

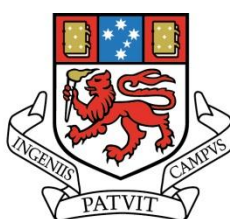
# Glycosylation analysis of therapeutic monoclonal antibodies

By

Lea Mauko

Submitted in fulfilment of the requirements for the Degree of

## Doctor of Philosophy



UNIVERSITY  
OF TASMANIA

November 2011

## **Declaration**

This thesis contains no material which has been accepted for a degree or diploma by the University or any other institution, except by way of background information and duly acknowledged in the thesis, and to the best of my knowledge and belief no material previously published or written by another person except where due acknowledgement is made in the text of the thesis, nor does the thesis contain any material that infringes copyright.

Lea Mauko

08/11/2011

This thesis may be made available for loan and limited copying and communication in accordance with the Copyright Act 1968.

Lea Mauko

08/11/2011

## **Abstract**

Pharmaceutical glycoproteins are one of the fastest growing therapeutic areas and glycosylation plays an important role in biological activity of the drugs. Most of the currently used therapeutic glycoproteins are expressed in non-human systems, often producing glycosylation patterns which can reduce the effectiveness and stability of the drugs or cause immune responses in patients. Due to the structural complexity of glycans, glycosylation analysis remains extremely challenging and frequently employs multiple separation and mass spectrometry based approaches. The standard approach for glycan profiling currently used in the pharmaceutical industry includes fluorescent labelling of enzymatically-released glycans and separation with hydrophilic interaction liquid chromatography (HILIC) coupled with fluorescence detection to achieve appropriate chromatographic resolution, sensitivity and relative quantification.

In this study, new methods employing zwitterionic-type HILIC (ZIC-HILIC) for the separation of 2-aminobenzamide (2-AB) labelled and reduced glycans from therapeutic monoclonal antibodies were developed. By using the new approach, the time of a chromatographic run was reduced compared to the standard method and the new proposed methods were suitable for on-line coupling with electrospray ionisation mass spectrometry detection (ESI-MS). Furthermore, it was demonstrated that by using ZIC-HILIC, fluorescent labelling was not required which significantly simplified the sample preparation.

To improve ESI-MS sensitivity of reduced glycans, the system was further downscaled employing nano ZIC-HILIC, which enabled the detection of minor glycan species. It was shown that coupling with high resolution MS provides information on glycan composition; however, due to high numbers of possible isobaric species, the confirmation of structures generally requires separation of glycans in combination with exoglycosidase digestions and tandem MS based approaches.

The HILIC analytical approaches were additionally compared to an orthogonal porous graphitized carbon (PGC) separation of reduced glycans coupled with ESI-MS. PGC exhibited excellent capability for the separation of isobaric glycan species and better sensitivity compared to HILIC. It was demonstrated that PGC is highly suitable for analysis of extremely complex glycan samples and the method was employed for structural characterisation of glycan species found in monoclonal antibodies. Since the PGC ESI-MS method resulted mainly in formation of protonated glycan species, the MS/MS spectra provided only limited structural information. On the other hand, exoglycosidase digestions enabled detailed characterisation of glycans from monoclonal antibodies. It was shown that multiple analytical approaches are generally required to obtain a complete glycan profile of a given glycoprotein.

## **Acknowledgments**

I would like to express my gratitude to people who made this thesis possible.

My supervisors, Prof Emily Hilder and Prof Paul Haddad, for opportunity to undertake this project, for support and guidance through the exciting world of science.

Dr Anna Nordborg, for numerous brilliant discussions and great help with practical aspects of laboratory work, especially in liquid chromatography.

Dr Nathan Lacher, for providing real samples used in the study, and for all suggestions and comments that helped to find the right direction in this project.

Dr Matthias Pelzing, for introduction to mass spectrometry, excellent ideas and advice, technical help, and for an opportunity to learn and work in Bruker laboratory.

Sebastiaan Dolman, for help with nano LC method development and instrumentation.

ACROSS colleagues, for making the lab an enjoyable place to work and for helping me in many different ways.

My friends, who kept me grounded and listened about all things great and small that didn't go quite as planned, in and out of the lab.

This thesis would not have been possible without support of my family. I am grateful for their patience and encouragement to follow this path. It has been an extraordinary journey with many great challenges.

## Contents

<b>Declaration .....</b>	<b>I</b>
<b>Abstract .....</b>	<b>II</b>
<b>Acknowledgments .....</b>	<b>IV</b>
<b>Contents .....</b>	<b>V</b>
<b>List of publications .....</b>	<b>VIII</b>
<b>Abbreviations .....</b>	<b>X</b>
<b>List of glycans .....</b>	<b>XII</b>
<b><i>Introduction .....</i></b>	<b><i>- 1 -</i></b>
<b><i>1. Chapter One - Literature review .....</i></b>	<b><i>- 3 -</i></b>
<b>1.1. Glycosylation.....</b>	<b>- 3 -</b>
<b>1.2. Analysis of intact and reduced MAbs.....</b>	<b>- 9 -</b>
<b>1.3. Analysis of glycopeptides .....</b>	<b>- 9 -</b>
<b>1.4. Glycans analysis.....</b>	<b>- 10 -</b>
1.4.1. Sample preparation.....	- 11 -
1.4.2. Capillary electrophoresis .....	- 15 -
1.4.3. Ion-exchange chromatography .....	- 15 -
1.4.4. Hydrophilic interaction liquid chromatography (HILIC) .....	- 16 -
1.4.5. Graphitized carbon liquid chromatography .....	- 19 -
1.4.6. Reversed phase chromatography .....	- 20 -
1.4.7. Analysis of glycans by mass spectrometry .....	- 21 -
1.4.7.1. MALDI-MS and ESI-MS in glycosylation analysis .....	- 21 -
1.4.7.2. Glycan fragmentation .....	- 22 -

<b>2. Chapter Two- Hydrophilic interaction liquid chromatography of glycans .....</b>	<b>- 29 -</b>
<b>2.1. Introduction .....</b>	<b>- 29 -</b>
<b>2.2. Materials and methods .....</b>	<b>- 31 -</b>
2.2.1. Reagents and chemicals .....	- 31 -
2.2.2. Sample preparation.....	- 32 -
2.2.3. Amide HILIC coupled with fluorescence detection.....	- 32 -
2.2.4. ZIC-HILIC of 2-AB labelled glycans .....	- 33 -
2.2.5. ZIC-HILIC of native and reduced glycans .....	- 33 -
<b>2.3. Results and discussion.....</b>	<b>- 34 -</b>
2.3.1. Separation of 2-AB-glycans using amide HILIC.....	- 34 -
2.3.2. ZIC-HILIC .....	- 39 -
2.3.2.1. Separation of 2-AB labelled glycans.....	- 39 -
2.3.2.2. Separation of native glycans .....	- 57 -
2.3.2.3. Separation of reduced glycans .....	- 66 -
<b>2.4. Conclusions.....</b>	<b>- 74 -</b>
<b>3. Chapter Three - Separation of glycans using graphitized carbon .....</b>	<b>- 75 -</b>
<b>3.1. Introduction .....</b>	<b>- 75 -</b>
<b>3.2. Materials and methods .....</b>	<b>- 77 -</b>
3.2.1. Reagents and chemicals .....	- 77 -
3.2.2. Graphitized carbon coupled with ESI-MS.....	- 77 -
<b>3.3. Results and discussion.....</b>	<b>- 78 -</b>
3.3.1. Separation of linear oligosaccharides using PGC .....	- 78 -
3.3.2. Separation of mannose glycan standards .....	- 80 -
3.3.3. Separation of glycans from RNase B .....	- 88 -
3.3.4. Glycan profiling of monoclonal antibodies using PGC .....	- 92 -
<b>3.4. Conclusions.....</b>	<b>- 103 -</b>

<b>4. Chpater Four - Nano LC separation of glycans.....</b>	<b>- 105 -</b>
<b>4.1. Introduction .....</b>	<b>- 105 -</b>
<b>4.2. Materials and Methods .....</b>	<b>- 106 -</b>
4.2.1. Sample preparation.....	- 106 -
4.2.2. Nano ZIC-HILIC coupled with ESI-MS.....	- 106 -
<b>4.3. Results and discussion.....</b>	<b>- 107 -</b>
4.3.1. Separation of high mannose glycans released from RNase B.....	- 107 -
4.3.2. Separation of glycans originating from monoclonal antibody .....	- 111 -
<b>4.4. Conclusions.....</b>	<b>- 120 -</b>
<b>5. Chapter Five - Exoglycosidase digestions and tandem mass spectrometry.....</b>	<b>- 121 -</b>
<b>5.1. Introduction .....</b>	<b>- 121 -</b>
<b>5.2. Materials and Methods .....</b>	<b>- 122 -</b>
5.2.1. Reagents and chemicals .....	- 122 -
5.2.2. Sample preparation.....	- 122 -
5.2.3. Tandem mass spectrometry .....	- 123 -
<b>5.3. Results and discussion.....</b>	<b>- 123 -</b>
5.3.1. Exoglycosidase digestions .....	- 123 -
5.3.2. Tandem mass spectrometry.....	- 146 -
<b>5.4. Conclusions.....</b>	<b>- 153 -</b>
<b>6. Chapter Six - Conclusions and future work .....</b>	<b>- 155 -</b>
<b>6.1. Project summary.....</b>	<b>- 155 -</b>
<b>6.2. Suggested future work.....</b>	<b>- 157 -</b>
<b>6.3. Conclusions.....</b>	<b>- 159 -</b>
<b>7. References .....</b>	<b>- 160 -</b>



## List of publications

### Papers

Mauko, L., Nordborg, A., Hutchinson, J.P., Lacher, N.A., Hilder, E.F., Haddad, P.R. Glycan profiling of monoclonal antibodies using zwitterionic-type hydrophilic interaction chromatography coupled with electrospray ionisation mass spectrometry detection, *Anal. Biochem.* 2011, **408** (2), 235-241, (**Chapter Two: 2.3.1., 2.3.2.2., 2.3.2.3.**).

Mauko, L., Pelzing, M., Dolman, S., Nordborg, A., Lacher, N.A., Haddad, P.R., Hilder, E.F. Zwitterionic-type hydrophilic interaction nano-liquid chromatography of complex and high mannose glycans coupled with high resolution time of flight mass spectrometry, in press, *J. Chromatogr. A* 2011, **1218**, 6419-6425 (**Chapter Four**).

Mauko, L., Hilder, E.F., Lacher, N.A., Pelzing, M., Nordborg, A., Haddad, P.R. Comparison of ZIC-HILIC and graphitized carbon-based analytical approaches combined with exoglycosidase digestions for analysis of glycans from monoclonal antibodies, waiting for Pfizer IP Committee and global disclosure approval prior to submission (**Chapter Two: 2.3.2.1., Chapters Three & Five**).

### Conference presentations

Mauko, L., Nordborg, A., Lacher, N.A., Hilder, E.F., Haddad, P.R. (2009) Glycan profiling of monoclonal antibodies-comparison of ZIC-HILIC and normal phase chromatography, coupled with CCAD, fluorescence and MS detection. *17<sup>th</sup> RACI Research & Development Topics, Griffith University, Gold Coast, QSL, 6<sup>th</sup>-9<sup>th</sup> Dec* (Oral)

Mauko, L., Nordborg, A., Lacher, N.A., Hilder, E.F., Haddad, P.R. (2010) Glycan profiling of monoclonal antibodies: Comparison of CCAD, fluorescence and ESI-MS detection, coupled with graphitized carbon and hydrophilic interaction

chromatography. *18<sup>th</sup> RACI Research & Development Topics, University of Tasmania, Hobart, TAS, 5<sup>th</sup>-8<sup>th</sup> Dec* (Oral)

Mauko, L., Nordborg, A., Lacher, N.A., Hilder, E.F., Haddad, P.R. (2010) Glycan profiling of monoclonal antibodies: Comparison of CCAD, fluorescence and ESI-MS detection, coupled with hydrophilic interaction chromatography. *30<sup>th</sup> ISPPP, Bologna, Italy, 6<sup>th</sup>-8<sup>th</sup> Sep* (Oral)

Mauko, L., Pelzing, M., Dolman, S., Nordborg, A., Lacher, N.A., Hilder, E.F., Haddad, P.R. (2011) Nanoscale zwitterionic-type hydrophilic interaction chromatography of complex and high mannose type glycans coupled with high resolution time of flight mass spectrometry. *23<sup>rd</sup> ANZSMS, Fremantle, WA, 29<sup>th</sup> Jan-03<sup>rd</sup> Feb* (Poster)

## Abbreviations

2-AA	2-anthranilic acid
2-AB	2-aminobenzamide
2-AP	2-aminopyridine
BPC	base peak chromatogram
CID	collision induced dissociation
dHex	deoxyhexose (fucose)
EIC	extracted ion chromatogram
Endo H	Endoglycosidase H
ESI-MS	electrospray ionisation mass spectrometry
Fuc	fucose
Gal	galactose
Glc	glucose
GlcNAc	N-acetylglucosamine
Hex	hexose
HexNAc	N-acetylhexosamine
HILIC	hydrophilic interaction liquid chromatography
HPLC	high-performance liquid chromatography
hrEIC	high resolution extracted ion chromatogram
IgG	Immunoglobulin G

LC	liquid chromatography
MAB	monoclonal antibody
MALDI	matrix-assisted laser desorption ionisation
Man	mannose
MS	mass spectrometry
MS/MS	tandem mass spectrometry
nano LC	nanoscale liquid chromatography
NeuAc	N-acetylneuraminic acid
NeuGc	N-glycolylneuraminic acid
PGC	porous graphitized carbon
PNGase F	Peptide: N-glycosidase F
QTOF	quadrupole-time of flight
RNase B	ribonuclease B
RP-HPLC	reversed phase high performance liquid chromatography
TIC	total ion chromatogram
TOF-MS	time of flight mass spectrometry
ZIC-HILIC	zwitterionic-type hydrophilic interaction liquid chromatography

## List of glycans

Table: List of glycans discussed in this study with theoretical monoisotopic masses of native, reduced and 2-aminobenzamide labelled forms.

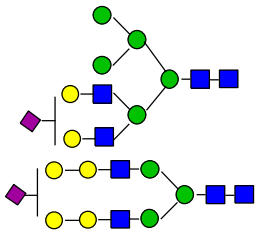
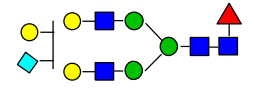
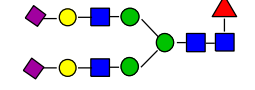
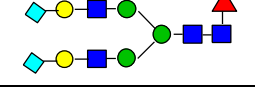
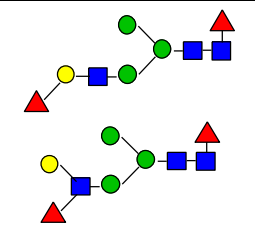
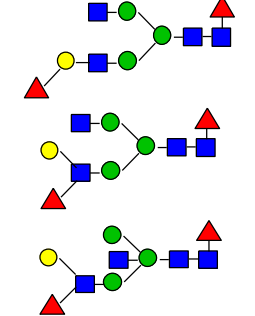
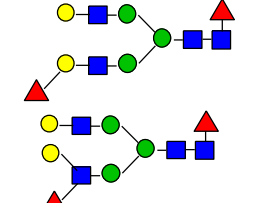
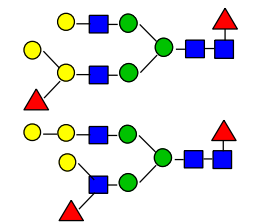
Composition	Glycan	Structure	Theoretical mass / Da, native	Theoretical mass / Da, reduced	Theoretical mass / Da, 2-AB labelled
High mannose glycans, cleaved by PNGase F.					
(Man) <sub>3</sub> (GlcNAc) <sub>2</sub>	Man3		910.33	912.34	1030.40
(Hex) <sub>2</sub> (Man) <sub>3</sub> (GlcNAc) <sub>2</sub>	Man5		1234.43	1236.45	1354.50
(Hex) <sub>3</sub> (Man) <sub>3</sub> (GlcNAc) <sub>2</sub>	Man6		1396.49	1398.50	1516.56
(Hex) <sub>4</sub> (Man) <sub>3</sub> (GlcNAc) <sub>2</sub>	Man7		1558.54	1560.55	1678.61
(Hex) <sub>5</sub> (Man) <sub>3</sub> (GlcNAc) <sub>2</sub>	Man8		1720.59	1722.61	1840.66
(Hex) <sub>6</sub> (Man) <sub>3</sub> (GlcNAc) <sub>2</sub>	Man9		1882.64	1884.66	2002.71
Truncated high mannose glycans, cleaved by Endoglycosidase H.					
(Hex) <sub>2</sub> (Man) <sub>3</sub> (GlcNAc) <sub>1</sub>	Man5-GlcNAc		1031.35	1033.37	1151.42
(Hex) <sub>3</sub> (Man) <sub>3</sub> (GlcNAc) <sub>1</sub>	Man6-GlcNAc		1193.41	1195.42	1313.48
(Hex) <sub>4</sub> (Man) <sub>3</sub> (GlcNAc) <sub>1</sub>	Man7-GlcNAc		1355.46	1357.48	1475.53
(Hex) <sub>5</sub> (Man) <sub>3</sub> (GlcNAc) <sub>1</sub>	Man8-GlcNAc		1517.51	1519.53	1637.58
(Hex) <sub>6</sub> (Man) <sub>3</sub> (GlcNAc) <sub>1</sub>	Man9-GlcNAc		1679.57	1681.58	1799.63

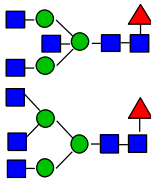
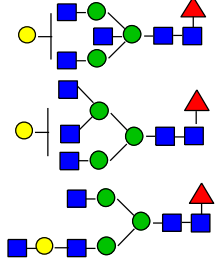
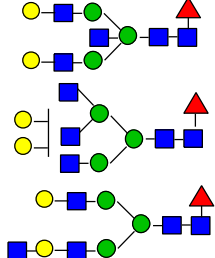
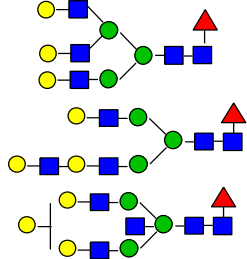
Neutral complex and hybrid glycans.					
(dHex) <sub>1</sub> (Man) <sub>3</sub> (GlcNAc) <sub>2</sub>	G0-2GlcNAc		1056.39	1058.40	1176.45
(HexNAc) <sub>1</sub> (Man) <sub>3</sub> (GlcNAc) <sub>2</sub>	G0-GlcNAc-Fuc		1113.41	1115.42	1233.48
(HexNAc) <sub>1</sub> (dHex) <sub>1</sub> (Man) <sub>3</sub> (GlcNAc) <sub>2</sub>	G0-GlcNAc		1259.47	1261.48	1379.53
(Hex) <sub>1</sub> (HexNAc) <sub>1</sub> (Man) <sub>3</sub> (GlcNAc) <sub>2</sub>	G0-GlcNAc-Fuc		1275.46	1277.48	1395.53
(HexNAc) <sub>2</sub> (Man) <sub>3</sub> (GlcNAc) <sub>2</sub>	G0-Fuc		1316.49	1318.50	1436.56
(HexNAc) <sub>2</sub> (dHex) <sub>1</sub> (Man) <sub>3</sub> (GlcNAc) <sub>2</sub>	G0		1462.54	1464.56	1582.61
(Hex) <sub>1</sub> (HexNAc) <sub>1</sub> (dHex) <sub>1</sub> (Man) <sub>3</sub> (GlcNAc) <sub>2</sub>	G1-GlcNAc		1421.52	1423.53	1541.59
(Hex) <sub>1</sub> (HexNAc) <sub>2</sub> (dHex) <sub>1</sub> (Man) <sub>3</sub> (GlcNAc) <sub>2</sub>	G1		1624.60	1626.61	1744.67
(Hex) <sub>2</sub> (HexNAc) <sub>1</sub> (dHex) <sub>1</sub> (Man) <sub>3</sub> (GlcNAc) <sub>2</sub>	G2-GlcNAc		1583.57	1585.59	1703.64
(Hex) <sub>2</sub> (HexNAc) <sub>2</sub> (dHex) <sub>1</sub> (Man) <sub>3</sub> (GlcNAc) <sub>2</sub>	G2		1786.65	1788.67	1906.72
(Hex) <sub>3</sub> (HexNAc) <sub>2</sub> (dHex) <sub>1</sub> (Man) <sub>3</sub> (GlcNAc) <sub>2</sub>	G3		1948.70	1950.72	2068.77
(Hex) <sub>4</sub> (HexNAc) <sub>2</sub> (dHex) <sub>1</sub> (Man) <sub>3</sub> (GlcNAc) <sub>2</sub>	G4		2110.76	2112.77	2230.82
(Hex) <sub>2</sub> (HexNAc) <sub>1</sub> (Man) <sub>3</sub> (GlcNAc) <sub>2</sub>	Hyb1		1437.51	1439.53	1557.58

$(\text{Hex})_2(\text{HexNAc})_1$ $(\text{dHex})_1$ $(\text{Man})_3(\text{GlcNAc})_2$	Hyb1F		1583.57	1585.59	1703.64
$(\text{Hex})_3(\text{HexNAc})_1$ $(\text{Man})_3(\text{GlcNAc})_2$	Hyb2		1599.57	1601.58	1719.63
$(\text{Hex})_3(\text{HexNAc})_1$ $(\text{dHex})_1$ $(\text{Man})_3(\text{GlcNAc})_2$	Hyb2F		1745.62	1747.64	1865.69
$(\text{Hex})_4(\text{HexNAc})_1$ $(\text{Man})_3(\text{GlcNAc})_2$	Hyb3		1761.62	1763.63	1881.69
$(\text{Hex})_4(\text{HexNAc})_1$ $(\text{dHex})_1$ $(\text{Man})_3(\text{GlcNAc})_2$	Hyb3F		1907.68	1909.69	2027.75

Sialylated complex and hybrid glycans.					
(Hex) <sub>1</sub> (HexNAc) <sub>1</sub> (dHex) <sub>1</sub> (NeuAc) <sub>1</sub> (Man) <sub>3</sub> (GlcNAc) <sub>2</sub>	G1-GlcNAc+NeuAc		1712.61	1714.63	1832.68
(Hex) <sub>2</sub> (HexNAc) <sub>1</sub> (NeuAc) <sub>1</sub> (Man) <sub>3</sub> (GlcNAc) <sub>2</sub>	Hyb1+NeuAc		1728.61	1730.62	1848.68
(Hex) <sub>1</sub> (HexNAc) <sub>1</sub> (dHex) <sub>1</sub> (NeuGc) <sub>1</sub> (Man) <sub>3</sub> (GlcNAc) <sub>2</sub>	G1-GlcNAc+NeuGc		1728.61	1730.62	1848.68
(Hex) <sub>3</sub> (HexNAc) <sub>1</sub> (NeuAc) <sub>1</sub> (Man) <sub>3</sub> (GlcNAc) <sub>2</sub>	Hyb2+NeuAc		1890.66	1892.68	2010.73
(Hex) <sub>2</sub> (HexNAc) <sub>1</sub> (dHex) <sub>1</sub> (NeuGc) <sub>1</sub> (Man) <sub>3</sub> (GlcNAc) <sub>2</sub>	Hyb1F+NeuGc		1890.66	1892.68	2010.73
(Hex) <sub>3</sub> (HexNAc) <sub>1</sub> (NeuGc) <sub>1</sub> (Man) <sub>3</sub> (GlcNAc) <sub>2</sub>	Hyb2F+NeuGc		1906.66	1908.67	2026.72
(Hex) <sub>1</sub> (HexNAc) <sub>2</sub> (dHex) <sub>1</sub> (NeuAc) <sub>1</sub> (Man) <sub>3</sub> (GlcNAc) <sub>2</sub>	G1+NeuAc		1915.69	1917.71	2035.76
(Hex) <sub>2</sub> (HexNAc) <sub>2</sub> (NeuAc) <sub>1</sub> (Man) <sub>3</sub> (GlcNAc) <sub>2</sub>	G2+NeuAc -Fuc		1931.69	1933.70	2051.76
(Hex) <sub>1</sub> (HexNAc) <sub>2</sub> (dHex) <sub>1</sub> (NeuGc) <sub>1</sub> (Man) <sub>3</sub> (GlcNAc) <sub>2</sub>	G1+NeuGc		1931.69	1933.70	2051.76
(Hex) <sub>4</sub> (HexNAc) <sub>1</sub> (NeuAc) <sub>1</sub> (Man) <sub>3</sub> (GlcNAc) <sub>2</sub>	Hyb3+NeuAc		2052.71	2054.73	2172.78
(Hex) <sub>3</sub> (HexNAc) <sub>1</sub> (dHex) <sub>1</sub> (NeuGc) <sub>1</sub> (Man) <sub>3</sub> (GlcNAc) <sub>2</sub>	Hyb2F+NeuGc		2052.71	2054.73	2172.78
(Hex) <sub>2</sub> (HexNAc) <sub>2</sub> (dHex) <sub>1</sub> (NeuAc) <sub>1</sub> (Man) <sub>3</sub> (GlcNAc) <sub>2</sub>	G2+NeuAc		2077.75	2079.76	2197.81
(Hex) <sub>3</sub> (HexNAc) <sub>2</sub> (NeuAc) <sub>1</sub> (Man) <sub>3</sub> (GlcNAc) <sub>2</sub>	G3+NeuAc -Fuc		2093.74	2095.76	2213.81
(Hex) <sub>2</sub> (HexNAc) <sub>2</sub> (dHex) <sub>1</sub> (NeuGc) <sub>1</sub> (Man) <sub>3</sub> (GlcNAc) <sub>2</sub>	G2+NeuGc		2093.74	2095.76	2213.81



(Hex) <sub>4</sub> (HexNAc) <sub>2</sub> (NeuAc) <sub>1</sub> (Man) <sub>3</sub> (GlcNAc) <sub>2</sub>			2255.79	2257.81	2375.86
(Hex) <sub>3</sub> (HexNAc) <sub>2</sub> (dHex) <sub>1</sub> (NeuGc) <sub>1</sub> (Man) <sub>3</sub> (GlcNAc) <sub>2</sub>	G3+NeuGc		2255.79	2257.81	2375.86
(Hex) <sub>2</sub> (HexNAc) <sub>2</sub> (dHex) <sub>1</sub> (NeuAc) <sub>2</sub> (Man) <sub>3</sub> (GlcNAc) <sub>2</sub>	G2+2NeuAc		2368.84	2370.86	2488.91
(Hex) <sub>2</sub> (HexNAc) <sub>2</sub> (dHex) <sub>1</sub> (NeuGc) <sub>2</sub> (Man) <sub>3</sub> (GlcNAc) <sub>2</sub>	G2+2NeuGc		2400.83	2402.85	2520.90
Complex glycans with fucosylated antenna.					
(Hex) <sub>1</sub> (HexNAc) <sub>1</sub> (dHex) <sub>2</sub> (Man) <sub>3</sub> (GlcNAc) <sub>2</sub>	F1-GlcNAc		1567.58	1569.59	1687.64
(Hex) <sub>1</sub> (HexNAc) <sub>2</sub> (dHex) <sub>2</sub> (Man) <sub>3</sub> (GlcNAc) <sub>2</sub>	F1		1770.66	1772.67	1890.72
(Hex) <sub>2</sub> (HexNAc) <sub>2</sub> (dHex) <sub>2</sub> (Man) <sub>3</sub> (GlcNAc) <sub>2</sub>	F2		1932.71	1934.72	2052.78
(Hex) <sub>3</sub> (HexNAc) <sub>2</sub> (dHex) <sub>2</sub> (Man) <sub>3</sub> (GlcNAc) <sub>2</sub>	F3		2094.76	2096.78	2214.83

Isobaric triantennary glycans and complex glycans with bisecting GlcNAc.					
(HexNAc) <sub>3</sub> (dHex) <sub>1</sub> (Man) <sub>3</sub> (GlcNAc) <sub>2</sub>	T0		1665.62	1667.64	1785.69
(Hex) <sub>1</sub> (HexNAc) <sub>3</sub> (dHex) <sub>1</sub> (Man) <sub>3</sub> (GlcNAc) <sub>2</sub>	T1		1827.68	1829.69	1947.75
(Hex) <sub>2</sub> (HexNAc) <sub>3</sub> (dHex) <sub>1</sub> (Man) <sub>3</sub> (GlcNAc) <sub>2</sub>	T2		1990.74	1992.75	2110.81
(Hex) <sub>3</sub> (HexNAc) <sub>3</sub> (dHex) <sub>1</sub> (Man) <sub>3</sub> (GlcNAc) <sub>2</sub>	T3		2151.78	2153.80	2271.85

■ GlcNAc (HexNAc); ● Man; ▲ Fuc; ● Gal; ◆ NeuGc; ◆ NeuAc

## ***Introduction***

The aim of this project is the development of new methods for glycosylation analysis of recombinant monoclonal antibodies (MAbs). MAbs and glycoproteins in general are one of the fastest growing therapeutic areas and their activity, stability, serum half-life and adverse reactions in patients are largely determined by glycosylation. Currently, there is no single method that could provide complete information on glycan profile, due to the complexity of glycan composition, structures and linkages. The sample preparation in glycosylation analysis is usually laborious and it can involve derivatization steps that are expensive and time-consuming. At the same time, numerous separation-based analytical approaches have been developed to provide detailed information on MAbs glycosylation and the current standardised separation procedures used in pharmaceutical industry require from several minutes to several hours. Since in quality control and clone selection high numbers of samples are being routinely analysed, there has been a lot of interest in improving and optimising current analytical methods.

The same principles of glycosylation analysis as in pharmaceutical industry apply also to the rapidly developing field of glycomics, the younger sibling of genomics and proteomics, where the entire range of sugars and their physiological and pathological aspects in a given organism are being studied. All these areas of glycobiology and pharmaceutical analysis require rapid, sensitive and quantitative analysis of glycan composition, structure and linkages.

The project is focused on several aspects of glycosylation analysis, including simplification of sample preparation, enhancing sensitivity of mass spectrometry (MS) detection by miniaturisation with emphasis on analysis of minor glycan species, comparing different stationary phases in order to achieve optimum selectivity, and employing enzymatic and mass spectrometry-based approaches for structural elucidation of glycans. The strategies and techniques used in this study are schematically represented in Figure 0–1.

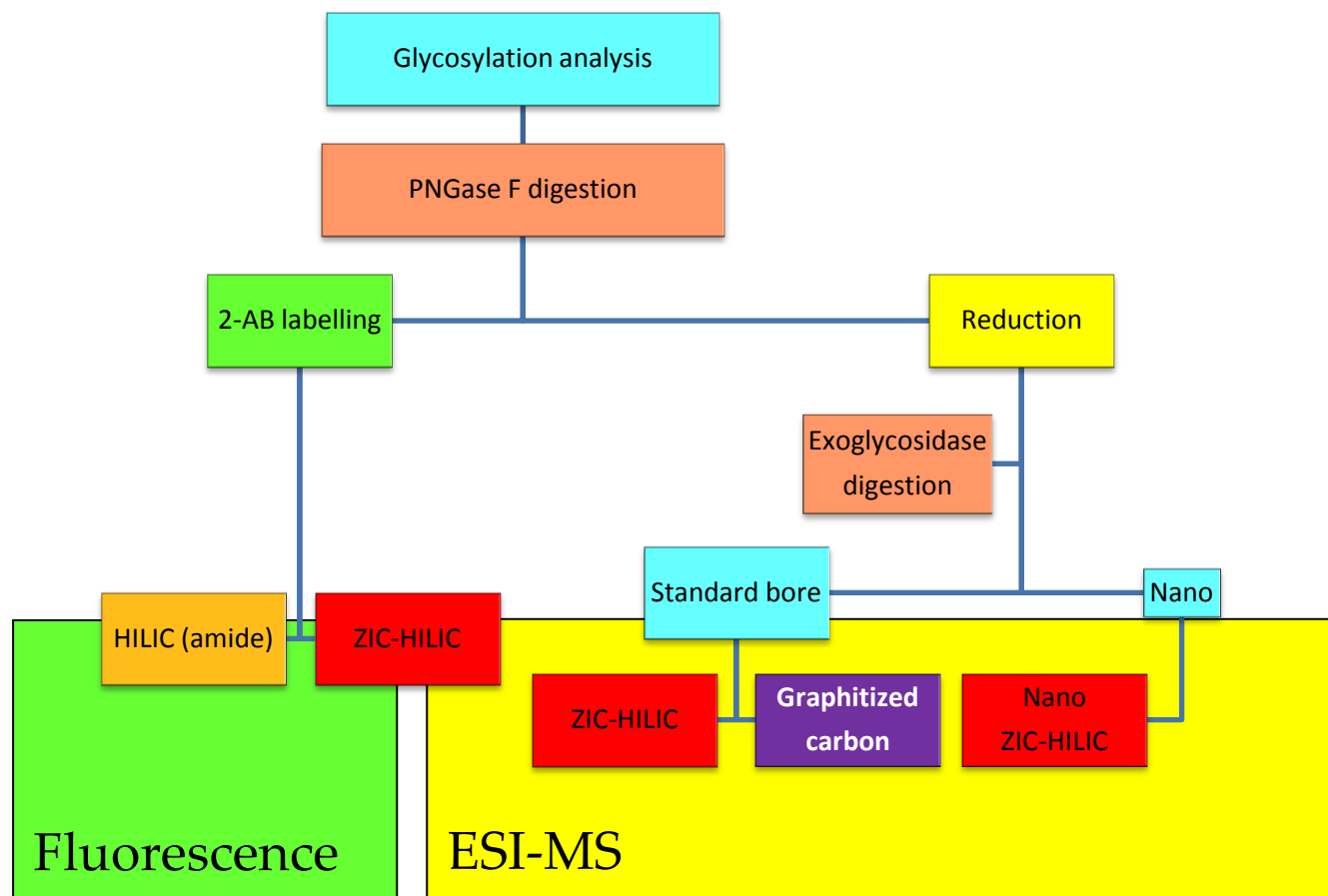


Figure 0–1: Schematic representation of methods used in this study.

# Chapter One

## ***1. Literature review***

Post-translational modifications (PTMs) are covalent modifications that change the properties of a protein by proteolytic cleavage or by addition of a modifying group to one or more amino acids. PTMs determine activity and localization of the protein, and interactions with other proteins [1]. Protein modifications are generally not homogeneous, and expression of a single gene can result in a large number of gene products [1]. The main PTMs associated with proteins are acetylation, acylation, carboxylation, hydroxylation, amidation, disulphide bond formation, glycosylation, phosphorylation, sulfation and proteolytic processing [1] and many of them are relevant also to therapeutic proteins [2]. The majority of approved therapeutic proteins, such as blood factors, anticoagulants, antibodies, hormones, erythropoietin and interferons, bear some form of PTMs [2].

### **1.1. Glycosylation**

Glycosylation is a very versatile post-translational modification and contributes to the complexity of protein molecules. Glycosylation determines biological activity and function of proteins and it has an important influence on their physicochemical properties [3, 4]. Malfunctions of glycan biosynthetic pathways lead to numerous disorders which indicate the importance of glycosylation in biological processes [5]. Several types of glycosylation are known and the most common and well-studied are O- and N-glycosylation. The N-linked glycans are attached to an asparagine residue via a (Man)<sub>3</sub>(GlcNAc)<sub>2</sub> core (where Man represents mannose and GlcNAc represents N-acetylglucosamine) and they are divided into the three main classes; high mannose, complex and hybrid type glycans (Figure 1–1). High mannose glycans have only mannose residues attached to the core, complex glycans have antennae starting with GlcNAcs, and hybrid glycans have one or two antennae attached to the 3-arm and mannose

residues at the 6-arm [4]. Most of the N-glycans are synthesised from a common precursor containing the (Glc)<sub>3</sub>(Man)<sub>9</sub>(GlcNAc)<sub>2</sub> residue. After the attachment to the protein, glycans are further exposed to the glucosidases and mannosidases which give the high mannose glycans with 5 to 9 mannose units as the final products of the processing (Figure 1–2). The glycans with the GlcNAc added to the terminal region are called complex type. In mammals, the antennae are commonly elongated by galactosylation and capped by sialylation or fucosylation. The additional fucosylation site is the core GlcNAc. Compared to the high mannose glycans, the complex glycans exhibit greater diversity [4, 6]. This thesis is mainly focused on N-glycosylation and N-glycan profiling of mammalian glycoproteins from natural sources and recombinant therapeutic glycoproteins with emphasis on monoclonal antibodies (MAbs). However, the same principles of the glycosylation analysis apply to glycomics research, where the entire range of saccharides and their physiological and pathological aspects in a given organism are being studied.

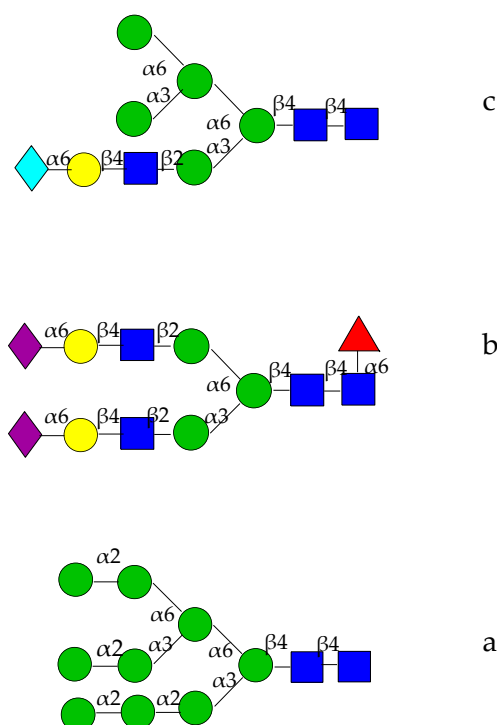


Figure 1–1: Chemical diversity of N-glycans with the most common representatives, (a) high mannose, (b) complex and (c) hybrid glycans. The structures are presented according to the scheme proposed by Consortium for Functional Glycomics [7]. The schematic representation has still not been unified [8].

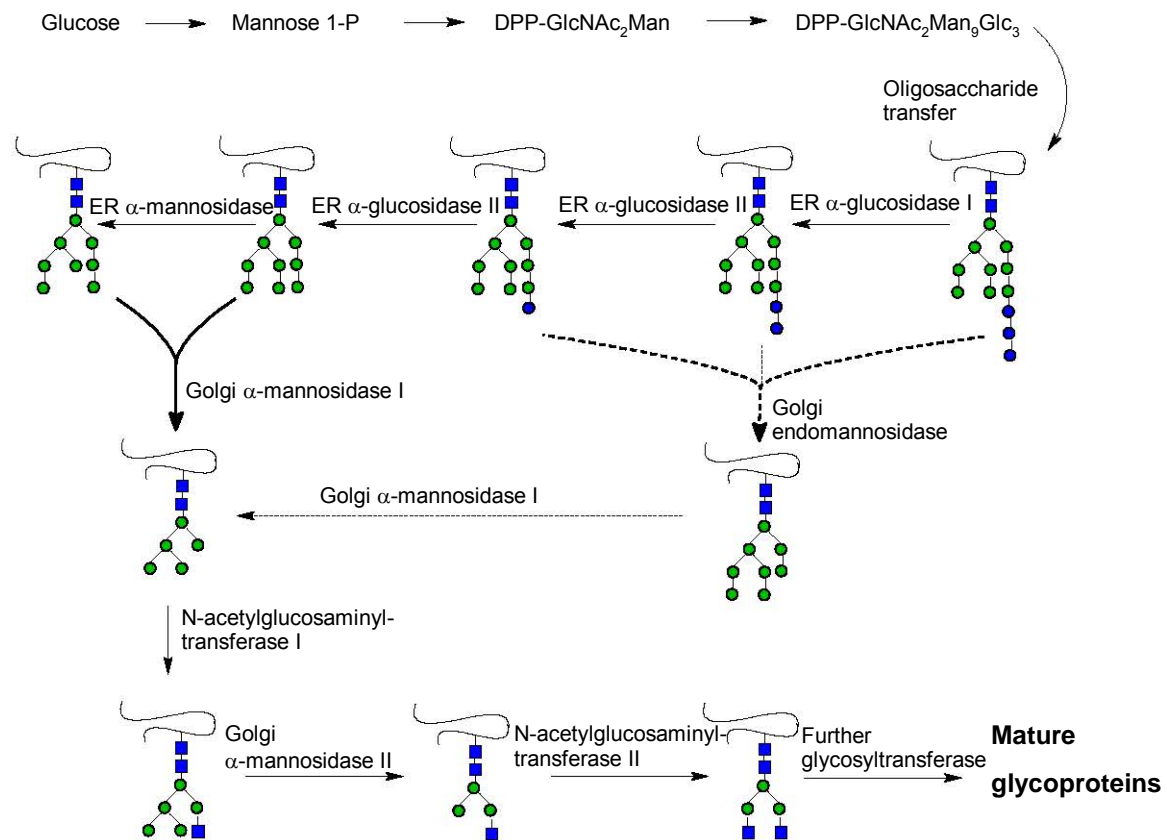


Figure 1-2: Biosynthesis on N-glycan side chains adapted from Dwek et al. [9]. ● Glucose; ■ N-acetylglucosamine; ● Mannose.

Most of the therapeutic MABs belong to the IgG subclass, with a basic structure that consists of two light and two heavy chains associated with covalent and non-covalent interactions, forming three regions. Two identical variable (Fv) regions express antigen-binding specific site and the constant region (Fc) determines interaction with effector molecules which results in the elimination of the antigen [10]. Monoclonal antibodies used in the treatment of cancers were primarily designed to target tumour antigens mainly involved in growth and proliferation of cancer cells and the main mechanism of action involved interaction with the antigen through the antigen-binding region of the MAB. Since it was established that the MAB anti-cancer activity can be enhanced by Fc mediated effects, which include killing the tumour cells via Antibody-dependent cytotoxicity (ADCC), Complement-dependent cytotoxicity (CDC) and Antibody-dependent phagocytosis (ADCP), novel approaches of engineering and optimising MAB activity have been developed. The main focus lies in enhancement of Fc effects through modifications of glycosylation and identifying Fc amino acid sequences for mutagenesis [11, 12]. Another important aspect of glycosylation of therapeutic glycoproteins is its effect on the *in vitro* and *in vivo* stability. The effects of glycosylation on proteolytic degradation, oxidation, chemical cross-linking and physical stability of glycoproteins have recently been reviewed [13].

A major general issue in MAB therapy has been immunogenicity, which originates either from the protein sequence or post-translational modifications, such as glycosylation. To minimize unwanted side-effects and increase efficiency, development of MABs therapeutics has moved from highly immunogenic murine to more human-like chimeric, humanised and fully human MABs [14].

The recombinant MABs are most commonly expressed in Chinese hamster ovary (CHO) and murine myeloma cells (NS0 and Sp2/0), which exhibit glycosylation patterns slightly different to those found in humans. While the most common glycans found in human polyclonal IgGs are of the biantennary complex type with various levels of core-fucose, galactose, bisecting N-acetylglucosamine and N-acetylneuraminic acid, IgGs expressed in CHO cell lines exhibit glycan profiles



with a higher degree of fucosylation and lower level of galactosylation. On the other hand, IgGs expressed in murine cell lines contain some glycan forms that are not present in humans and that can be immunogenic [10, 15, 16]. In murine systems but not in human, an active  $\alpha$ -galactosyltransferase is expressed, which adds a terminal  $\alpha$ -galactose to the  $\beta$ -galactose at the end of the antennae of complex glycans and it can sensitize patients if the drug is administered on the chronic basis [17, 18]. It has been generally accepted that CHO cell lines do not have all the enzymes required for synthesis of glycoproteins with  $\alpha$ -galactose epitope; however, the presence of  $\alpha$ -galactose in CHO cell line has been recently confirmed [19]. The  $\alpha$ -galactose levels in CHO glycoproteins are generally lower compared to those expressed in murine cell lines and it is believed that subclonal populations from the same parental cell lines can differ in the expression of the gene for  $\alpha$ -galactosyltransferase [19]. The other unusual glycan species found in glycoproteins from murine cells is N-glycolylneuraminic acid (NeuGc), which was also shown to be immunogenic [20]. Very recently, it has been reported that the presence of NeuGc in MAb can reduce serum half-life of the drug and consequently its efficacy [21]. It was suggested that the level of NeuGc in recombinant glycoproteins can be reduced simply by adding NeuAc in the culture medium, which would compete with the pre-existing NeuGc. This would be a much simpler solution than changing the cell lines that have already been approved by regulatory agencies [21]. On the other hand, the effect of high mannose glycans that are normally present in MAbs expressed in murine and CHO cells in low amounts is still unknown. It has been suggested that mannosylation can have a negative impact on the MAb half-life and clearance due to the binding to the mannose receptor-bearing cells [17, 22]. However, some other reports indicate that high mannose glycosylated MAbs are removed from the blood circulation with the same rate as the complex-type glycoforms [17, 23].

Some other, less frequently used, cell lines are mammalian (human), avian, insect, yeasts, bacteria or plant derived; and some of them have limited abilities to glycosylate proteins or they produce glycosylation patterns alternative to humans that can be problematic [16]. It is believed that human cell cultures

which could solve the problems related to glycosylation will gain more popularity in the future. A rapidly developing area is also glycoengineering where cell cultures and organisms are genetically manipulated to exhibit controlled expression of enzymes involved in glycosylation, producing proteins with specific and/or more uniform glycan profile [16, 24].

Glycosylation in the Fc region of MAbs also plays an important role in their activity and potency. MAbs used in treatment of various cancers exhibit ADCC and CDC which result in the killing and removal of the target cancer cells. As previously discussed, polyclonal human IgGs and therapeutic MAbs expressed in CHO and murine cell lines produce high level of core-fucosylated glycans. Recently it has been reported that ADCC activity of the MAbs dramatically increased for the MAbs with higher degree of defucosylation and it is expected that in the future cell lines with knocked out gene for  $\alpha$ -1,6-fucosyltransferase will be used for production of highly potent anti-tumour MAbs [25, 26]. On the other hand, a higher degree of sialylation in the Fc region of IgGs leads to increased anti-inflammatory activity which will direct the future design of therapeutics for treatment of inflammatory diseases, such as rheumatoid arthritis [27]. In order to understand complex structure-function relationships of glycans, multiple approaches to glycomics have to be integrated, including functional genetics that provides information on glycan diversification and glycosylation of proteins in relation to phenotype; analysis of glycan-protein interactions, development of glyco-gene microarrays, glycosylation analysis and bioinformatics [28].

In glycan profiling of recombinant glycoproteins, several questions must be addressed, such as glycan occupancy, presence of high mannose glycans and glycans containing sialic acids, degree of core-fucosylation and presence of intersecting GlcNAc. Glycosylation analysis can be performed on the level of glycoprotein, glycopeptides or glycans and the choice of the analytical strategy will depend on the question to be answered. Different approaches and strategies in glycosylation analysis of MAbs will be described.

## 1.2. Analysis of intact and reduced MAbs

Analysis of intact and reduced MAbs are described also as a “top-down” approach and provides information on glycan occupancy and the main glycosylation patterns. The simple method for evaluation of glycan occupancy employs capillary sodium dodecyl sulfate (SDS) gel electrophoresis coupled with UV detection. The non-glycosylated and glycosylated heavy chains of the protein can be efficiently separated and the method allows quantitative determination of both forms [29].

Another approach for analysis of intact MAbs employs reversed-phase (RP) HPLC coupled with high resolution MS. Separation of glycoforms by RP-HPLC is not possible; however, mass spectra contain information about glycan heterogeneity. Since deconvoluted mass spectra of intact MAbs can be difficult to interpret [30, 31], better differentiation between major glycoforms can be achieved after the reduction of MAbs and the separation of light and heavy chains by RP-HPLC due to the improved mass resolution and mass accuracy [30]. Several less common approaches using enzymes that cleave MAbs in the hinge region and analysis of MAb fragments have also been described and they have been recently summarised [32]. Although these methods are especially useful for fast analysis in production and formulation of MAbs, more detailed analysis on glycopeptide and glycan level is required to obtain a complete glycan profile of products for therapeutic use.

## 1.3. Analysis of glycopeptides

Analysis of glycopeptides is known also as glycosylation site-specific analysis and it is particularly useful in the field of glycomics and understanding of glycoproteins on a molecular level, where information about glycan heterogeneity as well as the glycosylation site are required. This analytical approach is also applicable to recombinant MAbs since it enables high-throughput characterisation of glycosylation [33]. Due to the method automation,

analysis of glycopeptides from human serum IgGs can also be used for screening and monitoring of pathological states [34]. Glycopeptides can be obtained by enzymatic cleavage commonly using trypsin, lysylendopeptidase (endo-Lys-C) or pronase [32, 35]. The size and complexity of peptides and glycopeptides formed depend on enzyme specificity. Trypsin digests often contain larger non-glycosylated peptides which reduce the ionisation efficiency of glycopeptides resulting in the suppression of the MS signal. On the other hand, pronase is a mixture of endo- and exopeptidases and the products of the enzyme digestion are complex mixtures of short peptides and glycopeptides [35]. Prior to MS detection, purification and enrichment steps are usually employed, which include RP-HPLC, hydrophilic interaction liquid chromatography (HILIC), lectin affinity and size-exclusion chromatography, which have been reviewed elsewhere [32, 35, 36]. Separation of glycosylated from non-glycosylated peptides can be achieved prior or during the LC-MS run. Glycopeptides can be differentiated from the non-glycosylated peptides by a specific ionisation pattern in collision-induced dissociation (CID) mass spectra, resulting in low molecular mass ions such as  $[\text{Hex}+\text{H}]^+$ ,  $[\text{HexNAc}+\text{H}]^+$ ,  $[\text{HexHexNAc}+\text{H}]^+$  and  $[\text{NeuAc}+\text{H}]^+$ . Alternatively, glycopeptides can be screened for specific fragments or neutral losses [32, 35]. When the separation of glycopeptides is performed by RP-HPLC, the glycopeptides with the same peptide chain are eluted closely together [37]. In some other case, the higher retention of glycopeptides containing acidic glycans compared to neutral glycans was observed [34]. Enhanced selectivity for separation of glycopeptides with the same amino acid sequence and different glycan structural isomers was achieved when zwitterionic-type HILIC (ZIC-HILIC) was used [38].

#### 1.4. Glycans analysis

The most widely used approach for glycan profiling of MAbs is a “bottom-up” approach, where glycans released from the protein are separated by capillary electrophoresis (CE) or LC and detected by MS or fluorescence detection.

### **1.4.1. Sample preparation**

Glycans are most commonly released from MAbs using Peptide: N-Glycosidase F (PNGase F). Due to accessibility of the glycosylation site, glycan cleavage in the Fc region of IgGs does not require prior denaturation with detergents or reducing agents or treatment with proteases. To increase the yields and accelerate the reaction, the use of monolithic supports for immobilization of PNGase F for glycoprotein digestion was demonstrated [39]. The enzyme reactors can be effectively coupled into a multidimensional system which could significantly simplify the procedure [40]. Recently, an integrated microfluidic device has been developed that was able to perform release of N-linked glycans by PNGase F, protein removal and glycan LC separation and it was coupled to nano electrospray ionisation (ESI)-MS. The sample preparation and analysis time was reduced to 10 min and the protocol was automated [41].

In special cases, such as MAbs expressed in plant systems with specific glycosylation patterns, PNGase A may be used as an alternative [32]. Hydrozinolysis is a less suitable method for releasing glycans from MAbs due to N-deacetylation and N-deglycolylation and therefore loss of information regarding sialylation [42]. Glycans can be analysed in native, reduced, permethylated or fluorescently-labelled forms. The choice of glycan derivatization is determined by the chosen separation and detection methods. Prior to fluorescent labelling, glycan samples should be purified from proteins, salts and detergents.

Glycans are generally labelled for detection by reductive amination via a Schiff base in the presence of an excess quantity of an appropriate tag (Figure 1–3) [43]. The choice of the fluorescent tag depends on the analytical approach. Labelling with a fluorescent tag enables fluorescence detection of glycans with high sensitivity (picomole level) as well as MS detection with higher sensitivity compared to native glycans, since the introduction of functional groups into the molecule increases ionisation efficiency. The yield of derivatization depends on

the first sugar at the reducing end of the glycan. For enzymatically released N-glycans with GlcNAc at the reducing end, the reaction might be incomplete [44]. The most commonly used labels are 2-aminobenzamide (2-AB) and 2-anthranilic acid (2-AA) [45]. The procedure was proposed by Bigge et al. [43] 15 years ago and since then it has been standardised and commercial kits for quantitative labelling of glycans are available.

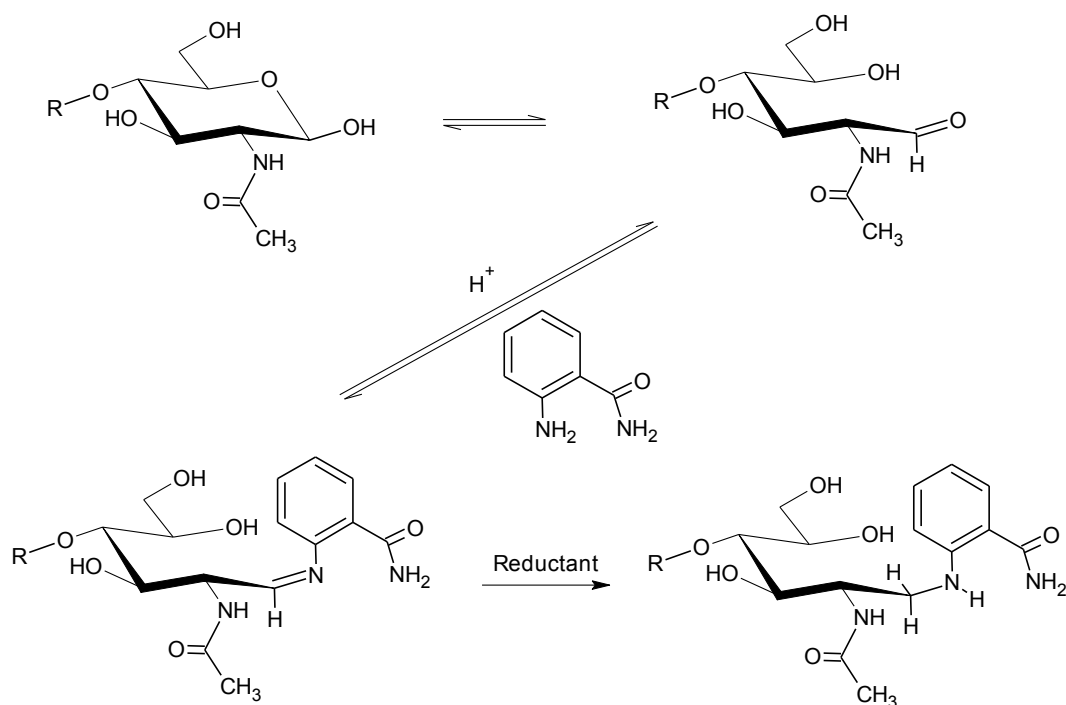


Figure 1–3: Reductive amination of glycans with 2-AB as proposed by Bigge et al. [43].

2-AB glycans are most frequently separated by HILIC with stationary phases having an amide functionality and databases for identification of glycans based on retention properties have been established [46]. One of the early introduced fluorescent tags was 2-aminopyridine (2-AP); however, non-quantitative yields and lower sensitivity are generally obtained [45]. Advances in fluorescent derivatization of glycans were reviewed by Anumula [45].

Detailed structural characterization of glycan species usually requires MS in combination with digestion by exoglycosidases which release a specific monosaccharide residue at the non-reducing terminus. Additional information about linkages and branching can be obtained where MS and tandem MS data are not sufficient for elucidation of glycan structures. Commonly used enzymes include  $\alpha$ -galactosidase,  $\beta$ -galactosidase,  $\alpha$ -mannosidase,  $\alpha$ -sialidase,  $\beta$ -N-acetylhexosaminidase and  $\alpha$ -L-fucosidase from various sources (Figure 1–4), and they can be used sequentially or as an array of exoglycosidase mixtures [47]. While the enzymatic sequencing is tedious, the parallel enzyme analysis is considerably shorter. Glycans are commonly labelled via reductive amination prior to the exoglycosidase digestion and separation [47, 48]. Another popular approach used for structural elucidation includes analysis of glycans in permethylated form without prior separation by matrix-assisted laser desorption ionisation (MALDI)-MS [49, 50] which will be further discussed below. Exoglycosidase digestions have been optimised for direct coupling with MALDI-MS to simplify the procedures, save time and increase throughput. Instead of classic sodium phosphate buffers, MS-friendly (i.e. volatile) ammonium acetate and ammonium formate buffers can be used [49, 51] and the digestion can be performed directly on the MALDI target [52, 53]. Similar strategies can be applied to analysis of glycoproteins from natural sources where glycosylation patterns have not been previously examined [54, 55].

$\alpha$ -galactosidase

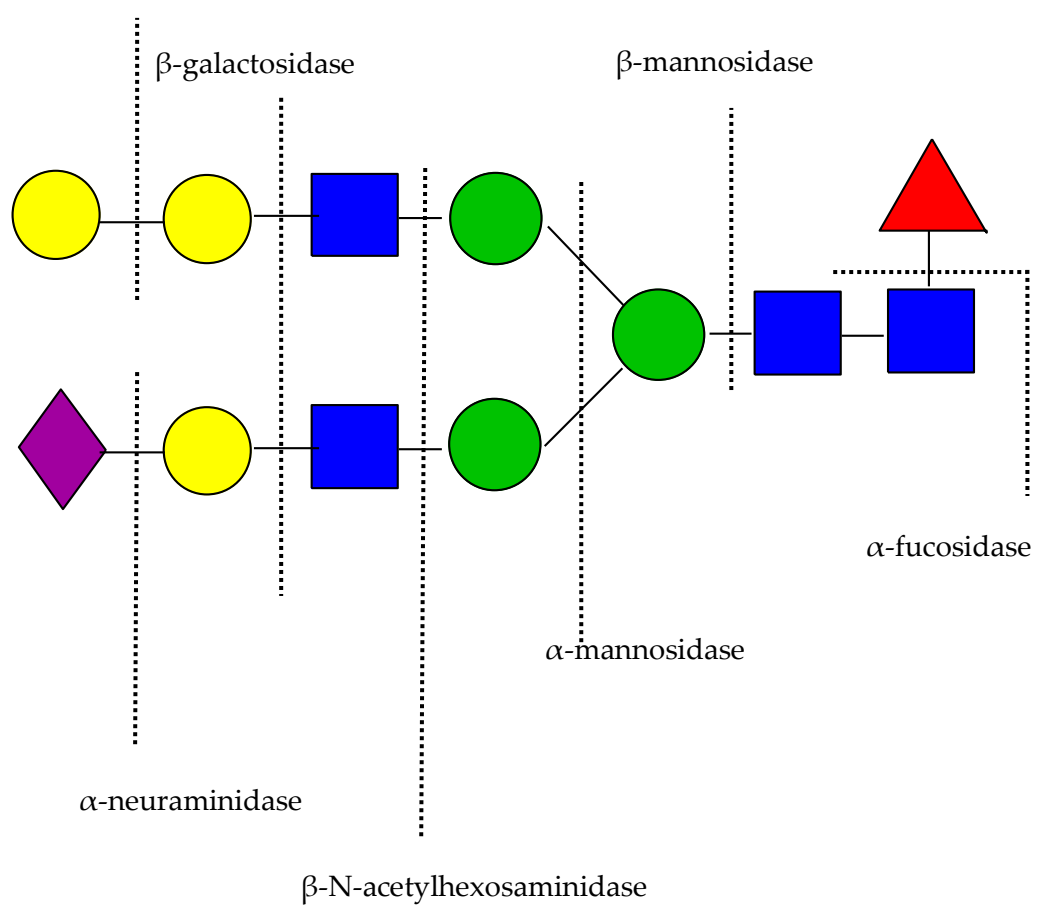


Figure 1–4: Schematic representation of exoglycosidases digestions with the most common exoglycosidases used for the cleavage of specific linkages.



### ***1.4.2. Capillary electrophoresis***

The most attractive feature of capillary electrophoresis (CE) analysis of glycans compared to HPLC approaches is reduced time of separation. However, CE analysis of glycans generally requires derivatization of oligosaccharides to introduce the charged group needed for migration in an electric field, to increase sensitivity by laser-induced fluorescence (LIF) detection, and to improve ionisation efficiency in MS. As an exception, sialylated glycans can be analysed by CE in the native form, since they can be easily deprotonated [56]. The electrophoretic mobility depends on the charge and the size of the glycan. Charged fluorescent tags, such as 2-aminobenzoic acid (2-AA) [29] and 8-aminopyrene-1,3,6-trisulfonate (APTS) [57, 58], are most often used. Since APTS carries 3 negative charges, APTS-labelled glycans can be analysed with high speed and resolution and major glycans found in MAbs can be analysed in less than 10 min [57, 59, 60]. Due to faster migrating rates and overlapping with reagent-derived peaks, some difficulties analysing minor species, sialic acids and high mannose glycans, have been reported [61]. The CE separation of APTS-labelled glycans was further developed for more detailed analysis of minor glycans, such as sialic acids and defucosylated species, and adapted for on-line coupling with MS [58]. Since 2-AA has a single negative charge, the CE-LIF analysis time is longer compared to analysis of APTS-labelled glycans. However, the 2-AA reagent is less expensive and easily commercially available, and collected 2-AA derivatives can be further analysed by LC-MS for further structural characterisation. CE analysis of MAbs and glycoproteins has recently been reviewed [44, 61].

### ***1.4.3. Ion-exchange chromatography***

Since glycans form anions at high pH, they are suitable for separation by high pH anion-exchange chromatography (AEC). The presence of redox-active functional groups makes glycans suitable analytes for pulsed amperometric detection (HPAEC-PAD) and low picomolar sensitivity can be achieved on analytical

columns [62]. Since high salt eluents are used in HPAEC, structure elucidation by MS requires off-line desalting. The demands for complex and detailed structural analysis require on-line coupling of HPAEC with mass spectrometry and an approach including on-line desalting was suggested [63]. HPAEC-PAD has been shown to be suitable for monitoring batch-to-batch variability of MAb glycosylation with simultaneous analysis of neutral and sialylated glycans [64]. Anion-exchange chromatography has recently been used as a part of 2D HILIC system where neutral and charged AP-glycans were sequentially eluted, based on the number of charged residues, and detected by fluorescence [65]. Although the progress in separation of glycans using AEC continues, the technique has not gained the same level of popularity as HILIC or use of graphitized carbon columns.

#### ***1.4.4. Hydrophilic interaction liquid chromatography (HILIC)***

Almost all HILIC stationary phases used for the separation of glycans are silica based with non-ionic (amide, diol) or ionic (amine, aminopropyl and zwitterionic) functionalities. Due to instability in aqueous solvents, adsorption or reactivity with analytes, bare silica, aminopropyl and amine columns tend to be less suitable for glycan separations [66]. In most of the recent publications use of amide and zwitterionic (ZIC-HILIC) columns is described. Glycans are retained on HILIC stationary phases in native, reduced or fluorescently-labelled forms. The interaction with HILIC stationary phases generally increases with increasing size of the glycan. One of the early strategies included separation of 2-AB labelled glycans using a silica-based stationary phase with amide functionality, coupled with fluorescence detection [67]. The method was shown to be suitable for analysis of neutral and sialylated glycans in a single run, providing information on their correct molar proportions. A dextran ladder was used to determine the elution positions of standard glycans in glucose units and incremental values for addition of monosaccharide residues to the glycan core were calculated. This information was used for interpretation of glycan profiles; and the glycans were confirmed with sequential exoglycosidase digestions [67].

Although this approach has been standardised, it is complex and time-consuming. A large effort has been put into increasing the sample throughput and simplifying the data analysis [68]. A database of 2-AB labelled glycan structures with retention times expressed as glucose units has been established, which shows the correlation between the retention properties and glycan composition, monosaccharide sequence and linkages [46]. The same research group developed an autoGU tool linked to the GlycoBase, which automatically assigns possible glycan structures to each HPLC peak [46]. On the other hand, coupling of HILIC separations with MS might simplify the procedure and provide more direct information about glycan composition. An ultra-high performance liquid chromatography (UHPLC) HILIC column packed with sub 2  $\mu\text{m}$  amide sorbent has recently been used for separation of 2-AB labelled N-glycans and faster analysis with improved resolution compared to standard packing material. The UHPLC column was used for identification of cancer associated alterations in serum glycosylation and correlation between branching, sialylation and galactosylation of serum proteins and progress of the stomach adenocarcinoma was confirmed [69].

An amide HILIC method using optimized sample preparation of 2-AB labelled glycans has recently been evaluated for analysis of N-glycans from recombinant pharmaceuticals. It was demonstrated that the procedure is in accordance with regulatory requirements of the biotechnology industry [70].

The amide HILIC method has also been widely used for the separation of glycans derivatized with 2-aminobenzoic acid (2-AA). The intensity in fluorescence detection is approximately twice as high compared to 2-AB and the reaction can be performed in aqueous medium [71], which makes the label particularly attractive for high-throughput glycosylation analysis [72]. Recently, it has been shown that structural isomers varying in linkage of core fucose can be effectively separated using this method and the structures were confirmed using MALDI TOF/TOF tandem mass spectrometry. A distinctive ion found in CID fragmentation spectra of 2-AA glycans confirmed the presence of allergenic 3-

linked core fucose found in insect and plant glycoproteins. On the other hand, MS/MS analysis of 2-AB labelled glycans did not provide the information on the linkage position [73]. The results indicate that the choice of an appropriate derivatizing agent may provide additional information when coupled to MS/MS.

A similar strategy as described for amide HILIC has recently been used for the separation of 2-AA and 2-AB labelled glycans in mixed mode, combining HILIC and anion-exchange chromatographic mechanisms, and it was termed hydrophilic interaction anion-exchange chromatography (HIAX). The idea is not new [71]; however, the proposed method allowed the use of an external standard to generate GU values for eluted glycans across the entire separation range. Using this it was possible to distinguish neutral from charged species in a single chromatographic run, which was an improvement compared to the generally used HILIC mode [74].

The need for fluorescent labelling can be successfully overcome by downscaling to capillary and nano formats. The amide HILIC method (using a 75  $\mu\text{m}$  I.D. column) was shown to separate underivatized N-glycans at low-femtomole sensitivity when coupled to ESI-MS. Since nano LC systems may exhibit run-to-run variations in elution times, co-chromatography of a dextran ladder may be required to standardise retention times [75]. Nanoscale amide HILIC has recently been coupled to the high resolution Orbitrap mass spectrometer. The method was applied to glycosylation analysis of plasma glycoproteins from healthy controls and cancer patients and two glycans with potential diagnostic value were identified [76]. A similar study was performed using micro amide HILIC [77]. These data suggest that improved sensitivity mainly due to the lower chromatographic dilution in miniaturised HILIC systems may be sufficient for glycan profiling without the need for time-consuming and expensive derivatization with fluorescent tags.

Another widely used stationary phase in glycosylation analysis is zwitterionic-type HILIC (ZIC®-HILIC, Merck SeQuant) with sulfobetaine functional groups. ZIC-HILIC has been used primarily for the separation or enrichment of

glycopeptides [78-80]; however, it has been demonstrated that ZIC-HILIC is also suitable for the separation of AP-labelled glycans and the column exhibited an enhanced capability of structural recognition [38, 80]. Our group recently reported the use of ZIC-HILIC stationary phase for separation of reduced glycans from monoclonal antibodies [81].

Both ZIC-HILIC and amide columns have been successfully coupled into 2D systems with anion-exchange chromatography [65], which shows the potential for improving chromatographic resolution in glycosylation analysis of complex samples.

#### ***1.4.5. Graphitized carbon liquid chromatography***

Porous graphitized carbon (PGC) has been shown to be a suitable stationary phase for separation of glycans from glycoproteins, either from natural sources [82-84] or produced by recombinant technology [37, 85]. Due to the high selectivity of PGC columns for separation of anomers, most of the separations are performed on reduced glycans, coupled with MS. The main advantage of PGC lies in the separation of underivatized glycans, although the method is also compatible with permethylated and fluorescently-labelled glycan forms, recently summarised by Ruhaak et al. [86]. PGC exhibits superior capability for the separation of structural and linkage isomers of high mannose [82] and complex glycans, with various degrees of sialylation [83] and sulfation [85]. Unlike for amide HILIC, currently no databases of retention properties of glycans on graphitized carbon are publicly available. However, a useful approach which included biosynthesis of all possible glycan mono- and disialylated glycan structures using recombinant transferases and establishment of a retention time library has been demonstrated [83]. Using this approach a detailed structural analysis of charged N-glycans from various mammalian sources was performed. It has to be noted that neutral and acidic glycans exhibit significantly different behaviour on graphitized carbon, therefore solvent, temperature and ion polarity have to be chosen accordingly [87]. Sensitivity in glycosylation analysis by PGC

was improved when the system was downscaled to nanoscale format columns and low femtomole quantities of oligosaccharides were detected by ion-trap MS [88]. Nanoscale separation has also been performed by graphitized carbon microchips and coupled with high resolution TOF-MS, which enabled sensitive analysis of glycans from human serum and identification of structures based on high mass accuracy spectra [89]. For the analysis of isobaric structures and studies of linkages, LC techniques exhibit a clear advantage over tandem MS approaches and the development will most certainly continue in both directions.

#### ***1.4.6. Reversed phase chromatography***

Reversed-phase chromatography of oligosaccharides is considered to exhibit orthogonal selectivity to HILIC and the combination of both approaches is commonly used for method evaluation. Glycans generally require derivatization to achieve retention on the RP stationary phases. Labels widely compatible with HILIC, such as 2-AB [90, 91], 2-AP [92] and 2-aminoacridone [93], are generally used in RP analysis of glycans. Analysis of fluorescently-labelled glycans by HILIC and RP, usually in combination with exoglycosidase digestions, is also called 2D chromatography or 2D-mapping [65, 93]. In the case of sialic acids 3D mapping can be employed, with additional separation by anion-exchange chromatography [94]. This approach provides more detailed information compared to the one-dimensional approach; however, it is extremely tedious and therefore is not suitable for routine analysis in glycomics research or quality control of pharmaceuticals. In HILIC, peaks for N-glycans from different classes can overlap, which can be an issue when separation is coupled to fluorescence detection. In contrast, in RP separation N-glycans from different classes are segregated in defined regions of the chromatogram which enables simpler and more accurate quantification [90]. The RP separation of 2-AB labelled N-glycans into classes, sialylated, high mannose, defucosylated complex, tri- and tetraantennary complex, and biantennary complex, has been demonstrated and the method was successfully applied to recombinant antibodies [90]. A high-throughput RP protocol for glycosylation analysis of recombinant glycoproteins,

involving microwave-assisted deglycosylation and labelling with 2-AB has also been recently proposed [91].

Another derivatization procedure for increasing glycan hydrophobicity and thereby allowing RP separation is permethylation. Permethylation was established by Ciucanu and Kerek [95] and it has become extensively used in combination with tandem MS due to the predictable and highly informative fragmentation of permethylated glycans. Permethylation was shown to be compatible with RP on its own or with additional derivatization of glycans with a fluorescent tag [96].

Human Proteome Organisation (HUPO) Human Disease Glycomics/Proteome Initiative (HGPI) conducted a study in collaboration with 20 laboratories, where various chromatographic and MS techniques were evaluated in order to establish technical standards for this complex type of analysis. The N-glycan analysis of the same transferrin and IgG samples performed using chromatography of 2-AB, 2-AA and 2-AP labelled glycans yielded good quantification. Graphitized carbon separation of reduced glycans coupled with ESI-MS in negative ion mode also provided acceptable quantification. The results indicate that both fluorescence and MS-based analysis is suitable for identification and quantification in glycomic studies [97].

#### ***1.4.7. Analysis of glycans by mass spectrometry***

In glycomics, commonly used techniques are MALDI and ESI which allow ionisation of non-volatile substances and are applicable to glycoproteins, glycopeptides and glycans, all of which can be detected at extremely low levels (femtomoles-picomoles) depending on the sample conditions [98].

##### **1.4.7.1. MALDI-MS and ESI-MS in glycosylation analysis**

MALDI was developed primarily for the analysis of macromolecules; however, the method became widely applicable to smaller molecules as well. In a MALDI experiment, the sample is mixed with an excess of a low molecular weight UV-

absorbing matrix which absorbs energy from a laser pulse and the energy is transformed from matrix to the sample. The energy transfer results in desorption of matrix and analyte from the surface and formation of ions in the gas phase. The ions are then electrostatically directed into a mass analyser [98]. MALDI is most commonly coupled with TOF mass analysers which can analyse ions with very high  $m/z$ . Higher resolution can be achieved when quadrupole orthogonal acceleration time-of-flight analysers (QTOF) are used. MALDI is a soft ionisation technique and fragmentation of oligosaccharides is usually low.

Electrospray is also a soft ionisation technique and it is suitable for analysis of a wide range of biomolecules. In principle, an electrolyte-containing analyte solution is pumped through a metal capillary, which is held at high potential. Due to the high electric field, a mist of highly charged droplets is generated. Dry gas and heat are applied to evaporate the solvent. As the droplet size decreases to the extent that surface-coulombic forces overcome surface-tension forces, the droplet breaks up to smaller droplets and the process continues until an ion desorbs from a droplet or solvent is completely removed. The beam of ions is then directed into a mass analyser through a series of lenses [98]. ESI-MS is ideally coupled to separation techniques, such as HPLC, and is usually combined with tandem mass analysers. Fragmentation is generally low and it can be produced by CID where a parent ion is selected by the first mass analyser and the fragment ions are analysed in the second mass analyser. The commonly used analysers are ion traps, triple quadrupole and QTOF instruments.

#### **1.4.7.2. Glycan fragmentation**

Fragmentation of glycans has been studied in fast atom bombardment (FAB)-MS, MALDI-MS and ESI-MS, either for native or derivatized glycans. Similar fragments are observed with all the techniques and they largely depend on the applied energy, type and the nature of the adduct, and lifetime of the ion before reaching the detector [99, 100]. Two major types of cleavages are reported, glycosidic cleavage and cross-ring cleavage (Figure 1–5). The glycosidic cleavage occurs between two rings, whereas the cross-ring cleavage results from breaking



two bonds on the same sugar residue [99]. Glycosidic cleavages predominate and give information on sequence and branching whereas the cross-ring cleavages provide information on linkages [100]. The degree of fragmentation depends strongly on the ion; the protonated species exhibit higher fragmentation than alkali metal coordinated oligosaccharides [101, 102].

Fragmentation can be performed in positive or negative ion mode and both methods provide complementary information. CID fragmentation of positive ions of underivatized N-glycans ionized by ESI showed that more energy was needed to fragment  $[M+Na]^+$  ions than  $[M+H]^+$  [100]. The protonated ions exhibited mainly glycosidic cleavage with main B- and Y-type fragments (Figure 1–6), whereas sodium adducts gave more complicated and informative spectra, also with cross-ring cleavages. The most abundant fragments resulted from loss of the terminal GlcNAc. Other prominent fragments were products of successive additional losses of residues at the non-reducing terminus [100]. CID spectra of oligosaccharides ionized by MALDI showed an additional effect of the matrix on fragmentation. While  $\alpha$ -cyano-hydroxycinnamic acid (CHCA) promoted the glycosidic cleavages, the 2,5-dihydroxybenzoic acid (DHB) promoted also cross-ring cleavages and formation of “internal” cleavage ions, derived from elimination of substituents from around the pyranose ring [103]. Also fragmentation of glycans derivatized with some common labels has been extensively studied. The CID fragmentation mass spectra of 2-AB labelled glycan sodium adducts provided rich information on glycan composition and sequence due to the dominating glycosidic cleavage [104]. As previously mentioned, additional linkage information was obtained from CID glycan spectra when 2-AA tags were used instead of 2-AB [73]. Another advantage of 2-AA over 2-AB is improved sensitivity in negative ion mode, which makes the 2-AA label suitable for analysis of minor species [105]. Recently, a method using a stable isotopic 2-AA tag for rapid direct infusion MS has been reported. Introduction of a stable isotopic tag at the reducing end alleviates the isomeric complexity and allows the segregation between the isomeric reducing and non-reducing end fragment ions [106].

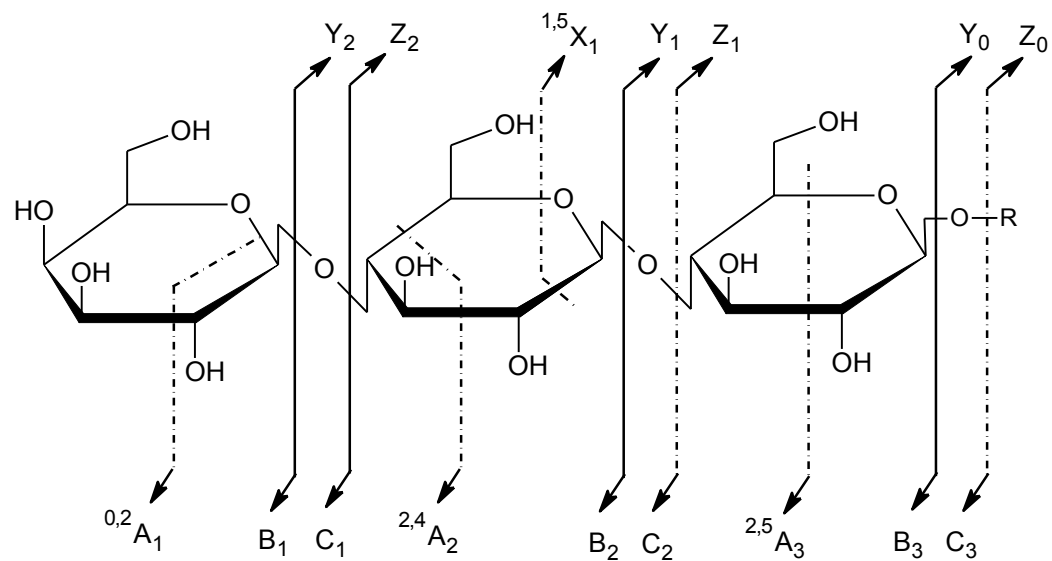


Figure 1-5: Types of carbohydrate fragmentation as proposed by Domon and Costello [99].

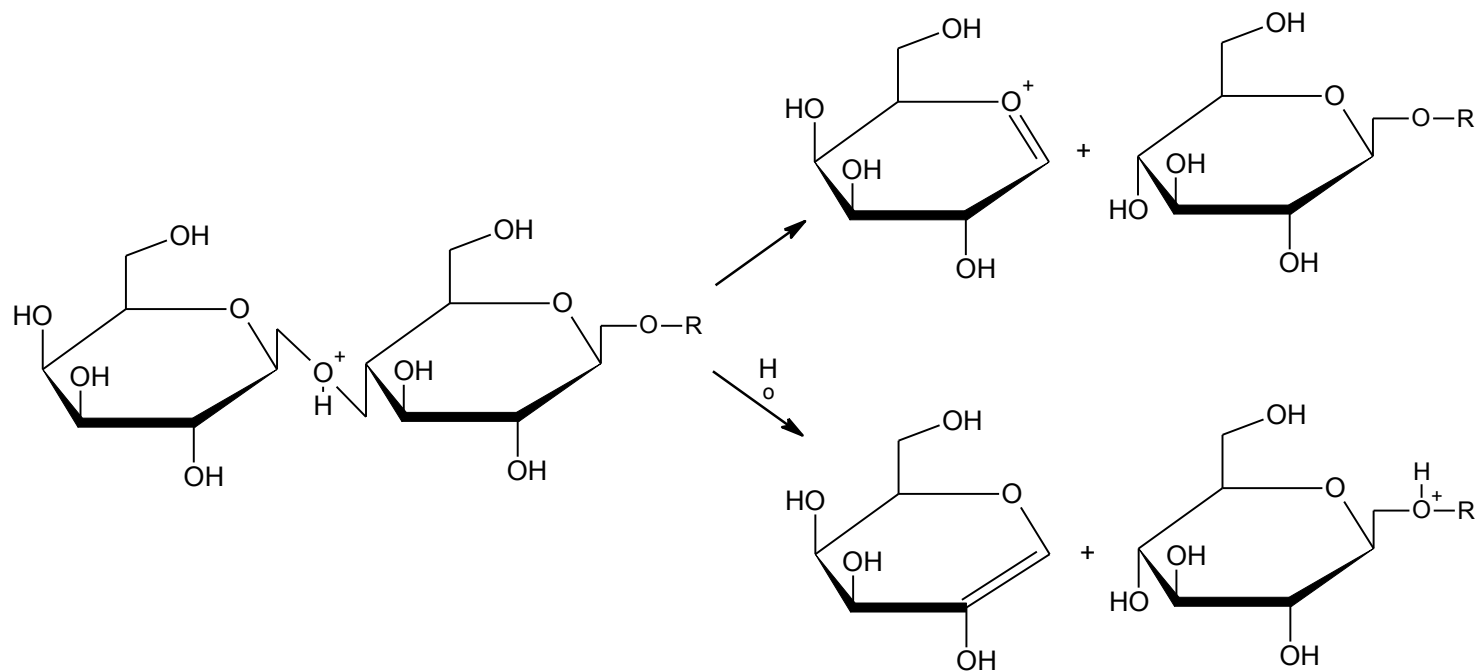


Figure 1-6: Glycosidic bond cleavage-formation of B- and Y-ions adapted from Domon and Costello [99].

Higher quality MS/MS spectra of sodiated adducts compared to protonated species is not the only reason why fragmentation of protonated adducts is generally avoided. It has been reported that fragmentation of protonated N-glycans with fucosylated antennae can lead to migration of fucose between the antennae and it can result in misleading fragments. It was suggested that fucose rearrangements are the result of the decomposition and similar spectra were obtained when ion trap and TOF/TOF mass analysers with very different lifetimes of the ions were used. The same pattern was observed for native and 2-AB labelled glycans; however, the fucose migration was not observed for permethylated glycans [107]. The rearrangement reactions are also known as internal residue loss and have been reported also for hexose residues in high mannose and biantennary complex glycans, either in glycopeptide or reductively aminated forms [108].

When the negative ion mode is used, oligosaccharides readily form  $[M-H]^-$  ions and the corresponding fragments. In the presence of various anions, such as  $SO_4^{2-}$ ,  $Cl^-$ ,  $Br^-$ ,  $I^-$  and  $NO_3^-$  [109-112], stable anion adducts are formed that are transmitted into the collision cell where they form identical fragment ions to those that originate from  $[M-H]^-$  ion, indicating the similar fragmentation mechanism [109]. CID spectra of  $[M-H]^-$  ions and negative adducts generates C-type glycosidic and cross-ring fragmentation, which provides additional information on linkage position. On the other hand, the positive ion mode results mainly in B- and Y-type fragmentations, which are less informative regarding the structure [109, 110, 113]. Fragmentation of negative ions has been studied for glycans in various forms, such as native or 2-AB labelled.

The most widely used approach in tandem MS of glycans includes permethylation and there are several advantages of performing this additional derivatization step, either on native or labelled glycans. Fragment spectra of permethylated glycans are usually more informative, containing extensive cross-ring cleavages, providing details on branching and linkages. An additional advantage of permethylation is stabilization of sialylated glycans which in the

underivatized form easily fragment with the loss of sialic acid. At the same time, permethylation neutralizes negative charges and thus makes the sialylated glycans suitable for analysis in the positive ion mode where higher sensitivity is generally achieved [114]. In the same study it was demonstrated that the specific cross-ring fragments allow distinction between  $\alpha$ 2-3 and  $\alpha$ 2-6 linkages of sialic acid residues. Since permethylation can cause degradation of sialic acids, an alternative approach without derivatization using the negative ion mode fragmentation has also been suggested. It has been shown that permethylation is not necessarily required to distinguish between  $\alpha$ 2-3 and  $\alpha$ 2-6 linkages of sialic acid residues [115].

There has still been a lot of discussion whether MS is suitable for quantitative analysis due to the different ionisation efficiencies for charged and neutral glycans and in-source decomposition of sialic acids. The standard approach for analysis of glycans includes permethylation; however, the harsh conditions used in the procedure can cause partial hydrolysis of sialic acids and is therefore not recommended for quantification of acidic glycans. Several alternative derivatization procedures have been suggested, including methyl esterification and amidation of carboxyl groups. The first method is based on neutralisation of negatively charged groups by methyl esterification without oxidative degradation, followed by derivatization with Girard's reagent T to introduce permanent charge into the molecule. The final product of the reaction gives a simple MS spectrum without additional metal adducts. The quantification of sialic acids by the new method was demonstrated on recombinant therapeutic glycoprotein expressed in two CHO cell lines, giving significantly different glycan profiles [116].

Another approach for quantitative analysis of N-glycans included amidation of acidic glycans, PNGase F digestion, and desalting, using a single-pot approach enabling high-throughput analysis. The new method was based on amidation of sialic acids under mild acidic conditions while the glycan was still attached to the protein. Release of neutral glycans followed by derivatization at the reducing

end resulted in the final products with permanent charges that could be quantitatively analysed by MALDI-TOF [117].

Since correlation between breast cancer and changed ratio of  $\alpha$ 2-3 and  $\alpha$ 2-6 linkages of sialic acid has been observed, a MS method has been developed that enables observing differences in the ratio between the two in healthy and diseased populations. The method is based on selective amidation of  $\alpha$ 2-6 linked sialic acids; while  $\alpha$ 2-3 linked undergo spontaneous lactonization. The glycans are subsequently permethylated and analysed by a MALDI-TOF-MS analysis [118].

When it comes to analysis of structural isomers, sequential mass spectrometry ( $MS^n$ ) can be a valuable tool, especially when MS is not coupled to the prior separation of glycans. Sequential mass spectra can be interpreted manually; however, computational interpretation may be used as an aid and it is believed in the future it might be completely automated [119]. The same strategy has been applied to recognizing and studying differences in metastatic and non-metastatic tumour cells, which demonstrates the potential use of this approach in glycomics studies [120]. Sequential mass spectrometry is useful also in combination with LC techniques where separation of glycan isomers might not be achieved [92].

## Chapter Two

### ***2. Hydrophilic interaction liquid chromatography of glycans***

#### **2. 1. Introduction**

Immunoglobulin G (IgG) is the most abundant immunoglobulin and it is generally responsible for recognition of pathogens and toxic antigens and their subsequent neutralization and elimination through activation of biologic effector mechanisms. Monoclonal IgGs represent a rising group of pharmaceuticals and their potency, stability and immunogenicity largely depend on their post-translational modifications, especially N-glycosylation in the conserved domain. The N-glycans are generally of biantennary complex type, most of them core-fucosylated [10] and variations in structure, such as defucosylation and sialylation, can have great effect on the biological activity of a product [25, 27]. Therefore, the glycan profiling of IgGs of pharmaceutical interest is of high importance. However, rapid glycosylation profiling of large numbers of samples for quality control and clone selection remains a challenge [32].

Standard procedures for glycan analysis include in-solution digestion of glycoprotein samples with PNGase F, thus releasing the glycans from the glycoprotein. Following this step, the most common strategy for analysing enzymatically-released glycans from antibodies and glycoproteins generally includes labelling at the reducing end of oligosaccharides followed, by liquid chromatography (LC), combined with either fluorescence or MS detection. Labelling of glycans for fluorescence detection is most commonly achieved via reductive amination with aromatic amines, such as 2-aminobenzamide (2-AB), 2-anthranilic acid (2-AA) or 2-aminopyridine (AP) [43, 45]. As well as enabling fluorescence detection, pre-column derivatization, such as fluorescent labelling or permethylation, is also usually required to improve chromatographic

resolution, sensitivity in ESI-MS and formation of fragment ions which provide additional structural information [66, 121].

Separations of oligosaccharides derived from glycoproteins have been achieved using a range of stationary phases including reversed-phase (RP), HILIC and graphitized carbon, each coupled with MS or fluorescence detection [32]. The use of graphitized carbon columns has recently been shown to be very promising for glycan analysis, showing improved performance in the separation of isomeric oligosaccharides, usually in the reduced or fluorescently-labelled form [37, 82]. These methods mostly use MS, rather than fluorescence detection. A minor disadvantage of this approach is that the use of graphitized carbon columns for reducing glycans usually results in an undesirable separation of anomers.

A widely used method for analysis of protein glycosylation is HILIC using TSK amide-80 columns (Tosoh biosciences) in combination with fluorescence detection of 2-AB labelled glycans. Acetonitrile-water gradients with volatile buffers are used for elution, which makes the method compatible with MS. In general, the retention of oligosaccharides increases with the increasing number of sugar residues and a dextran ladder which enables measuring retention relative to glucose units is commonly used for identification of oligosaccharides. Improved sensitivity can be achieved by down-scaling to a 75  $\mu\text{m}$  internal diameter TSK Amide-80 column and coupling on-line with nano-ESI-MS [75]. As nano LC systems often exhibit poor reproducibility in retention times, co-chromatography of a 2-AB labelled glycan ladder and 2-AB labelled samples may be required using this approach [75]. Alternatively, HILIC amide columns can also be used for the separation of unlabelled glycans [77], although this approach is less common.

Recently, as an alternative to amide HILIC columns, the use of ZIC-HILIC columns with sulfobetaine groups has been reported for the separation of sialylated AP-derivatized N-glycans and N-glycopeptides [38, 80]. These columns have been shown to be capable of structural recognition and allow



better separation of AP-glycan structural isomers compared to amide columns [32].

Since MALDI-MS and ESI-MS commonly do not fragment oligosaccharides, they are the most suitable approaches for the MS analysis of complex mixtures of glycans. Native neutral glycans are commonly detected with the best sensitivity in the positive ion mode and sialylated glycans are best detected in the negative ion mode [98]. The 2-AB labelled oligosaccharides are usually detected in the positive ion mode as sodium adducts [98], although detection in the negative ion mode has some advantages, such as higher stability of fucose linkages and various possible cross-ring fragmentations which give additional structural information [113].

In this chapter, the use of a ZIC-HILIC column for the simple analysis of 2-AB labelled, native and reduced glycans from monoclonal antibodies is demonstrated. These new methods have been compared to a standard method commonly used in the pharmaceutical industry. Using a ZIC-HILIC column demonstrates several advantages and is shown to have the capability of structural recognition of reduced oligosaccharides, a feature that is similar to graphitized carbon columns.

## **2.2. Materials and methods**

### ***2.2.1. Reagents and chemicals***

Unless otherwise noted, all chemicals were of analytical grade. Acetonitrile was obtained from VWR International (Poole, UK). Acetic acid, ethanol, 2-aminobenzamide labelling kit, ribonuclease B (R7884), sodium borohydride, mannose 3 glycan, mannose 9 glycan, maltopentaose, maltohexaose and maltoheptaose were obtained from Sigma (St. Louis, MO, USA). Formic acid, ammonium hydroxide and ammonium bicarbonate were obtained from Fluka (Steinheim, Germany).

Samples of MAbs prepared by recombinant DNA technology (denoted as MAb1, MAb2 and MAb3) were kindly donated by Pfizer Inc. (St. Louis, MO, USA).

### ***2.2.2. Sample preparation***

Glycoprotein samples were desalted prior to digestion using centrifugal filter units (Amicon Ultra, 10.000 MWCO, Millipore, Carrigtwohill, Ireland). Glycans were released from glycoproteins (250 µg) by incubation with 3 µL of PNGase F (500 units/mL, from *Elizabethkingia meningoseptica*; Sigma) per 100 µL of 50 mM ammonium bicarbonate buffer, pH 8.0, overnight at 37 °C. Proteins were removed by precipitation with 400 µL of ice-cold ethanol. Dried supernatants were stored at -20 °C for further analysis, labelling with 2-AB or reduction with sodium borohydride. 2-AB labelled glycans were prepared by following the protocol provided by the manufacturer and reconstituted in 100 µL of water prior to analysis. The dried samples were reduced by adding 20 µL of 0.5 M sodium borohydride in 50 mM sodium hydroxide and incubating at room temperature overnight. The samples were then acidified by adding 5 µL of glacial acetic acid and desalted by ion-exchange chromatography (Dowex MR-3 mixed bed, Sigma).

### ***2.2.3. Amide HILIC coupled with fluorescence detection***

The glycans released from the MAbs were derivatized with 2-AB to enable fluorescence detection. Glycan profiling in HILIC mode with fluorescence detection was performed on a Waters 2690 Separation Module equipped with a Waters 474 Scanning Fluorescence detector (Waters, Milford, MA, USA). The excitation wavelength was set at 330 nm and the emission wavelength at 420 nm. The column used was a TSK Gel Amide-80 (4.6 x 250 mm, 5 µm) from TOSOH Bioscience (Tokyo, Japan). Eluent A consisted of acetonitrile and Eluent B of 250 mM ammonium formate, pH 4.4. Eluent flow-rate was 0.4 ml/min and the column oven temperature was thermostated to 30 °C. Elution was achieved using a binary step gradient from 70 to 60% Eluent A from 0-90 min, followed by a linear gradient 60 to 5% A from 90-140 min, finally reaching 0% A at 145 min.

The eluent composition was thereafter returned to 70% A in 1 min and the system re-equilibrated for 14 min. 25  $\mu$ L of the sample was injected onto the column.

#### ***2.2.4. ZIC-HILIC of 2-AB labelled glycans***

The glycans released from the MAbs and the RNase B were derivatized with 2-AB. Glycan profiling with fluorescence detection was performed on a Waters 2690 Separation Module equipped with thermostated column compartment and a waters 474 Scanning Fluorescence detector (Waters, Milford, MA, USA). The excitation wavelength was set at 330 nm and the emission wavelength at 420 nm. Separations were performed with SeQuant™ ZIC®-HILIC column (2.1 x 150 mm, 3.5  $\mu$ m) from Merck SeQuant (Umeå, Sweden). Eluent A consisted of acetonitrile and eluent B from 17 mM acetic acid, pH 3.25. The flow-rate was 0.3 ml/min and the column oven temperature was thermostated to 30 °C. 2-AB glycans were eluted using gradient elution, starting with a 10 min isocratic step at 20% B, followed by a linear gradient from 20 to 30% B in 50 min, followed by a wash step at 80% B for 5 min. Prior to the next injection, the system was equilibrated for 15 min at 80% B. The sample was reconstituted in 100  $\mu$ L of deionised water and 5  $\mu$ L of the sample was injected onto the column. Glycan profiling with ESI-MS detection was performed using a MicrOTOF-Q™ (Bruker Daltonik, Bremen, Germany) with an Agilent 1200 series binary pump and autosampler (Agilent, Santa Clara, CA, USA) with the column installed in a column oven (Thermosphere, TS-130, Phenomenex, USA) operated at 30 °C. Gradient conditions were the same as described for the fluorescence detection. The ESI-MS conditions were: capillary voltage, 4.5 kV; drying gas temperature, 200 °C; drying gas flow, 8 L/min; nebulizer pressure, 1.5 bar; scan range m/z 50-3000.

#### ***2.2.5. ZIC-HILIC of native and reduced glycans***

Experiments were performed using a MicrOTOF-Q™ (Bruker Daltonik, Bremen, Germany) with an Agilent 1200 series binary pump and autosampler (Agilent,

Santa Clara, CA, USA). Separations of glycans released from RNase B and MAbs were performed with SeQuant™ ZIC®-HILIC column (2.1 x 150 mm, 3.5 µm; Merck SeQuant, Umeå, Sweden) installed in a column oven (Thermosphere, TS-130, Phenomenex, USA) at 30 °C. The flow-rate was 0.3 mL/min. Eluent A consisted of acetonitrile and eluent B of 34 mM acetic acid, pH 3.0. Native and reduced glycans were eluted using gradient elution starting at 90% A, a linear gradient 90 to 75% A from 0 to 10 min, followed by a linear gradient 75-70% from 10 to 80 min and a linear gradient 70-40% A from 80 to 100 min, followed by an isocratic step at 40% A for 5 min. At 106 min the eluent composition was returned to 90% A and the system equilibrated for 14 min. Separation of linear oligosaccharides maltopentaose, maltohexaose and maltoheptaose was performed using the same eluents as for RNase B and MAbs glycans. The flow-rate was set at 0.3 mL/min. Reducing oligosaccharides were eluted using a linear gradient 90 to 35% A from 0 to 20 min, followed by an isocratic step at 35% A for 5 min. At 26 min the eluent composition was returned to 90% A and the system equilibrated for 14 min. Acquisition of mass spectra was performed in the positive ion mode. The ESI-MS conditions were: capillary voltage, 4.5 kV; drying gas temperature, 200 °C; drying gas flow, 8 L/min; nebulizer pressure, 1.5 bar; scan range m/z 50-3000.

## 2.3. Results and discussion

### 2.3.1. Separation of 2-AB-glycans using amide HILIC

One of the most commonly used procedures for the analysis of glycans in the pharmaceutical industry is to label glycans with 2-AB followed by separation of labelled glycans using a HILIC column with amide functionality, coupled with fluorescence detection. Peaks are usually assigned based on the retention times of 2-AB labelled standards; however, standards for low abundance glycans are not commercially available and collection of fraction with offline MS analysis may be required for identification when less common glycan species are present in a sample.

RNase B and monoclonal antibodies MAb1, MAb2 and MAb3 used in this study were digested using the enzyme PNGase F and the released glycans were labelled with 2-AB and analysed by the standard procedure, using an Amide-80 column and fluorescence detection. Glycan profiles obtained by this standard procedure were used for comparison with the new methods for analysis of 2-AB labelled, native and reduced glycans separated on the ZIC-HILIC column coupled with fluorescence and ESI-MS.

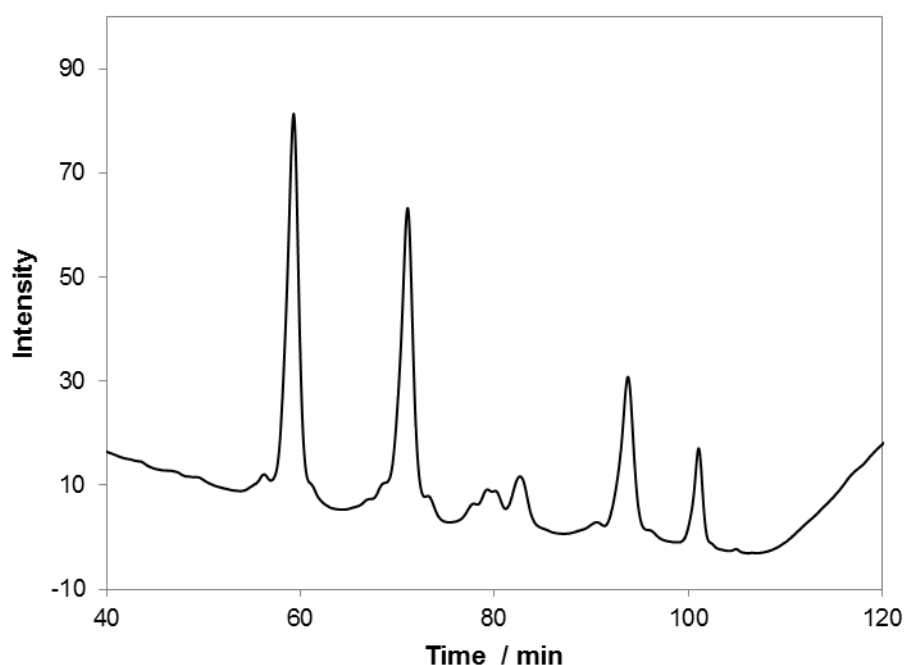
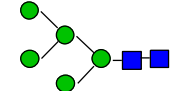
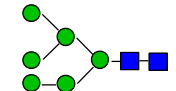
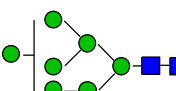
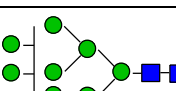
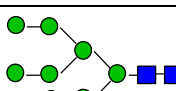


Figure 2-1: Separations achieved on an Amide-80 column with fluorescence detection of 2-AB labelled glycans released from RNase B. Man5-Man9 glycans were identified; the retention time increases with the increasing molecular weight of glycans. Man7 structural isomers were partially separated. Gradient elution: mobile phase A-acetonitrile; mobile phase B-250 mM ammonium formate, pH 4.4.

Table 2-1: Relative quantification of high mannose glycans from RNase B obtained by Amide-80 column coupled with fluorescence detection.

Structure	Abbr.	Retention time [min]	Relative peak area [%]
	Man5	64.8	37.4
	Man6	77.4	28.0
	Man7	84.5 86.2 89.4	2.3 4.4 5.0
	Man8	100.5	16.6
	Man9	104.7	6.3

■ GlcNAc; ● mannose

RNase B is a relatively simple and well-studied glycoprotein, which contains high mannose oligosaccharides with 5 to 9 mannose residues. Peaks in the fluorescence chromatogram of RNase B glycans can be assigned based on the general rule in HILIC that elution time increases with the size of the glycan. As illustrated in Figure 2-1, between 75 and 84 min a cluster of partially separated peaks can be observed, which most likely correspond to partial separation of Man7 structural isomers. As expected, all glycans Man5 to Man9 were found in the RNase B glycan profile, with relative % areas summarised in Table 2-1.

Figure 2-2 shows glycan profiles of the different MAbs studied in this work, obtained by the standard procedure. The observed glycosylation patterns are consistent with glycosylation expected in mammalian expression systems, containing mainly fucosylated biantennary complex glycans, G0 (45.6-84.8% relative area), G1 (11.3-33.4%), G0-GlcNAc (2.4-3.1%) and G2 (0.7-5%).

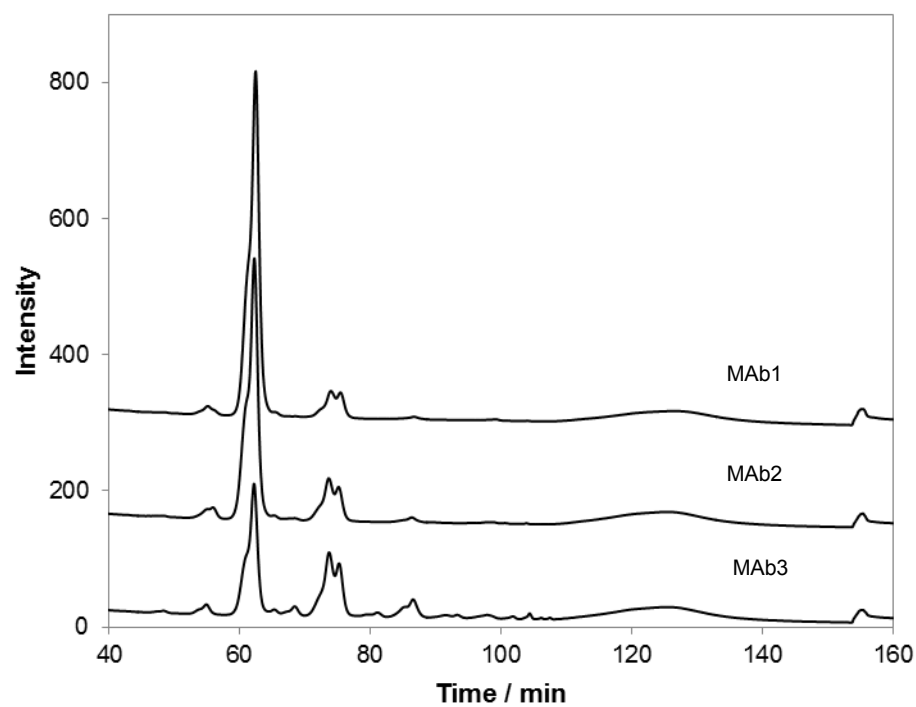
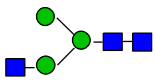
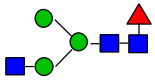
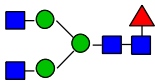

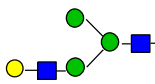
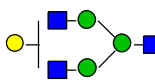
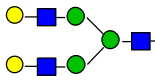
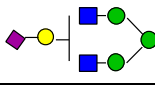


Figure 2-2: Separations achieved on an Amide-80 column with fluorescence detection of 2-AB-labeled glycans released from MAbs. The retention time increases with the increasing molecular weight of glycans. The main glycan species in all the MAbs are G0, G1 and G2. Glycosylation pattern of MAb3 is different to those for MAb1 and MAb2, containing numerous peaks in the elution range of negatively charged complex glycans. Gradient elution: mobile phase A-acetonitrile; mobile phase B-250 mM ammonium formate, pH 4.4.

Table 2-2: Relative quantification of glycoforms from the monoclonal antibodies obtained by Amide-80 column coupled with fluorescence detection.

Glycan	Structure	% Area		
		MAb1	MAb2	MAb3
Unknown				<0.2
G0-Fuc-GlcNAc		<0.2	<0.2	0.5
G0-GlcNAc		2.4	3.7	3.1
G0		84.8	74.0	45.6
Man5		0.5	0.8	1.4
Unknown			<0.2	
G1-GlcNAc		<0.2	0.4	2.7
G1		6.8	12.1	21.5
		4.5	6.6	11.9
Unknown				0.3
Unknown				0.9
Unknown				2.4
G2		0.7	1.5	5.0
Unknown				0.9
Unknown				0.6
Unknown			<0.2	
Unknown				1.3
G1+NANA		<0.2		
Unknown				0.5
Unknown			<0.2	
Unknown		<0.2	<0.2	0.9
Unknown				<0.2
Unknown				<0.2

■ GlcNAc; ▲ fucose; ● mannose; ● galactose; ◆ NeuAc



The peaks have been identified based on the retention times, since the procedure is standardised. Some minor species, such as Man5, G0-GlcNAc, G1-GlcNAc can also be identified, but they all represent less than 1% of the total peak area. It was not possible to identify peaks with less than 0.2% of the total peak area (Table 2-2) and under these experimental conditions G1 structural isomers were only partially separated. MAb3 was shown to be significantly different to MAb1 and MAb2, containing a wide range of minor glycans that could not be identified by the standard procedure. The difference between these MABs is expected, since MAb1 and MAb2 were expressed in Chinese hamster ovary (CHO) cell lines and MAb3 was expressed in murine NS0 cell line. The major differences in galactosylation and sialylation have been reported for the two cell lines [15, 18] which can also contribute to the immunogenicity of the drugs in humans [19, 20]. It is reasonable to expect that antibodies expressed in similar systems would present similar glycan profiles to these MABs.

Despite the high sensitivity of the fluorescence detection and the commercial availability of labelling kits, there are several limitations to this procedure. Fluorescent labelling is expensive and time-consuming, especially when large numbers of samples are analysed. Furthermore, fluorescence detection does not provide direct information about the structure of glycans and a single chromatographic run the using standard procedure requires nearly 3h. Therefore, a new approach was investigated for the separation of 2-AB labelled, native and reduced glycans from MABs using a HILIC column with zwitterionic functionality (ZIC-HILIC), coupled with fluorescence and ESI-MS detection.

### **2.3.2. ZIC-HILIC**

#### **2.3.2.1. Separation of 2-AB labelled glycans**

A HILIC column with zwitterionic functionality (ZIC-HILIC) which was previously shown to separate glycopeptides and 2-aminopyridine labelled glycans [38, 78, 80] was tested for separation of 2-AB labelled glycans from RNase B and monoclonal antibodies. ZIC-HILIC was coupled to fluorescence

detection to achieve optimum sensitivity and for relative quantification of glycans. The ZIC-HILIC was further coupled with ESI-MS for identification of glycans previously observed using fluorescence detection.

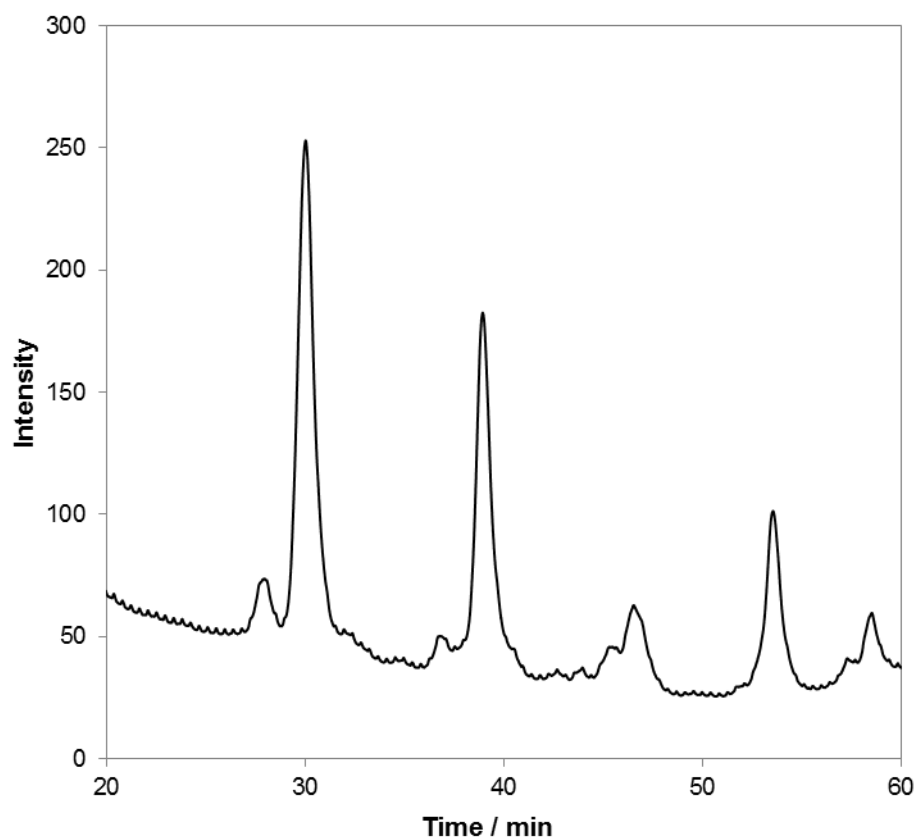


Figure 2-3: Fluorescence chromatogram of 2-AB labelled RNase B glycans. Additional peaks that correspond to 2-AB labelled high mannose glycans cleaved by Endo H are observed in fluorescence chromatogram and they were eluted before the PNGase F released glycans with the same number of mannose residues.

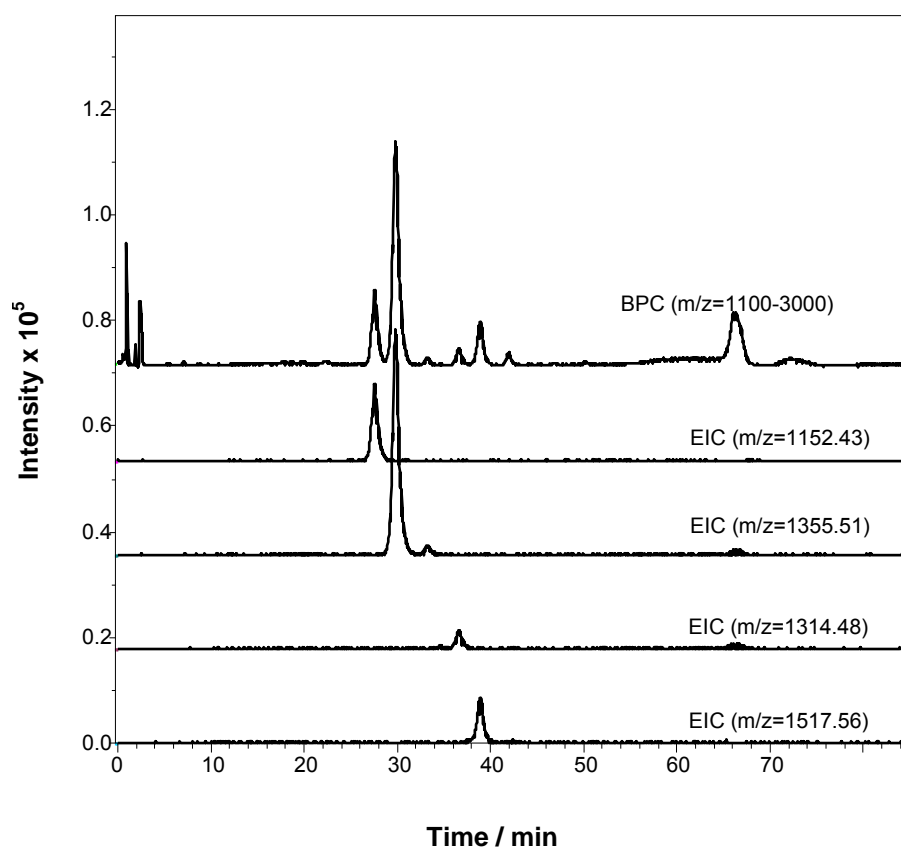


Figure 2-4: Separation of 2-AB labelled glycans from RNase B using ZIC-HILIC coupled with ESI-MS. Base peak chromatogram (BPC) in mass range from 1100 to 3000 and extracted ion chromatograms (EIC) of singly protonated Man5-GlcNAc, Man5, Man6-GlcNAc and Man6. Width for selected chromatogram traces was  $\pm 0.03$  Da.

Figure 2–3 shows a fluorescence chromatogram of RNase B obtained using ZIC-HILIC column and considering the most likely HILIC separation mechanism, the expected retention time would increase with increasing molecular weight of glycans. Compared to the amide HILIC column, several additional smaller peaks were observed in the ZIC-HILIC chromatogram, that were eluted before the main peaks of Man5-Man9 glycans. It is assumed that some of the glycans that are clearly resolved in the ZIC-HILIC chromatogram, co-eluted when HILIC amide was used as a stationary phase. The structures of 2-AB labelled glycans were further characterised using ZIC-HILIC coupled with ESI-MS (Figure 2–4). This confirmed the proposed order of elution, where larger glycans were more strongly retained by the ZIC-HILIC stationary phase. The retention times with relative peak areas and proposed structures as discussed below are summarised in Table 2-3. With ESI-MS only Man5 and Man6 were identified, observed as the singly protonated ions. However, sensitivity in ESI-MS was lower compared to the fluorescence detection, which resulted in the loss of signals for Man7, Man8 and Man9 glycans. Due to the correlation between relative quantitative data obtained by amide HILIC and ZIC-HILIC coupled with fluorescence, the proposed peak assignment is as shown in Table 2-3.

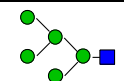
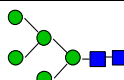
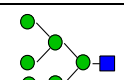
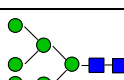
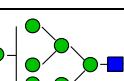
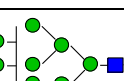
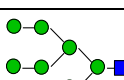
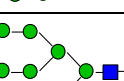
Additional peaks, previously not observed by HILIC-amide/fluorescence, were found in the fluorescence chromatogram of RNase B and were eluted before the high mannose glycans. Using ESI-MS, they were identified as truncated high mannose glycans, lacking a core GlcNAc. Truncated glycans are common degradation products of enzyme Endoglycosidase H (Endo H), which has specificity for high mannose glycans and hydrolyses the bond between the core GlcNAcs. It is suggested that contamination with Endo H was present in the PNGase F. When HILIC with an amide type column was used, the truncated glycans were most likely co-eluted with the main glycan products of cleavage by PNGase F, which explains the bad peak shapes in the fluorescence chromatogram (Figure 2–1). The ZIC-HILIC column exhibited enhanced resolving power for 2-AB labelled high mannose glycans compared to the HILIC

amide-80, resulting in the complete separation of various products of PNGase F and Endo H degradation in the shorter chromatographic run.

The ZIC-HILIC column was also used for separation of 2-AB labelled glycans from monoclonal antibodies. A binary gradient consisting of acetonitrile and an aqueous solution of acetic acid was used for elution in order to make the method compatible for on-line coupling with ESI-MS. Fluorescence chromatograms of MAb1, MAb2 and MAb3 are shown in Figure 2-5 to Figure 2-7, with relative quantification data summarised in Table 2-4. The peaks were assigned based on the ESI-MS results described below.

Some differences were observed when ZIC-HILIC was compared to the results obtained by the amide HILIC method. The selectivity of ZIC-HILIC for 2-AB labelled glycans was different to amide HILIC, with Man5 being eluted before G0. G0-Fuc glycan species was identified in MAb1 and MAb2 samples, which was not previously seen by using the amide HILIC column. G0-Fuc and Man5 glycans were not fully resolved. The loss of separation could be due to the large dead volume after the column, mainly contributed by the tubing and the flow-cell (16  $\mu$ L) of the fluorescence detector. The peaks could appear as only partially separated if the data acquisition rate was not sufficient (0.25 points/s). Due to the peak overlapping, the relative peak areas of minor glycans are approximate and correlation between amide HILIC and ZIC-HILIC for the major glycan species is satisfactory. Differences in relative quantification could be mainly contributed by co-elution of glycans. Several minor glycans were observed in MAb samples when LC was coupled with fluorescence, but these could not be identified by ESI-MS due to lower sensitivity. A lower number of peaks was observed using ZIC-HILIC compared to the HILIC amide standard method. This could be explained by incomplete separation of 2-AB glycans using ZIC-HILIC and therefore minor species were hidden in the broad peaks of major glycan species. However, it has to be emphasized that a lower sample amount was injected onto the ZIC-HILIC column than the amide HILIC column, which could contribute to the lower number of observed peaks.

Table 2-3: Relative quantification of glycoforms from the RNase B obtained by ZIC-HILIC column coupled with fluorescence detection. Theoretical m/z of most likely ions to be found by ESI-MS are listed in the table. The Man5, Man5-GlcNAc, Man6 and Man6-GlcNAc were confirmed by ESI-MS.

	Glycan	Structure	(m/z) <sub>theoretical</sub> , 2-AB [M+H] <sup>+</sup> [M+2H] <sup>2+</sup>	Ions found	Retention time / min	Relative peak area / %
(Man) <sub>2</sub> (Man) <sub>3</sub> (GlcNAc) <sub>1</sub>	Man5-GlcNAc		1152.43 576.72	[M+H] <sup>+</sup>	27.9	10.8
(Man) <sub>2</sub> (Man) <sub>3</sub> (GlcNAc) <sub>2</sub>	Man5		1355.51 678.26	[M+H] <sup>+</sup>	30.0	35.0
(Man) <sub>3</sub> (Man) <sub>3</sub> (GlcNAc) <sub>1</sub>	Man6-GlcNAc		1314.48 657.74	[M+H] <sup>+</sup>	36.7	4.6
(Man) <sub>3</sub> (Man) <sub>3</sub> (GlcNAc) <sub>2</sub>	Man6		1517.56 759.28	[M+H] <sup>+</sup>	38.9	22.6
(Man) <sub>4</sub> (Man) <sub>3</sub> (GlcNAc) <sub>2</sub>	Man7		1679.61 840.31		45.3 46.5	9.5
(Man) <sub>5</sub> (Man) <sub>3</sub> (GlcNAc) <sub>2</sub>	Man8		1841.67 921.34		53.5	10.7
(Man) <sub>6</sub> (Man) <sub>3</sub> (GlcNAc) <sub>1</sub>	Man9-GlcNAc		1800.64 900.82		57.3	2.1
(Man) <sub>6</sub> (Man) <sub>3</sub> (GlcNAc) <sub>2</sub>	Man9		2003.72 1002.36		58.5	4.6

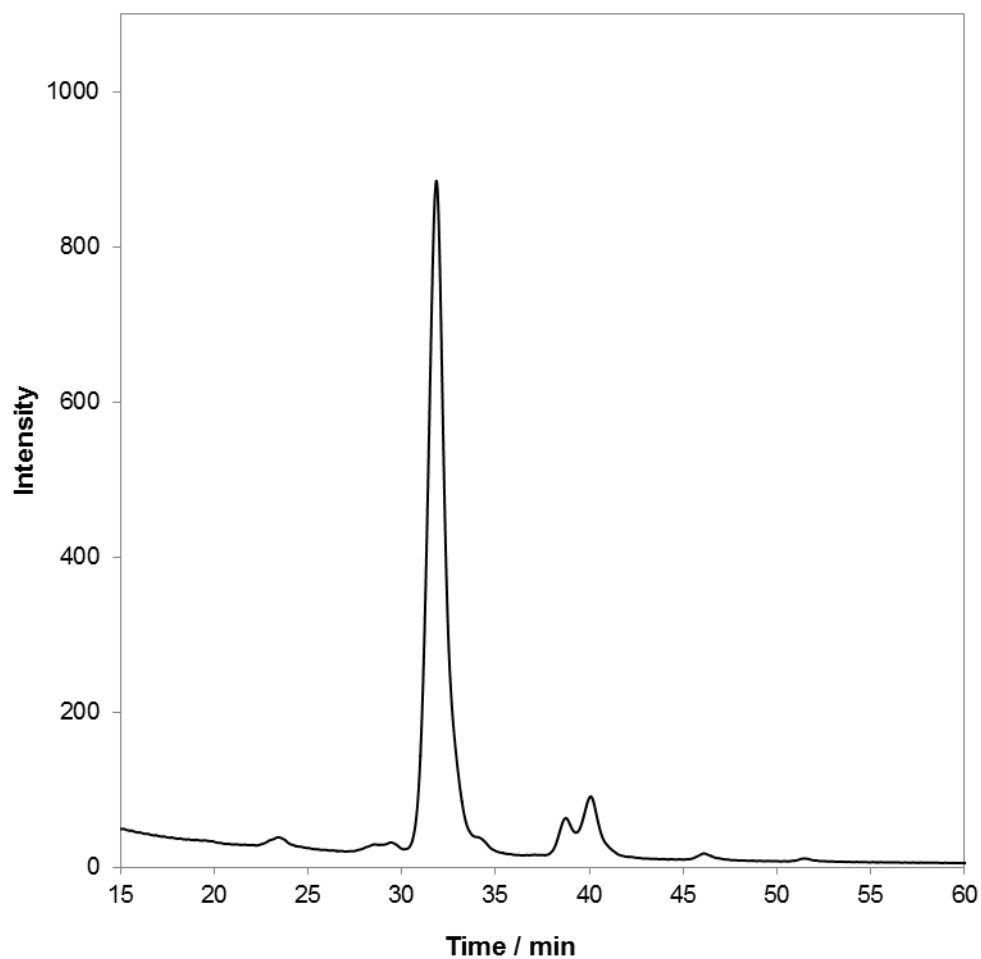


Figure 2-5: Fluorescence chromatogram of 2-AB labelled glycans from MAb1. Gradient elution: mobile phase A-acetonitrile; mobile phase B-17 mM acetic acid, pH 3.25. The chromatogram confirmed the high degree of fucosylation and low level of galactosylation in MAb1 as expected for the MAb expressed in CHO cell line.

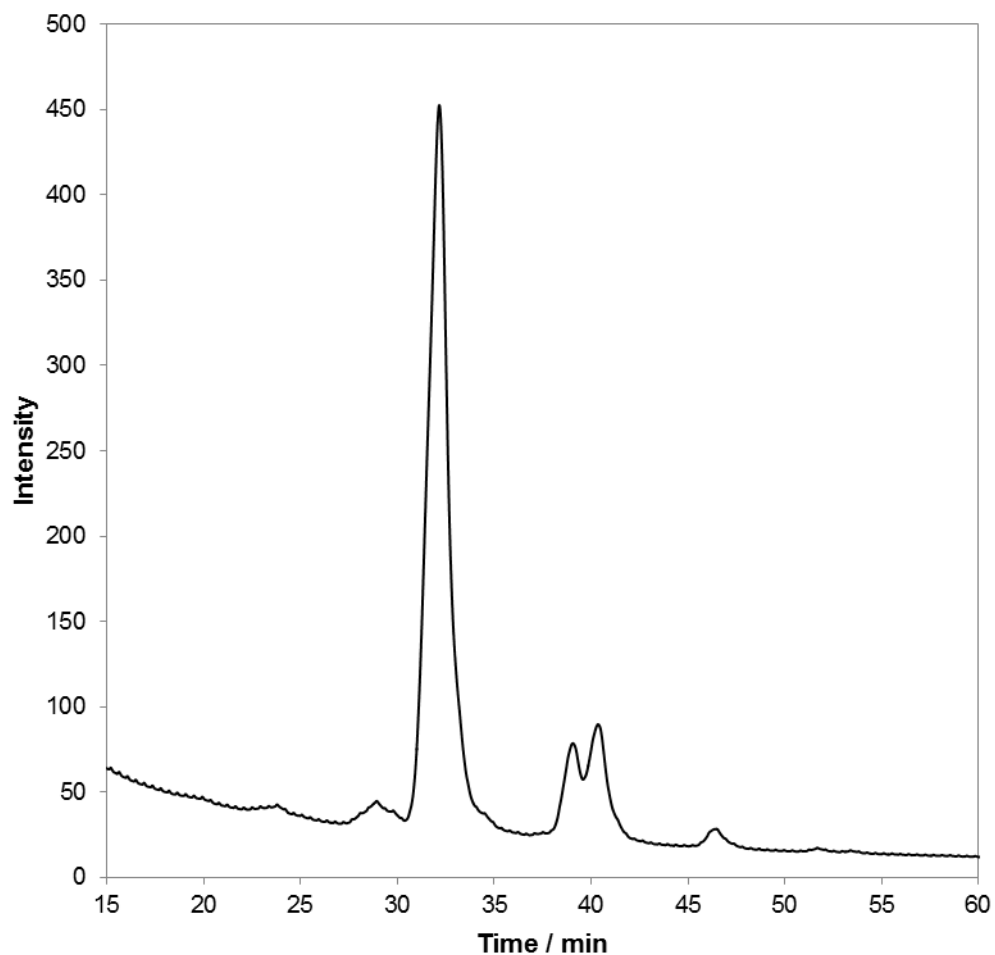


Figure 2–6: Fluorescence chromatogram of 2-AB labelled glycans from MAb2. Gradient elution: mobile phase A-acetonitrile; mobile phase B-17 mM acetic acid, pH 3.25. Similarly as for MAb1, a high content of fucosylated species with low degree of galactosylation was observed in the MAb2 glycan profile.



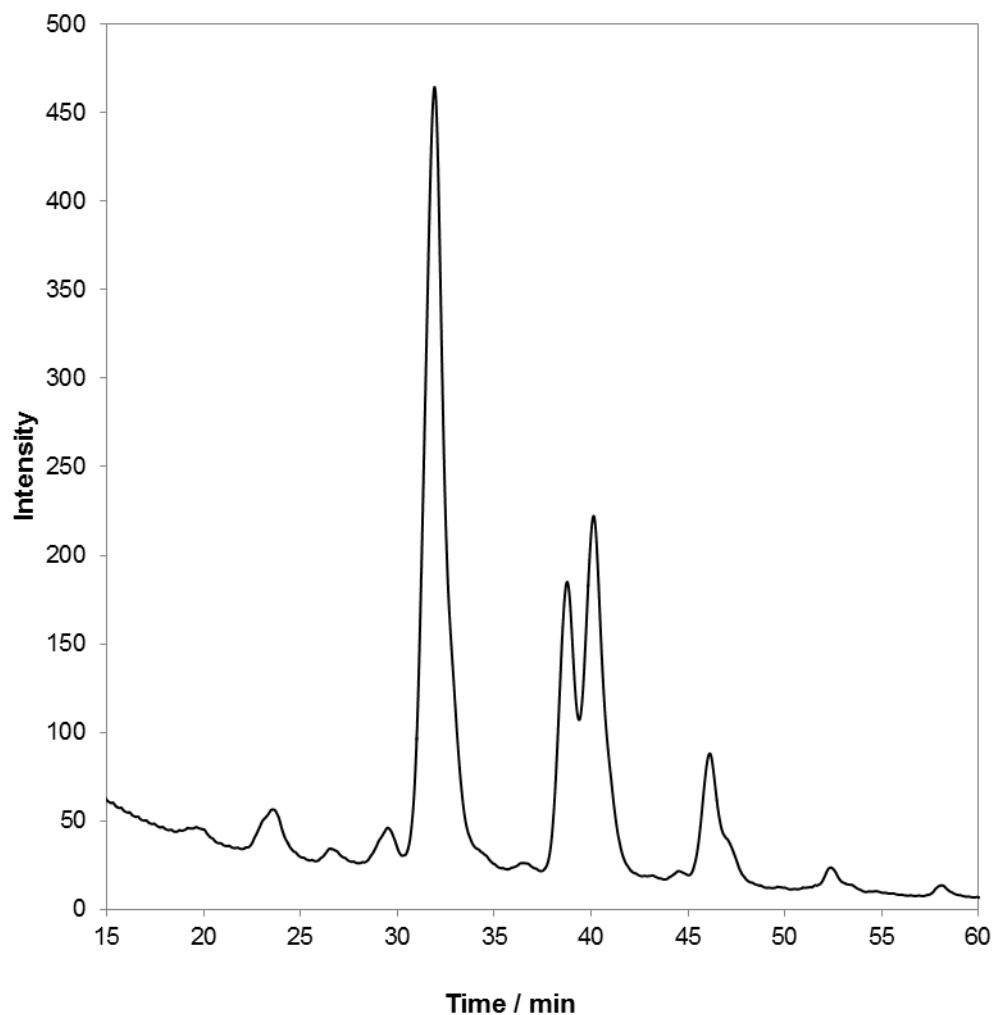


Figure 2-7: Fluorescence chromatogram of 2-AB labelled glycans from MAb3. Gradient elution: mobile phase A-acetonitrile; mobile phase B-17 mM acetic acid, pH 3.25. Mab3 exhibited higher degree of galactosylation compared to MAb1 and MAb2. Multiple unassigned peaks were observed, indicating more complex glycan profile, as previously confirmed by amide HILIC.

Table 2-4: Relative quantification of glycoforms from the monoclonal antibodies obtained by ZIC-HILIC coupled with fluorescence detection.

Glycan	Structure	% Area		
		MAb1	MAb2	MAb3
G0-GlcNAc-Fuc				0.4
G0-GlcNAc		4.1	<0.2	2.9
Unknown				0.62
G0-Fuc		1.6	0.9	
Man5		1.3	<0.2	1.9
G0		80.2	79.4	49.8
Unknown				0.4
Unknown		1.5		
G1		3.4	7.3	13.7
		7.0	10.9	21
Unknown				<0.2
G2		0.7	1.0	8.0
Unknown		0.2	<0.2	
Unknown				0.7
Unknown				0.4

Reproducibility of retention times and peak intensities was good when the same sample was injected consecutively. A relative standard deviation of retention times of approximately 0.5-1.1% was observed between different samples (not shown), with the difference increasing with the increasing retention time. It is assumed that some of the components in the original formulations of monoclonal antibodies were not fully removed during the sample preparation and they interfered with the column chemistry. The issue regarding sample additives will be further discussed later in the section on separation of 2-AB labelled glycans using ZIC-HILIC coupled with ESI-MS.

The ZIC-HILIC separation was further coupled to ESI-MS for structural assignment of peaks obtained by ZIC-HILIC/Fluorescence. The MS chromatograms are shown in Figure 2-8 to Figure 2-10. The main ion species for all the identified glycans were singly protonated and sodiated ions (not shown). Slightly lower sensitivity compared to the fluorescence detection was achieved; however, all main glycans that were previously observed by the amide HILIC have been identified and they are summarised in Table 2-5. Furthermore, besides G0-Fuc, two other previously unobserved glycan species were identified (Table 2-5), with the compositions  $(\text{Hex})_2(\text{HexNAc})_1(\text{Man})_3(\text{GlcNAc})_2$  and  $(\text{Hex})_2(\text{HexNAc})_1(\text{dHex})_1(\text{Man})_3(\text{GlcNAc})_2$ . Three possible structures could be assigned to both observed  $m/z$  values; one complex structure with  $\alpha$ -galactosylation on the 3-arm, and two hybrid type structures with one or two mannose units on the 6-arm. For the  $m/z$  1704.65 two peaks were found, however it was not possible to elucidate the structure for the two peaks and three possible structures were proposed for the observed  $m/z$ . For the early eluted peak only singly charged  $[\text{M}+\text{H}]^+$  ion was observed, whereas for the late eluted peak singly and doubly protonated species were found. All proposed structures would be possible to find in MAbs expressed in murine NS0 cell line [18]; however, the obtained data do not provide enough information to conclude which structure is correct.

In MAb1 and MAb2 samples, two peaks have been observed for G0-GlcNAc-Fuc chromatogram trace ( $m/z=1234.48$ ), which could be due to the separation of structural isomers. Using the GlycoSuite database of glycan structures, two likely structures were found, with GlcNAc attached to 3- or 6-arm of the glycan core; however, the confirmation and structural elucidation with the existing data are not possible. Interestingly, for MAb3 only one G0-GlcNAc-Fuc peak was observed, which might suggest that the difference in glycosylation pattern was due to the different expression systems of these MAbs.

The main advantage of the new ZIC-HILIC method compared to the standard HILIC procedure is shorter analysis time, which was reduced from 160 min to 85 min, including the equilibration time. Furthermore, the method was optimised for on-line coupling with ESI-MS, since a low concentration of acetic acid was used as an eluent. On the other hand, the standard procedure required a high concentration of ammonium formate buffer and was not suitable for the on-line ESI-MS detection of 2-AB labelled glycans due to the ionisation suppression. A common approach for identification of glycans using the HILIC amide column includes the use of 2-AB glycan standards and identification based on the retention time may require further collection of glycan fractions for confirmation of structures by MS. It is important to emphasise that not all the glycans that can be found in monoclonal antibodies are commercially available and prices for purified and labelled glycans are often very high. The analysis of minor species is therefore extremely challenging and complete structural assignment of peaks in fluorescence chromatograms is not always possible.

Despite the lower sensitivity there are some clear advantages of using ESI-MS instead of fluorescence detection. The MS detection enables extraction of a single chromatogram trace which is very useful when complex samples with co-eluting compounds are being analysed. As shown in Figure 2-10, the glycan G1-GlcNAc co-eluted with G0 glycan under the applied experimental conditions and it cannot be seen by using fluorescence detection alone. Since the dead volume after the column is reduced when using ESI-MS detection, the G0-Fuc and Man5

that were only partially resolved when using fluorescence detection, were now almost completely separated.

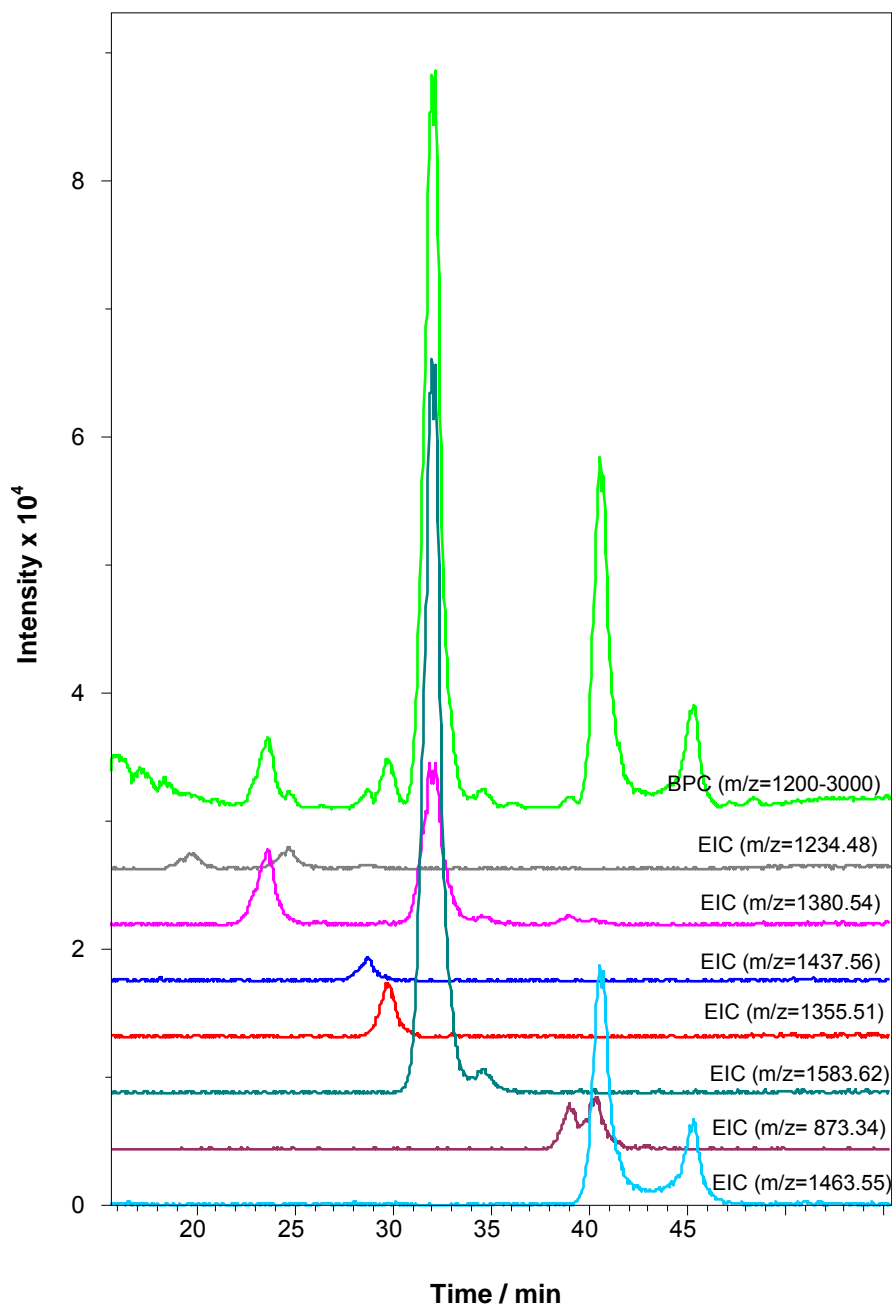


Figure 2-8: Separation of 2-AB labelled glycans from MAb1 using ZIC-HILIC coupled with ESI-MS. Base peak chromatogram in mass range 1200-3000, extracted ion chromatograms of singly and doubly protonated ions of major 2-AB glycans and native G0 glycan, indicating incomplete labelling.

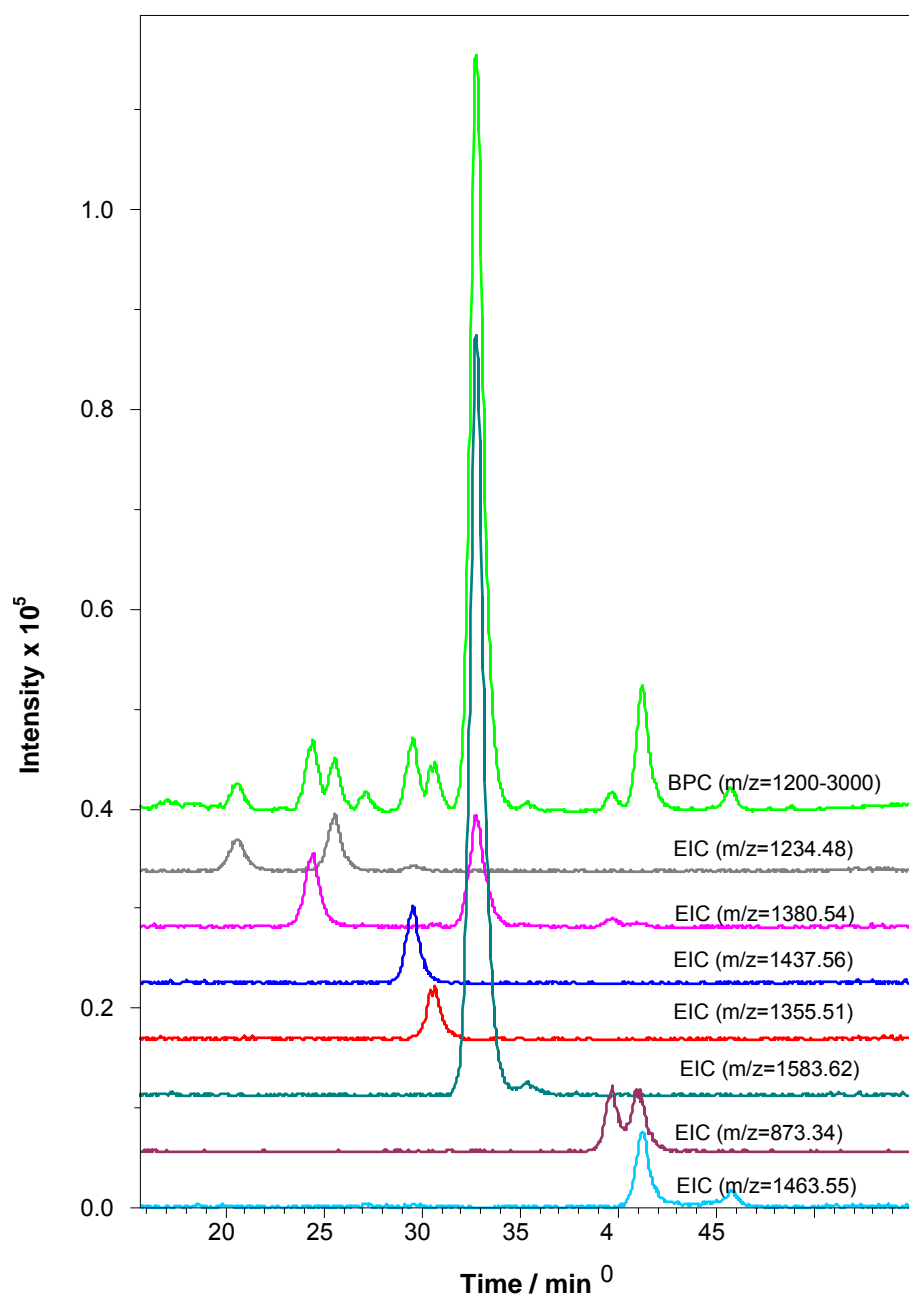


Figure 2-9: Separation of 2-AB labelled glycans from MAb2 using ZIC-HILIC coupled with ESI-MS. Base peak chromatogram in mass range 1100-3000 and extracted ion chromatograms of singly and doubly protonated ions of major 2-AB glycans and native G0 glycan. Double peak of G0-GlcNAc indicates in-source fragmentation. Two peaks are observed for G0-GlcNAc-Fuc.

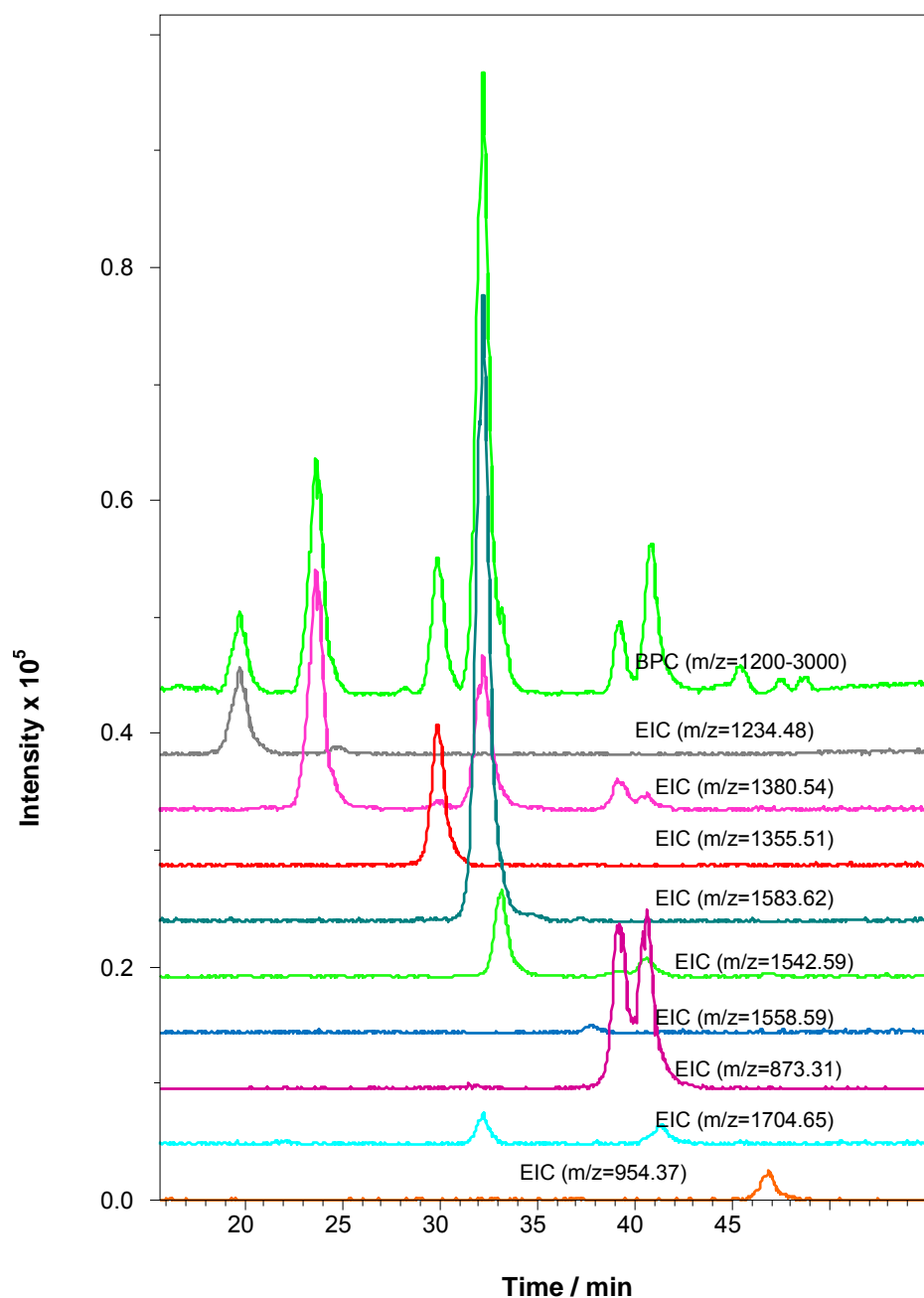


Figure 2-10: Separation of 2-AB labelled glycans from MAb3 using ZIC-HILIC coupled with ESI-MS. Base peak chromatogram in mass range 1100-3000, extracted ion chromatograms of singly and doubly protonated ions of major 2-AB glycans and native G0 glycan. Double peaks of G0-GlcNAc and G1-GlcNAc indicate in-source fragmentation.

Various aqueous mobile phases were tested for the elution of 2-AB labelled glycans, including acetic acid, ammonium formate and ammonium acetate, using the same gradient profile as previously described. The composition of the mobile phase did not significantly affect the retention of the 2-AB glycans; however, it had a large impact on elution of contaminants originating from the samples. The MABs and other biological formulations usually contain detergents, such as polysorbates (Tween), that might not be completely removed during the sample clean-up. If they are present in sufficiently high concentrations, the surface chemistry can be changed which could explain sample-to-sample variations in retention times. Since the detergents are polymeric mixtures, they did not elute as a single peak but over a large time window, which interfered the least with the elution of glycans when acetic acid was used as the mobile phase (not shown). When ammonium formate and ammonium acetate were used as a mobile phase, the contaminants started to elute earlier and due to their good ionisation in ESI-MS source, the ionisation of co-eluting glycans was suppressed and the signal was therefore reduced. Late-eluted minor glycans found in MAb3 could not be detected by ESI-MS, most likely due to the presence of contaminants in the sample. The sample preparation was further optimised in later chapters, where additional cleaning steps were introduced. Fluorescence detection offers an advantage compared to the ESI-MS detection, since contaminants present from the original formulation do not interfere with the signal for fluorescently-labelled glycans. However, it is important to emphasise that labelling is not always quantitative and in all the MAb samples, native G0 glycan was found, which exhibited higher retention compared to the 2-AB labelled form.

Similarly as observed for amide HILIC, the MAb3 glycan profile obtained by ZIC-HILIC was different to glycan profiles of MAb1 and Mab2, which is in agreement with the proposal that these MABs originate from different expression systems. However, minor glycans in these MABs could not be identified with amide HILIC or ZIC-HILIC separation of 2-AB labelled glycans.





Table 2-5 continued...

$(\text{Hex})_2(\text{HexNAc})_1$ $(\text{Man})_3(\text{GlcNAc})_2$		Hyb1	1558.59 779.80	$[\text{M}+\text{H}]^+$	37.7	-	-	+
$(\text{Hex})_1(\text{HexNAc})_2$ $(\text{dHex})_1$ $(\text{Man})_3(\text{GlcNAc})_2$		G1	1745.67 873.34	$[\text{M}+\text{H}]^+$ $[\text{M}+2\text{H}]^{2+}$	39.1 40.5	+	+	+
$(\text{Hex})_2(\text{HexNAc})_1$ $(\text{dHex})_1$ $(\text{Man})_3(\text{GlcNAc})_2$		Hyb1F / G2-GlcNAc	1704.65 852.83	$[\text{M}+\text{H}]^+$ $[\text{M}+2\text{H}]^{2+}$	41.3	-	-	+
$(\text{Hex})_2(\text{HexNAc})_2$ $(\text{dHex})_1$ $(\text{Man})_3(\text{GlcNAc})_2$		G2	1907.73 954.37	$[\text{M}+2\text{H}]^{2+}$	46.8	+	+	+

+ confirmed; - not found in the sample.

### 2.3.2.2. Separation of native glycans

Initially, the ZIC-HILIC column was tested for the separation of 2-AB labelled glycans. Several aqueous mobile phases with different pH and ionic strength, using ammonium formate, ammonium acetate or acetic acid as the buffer were tested. A number of different gradient profiles were evaluated, with the best profile obtained using 17 mM acetic acid. The experimental conditions showing the best separation of 2-AB labelled glycans were used for further method development for the separation of native and reduced glycans. In this initial work, better sensitivity in ESI-MS experiments was achieved by using a low concentration of acetic acid as the aqueous mobile phase. This composition reduced the background noise and improved the ionisation efficiency, which was significantly reduced when ammonium was present in the buffer solution.

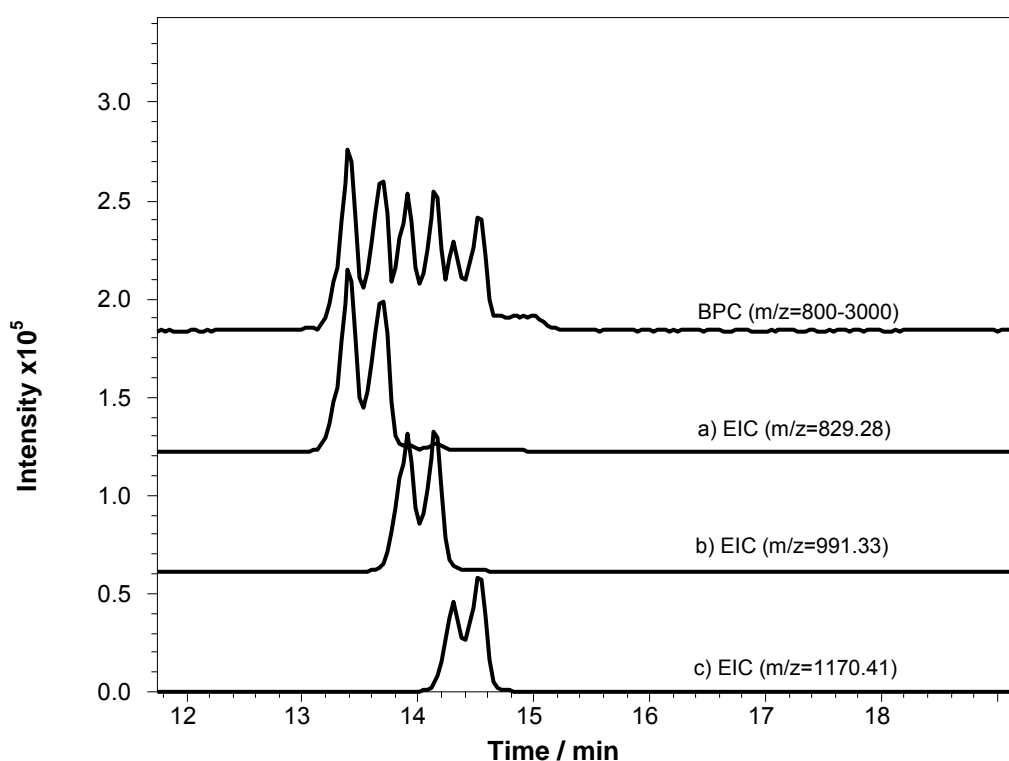


Figure 2–11: Separation of linear oligosaccharides at a concentration of 3 µg/ml: (a) maltopentaose; (b) maltohexaose; (c) maltoheptaose. Gradient elution: mobile phase A-acetonitrile; mobile phase B-34 mM acetic acid, pH 3.0.

Linear oligosaccharides containing 5-7 glucose units and high mannose, mannose 3 (Man3) and mannose (Man9), glycan standards were used for testing the capability of the ZIC-HILIC column for the separation of reducing glycans. For all types of reducing glycan standards, linear oligosaccharides and high mannose, the same behaviour was observed. Glycan anomers were separated and signals for glycans appeared as double peaks due to mutarotation (Figure 2-11 and Figure 2-12).

Separation of Man3 and Man9 glycan standards on the ZIC-HILIC column was further tested under different chromatographic conditions, using various acids and buffers as the eluent B, with the same gradient profile as previously described. When 0.1% formic acid, 0.1% acetic acid, 0.1% propionic acids were used, a strong double peak was observed in the base peak chromatogram (BPC) that corresponded to Man3 glycan, with no significant difference in sensitivity or retention time. For Man9 glycan, which was eluted at higher water content, sensitivity was much lower compared to Man3 (Figure 2-12). On the other hand, sensitivity for Man3 and Man9 was greatly reduced when ammonium buffers were used as aqueous mobile phase due to the reduced ionisation efficiency. Sensitivity decreased with the increasing ammonium concentration in the mobile phase and when 60 mM ammonium formate buffer was used as an eluent, the peak for the Man9 glycan could no longer be seen in the BPC, whereas the intensity of the peak for Man3 remained the same as in 10 mM ammonium formate and shifted to the lower retention time (Figure 2-13).

The mobile phase composition had also a great effect on the formation of ions in the ESI source. Other parameters that affected the formation of ions were the presence of contaminants in the sample, and the size and structure of glycans. In positive ion ESI-MS mode glycans tend to form protonated species and sodium adducts; a higher proportion of ammonium glycan adducts is expected when ammonium is present in the sample or in the mobile phase.

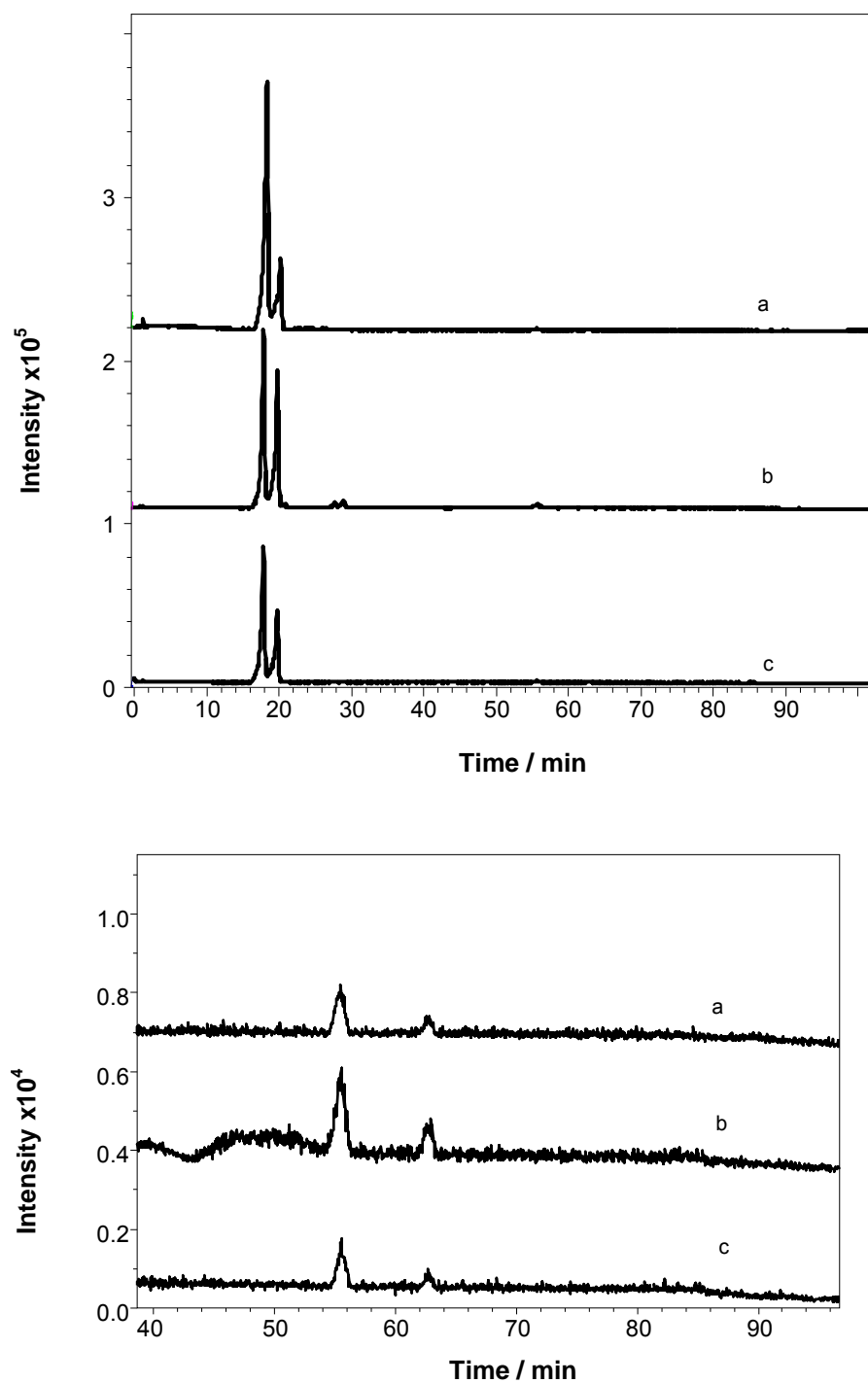


Figure 2-12: Man3 (concentration of 10  $\mu\text{g/mL}$ ) and Man9 (concentration of 20  $\mu\text{g/mL}$ ) standards. Gradient elution: mobile phase A-acetonitrile, mobile phase B-0.1% formic acid (a), 0.1% acetic acid (b), 0.1% propionic acid (c). No significant difference in retention times or signal intensity is observed in BPC ( $m/z=800-3000$ ).

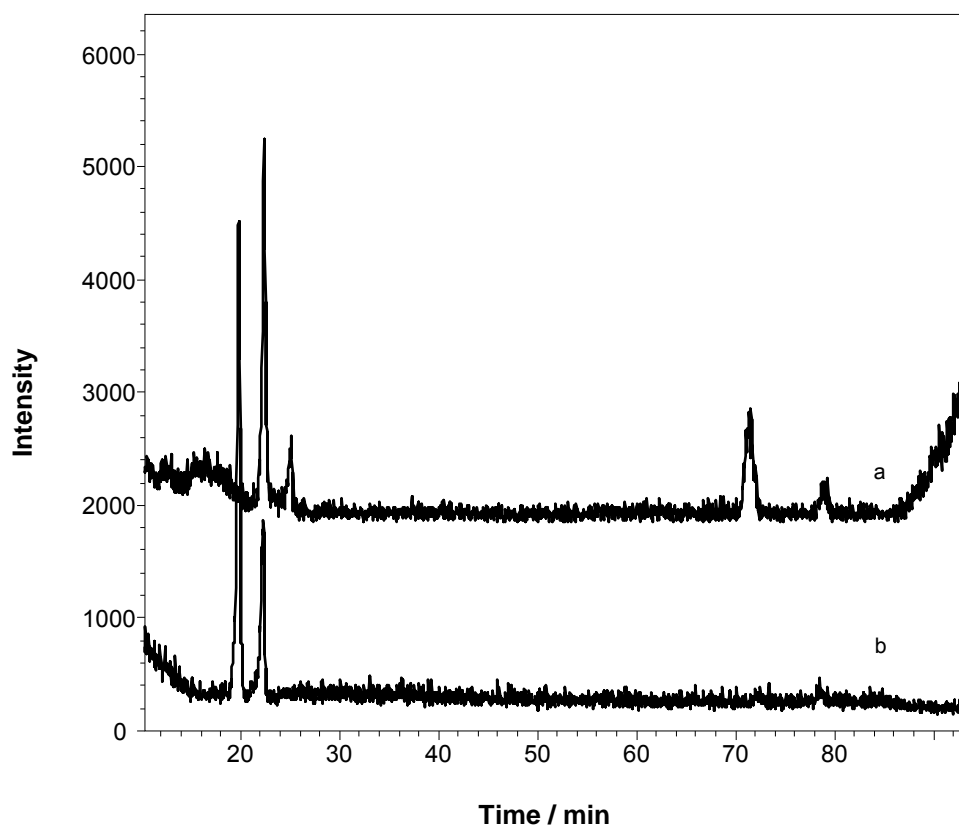


Figure 2–13: Man3 (concentration of 10  $\mu\text{g/mL}$ ) and Man9 (concentration of 20  $\mu\text{g/mL}$ ) standards. Gradient elution: mobile phase A-acetonitrile, mobile phase B-10 mM (a) and 60 mM (b) ammonium formate pH 4.0. Intensity of the signal for Man3 glycan in BPC ( $m/z=800\text{--}3000$ ) remained the same when higher buffer concentration was used and it shifted to a lower retention time. Signal for Man9 glycan can no longer be observed when higher buffer concentration was used.

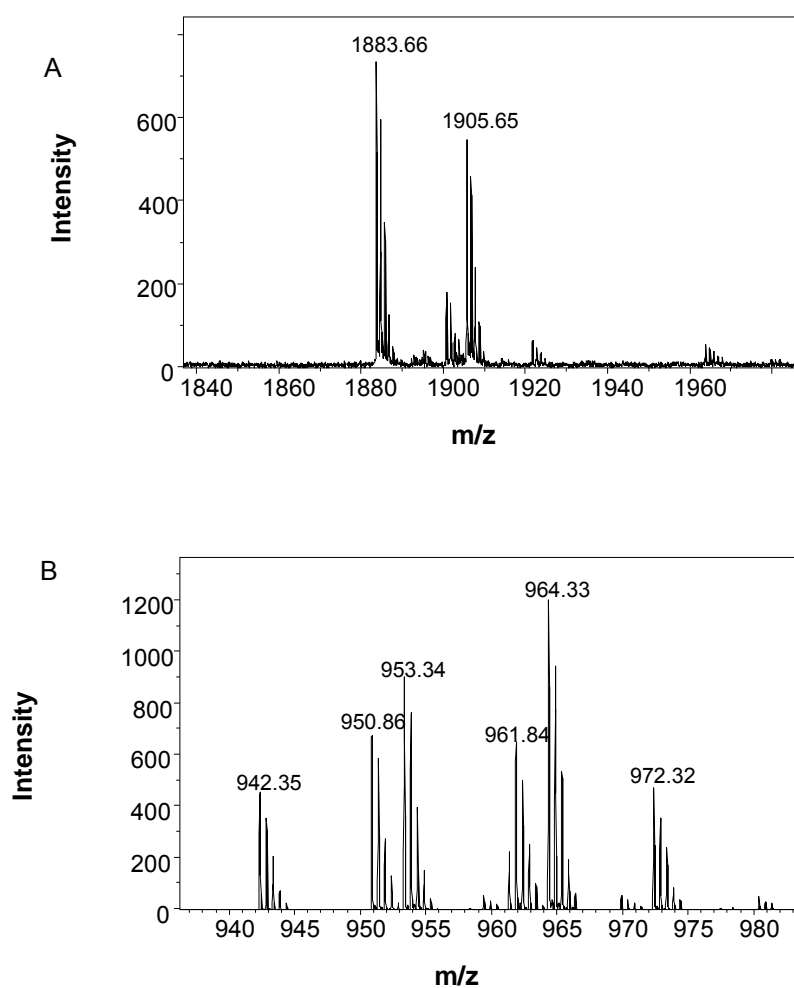


Figure 2-14: Mass spectra of Man9 glycan: singly charged ions (A) and doubly charged ions (B). Gradient elution: mobile phase A-acetonitrile, mobile phase B-0.1% acetic acid. The main adducts are singly and doubly protonated and sodiated ions. Ammonium adducts are present, most likely due to the ammonium contamination in the sample.

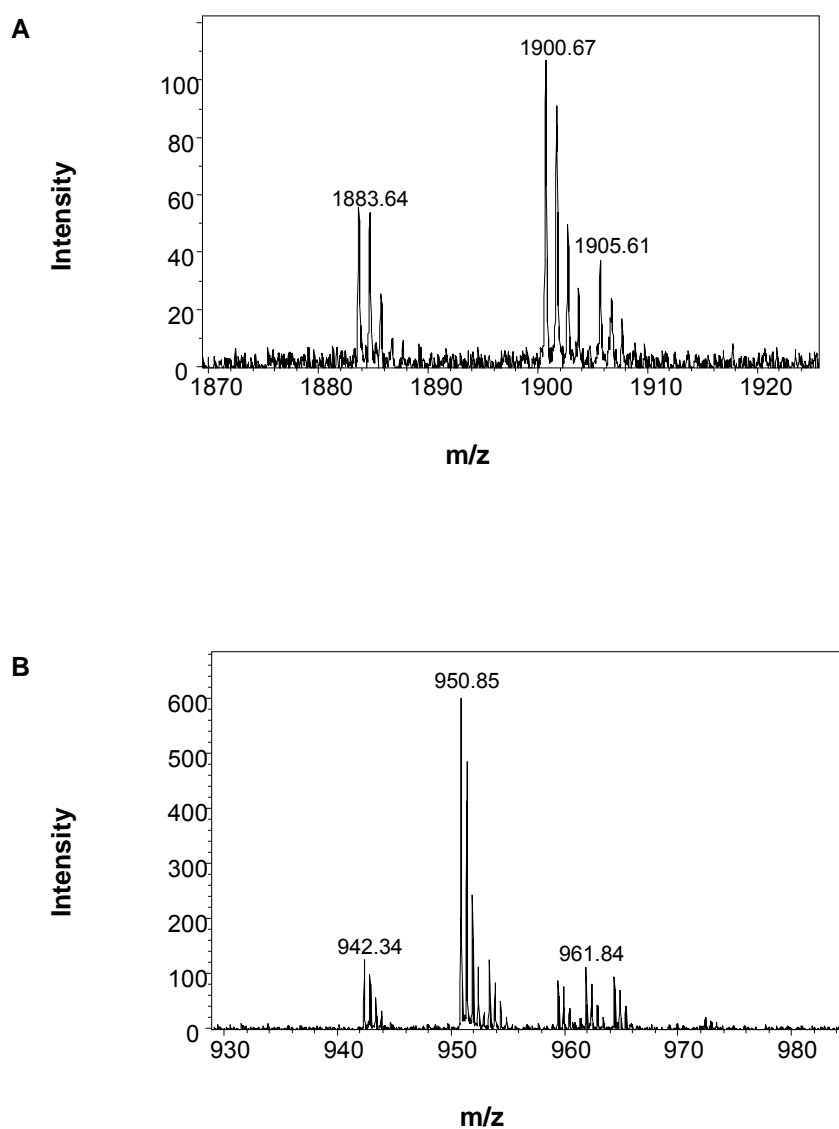
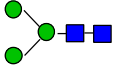
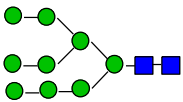


Figure 2–15: Mass spectra of Man9 glycan: singly charged ions (A) and doubly charged ions (B). Gradient elution: mobile phase A-acetonitrile, mobile phase B-10 mM ammonium formate. The dominating ions are singly and doubly charged ammonium adducts.



Table 2-6: Man3 and Man9 adducts found in mass spectra under different experimental conditions.

Possible ions	Theoretical m/z	
		
$[M+H]^+$	911.35 <sup>*</sup> , <sup>‡</sup>	1883.68
$[M+Na]^+$	933.33	1905.66
$[M+NH_4]^+$		1900.71
$[M+2H]^{2+}$		942.34
$[M+2Na]^{2+}$		964.33 <sup>*</sup>
$[M+2NH_4]^{2+}$		959.37
$[M+H+Na]^{2+}$		953.33
$[M+H+NH_4]^{2+}$		950.86 <sup>‡</sup>
$[M+Na+NH_4]^{2+}$		961.85
<sup>*</sup> the most abundant ion in acetic acid		
<sup>‡</sup> the most abundant ion in 10 mM ammonium formate		

For Man3 the most abundant ion under all experimental conditions used was the pseudomolecular ion  $[M+H]^+$  and it did not form any doubly charged species. With increasing molecular mass, formation of doubly charged ions becomes more prominent. For Man9 glycan besides the main protonated and sodiated ions, singly and doubly charged ammonium adducts were observed when 0.1% acetic acid was used as the eluent B, which indicated the presence of ammonium in the sample (Figure 2–14). When ammonium was present in the mobile phase, the ammonium adducts became the dominant ions for Man9 glycan (Figure 2–15). The observed ions for Man3 and Man9 glycans are summarised in Table 2-6. When the typical ionisation pattern under certain experimental conditions is understood, it can be a valuable tool in identifying unknown glycans in a sample. Glycans also exhibit a specific isotope pattern which can be calculated by appropriate software. The relative intensity of peaks in the isotope pattern can be used for an additional confirmation of glycan MS signal.

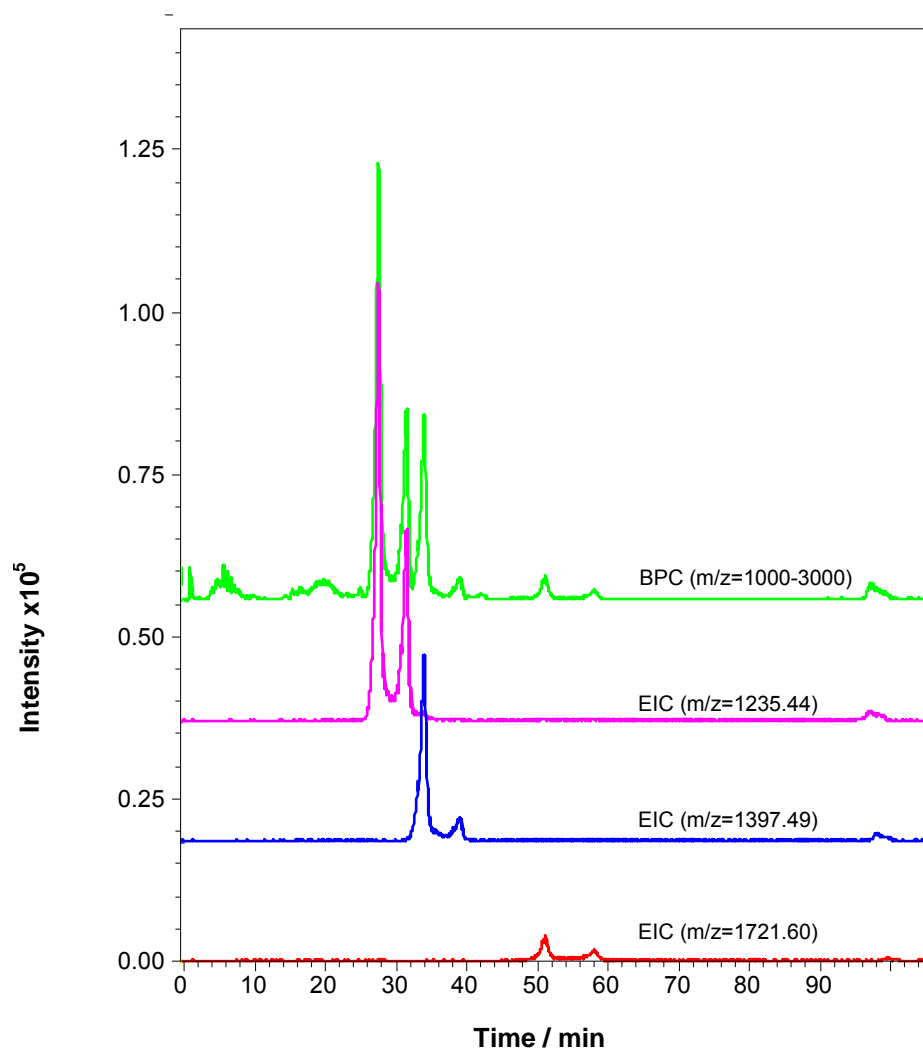


Figure 2–16: Separation of native glycans from RNase B using ZIC-HILIC column coupled with ESI-MS. Gradient elution: mobile phase A-acetonitrile; mobile phase B-34 mM acetic acid, pH 3.0. Only the most abundant glycans, Man5, Man6 and Man8, are found in the BPC. Due to the mutarotation, glycans eluted as double peaks. Man7 and Man9 are not observed due to the peak broadening.

The method was applied to the RNase B glycans and under the conditions used, only peaks for the most abundant glycans, Man5, Man6 and Man8, could be identified. Reducing oligosaccharides appeared as double peaks due to mutarotation and were only partially resolved (Figure 2–16). In addition, it was observed that peak broadening due to the mutarotation process reduced the sensitivity, therefore minor species such as Man7 and Man9 could not be found in the BPC, although the MS signals were observed in the accumulated mass spectrum (Figure 2–17).

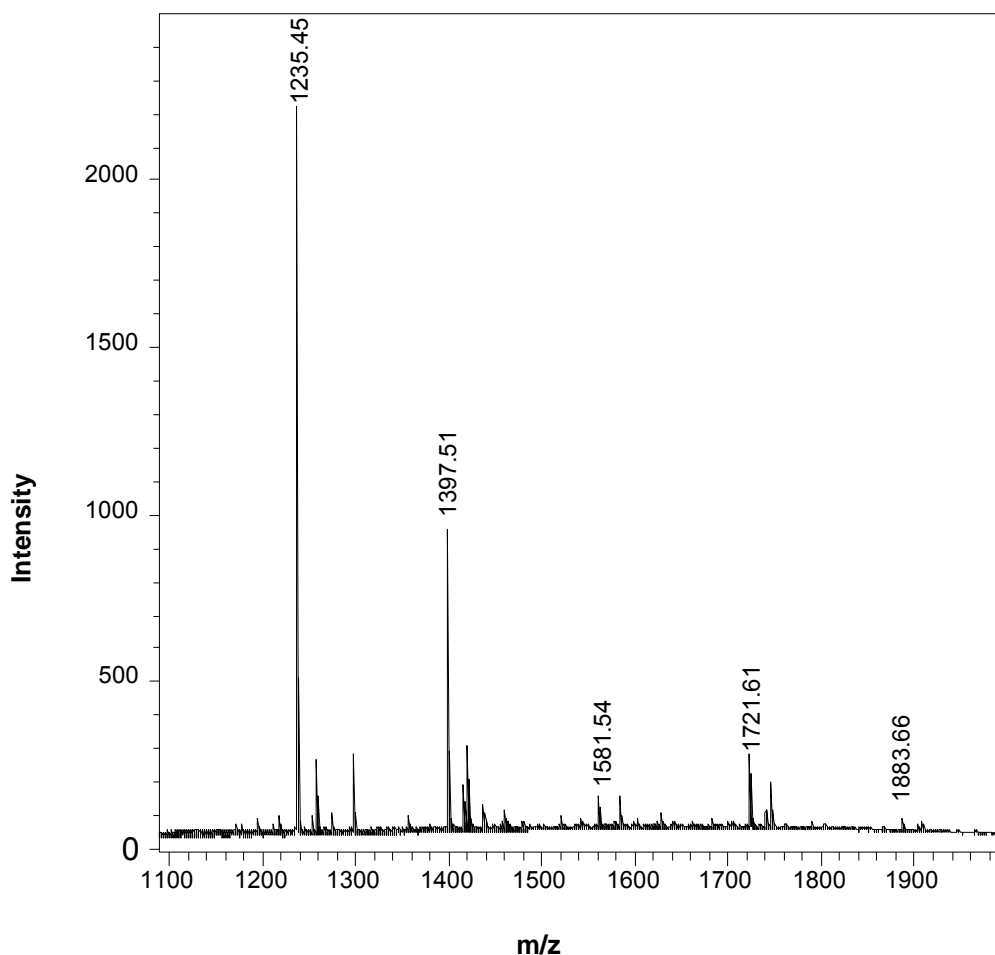


Figure 2–17: Accumulated mass spectrum of the whole native glycan elution range. All glycans expected to be present in RNase B, Man5–Man9, are found in the mass spectrum. Relative intensities are in agreement with the data obtained by fluorescence detection.

Similar behaviour has already been reported for the separation of glycans on graphitized carbon columns [82, 122]. The double peaks appearing due to mutarotation could be avoided either by reducing the glycans to alditols using sodium borohydride, or by increasing the pH which accelerates the mutarotation process.

### 2.3.2.3. Separation of reduced glycans

Due to the pH limitations of the silica-based ZIC-HILIC column, the anomers of RNase B oligosaccharides were removed by reduction prior to the separation (Figure 2–18). Following the reduction, single peaks corresponding to Man5 to Man9 were found in the BPC. For the most abundant glycans, Man5 and Man6, double peaks that correspond to the native forms could be observed due to incomplete reduction but they did not interfere with the separation of the reduced glycans. In addition, peaks for Man7 structural isomers were partially resolved (Figure 2–18). The RNase B glycan profile corresponded well to the glycan profile obtained by the standard method for separation of 2-AB labelled glycans on an amide and a ZIC-HILIC column, coupled with fluorescence detection. The order of elution was also the same for the reduced glycans as was observed for the separation of 2-AB glycans on either amide HILIC or ZIC-HILIC stationary phases, which confirmed the HILIC separation mechanism. The accumulated mass spectrum over the glycan elution range, Figure 2–19, shows that under the given conditions, oligosaccharides gave the strongest signal for the pseudomolecular ions  $[M+H]^+$  and  $[M+Na]^+$ . Most significantly, using this new approach the sample preparation was simplified and the analysis time was reduced from 145 min to 105 min without the equilibration time, compared to the standard procedure.

Similar behaviour was observed for the glycans released from MABs as for RNase B oligosaccharides, with native glycans appearing as double peaks due to mutarotation (data not shown). The ZIC-HILIC chromatograms for reduced oligosaccharides obtained from MABs are shown in Figure 2–20 and Figure 2–21 and the data are summarised in Table 2-7. The MAB glycan profiles also

correlated well with the profiles obtained using the standard procedure for 2-AB labelled glycans. In all of the samples a small double peak correlating to a small amount of unreduced G0 was observed, but it did not interfere with the separation of the reduced glycans.

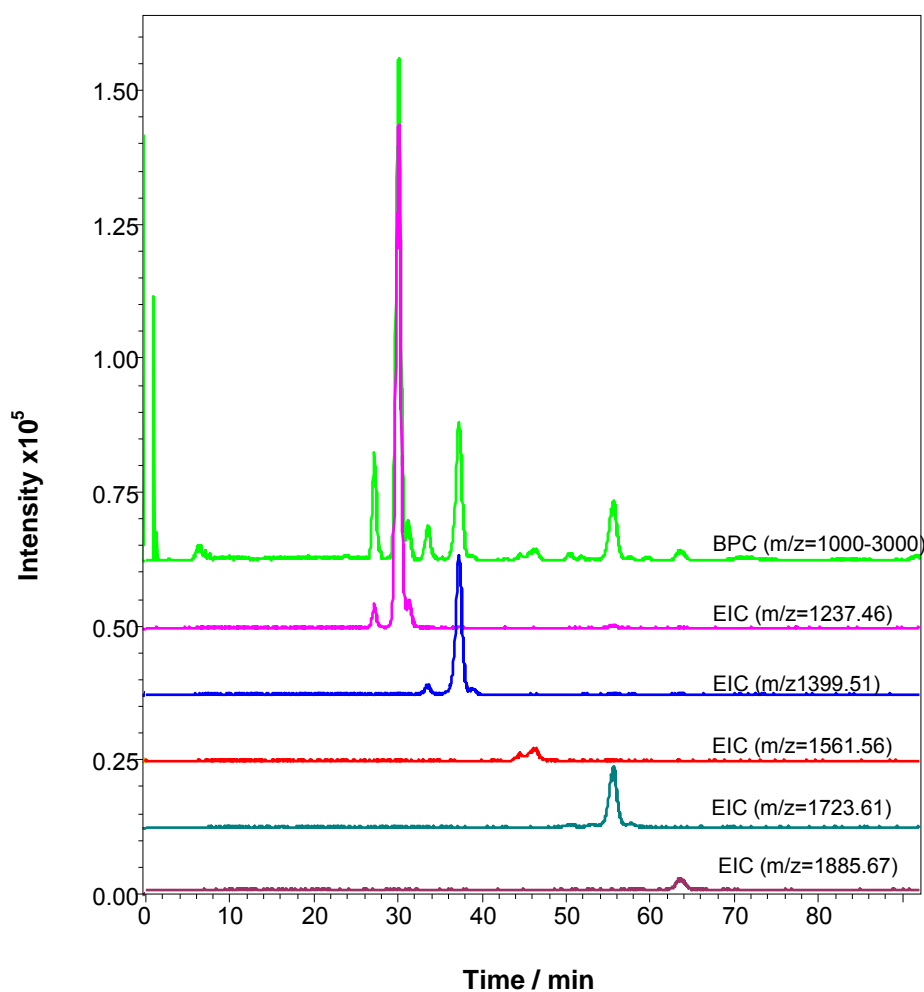


Figure 2–18: Separation of reduced glycans from RNase B using ZIC-HILIC column coupled with ESI-MS. Gradient elution: mobile phase A-acetonitrile; mobile phase B-34 mM acetic acid, pH 3.0. Man5-Man9 glycans are found in the BPC. Man7 glycans are partially separated. Small amounts of unreduced glycans which do not interfere with the separation of reduced glycans are present in the sample.

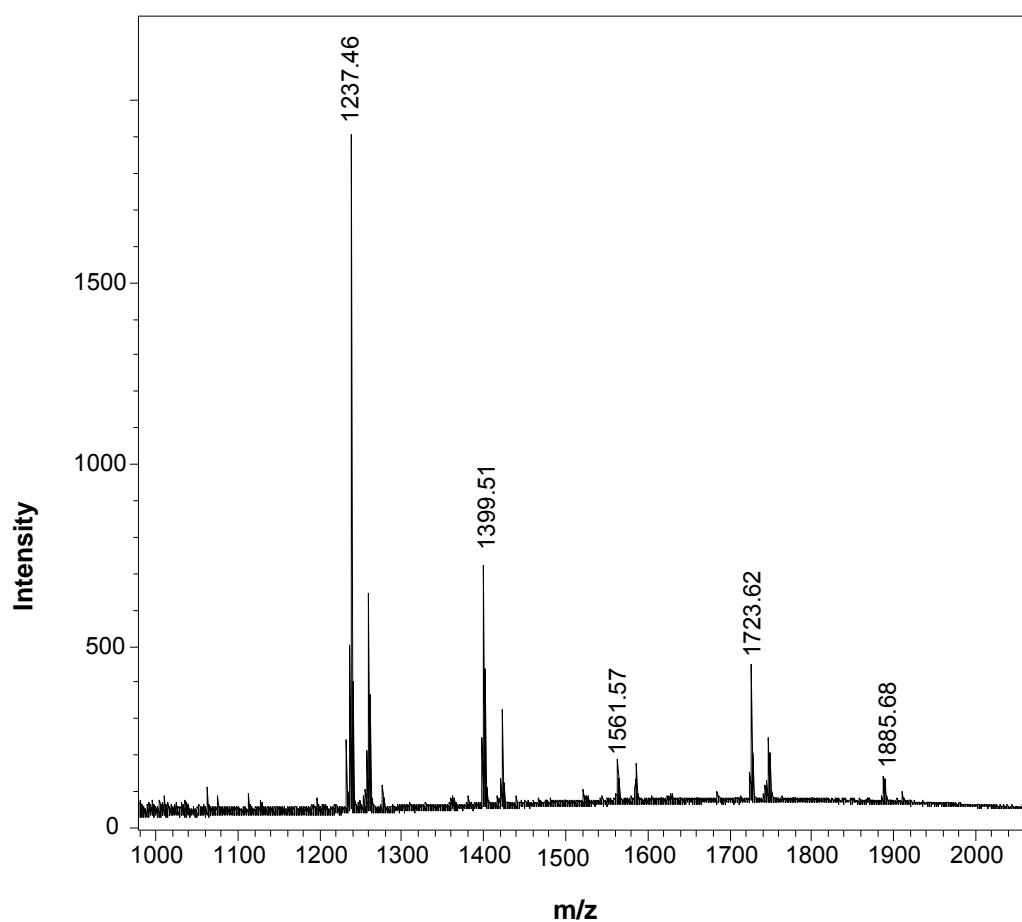


Figure 2–19: Accumulated mass spectrum of the whole reduced RNase B glycan elution range. Man5-Man9 glycans are found in the mass spectrum, with relative amounts: Man5>Man6>Man8>Man7>Man9.

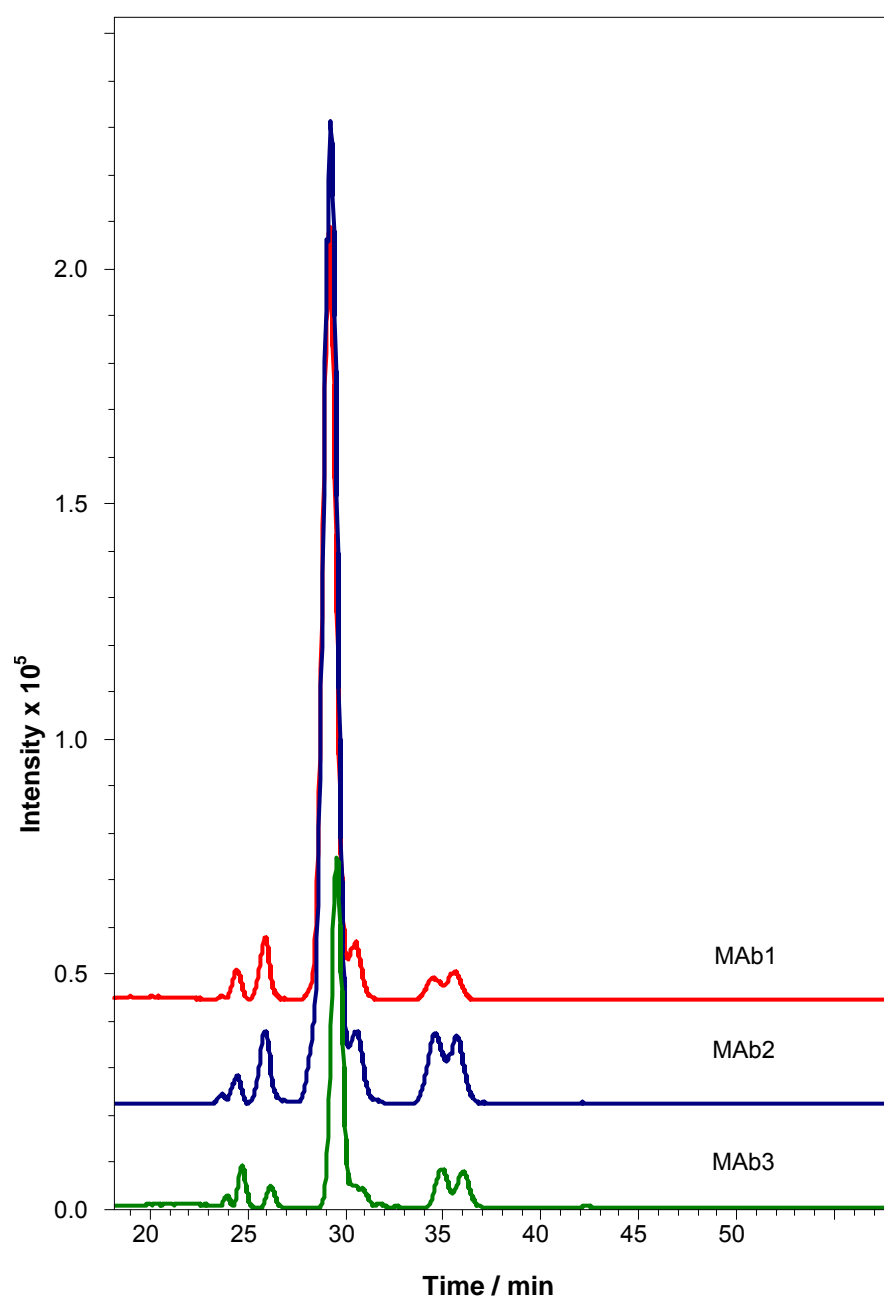


Figure 2–20: Base peak chromatograms ( $m/z=1100-3000$ ) of reduced glycans released from MAbs obtained with ZIC–HILIC coupled with ESI–MS. Gradient elution: mobile phase A–acetonitrile; mobile phase B–34 mM acetic acid, pH 3.0. Major glycans: G0–GlcNAc–Fuc, G0–GlcNAc, G0, G1 and G2 are found in the BPC. G1 isomers are partially separated.

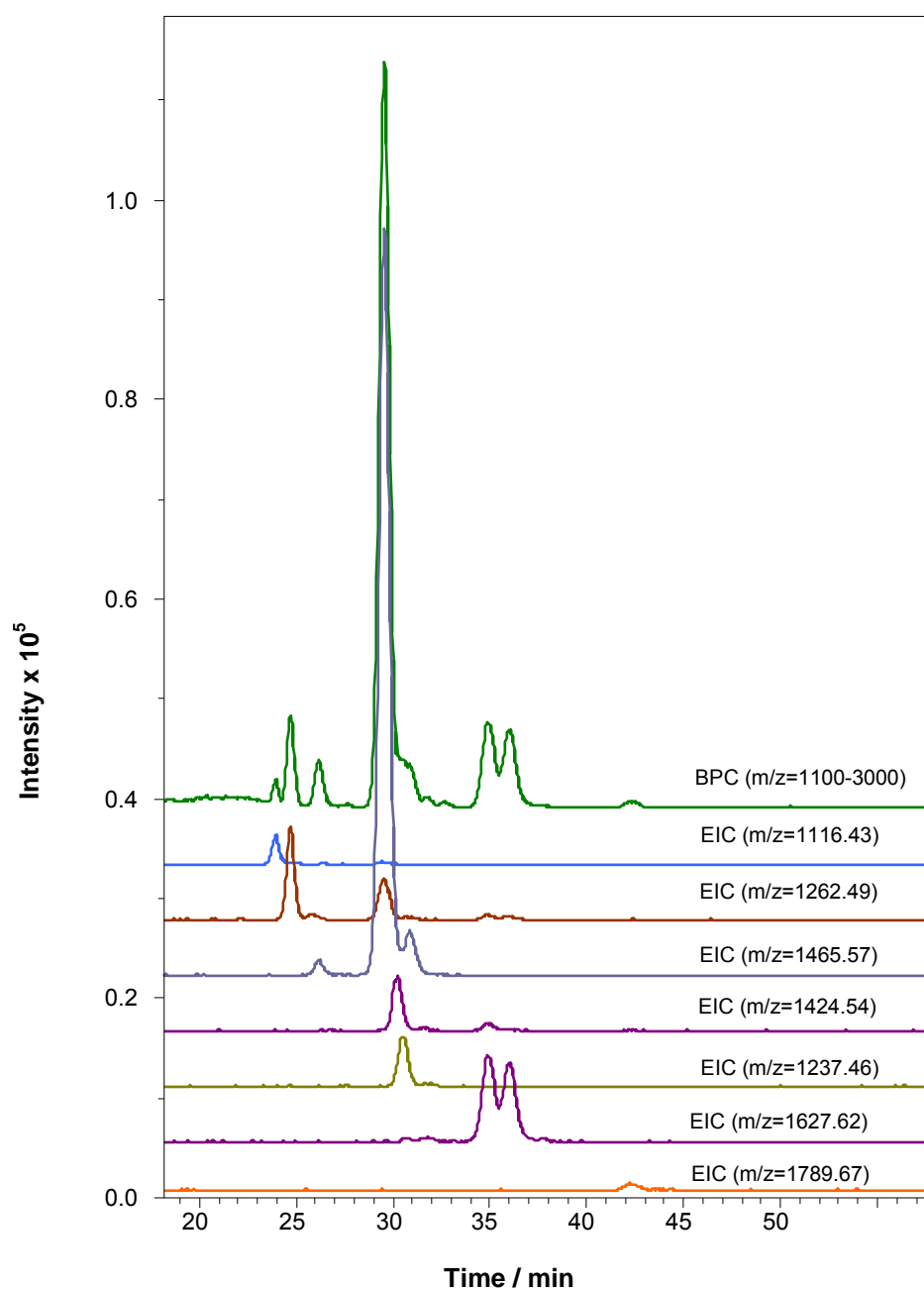


Figure 2-21: BPC and extracted ion chromatograms (EICs) of glycans from MAb3. Gradient elution: mobile phase A-acetonitrile; mobile phase B-34 mM acetic acid, pH 3.0. G0, Man5 and G1-GlcNAc are partially overlapped.



Table 2-7: Reduced glycans, found in MAbs by ZIC-HILIC method.

Glycan composition	Structure	Abbr.	(m/z) <sub>theoretical, red</sub> [M+H] <sup>+</sup> [M+2H] <sup>2+</sup>	Ions found	Retention time / min	MAb1	MAb2	MAb3
(HexNAc) <sub>1</sub> (Man) <sub>3</sub> (GlcNAc) <sub>2</sub>		G0-GlcNAc-Fuc	1116.43 558.72	[M+H] <sup>+</sup>	23.9 26.3	+	+	+
(HexNAc) <sub>1</sub> (dHex) <sub>1</sub> (Man) <sub>3</sub> (GlcNAc) <sub>2</sub>		G0-GlcNAc	1262.49 631.75	[M+H] <sup>+</sup>	24.6	+	+	+
(HexNAc) <sub>2</sub> (dHex) <sub>1</sub> (Man) <sub>3</sub> (GlcNAc) <sub>2</sub>		G0	1465.57 733.29	[M+H] <sup>+</sup>	29.3	+	+	+
(Hex) <sub>1</sub> (HexNAc) <sub>1</sub> (dHex) <sub>1</sub> (Man) <sub>3</sub> (GlcNAc) <sub>2</sub>		G1-GlcNAc	1424.54 712.77	[M+H] <sup>+</sup>	30.0	-	+	+
(Hex) <sub>2</sub> (Man) <sub>3</sub> (GlcNAc) <sub>2</sub>		Man5	1237.46 619.23	[M+H] <sup>+</sup>	30.3	+	+	+
(Hex) <sub>1</sub> (HexNAc) <sub>2</sub> (dHex) <sub>1</sub> (Man) <sub>3</sub> (GlcNAc) <sub>2</sub>		G1	1627.62 814.31	[M+H] <sup>+</sup> [M+2H] <sup>2+</sup>	34.7 35.8	+	+	+
(Hex) <sub>2</sub> (HexNAc) <sub>2</sub> (dHex) <sub>1</sub> (Man) <sub>3</sub> (GlcNAc) <sub>2</sub>		G2	1789.67 895.34	[M+H] <sup>+</sup> [M+2H] <sup>2+</sup>	42.0	-	+	+

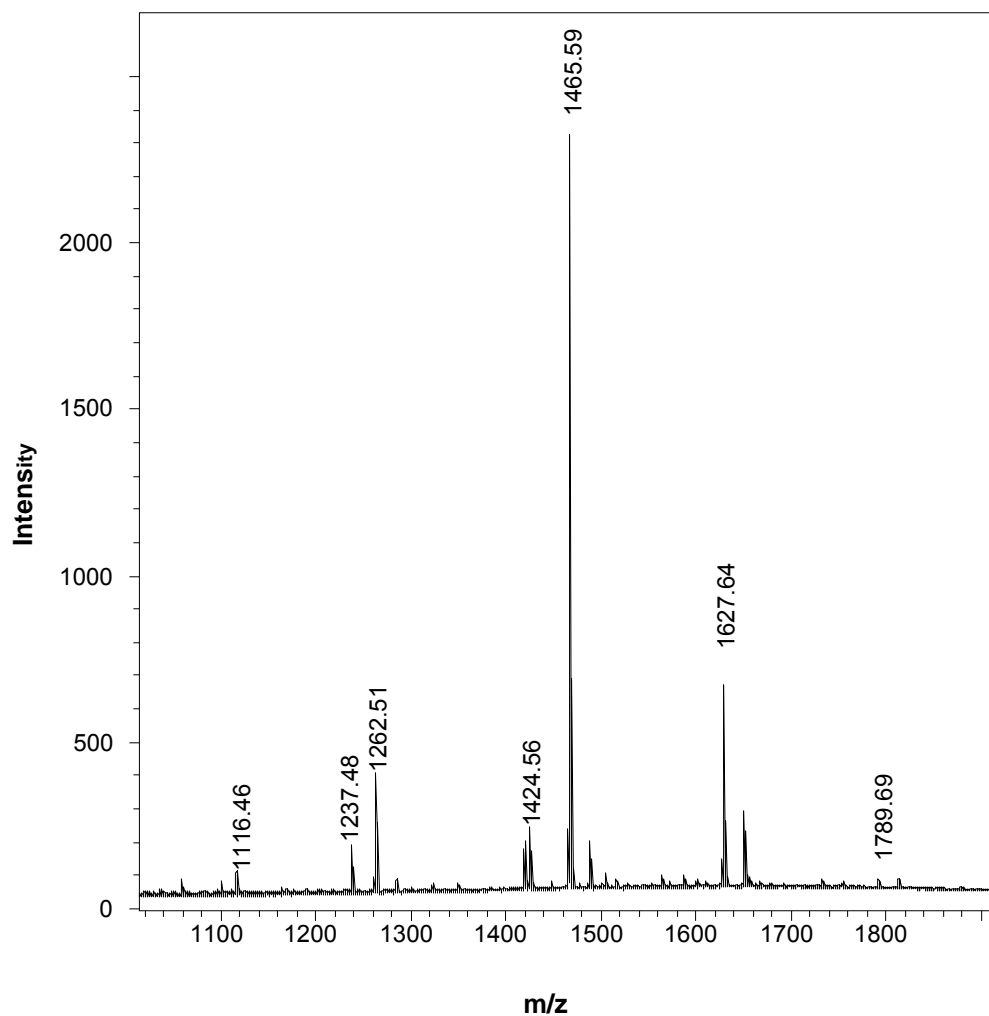


Figure 2–22: Accumulated mass spectrum of the whole reduced MAb3 glycan range. All the major glycan species are identified with the main singly charged protonated ion. Singly charged sodium adducts are observed for the most abundant glycans.

Similar to the results for the RNase B glycans, the accumulated mass spectrum (Figure 2–22) over the glycan elution range shows that the most abundant species were the protonated species and sodium adducts. The G1 structural isomers were partially resolved, indicating that the ZIC-HILIC column has the capability to separate structural isomers, as also previously reported for AP-labelled glycans and glycopeptides [38, 80]. Similarly as seen for the separation of 2-AB labelled glycans, two peaks for G0-GlcNAc-Fuc were observed in MAb1 and MAb2, and one peak was observed in MAb3 glycan samples. Although the retention mechanism governing the ZIC-HILIC separation of glycans is not completely understood, it has been suggested that the structural recognition capability is based on hydrophilic partitioning of glycans and electrostatic interaction between glycans and zwitterionic sulfobetaine groups on the surface [80]. For G0-GlcNAc several peaks were also observed which indicated the presence of in-source fragmentation of G0 and G1 glycans. Fragmentation will be discussed in detail in Chapter 3.

Due to the poor ionisation of native and reduced glycans in the ESI source, the main disadvantage of using ESI-MS instead of fluorescence is the loss of sensitivity. However, despite lower sensitivity, all of the most abundant glycans in the MAbs were identified under the described experimental conditions and the glycan profiles correlated well with the profiles obtained with the standard procedure. At the same time, fluorescence labelling has the disadvantage of being both relatively expensive and sometimes non-quantitative. Therefore, this new approach offers a good alternative for fast and reliable glycan profiling of MAbs. None of the described methods provided complete information about MAb glycosylation, which indicated the need for further method development and testing new stationary phases in order to save time required for derivatization procedures or chromatographic separation. There are a few parameters to be considered; sample preparation time and costs, sensitivity in fluorescence and ESI-MS detection, structural information and time of a chromatographic run.

In quality control, a consistent glycan profile over time obtained by fluorescence detection may provide sufficient information about the protein glycosylation. On the other hand, clone selection in production of biotherapeutics, looking for correlations between glycosylation and illnesses, or understanding biological activity of the naturally occurring and recombinant glycoproteins may require detailed information about glycosylation patterns which cannot be obtained by a single method.

## **2.4. Conclusions**

In this chapter, a simpler and faster HILIC separation of 2-AB labelled, native and reduced glycans from RNase B and monoclonal antibodies using a ZIC-HILIC column has been described. It is demonstrated that the ZIC-HILIC column has a good capability for structural recognition for isomeric, neutral, reduced and 2-AB labelled glycans. The new ZIC-HILIC methods were compared to a separation of 2-AB labelled glycans on an Amide-80 column, coupled with fluorescence detection, yielding a good correlation between the glycan profiles. Using a ZIC-HILIC column, the time required for separation of 2-AB glycans was significantly reduced compared to the standard procedure. The separation of 2-AB glycans was optimized for on-line coupling with fluorescence and ESI-MS detection to obtain quantitative information and for structural assignment of peaks. Different selectivity of ZIC-HILIC was observed compared to the Amide-80 column and two glycan species that were not previously identified by the standard method were found in the MAb samples. Furthermore, the use of the ZIC-HILIC method for separation of reduced glycans was demonstrated. The ZIC-HILIC method exhibited good retention time reproducibility and due to the good chromatographic resolution and ESI-MS sensitivity, additional fluorescence labelling was not required which significantly lowers the cost of the analysis. This work demonstrates that the ZIC-HILIC separation is suitable for routine profiling of monoclonal antibodies and offers a good alternative to the more conventional separations using HILIC amide-80 and graphitized carbon columns.

## Chapter Three

### *3. Separation of glycans using graphitized carbon*

#### **3.1. Introduction**

A very promising method for analysis of glycans from recombinant proteins is the use of a graphitized carbon column coupled with ESI-MS. It still has not gained the popularity of HILIC, since the separation mechanism is not yet well understood and no databases for structural assignment are available [86]. The most widely used porous graphitized carbon (PGC) columns in glycosylation analysis are Hypercarb<sup>TM</sup> columns (Thermo Fisher Scientific). Graphitized carbon has a stereo-selective surface with the capability to separate closely related compounds and it is stable over a wide pH range (pH 1-14). Retention of native and reduced glycans on graphitized carbon is driven by hydrophobic, polar and ionic interactions [86, 122, 123]. The strength of the interaction with the PGC stationary phase depends on the area in contact with the surface, and consequently also on the geometry and type of the functional groups in the molecule [124]. Due to the described properties, one of the main advantages of graphitized carbon is its isomer separation power, which is superior compared to HILIC. Binary gradients consisting of acetonitrile and an aqueous phase containing volatile buffers are commonly used for elution of glycans. Ionic strength and pH of the mobile phase have little impact on the elution of neutral glycans; however, the effect is much more pronounced for highly sialylated glycans which require use of buffers with some ionic strength to achieve elution [87]. Since the higher buffer concentrations negatively influence the ionisation efficiency for glycans, the choice of the mobile phase will strongly depend on the type and charge of analysed glycans.

PGC has been shown to successfully separate high mannose, hybrid and complex type glycans from natural sources [37, 82-84, 125], and recombinant

glycoproteins [37, 85]. Most of the published work has been performed using reduced [37, 84, 85, 126-128] and 2-aminopyridine labelled glycans [129, 130], since analysis of native glycans usually results in undesirable separation of anomers [122]. Separation of anomers can be partially suppressed by using ammonia with high pH > 10 which enhances mutarotation [122, 131]; however, if the process is not fast enough, peak broadening may be observed [86, 122]. Graphitized carbon stationary phases can also be applied to permethylated glycans [132]. Permethylation increases ionisation efficiency of glycans and it is useful for fragmentation of glycans using tandem MS and can provide additional information about linkages and branching due to the extensive cross-ring fragmentations. On the other hand, the separation of permethylated glycan isomers using graphitized carbon might be more challenging compared to the separation of native and reduced glycan isomers.

In a majority of cases, the separation of glycans by graphitized carbon has been coupled with MS detection. Glycans can be detected in positive or negative ion mode; however, the ionisation efficiency for negatively charged glycans is promoted in the negative ion mode [88] which can also lead to incorrect estimation of the relative amounts of charged and neutral glycans in the sample. The sensitivity in ESI-MS detection is largely enhanced using nano LC, due to the lower chromatographic dilution of the sample and more efficient ion transfer in the nano ESI-MS source [88, 131]. Improved absolute signal intensity in nano LC enables accumulation of high quality fragmentation data in the MS/MS mode and assignment of glycan structures [88]. Nano graphitized carbon LC in the form of a microfluidic chip was employed in profiling of complex N-glycan mixtures from human serum [89]. The nano LC separation method was coupled to orthogonal TOF-MS, which enabled identification of glycans based on high mass accuracy. In a similar way, graphitized carbon chips were used for the analysis of mucin oligosaccharides and oligosaccharides from human milk and separation of a large number of components in a single run was demonstrated [133]. Recently, the use of an integrated microfluidics chip for glycan cleavage, clean-up, capture, separation using graphitized carbon stationary phase, and

nano ESI-TOF-MS has been reported. With the integrated chip, the complete analysis time was reduced from several hours to 10 min [134].

In this chapter, the use of a standard-bore PGC column for separation of reduced glycans from monoclonal antibodies is demonstrated. Using graphitized carbon demonstrates several advantages compared to the amide HILIC and ZIC-HILIC approaches, with higher sensitivity obtainable. Additionally, PGC exhibits superior capability for separation of isobaric species with reduced time required for a chromatographic run compared to the HILIC methods.

## **3.2. Materials and methods**

### ***3.2.1. Reagents and chemicals***

Unless otherwise noted, all chemicals were of analytical grade. Acetonitrile was obtained from VWR International (Poole, UK). Acetic acid, ethanol, PNGase F, ribonuclease B (R7884), sodium borohydride, mannose 3 glycan, mannose 9 glycan, maltopentaose, maltohexaose and maltoheptaose were obtained from Sigma (St. Louis, MO, USA). Formic acid, ammonium hydroxide and ammonium bicarbonate were obtained from Fluka (Steinheim, Germany). Propionic acid was purchased from Chem-Supply (Port Adelaide, Australia).

### ***3.2.2. Graphitized carbon coupled with ESI-MS***

The glycans released from the MAbs and the RNase B were reduced with sodium borohydride and desalted by ion-exchange chromatography, as described previously. Experiments were performed using a MicrOTOF-Q™ (Bruker Daltonik, Bremen, Germany) with an Agilent 1200 series binary pump and autosampler (Agilent, Santa Clara, CA, USA). Separations of native and reduced glycans were performed with Hypercarb™ column (2.1 x 150 mm, 5 µm; Thermo Fisher Scientific) installed in a column oven (Thermosphere, TS-130, Phenomenex, USA) at 30 °C.

Glycan standards and glycans released from RNase B were eluted using a binary step gradient; eluent A consisted of acetonitrile and eluent B consisted of aqueous solutions of various acids and volatile buffers, as noted. The flow-rate was set to 0.3 mL/min. Gradient: 7 to 40% A in 50 min, followed by a linear gradient 40 to 60% A in 10 min. The eluent composition was returned thereafter to 7% A in 1 min and the system re-equilibrated for 19 min prior to the next injection.

Elution of glycans from MAbs was achieved using a binary gradient; eluent A consisted of acetonitrile and eluent B consisted of a aqueous solution of 17 mM (0.1% v/v) acetic acid in water, unless otherwise noted. The flow-rate was set to 0.3 mL/min. Elution was achieved using a gradient from 7 to 30% A from 0-40 min, followed by an isocratic wash step for 5 min at 60% A, and followed by an equilibration step for 15 min at 7% A. ESI-MS conditions were: capillary voltage, 4.0 kV; drying temperature, 200 °C; drying gas flow, 8 L/min; nebulizer pressure, 1.5 bar; scan range m/z 50-3000.

### 3.3. Results and discussion

#### 3.3.1. Separation of linear oligosaccharides using PGC

A graphitized carbon column was used for the separation of native and reduced glycans. For the method development, linear oligosaccharides, maltopentaose, maltohexaose, maltoheptaose, and high mannose glycan standards, Man3 and Man9, were used, all in the reducing form. Various experimental conditions were tested in order to achieve optimum separation with high ESI-MS sensitivity. It was expected that the presence of ammonium would reduce the ionisation efficiency, as previously demonstrated for ZIC-HILIC; however, ionisation of glycans in ESI-MS could be significantly different when graphitized carbon is used due to the mobile phase having a low content of acetonitrile. Since in HILIC the acetonitrile was the main source of chemical background, it was expected that sensitivity could be enhanced when graphitized carbon is used as a stationary phase.



Initially, the effect of mobile phase composition and pH on retention, ionisation of glycans and sensitivity was examined. Native linear oligosaccharides, maltopentaose, maltohexaose and maltoheptaose, were injected onto the graphitized carbon column and detected with ESI-MS in the positive ion mode.

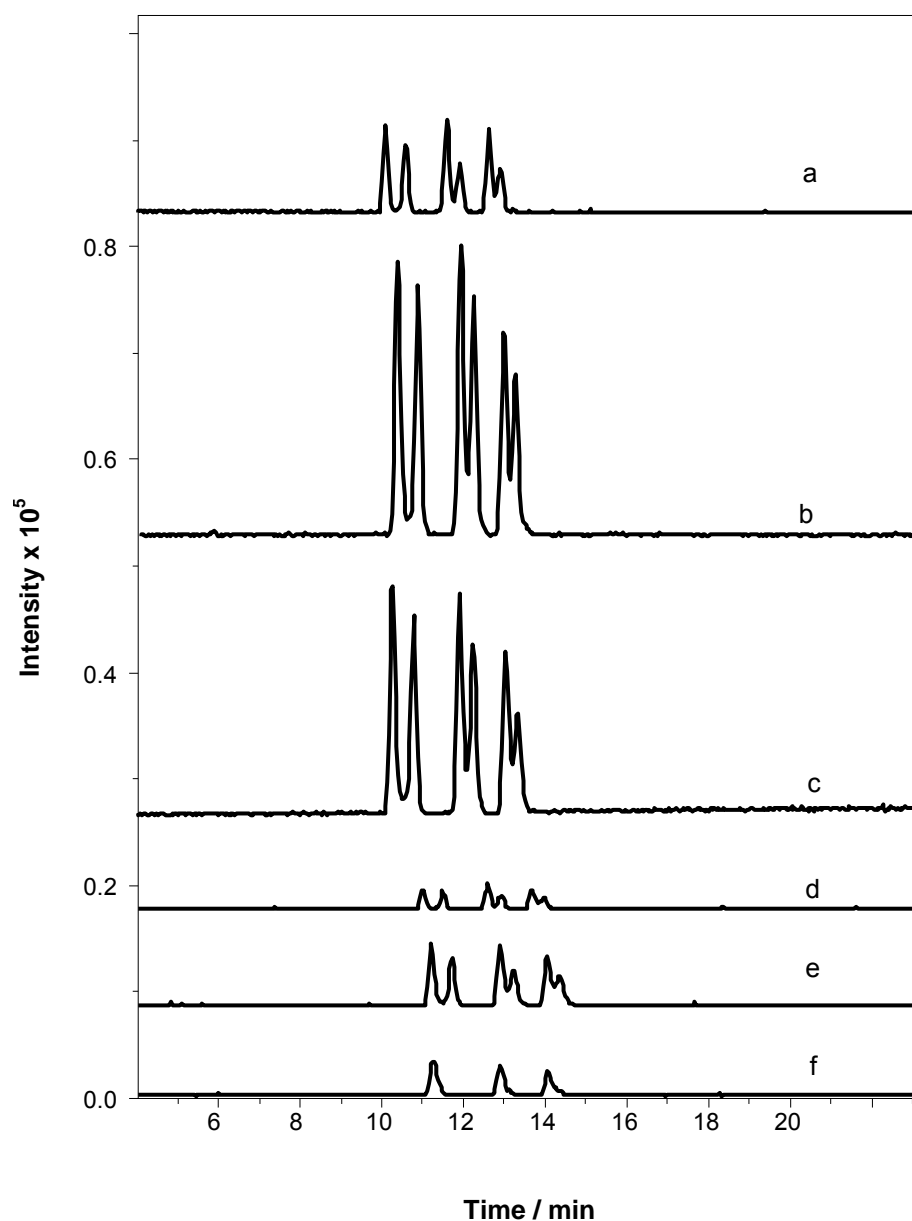


Figure 3-1: Separation of linear oligosaccharides at a concentration of 3 µg/ml. Gradient elution: mobile phase A-acetonitrile; mobile phase B-(a) 0.1% v/v formic acid,  $V_{inj}$  5 µl; (b) 0.1% v/v acetic acid,  $V_{inj}$  5 µl; (c) 0.1% v/v propionic acid,  $V_{inj}$  5 µl; (d) 10 mM ammonium formate pH 4.0,  $V_{inj}$  10 µl; (e) 10 mM ammonium acetate pH 7.2,  $V_{inj}$  10 µl; (f) 0.01% ammonia,  $V_{inj}$  5 µl.

Due to the separation of anomers, the oligosaccharides were eluted as double peaks when acids or ammonium buffers were used. This behaviour has been previously reported for graphitized carbon and HILIC stationary phases. However, compared to the amide HILIC and ZIC-HILIC, the graphitized carbon can be used over a wider pH range which allows additional choices of mobile phases with high pH, such as ammonia. When 0.01% ammonia solution, pH 10.6, was used as the aqueous mobile phase, the mutarotation was accelerated and oligosaccharides were eluted as a single broad peak. However, sensitivity was greatly reduced due to ionisation suppression. Aqueous acid solutions were therefore considered as more suitable mobile phases for the glycosylation analysis of MAbs, with emphasis on structural elucidation of minor glycan species. The highest sensitivity was achieved when mobile phases containing acetic and propionic acid were used (Figure 3–1). As expected, the sensitivity was reduced approximately by an order of magnitude for ammonium buffer solutions due to the ionisation suppression. Sensitivity was also three-fold lower when formic acid was used instead of acetic acid, and the similar decrease in sensitivity was observed when ammonium formate and ammonium acetate were compared. Since the method development was also focused on identification of charged glycans in the MAbs, ammonium acetate was not excluded as a possible mobile phase in the analysis of real samples. The choice of suitable eluents for glycosylation analysis of RNase B and MAbs required a further reduction of glycans with sodium borohydride in order to avoid the undesirable separation of anomers.

Variation in composition of the aqueous phase did not significantly affect the retention of the oligosaccharides, but it had a major effect on the ionisation of the oligosaccharides. When ammonium was not present in the eluent,  $[M+H]^+$  pseudomolecular ions were the dominant species, however a low amount of  $[M+NH_4]^+$  species was observed for all oligosaccharides (Figure 3–2A). It is suggested that ammonium originated from the sample. When ammonium buffers or ammonia were used, for larger oligosaccharides maltohexaose and

maltoheptaose, the strongest peaks observed were singly charged ammonium adducts and for the maltopentaose, the dominant peak was the protonated ion (Figure 3–2B).

The results suggest that the tendency to form ammonium adducts increases with increasing molecular mass of the glycan. Similar results were observed for the glycan standards separated in the HILIC mode. Under both experimental conditions, neutral losses of water and one glucose residue were observed and the prominence of in-source fragmentation decreased in the following order, M5>M6>M7 (Figure 3–2). The fragment ions resulting from neutral loss of one glucose residue were observed only for protonated species,  $[M+H]^+$  and  $[M-H_2O+H]^+$ , but not for ammonium adducts (not shown). The ionisation pattern suggests that ammonium stabilises oligosaccharides, similarly as reported for sodium adducts [101], therefore the ammonium adducts could not be fragmented in the ESI source. Since larger oligosaccharides exhibited greater preference to form ammonium adducts, the amount of in-source fragmentation decreased with increasing molecular weight, whereas the amount of ammonium adducts decreased in the reversed order.

### 3.3.2. Separation of mannose glycan standards

The same set of experiments was repeated for Man3 and Man9 glycan standards, which are more closely related to the glycans expected to be found in RNase B and the MABs. For both mannose glycans, separation of anomers on graphitized carbon column was observed, except for the separation when ammonia solution was used as the eluent, which was in agreement with previously obtained results for linear oligosaccharides (Figure 3–3 and Figure 3–4). The same negative effect of ammonium on sensitivity as described for linear oligosaccharides was observed. The sensitivity for M5–M7 and Man3 glycans was also three-fold lower for formic acid than when acetic acid was used as the mobile phase. Opposite to M5–M7, Man9 glycan eluted earlier than the smaller Man3 glycan. Since the

separation mechanism of oligosaccharides on PGC is not completely understood [86], the elution order of glycans is harder to predict compared to HILIC.

The effect of the mobile phase composition and pH on the retention of both glycans was negligible. However, differences in ionisation of Man3 and Man9 glycans were observed. Man3 glycan with a molecular weight similar to linear maltopentaose exhibited a similar ionisation pattern with dominating singly charged protonated ion under all experimental conditions used. For Man3 glycan, a neutral loss of water and one mannose residue was observed when acetic acid was used as a mobile phase; however, the intensity of fragment ions was very low (Figure 3–5A). Under all experimental conditions, a singly charged sodium adduct was present in the mass spectrum and no fragmentation was observed for this ion which is in agreement with results described above. When ammonium acetate was used as a mobile phase, only small peaks for ammonium and potassium adducts were observed (Figure 3–5B).

On the other hand, the larger Man9 glycan tended to form doubly charged species and under certain conditions extensive in-source fragmentation was observed (Figure 3–6). When low concentrations of acids were used as the mobile phase, a series of doubly charged ions with similar intensity were observed,  $[M+2H]^{2+}$ ,  $[M+H+NH_4]^{2+}$ ,  $[M+NH_4+Na]^{2+}$ . A strong singly protonated ion was also found in the mass spectrum. When acetic acid was used as an eluent, strong peaks for doubly protonated Man4 to Man8 fragment ions were observed; however the other doubly charged species of fragment ions were not found in the mass spectrum. The fragmentation pattern suggests that the doubly protonated ions are less stable in the ESI source, as previously observed for the oligosaccharides and this results in the neutral loss of mannose residues. It is suggested that formation of ammonium and sodium adducts stabilises the ions in the ESI source.

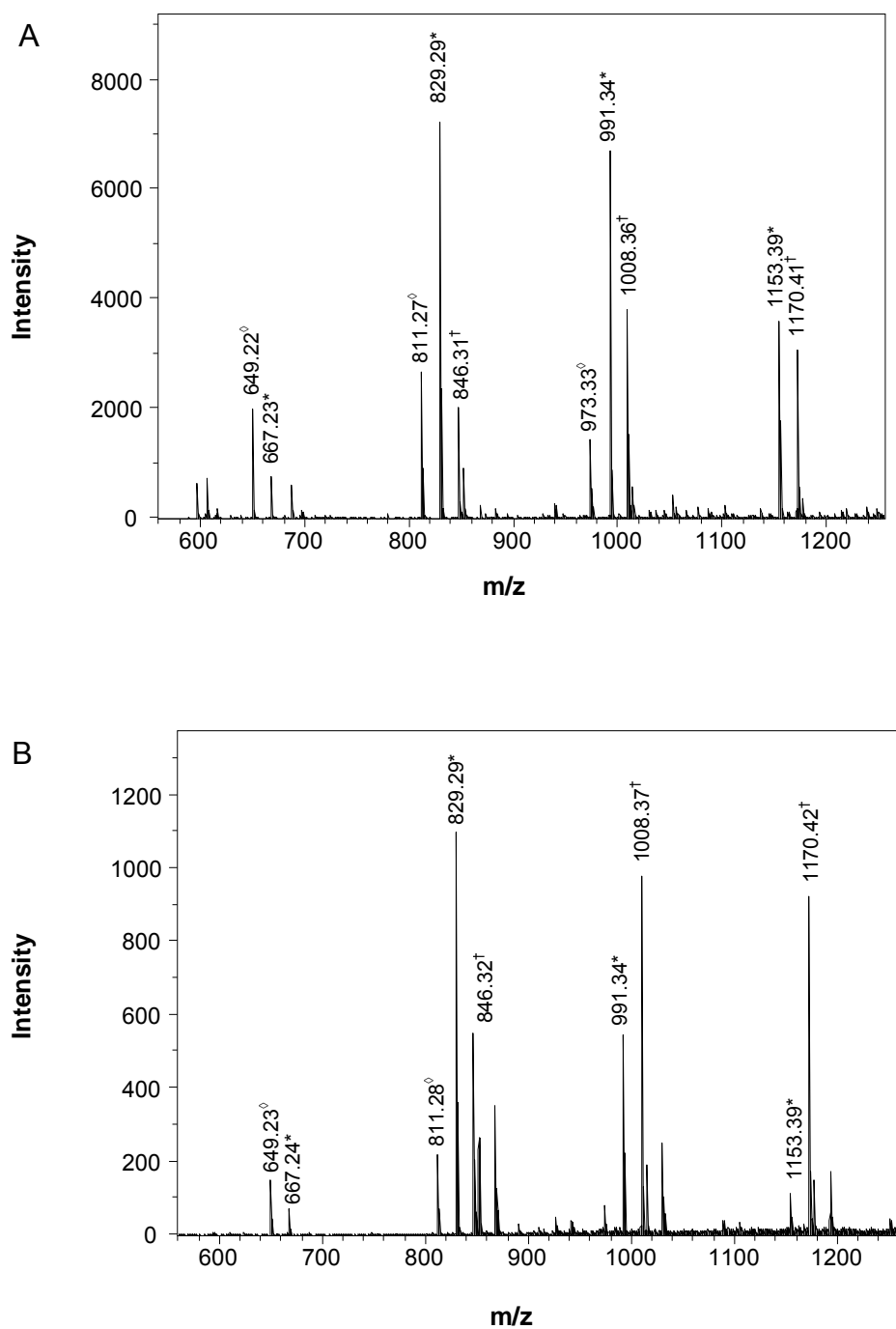


Figure 3-2: Average mass spectra over the maltopentaose, maltohexaose and maltoheptaose elution range. Gradient elution: mobile phase A-acetonitrile, mobile phase B-(A) 0.1% acetic acid, (B) 10 mM ammonium acetate pH 7.2. \* Protonated species  $[M+H]^+$ ;  $^{\diamond}$  protonated fragments with neutral loss of water  $[M-H_2O+H]^+$ ;  $^{\dagger}$  ammonium adducts  $[M+NH_4]^+$ .

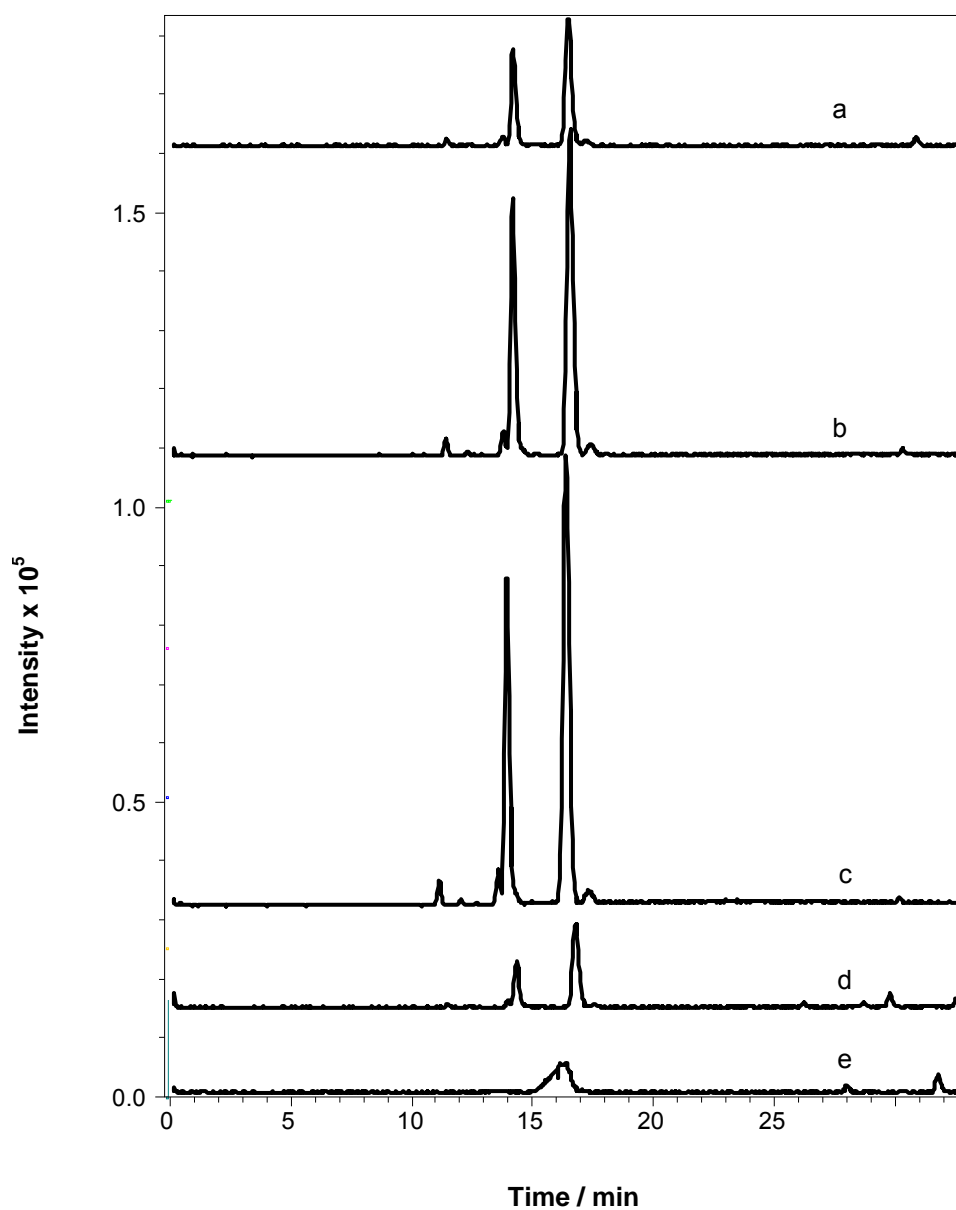


Figure 3-3: Base peak chromatograms of Man3 glycan at a concentration of 10 µg/ml. Gradient elution: mobile phase A-acetonitrile; mobile phase B-(a) 0.1% v/v formic acid,  $V_{inj}$  5 µl; (b) 0.1% v/v acetic acid,  $V_{inj}$  5 µl; (c) 0.1% v/v propionic acid,  $V_{inj}$  5 µl; (d) 10 mM ammonium acetate pH 7.2,  $V_{inj}$  10 µl; (e) 0.01% ammonia,  $V_{inj}$  5 µl. When ammonium was present in the mobile phase, the sensitivity was reduced for an order of magnitude. When ammonia was used, the Man3 glycan eluted as a single broad peak.

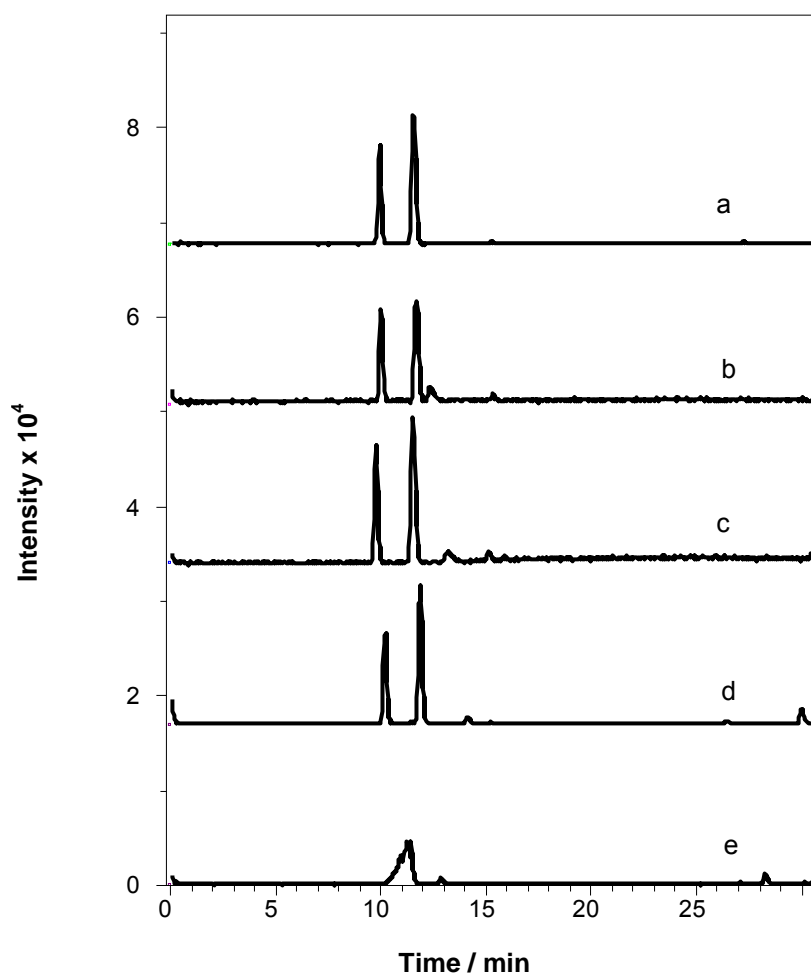


Figure 3-4: Base peak chromatograms of Man9 glycan at a concentration of 20 µg/ml. Gradient elution: mobile phase A-acetonitrile; mobile phase B-(a) 0.1% v/v formic acid,  $V_{inj}$  5 µl; (b) 0.1% v/v acetic acid,  $V_{inj}$  5 µl; (c) 0.1% v/v propionic acid,  $V_{inj}$  5 µl; (d) 10 mM ammonium acetate pH 7.2,  $V_{inj}$  10 µl; (e) 0.01% ammonia,  $V_{inj}$  5 µl.

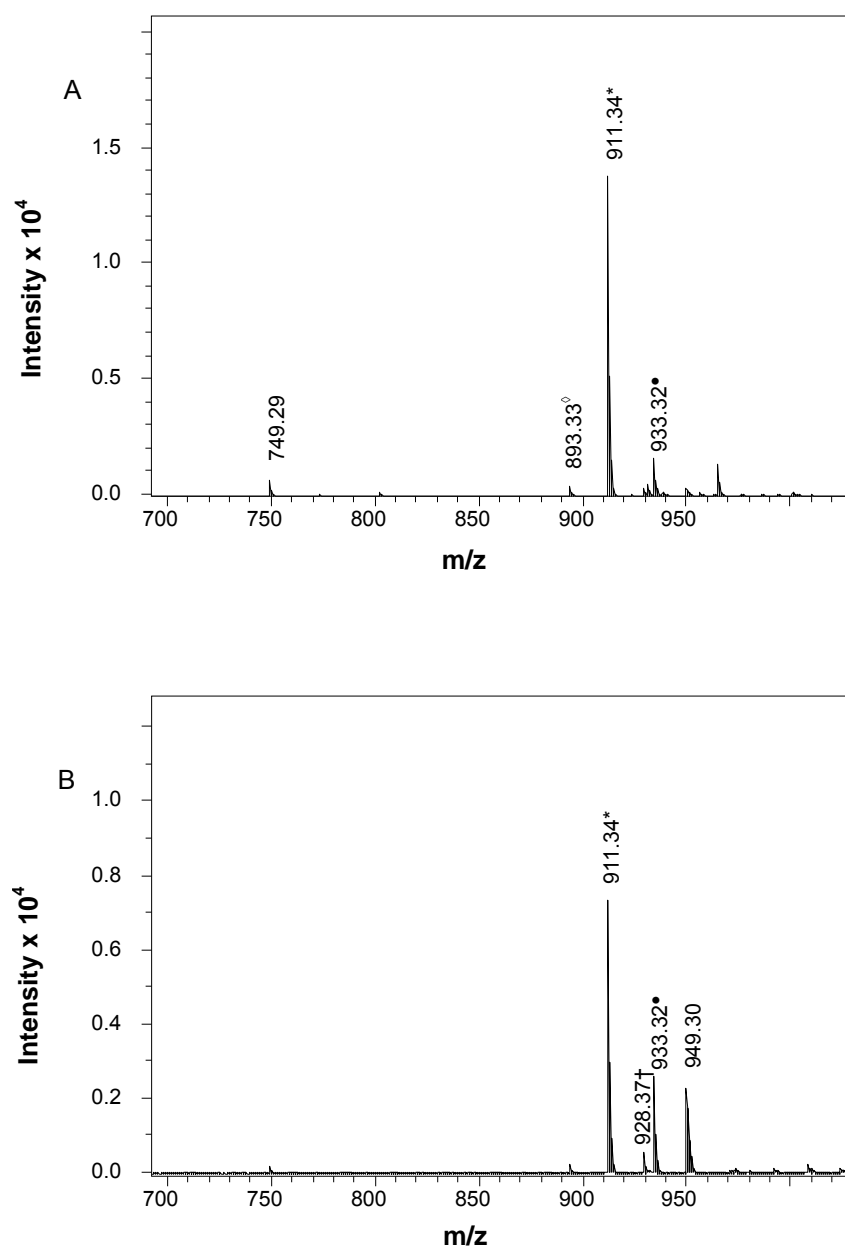


Figure 3-5: Average mass spectra over the Man3 elution range. Gradient elution: mobile phase A-acetonitrile, mobile phase B-(A) 0.1% acetic acid, (B) 10 mM ammonium acetate pH 7.2. \* Protonated species  $[M+H]^+$ ;  $\diamond$  protonated fragments with neutral loss of water  $[M-H_2O+H]^+$ ;  $\dagger$  ammonium adducts  $[M+NH_4]^+$ ;  $\bullet$  sodium adduct  $[M+Na]^+$ .



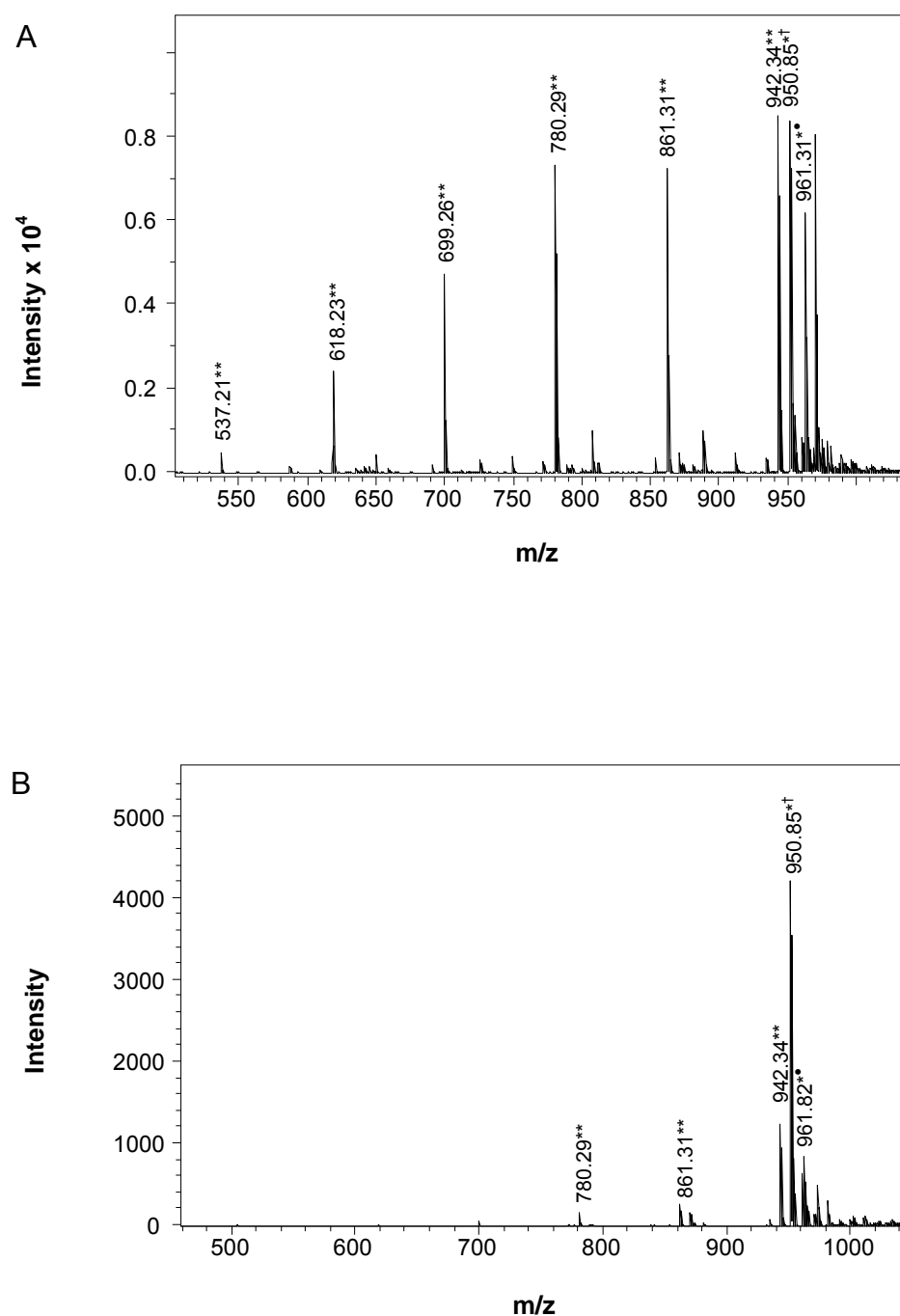


Figure 3-6: Average mass spectra over the Man9 elution range. Gradient elution: mobile phase A-acetonitrile, mobile phase B-(A) 0.1% acetic acid, (B) 10 mM ammonium acetate pH 7.2 \*\* Protonated species  $[M+2H]^{2+}$ ; \*† proton and ammonium adducts  $[M+H+NH_4]^{2+}$ , \*• proton and sodium adducts  $[M+H+Na]^{2+}$ .

When ammonium was present in the eluent, the dominant peak found in the mass spectrum was the  $[M+H+NH_4]^{2+}$  ion. A small peak for the singly charged ammonium adduct was also observed. The in-source fragmentation was almost negligible when ammonium acetate was used as a mobile phase. Only small peaks for doubly protonated fragment ions were observed in the mass spectrum, indicating the neutral loss of mannose residues. Again, the ionisation pattern suggested the stabilising effect of ammonium on fragmentation of glycans in the ESI source. The effect of mobile phase on the sensitivity of Man9 glycan was less pronounced compared to the smaller glycans used in the experiment. Understanding the ionisation of glycans in the ESI-MS source is vital for identification of glycans in complex real samples. Mobile phases containing acetic acid and ammonium acetate were selected as the most suitable mobile phases for further method development for separation of high mannose and complex-type glycans from RNase B and MAbs.

### ***3.3.3. Separation of glycans from RNase B***

PGC was used for the separation of glycans from RNase B and the chromatograms of high mannose glycans are shown in Figure 3-7. Acetic acid was used as an aqueous mobile phase in order to achieve optimum sensitivity. Truncated Man5-GlcNAc and Man6-GlcNAc glycans were found in the sample confirming the Endo H contamination previously observed for 2-AB labelled glycans separated by ZIC-HILIC. The truncated high mannose glycans exhibited lower retention on PGC compared to the PNGase F cleavage products. Opposite to the HILIC separation, the order of elution of Man5-Man9 glycans did not correlate with the molecular weight of the glycans. The most strongly retained was Man5 glycan, whereas Man6 to Man9 glycans were eluted in a very narrow elution window without a specific order. More important, the three Man7 glycans were completely separated, which confirms the previously reported capability of graphitized carbon to separate structural isomers [37].

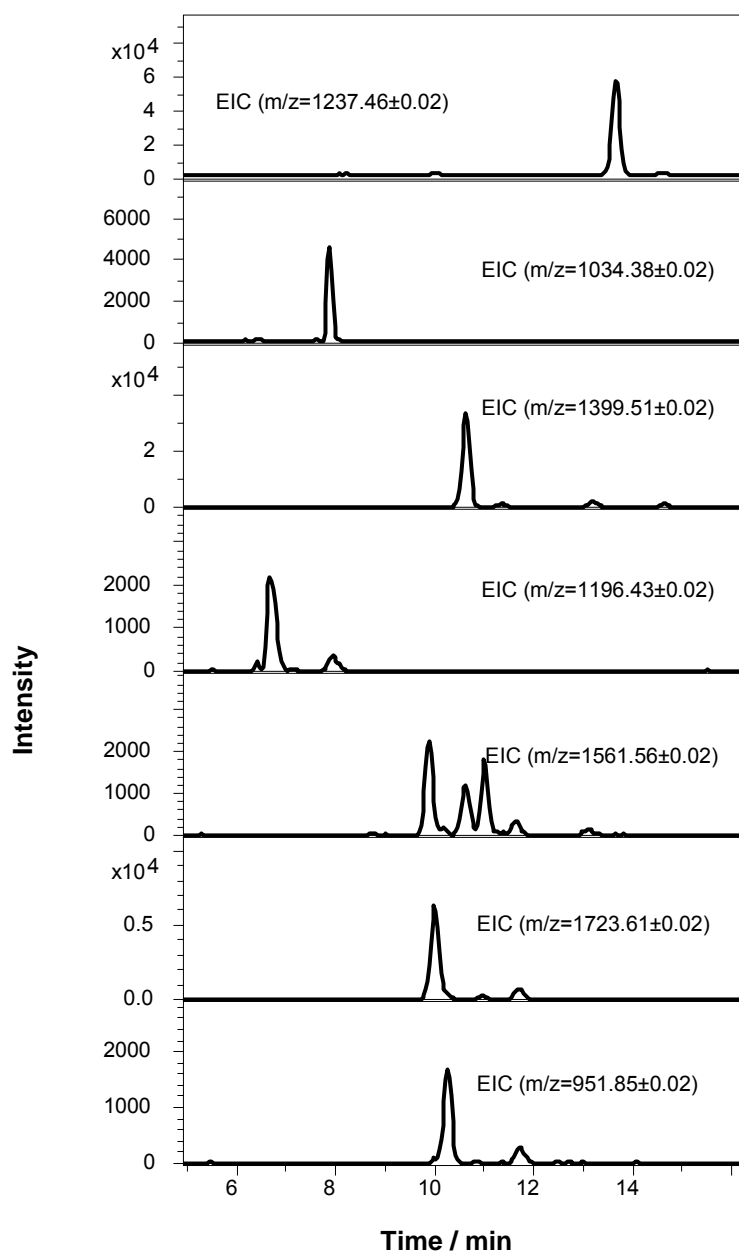


Figure 3-7: Extracted ion chromatograms of reduced glycans from RNase B obtained with graphitized carbon coupled with ESI-MS. Gradient elution: mobile phase A-acetonitrile; mobile phase B-0.1% v/v acetic acid, pH 3.25. Three Man7 structural isomers are baseline resolved. A small amount of unreduced glycans is found in the sample, and was eluted after the corresponding reduced form.

For Man5-Man7 glycans, a strong singly charged protonated ion was observed (Figure 3–8), whereas Man8 and Man9 exhibited more complex mass spectra with singly and doubly charged species, as summarised in Table 3-1. This result is consistent with the data obtained for the reducing Man3 and Man9 glycan standards, indicating that ionisation of high mannose glycans depends on the size of the molecule, with higher preference for doubly charged ions for larger glycan species.

The glycan profile of RNase B was consistent with the results previously obtained by amide HILIC and ZIC-HILIC. Furthermore, graphitized carbon allowed baseline separation of Man7 structural isomers, which in the HILIC mode were only partially resolved.

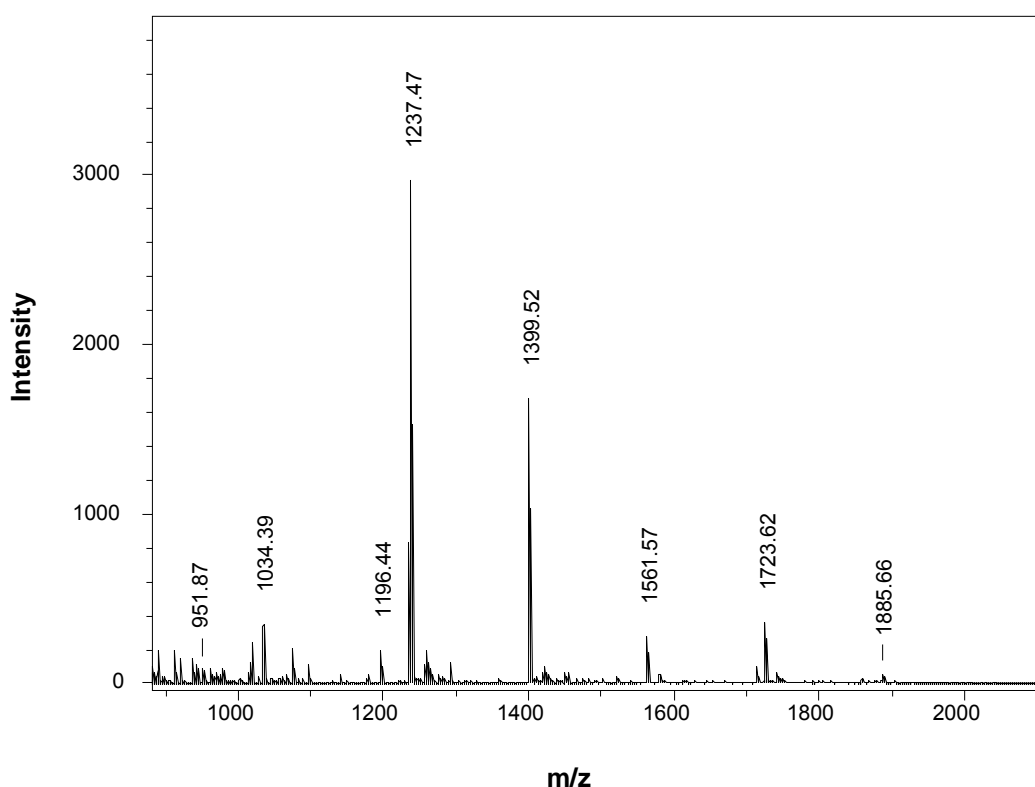
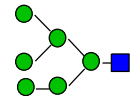
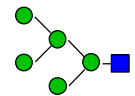
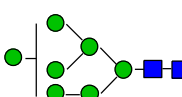
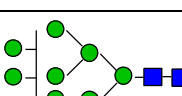
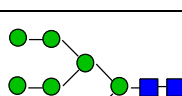
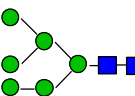
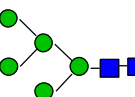


Figure 3–8: Average mass spectrum of reduced glycans from RNase B obtained with graphitized carbon coupled with ESI-MS. Gradient elution: mobile phase A-acetonitrile; mobile phase B-0.1% acetic acid. For Man5-Man8 the strongest observed peaks are  $[M+H]^+$  ions, and for Man9 a number of singly and doubly charged ions were identified. Endo H cleavage products, Man5-GlcNAc and Man6-GlcNAc, are observed.

Table 3-1: Retention times and measured m/z for reduced glycans found in RNase B.

Glycan composition	Glycan	Structure	(m/z) <sub>theoretical, red</sub> [M+H] <sup>+</sup> [M+2H] <sup>2+</sup>	Ions found	Retention time / min
(Man) <sub>3</sub> (Man) <sub>3</sub> (GlcNAc) <sub>1</sub>	Man6-GlcNAc		1196.43 598.72	[M+H] <sup>+</sup>	6.7
(Man) <sub>2</sub> (Man) <sub>3</sub> (GlcNAc) <sub>1</sub>	Man5-GlcNAc		1034.38 517.69	[M+H] <sup>+</sup>	7.9
(Man) <sub>4</sub> (Man) <sub>3</sub> (GlcNAc) <sub>2</sub>	Man7		1561.56 781.28	[M+H] <sup>+</sup>	9.9 10.6 11.0
(Man) <sub>5</sub> (Man) <sub>3</sub> (GlcNAc) <sub>2</sub>	Man8		1723.61 862.31	[M+H] <sup>+</sup> [M+2H] <sup>2+</sup>	10.0
(Man) <sub>6</sub> (Man) <sub>3</sub> (GlcNAc) <sub>2</sub>	Man9		1885.67 943.34	[M+H] <sup>+</sup> [M+2H] <sup>2+</sup> [M+H+NH <sub>4</sub> ] <sup>2+</sup>	10.2
(Man) <sub>3</sub> (Man) <sub>3</sub> (GlcNAc) <sub>2</sub>	Man6		1399.51 700.26	[M+H] <sup>+</sup>	10.6
(Man) <sub>2</sub> (Man) <sub>3</sub> (GlcNAc) <sub>2</sub>	Man5		1237.46 619.23	[M+H] <sup>+</sup>	13.6

### 3.3.4. Glycan profiling of monoclonal antibodies using PGC

The use of graphitized PGC was also demonstrated for reduced glycans from monoclonal antibodies, which are summarised in Table 3-2. Symbols (a)-(l) are used for glycan chromatogram traces shown in Figure 3-9 to Figure 3-11. Similar glycan profiles compared to the profiles obtained by the HILIC amide and ZIC-HILIC methods were expected; however, a few significant differences were observed. Opposite to the high mannose glycans, the order of elution of the most abundant G0, G1 and G2 complex-type glycans was the same as in the amide HILIC and ZIC-HILIC separation, where retention increased with increasing molecular weight. The difference in retention properties for high mannose and complex-type glycans suggested a more complex mechanism of interaction with the stationary phase which depends on the glycan composition, structure and size of the glycans.

For MAb1 and MAb2 most of the glycans identified with the HILIC amide and ZIC-HILIC methods were found in the samples. Using the PGC column, a G0-Fuc glycan was identified ((a) in Figure 3-9 and Figure 3-10), which was eluted before the G0-GlcNAc. The G0-Fuc glycan has not been identified by the standard amide HILIC method for the separation of 2-AB labelled glycans, but it was observed in the 2-AB labelled form when analysed by ZIC-HILIC. The results indicate that the new method is complementary to the standard procedure and the complete glycan profile could not be obtained by a single method only.

Under the conditions applied, the G1 glycans were partially separated ((g), Figure 3-9 to Figure 3-11). For the G0-GlcNAc ((c), Figure 3-9 to Figure 3-11), several peaks were found, where the first peak belonged to the glycan and the later peaks were in-source fragments of G0 and G1. The fragmentation pattern suggests a neutral loss of terminal GlcNAc of non-galactosylated antenna in G0.

Table 3-2: Proposed structures and retention times of the reduced glycans found in MAb.

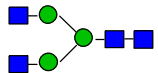
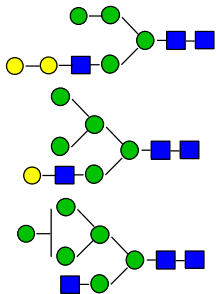
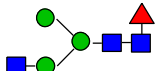
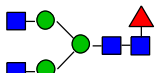
Glycan composition	Symbol	Possible structures	(m/z) <sub>theoretical, red</sub> [M+H] <sup>+</sup> [M+2H] <sup>2+</sup>	Ions found	Retention time / min	MAb1	MAb2	MAb3
(HexNAc) <sub>2</sub> (Man) <sub>3</sub> (GlcNAc) <sub>2</sub>	a / G0-Fuc		1319.51 660.26	[M+H] <sup>+</sup>	10.3	+	+	-
(Hex) <sub>3</sub> (HexNAc) <sub>1</sub> (Man) <sub>3</sub> (GlcNAc) <sub>2</sub>	b / Hyb2		1602.59 801.80	[M+2H] <sup>2+</sup>	12.2	-	-	+
(HexNAc) <sub>1</sub> (dHex) <sub>1</sub> (Man) <sub>3</sub> (GlcNAc) <sub>2</sub>	c / G0-GlcNAc		1262.49 631.75	[M+H] <sup>+</sup>	12.6 13.6 14.4 14.7	+	+	+
(HexNAc) <sub>2</sub> (dHex) <sub>1</sub> (Man) <sub>3</sub> (GlcNAc) <sub>2</sub>	d / G0		1465.57 733.29	[M+H] <sup>+</sup> [M+2H] <sup>2+</sup>	13.6	+	+	+

Table 3-2 continued...

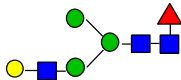
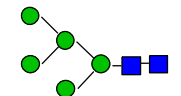
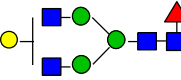
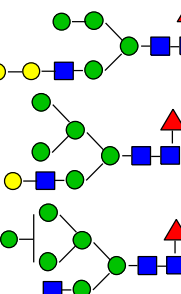
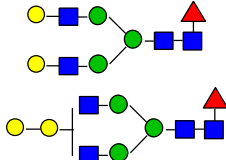
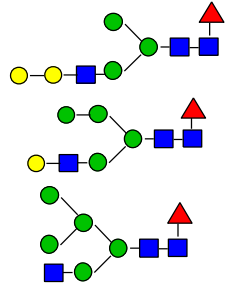
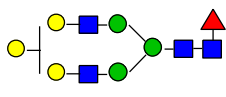
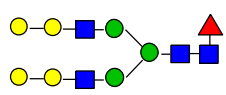
(Hex) <sub>1</sub> (HexNAc) <sub>1</sub> (dHex) <sub>1</sub> (Man) <sub>3</sub> (GlcNAc) <sub>2</sub>	e / G1-GlcNAc		1424.54 712.77	[M+H] <sup>+</sup>	14.0 14.4 14.7 15.5	-	-	+
(Hex) <sub>2</sub> (Man) <sub>3</sub> (GlcNAc) <sub>2</sub>	f / Man5		1237.46 619.23	[M+H] <sup>+</sup>	14.3	+	+	+
(Hex) <sub>1</sub> (HexNAc) <sub>2</sub> (dHex) <sub>1</sub> (Man) <sub>3</sub> (GlcNAc) <sub>2</sub>	g / G1		1627.62 814.31	[M+2H] <sup>2+</sup> [M+H] <sup>+</sup>	14.4 14.7	+	+	+
(Hex) <sub>3</sub> (HexNAc) <sub>1</sub> (dHex) <sub>1</sub> (Man) <sub>3</sub> (GlcNAc) <sub>2</sub>	h / Hyb2F		1748.65 874.83	[M+2H] <sup>2+</sup>	15.1 15.7	-	-	+



Table 3-2 continued...

(Hex) <sub>2</sub> (HexNAc) <sub>2</sub> (dHex) <sub>1</sub> (Man) <sub>3</sub> (GlcNAc) <sub>2</sub>	i / G2		1789.67 895.34	[M+2H] <sup>2+</sup>	15.5 16.3 17.0	+	+	+
(Hex) <sub>2</sub> (HexNAc) <sub>1</sub> (dHex) <sub>1</sub> (Man) <sub>3</sub> (GlcNAc) <sub>2</sub>	j / G2-GlcNAc / Hyb1F		1586.59 793.80	[M+2H] <sup>2+</sup>	13.2 16.4	-	-	+
(Hex) <sub>3</sub> (HexNAc) <sub>2</sub> (dHex) <sub>1</sub> (Man) <sub>3</sub> (GlcNAc) <sub>2</sub>	k / G2+Gal		1951.73 976.37	[M+2H] <sup>2+</sup>	17.2 17.7	-	-	+
(Hex) <sub>4</sub> (HexNAc) <sub>2</sub> (dHex) <sub>1</sub> (Man) <sub>3</sub> (GlcNAc) <sub>2</sub>	l / G2+2Gal		2113.78 1057.39	[M+2H] <sup>2+</sup>	18.9	-	-	+

+ glycan was confirmed; - glycan not found in the sample.

In-source fragmentation.

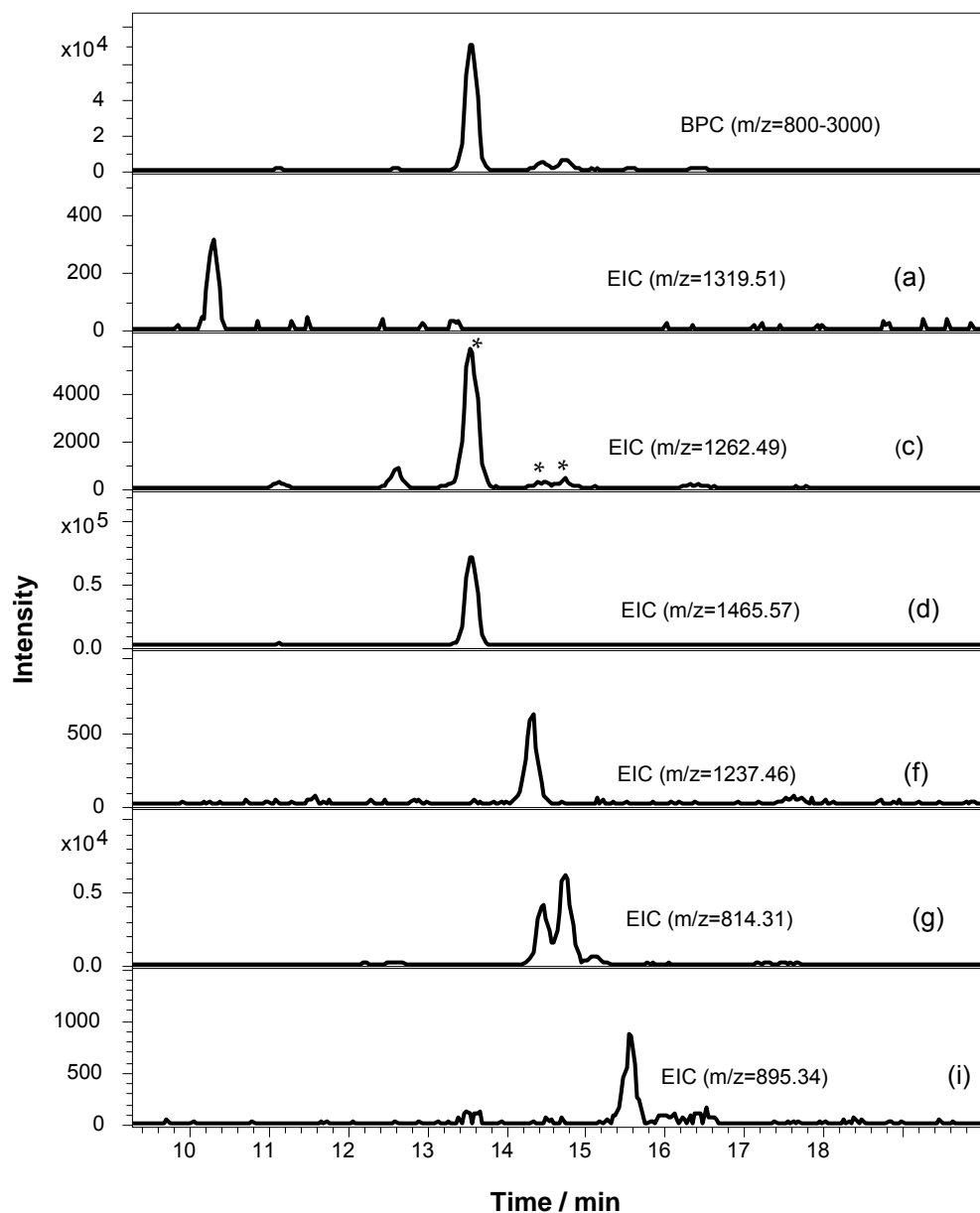


Figure 3-9: Base peak chromatogram and extracted ion chromatograms of reduced glycans from MAb1 obtained with graphitized carbon coupled with ESI-MS. Gradient elution: mobile phase A-acetonitrile; mobile phase B-0.1% v/v acetic acid, pH 3.25. G1 glycan isomers are partially separated. Extensive in-source fragmentation (\*) of terminal GlcNAc is observed.

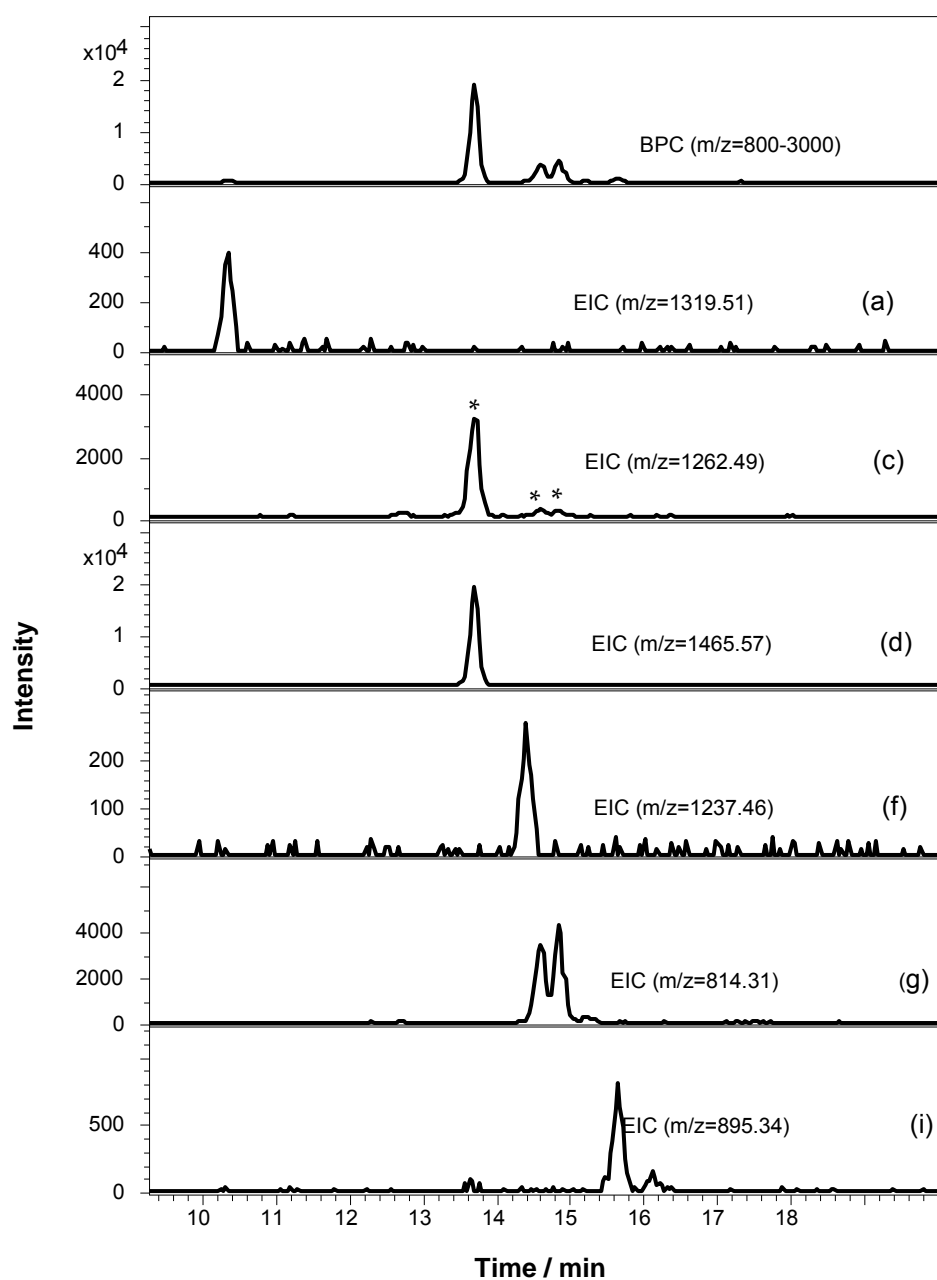


Figure 3-10: Base peak chromatogram and extracted ion chromatograms of reduced glycans from MAb2 obtained with graphitized carbon coupled with ESI-MS. Gradient elution: mobile phase A-acetonitrile; mobile phase B-0.1% v/v acetic acid, pH 3.25. \* In-source fragmentation.

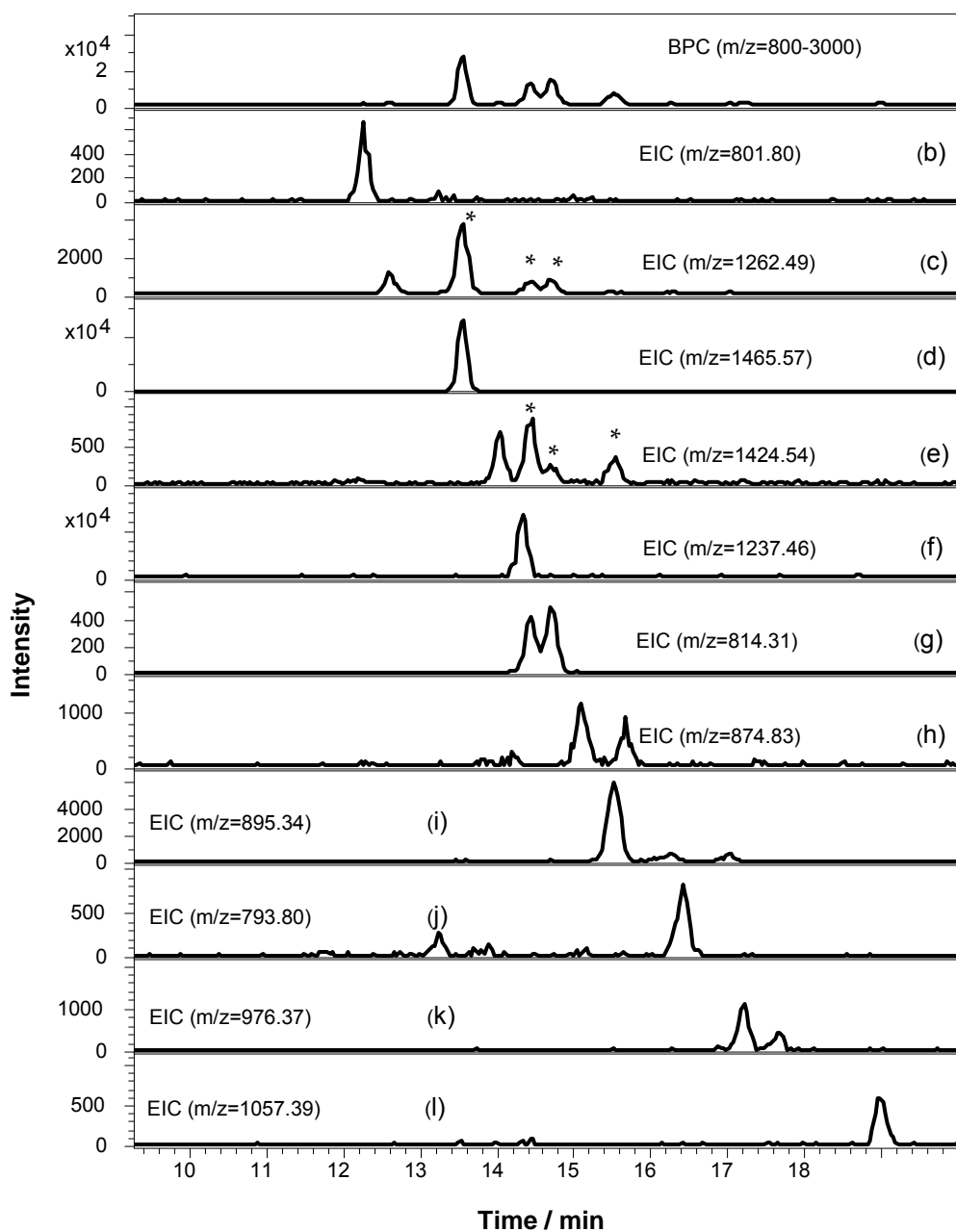


Figure 3–11: Base peak chromatogram and extracted ion chromatograms of reduced glycans from MAb3 obtained with graphitized carbon coupled with ESI-MS. Gradient elution: mobile phase A-acetonitrile; mobile phase B-0.1% v/v acetic acid, pH 3.25. Several isobaric structures of (h), (i), (j) and (k) glycan species are observed. Extensive in-source fragmentation (\*) of G0, G1 and G2 glycan is observed.

However, the G1 fragmentation seemed more complex. For none of the G1 isomers was the loss of galactose confirmed, and for both G1 glycan isomers, a fragment peak of G0-GlcNAc with the same intensity was observed, indicating the loss of GlcNAcGal fragment with no preference for either 3- or 6- arm of the glycans.

A very low intensity peak was found for G1-GlcNAc glycan (not shown), with the same retention time as the first G1 glycan isomer, and it cannot be confirmed whether the peak represents the G1-GlcNAc glycan or an in-source fragment of the G1 glycan isomer. Extensive fragmentation in the position between the core mannose and GlcNAc of both arms, suggested the instability of this bond which was further destabilised by the terminal galactose. Abundant fragment ions resulting from loss of terminal GlcNAc have been previously observed for complex N-glycans [100]. The fragmentation will be further discussed by reference to the glycans from MAb3, which exhibited a different distribution of galactosylated glycan species and presence of  $\alpha$ - and  $\beta$ -galactosylation. In MAb1 and MAb2, which were expressed in CHO cells, only  $\beta$ -linked terminal galactose is expected to be found and the single peak observed for G2 glycan was in agreement with the theoretical prediction ((i) in Figure 3–9 and Figure 3–10).

The glycan profile of MAb3 (Figure 3–11) exhibited greater complexity compared to MAb1 and MAb2, with several previously unidentified glycans observed. No defucosylated complex glycans were confirmed in this sample, and a different galactosylation pattern compared to MAb1 and MAb2 was observed. Single peaks were observed for G0 and Man5 glycans with single likely structural isomers. G1 structural isomers were partially separated, as observed already for MAb1 and MAb2. For the G2 chromatogram ((i) in Figure 3–11), three baseline-separated peaks were observed. The first and the most intense peak exhibited the same retention as G2 glycans from MAb1 and MAb2 and indicated the presence of the glycan with 2  $\beta$ -linked galactose units attached to two terminal GlcNAcs, which forms one possible structural isomer. The other two minor peaks most likely corresponded to two glycan isomers with two elongated galactose units on

one antenna, where the first galactose is  $\beta$ -linked to GlcNAc and the second one is  $\alpha$ -linked to the galactose. No preference for either of the antennae is expected and similar peak intensity for both isomers is in agreement with the predicted structures.

Two new structures, G3 and G4, which additionally confirmed the  $\alpha$ -galactosylation pattern in MAb3, were observed ((k) and (l) in Figure 3–11). For the G4 glycan a single peak was observed in the chromatogram which probably corresponded to the only likely structure containing two  $\alpha$ -linked galactose residues on both of the antennae. On the other hand, for the G3 glycan two peaks were observed in the chromatogram, which most likely represent two structural isomers with an  $\alpha$ -linked galactose on either of the antennae. Both isomers are likely to exist as structures represented in the Table 3-2.

At 12.2 min a peak of defucosylated hybrid Hyb2 glycan species was observed ((b), Figure 3–11), which could represent any of 3 possible structures in Table 3-2. Since the  $\alpha$ -galactosylation was confirmed in MAb3, it is suggested that the  $\alpha$ -galactosylated structure is the most likely glycan species; however, structural elucidation is not possible for this chromatogram trace. As previously observed, the only defucosylated glycan species G0-Fuc, found in MAb1 and MAb2 was also eluted earlier compared to the fucosylated glycan form G0 ((a) and (d) in Figure 3–9 Figure 3–10). For the Hyb2F glycan ((h), Figure 3–11) which contains additional fucose compared to Hyb2, two peaks were observed and three possible hybrid structures with the same elemental composition are suggested, each with 3 hexose (galactose or mannose) residues (Table 3-2). Hyb2 and Hyb2F structures with GlcNAc on the 3-arm and mannose residues on the 6-arm are likely to exist in the MAb3 sample. With the existing data it was impossible to conclude which of the structures are present in the sample.

For  $m/z=793.80$  two peaks were observed, with very different retention properties ((j), Figure 3–11). Similarly as for Hyb2 and Hyb2F glycans, three possible glycan structures with the same elemental composition and various degrees of mannosylation and galactosylation were predicted. Since glycans

containing one GlcNAc generally exist only as the 3-arm isomers, all the three glycans are likely to exist in one structural form, as presented in Table 3-2. Due to the significant amount of  $\alpha$ -galactosylation present in the MAb3, hypergalactosylated species G2-GlcNAc and a Hyb1F glycan seem to be the most likely candidates, however further analysis will be required to elucidate the possible structures of the two glycan species.

Extensive in-source fragmentation was also observed in the MAb3 chromatogram. For G0-GlcNAc and G1-GlcNAc several peaks were observed ((c) and (e), Figure 3–11). The first peak for both chromatogram traces corresponded to G0-GlcNAc and G1-GlcNAc glycans, and later peaks that overlap with G0, G1 and G2, corresponded to fragments of these glycan species. It was again confirmed that the fragmentation occurred on the bond between the core mannose and GlcNAc. The neutral loss of GlcNAc and GlcNAcGal fragments was observed, where the loss of GlcNAc occurred on both G1 isomers with similar intensity and the loss of GlcNAcGal was more prominent on the early eluted G1 isomer. The results were not sufficient for the final conclusion of the terminal galactose position in G1 structural isomers; however, they indicated that stabilities of 3- and 6-linked GlcNAcs were not the same.

The complex galactosylation pattern in MAb3 was not surprising, considering that MAb3 was expressed in NS0 murine cell line which exhibits  $\alpha$ -galactosyltransferase activity which is generally not found in CHO cells.

Further MS/MS experiments in combination with exoglycosidase treatment will be required for complete structural elucidation of glycan species found in MAb3. However, it is noted that the MS/MS experiments alone may not be sufficient to confirm the isobaric structures containing mannose and/or galactose building blocks, since the fragmentation pattern of these glycan species would be very similar. On the other hand, treatment of glycans with various exoglycosidases (mannosidase,  $\alpha$ - and  $\beta$ -galactosidase, fucosidase) will provide not only the information on terminal glycan residues but also the linkages.

The ionisation pattern for MAb glycans was significantly different to that of high mannose glycans from RNase B. The dominant ions were singly and doubly charged protonated ions, and ammonium adducts were observed for the oligomannosidic glycans. Again, the higher preference for doubly charged glycans was observed for larger glycans, as shown in Figure 3–12. For G0-GlcNAc the main singly protonated ion was observed, whereas G0 exhibited two strong signals for  $[M+H]^+$  and  $[M+2H]^{2+}$ , with lower intensity for the latter. The situation for G1 was reversed, with the stronger peak for doubly protonated species. For G2 and  $\alpha$ -galactosylated glycans G3 and G4, only the  $[M+2H]^{2+}$  was found in the mass spectrum.

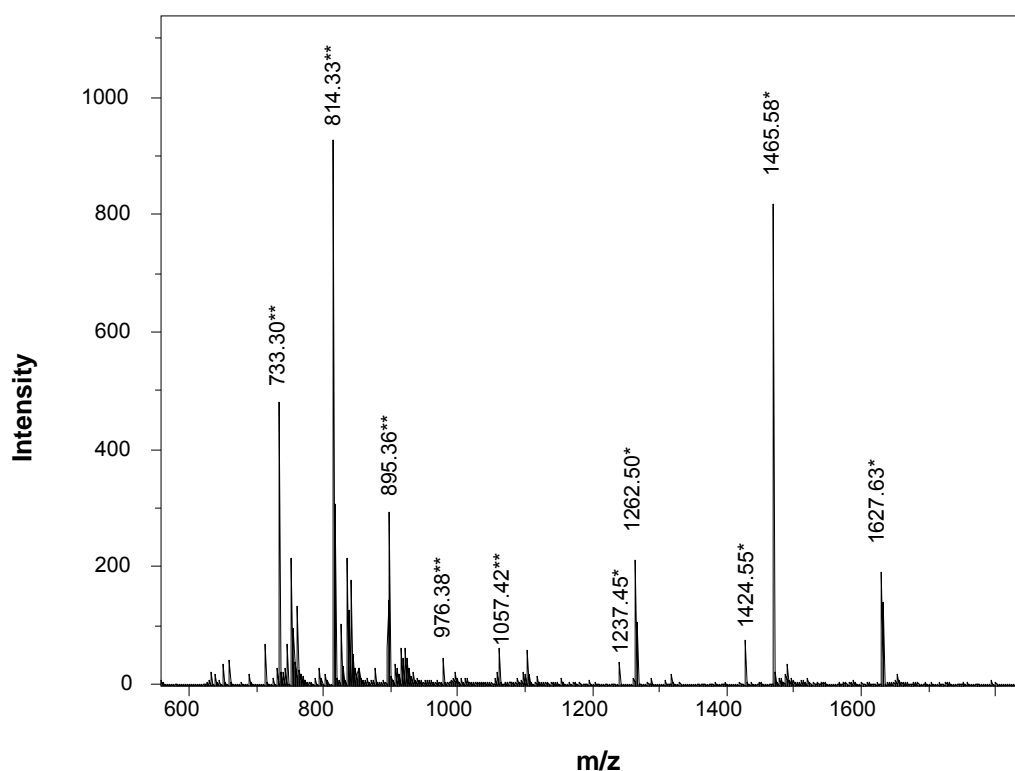


Figure 3–12: Average mass spectrum of reduced glycans from MAb3 obtained with graphitized carbon coupled with ESI-MS. Gradient elution: mobile phase A-acetonitrile; mobile phase B-0.1% acetic acid. Singly and doubly protonated species were observed for G0 and G1 glycans. Doubly protonated forms were dominant for larger glycans. \*Singly protonated ions; \*\*doubly protonated ions.



It is important to emphasize that it is possible that under the conditions applied, the charged glycans may not have been eluted and absence of peaks for sialic acids containing glycans, observed with the HILIC amide separation of 2-AB labelled glycans, might not be due only to the low sensitivity. It has been previously suggested that for elution of charged glycans from the graphitized carbon column, a mobile phase with acid is not sufficient and ammonium buffers with certain ionic strength are required [87]. To see if any sialic acid-containing glycans can be detected, the glycans were separated on graphitized carbon using 6 mM ammonium acetate pH 7.2 in water as an eluent B. When ammonium was present in the mobile phase, a significant suppression of ionisation was observed and only the peaks for the most abundant glycans were identified (not shown) and therefore the presence of sialic acids glycans could not be confirmed.

It has been demonstrated that none of the described methods provided the complete glycan profile of the monoclonal antibodies and the separation using graphitized carbon gave complementary results with more detailed information about the presence of structural isomers in the sample and the less common glycosylation patterns, such as additional  $\alpha$ -linked galactose in the antennae of complex glycans.

### 3.4. Conclusions

Graphitized carbon is shown to be a good alternative to HILIC in glycosylation analysis; however, none of the described HILIC and graphitized carbon methods provided the complete glycan profile of the monoclonal antibodies used in this study. Graphitized carbon is commonly used for separation of reduced glycans and coupled to ESI-MS. Compared to the standard method for separation of 2-AB labelled glycans using HILIC amide coupled with fluorescence detection the graphitized carbon separation exhibits lower sensitivity, which is the main drawback of methods which do not include fluorescent labelling. On the other hand, the chromatographic run time was shorter compared to the previously described HILIC amide and ZIC-HILIC methods and expensive and time

consuming labelling was replaced by simple reduction using sodium borohydride. The graphitized carbon separation mechanism is not yet completely understood and the order of elution of glycans does not necessarily correlate with the size of glycans, as previously seen for HILIC separations. However, the graphitized carbon has superior capabilities for the separation of isobaric glycans compared to the HILIC columns used in this study and several structural isomers were successfully resolved using this method. The separation of structural isomers can be extremely important when monoclonal antibodies with more complex glycosylation patterns consisting of hybrid and highly galactosylated complex glycans with elongated antennae are being analysed. Frequently, a variety of structures with different branching or degree of mannosylation and galactosylation are possible for a single molecular mass. Although some of the isomers can be completely separated using graphitized carbon, structural elucidation is often not possible and analysis combined with exoglycosidases treatment may be required. It was demonstrated that the best sensitivity was achieved when a low concentration of acid was used as an aqueous mobile phase, although this promoted the in-source fragmentation of larger glycans. Ionisation of glycans was significantly suppressed when ammonium buffers were used as a mobile phase, which reduced sensitivity and resulted in the loss of signals for minor glycans species. No charged glycans were identified using graphitized carbon, probably due to two reasons. It is likely that the sialic acids-containing glycans were strongly retained by the stationary phase when low concentrations of acids were used as a mobile phase. When ammonium buffers were used, the sensitivity of ESI-MS detection was reduced due to the suppressed ionisation and low abundance negatively charged glycans could not be detected. The sensitivity of ESI-MS detection of reduced glycans could be enhanced by miniaturisation and this will be further examined in the following chapter.

## Chapter Four

### *4. Nano LC separation of glycans*

#### **4.1. Introduction**

An alternative strategy for glycan profiling with improved sensitivity is the separation of underivatized glycans using nanoscale LC coupled with mass spectrometric detection. The improved sensitivity is mainly due to lower chromatographic dilution in nano LC and improved ionisation efficiency in the nano ESI source [135]. Nanoscale graphitized carbon and HILIC amide stationary phases have been used for the separation of underivatized O- and N-glycans with low-femtomole sensitivity [75, 76, 88, 131, 136]. The nanoscale graphitized carbon columns have also been used in a microchip format [133]. The use of porous layer open tubular HILIC columns with 10  $\mu\text{m}$  I.D. for sensitive glycan analysis with ESI-MS detection has also been demonstrated [137]. Recently, a chip-based reversed phase LC separation of permethylated glycans has also been reported [138].

In this chapter, the use of nano ZIC-HILIC for a simple, rapid, and sensitive analysis of reduced high mannose and complex glycans from ribonuclease B and a recombinant monoclonal antibody is demonstrated. With this new method, higher sensitivity was achieved compared to the conventional approach. The ZIC-HILIC column exhibited different selectivity for neutral and sialylated glycans and a wide range of charged minor glycan species was identified. The nano ZIC-HILIC was coupled to a high resolution mass spectrometer which enabled study of structures that could not previously be identified by any current conventional approach.

## 4.2. Materials and Methods

### 4.2.1. Sample preparation

Glycoprotein samples (250 µg) were desalted prior to digestion using centrifugal filter units (Amicon Ultra, 10.000 MWCO, Millipore, Carrigtwohill, Ireland). Glycans were released from glycoproteins by incubation with 3 µL of PNGase F (500 units/mL, from *Elizabethkingia meningoseptica*); per 100 µL of 50 mM ammonium bicarbonate buffer, pH 8.0, overnight at 37 °C. Proteins were removed by precipitation with 400 µL ice-cold ethanol and dried in the vacuum oven overnight at 40 °C. The dried supernatants were reduced by adding 20 µL of 0.5 M sodium borohydride in 50 mM sodium hydroxide and incubating at room temperature overnight. The samples were then acidified by adding 5 µL of glacial acetic acid and desalted by ion-exchange chromatography (Dowex MR-3 mixed bed, Sigma). Prior to analysis, the samples were diluted by a factor of ten in acetonitrile and 2 µL of the sample was injected onto the column.

### 4.2.2. Nano ZIC-HILIC coupled with ESI-MS

Nano ZIC-HILIC chromatography was performed with a Merck SeQuant (Umeå, Sweden) nano ZIC®-HILIC column (75 µm I.D. × 150 mm) with 5 µm particle size. The analyses were performed on a Dionex Ultimate 3000 HPLC system, including a ternary low-pressure-mixing gradient pump (DGP-3600) equipped with a membrane degasser unit (SRD-3600), a temperature-controlled column oven with a flow manager (FLM-3100) and a thermostated autosampler (WPS-3000T). Mobile phase A and B consisted of acetonitrile and 2 mM ammonium acetate in water, pH 6.9, respectively. The flow-rate was set to 600 nL/min and the temperature of the column was maintained at 40 °C. Ribonuclease B and MAb3 glycans were analysed using gradient elution, starting with a 3 min isocratic step at 10% B, followed by a linear gradient from 10 to 45% B in 15 min and finished with a wash step at 95% B for 5 min. Prior to the next injection, the column was equilibrated for 25 min at 10% B. The LC system was coupled to the high resolution orthogonal TOF MS (MaXis™, Bruker- Daltonik, Bremen,

Germany). The transfer capillary was kept at a voltage of - 4500 V (positive ion polarity mode) or 3500 V (negative ion polarity) respectively. The nebulizer was set to 0.6 bar using an ESI nano sprayer (Bruker, Bremen, Germany), the dry gas temperature to 180 °C and the dry gas flow rate to 3 L/min. The ion transfer was optimized in the range  $m/z$  200-3000 for highest sensitivity while keeping the resolution  $R > 50,000$  across the whole mass range. The TOF MS mass calibration was carried out prior to the LC-MS experiment by direct infusion of a 100 fold dilution of ES Tuning Mix (Agilent Technologies, Waldbronn, Germany) at 4  $\mu\text{L}/\text{min}$ .

### 4.3. Results and discussion

#### 4.3.1. Separation of high mannose glycans released from RNase B

RNase B is a glycoprotein with a molecular weight of approximately 15 kDa containing a single N-linked glycosylation site for high mannose glycans with 5 to 9 mannose units and several possible structural isoforms [139]. Prior to the separation, the PNGase F released glycans were reduced to avoid a complex chromatogram resulting from the presence of anomers. The glycan profile of RNase B obtained by ZIC-HILIC nano LC-ESI-TOF-MS in positive ion mode is shown in Figure 4-1. The expected order of elution according to the glycan size was achieved; the glycans with higher molecular weight exhibited longer retention times. The observed behaviour was in agreement with the accepted HILIC separation mechanism. All high mannose glycans were eluted over a 3 minute range and most of them were baseline resolved. Some unreduced glycans present in the sample led to additional peaks being observed in the base peak chromatogram (BPC). The high resolution of the mass spectrometer enabled a clear distinction to be made between the reduced and unreduced peaks, which can otherwise give a partially overlapping pattern. All high mannose glycans exhibited a similar ionisation pattern, with dominating doubly charged  $[M+H+NH_4]^{2+}$  ions. Singly charged protonated and sodiated molecular ion was observed for the Man5 glycan, however with increasing molecular weight the

proportion of doubly charged species increased. In-source fragmentation was observed for singly and doubly protonated ions, with the loss of one or two mannose residues (Figure 4–2). Less fragmentation was observed for  $[M+H+NH_4]^{2+}$  ions, which indicated the stabilizing effect of  $NH_4^+$  ion. It has been previously reported that oligomannosidic glycans are prone to in-source fragmentation depending on the solvent composition [37]. Compared to the original procedure, the complete analysis time was reduced from 105 min to 48 min, with a 70 fold increase in sensitivity which results from the lower chromatographic dilution of the sample. The mass sensitivity in chromatographic detection increases with the inverse square of the column diameter and lower flow-rates additionally improve the ionisation efficiency in nano ESI [135]. RNase B glycans are summarised in Table 4-1.

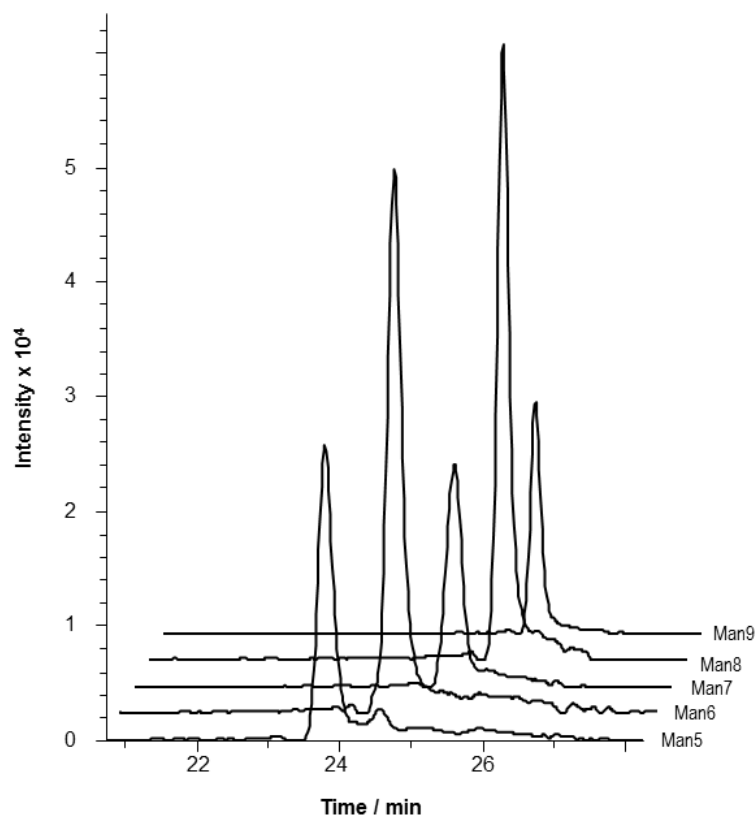


Figure 4–1: Separation of reduced high mannose glycans from RNase B. Gradient elution, 10 to 45% B; mobile phase A (acetonitrile) and mobile phase B (2 mM ammonium acetate pH 6.9 in water); ESI-MS, positive ion mode. High resolution extracted ion chromatograms (hrEIC),  $m/z$ : (Man5)  $627.7451 \pm 0.002$ ; (Man6)  $708.7715 \pm 0.002$ ; (Man7)  $789.7979 \pm 0.002$ , (Man8)  $870.8243 \pm 0.002$ ; (Man9)  $951.8507 \pm 0.002$ .

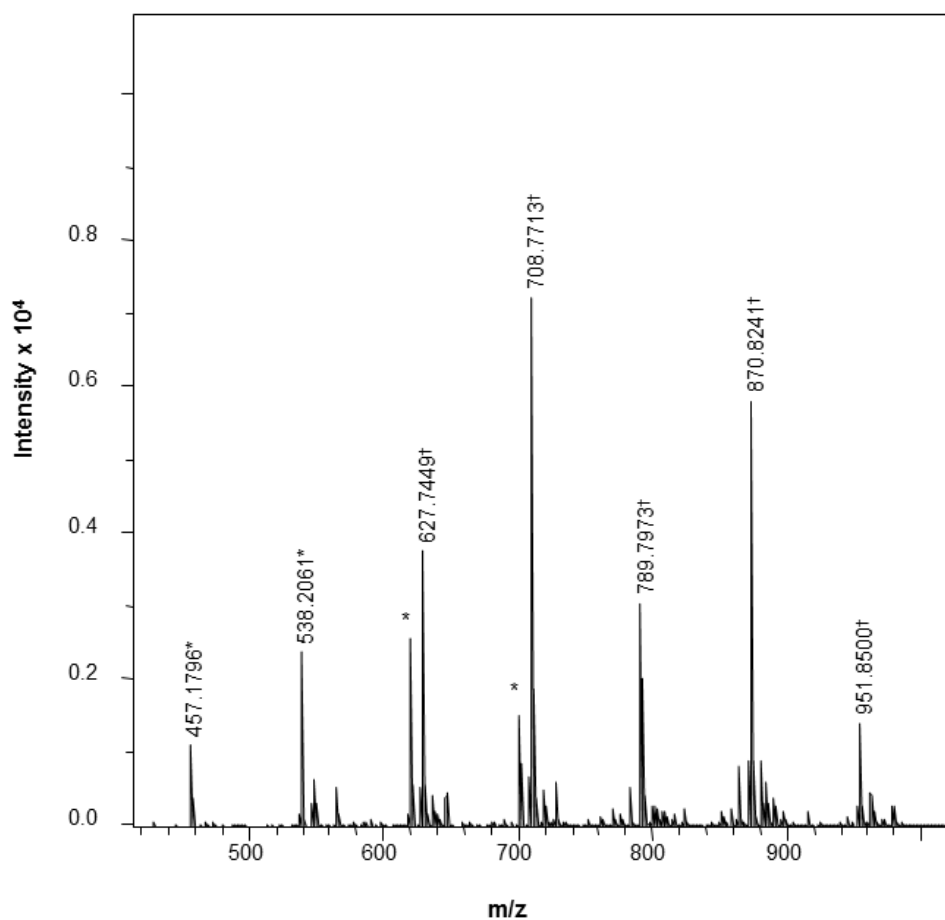
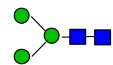
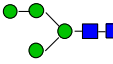

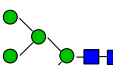
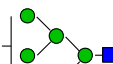
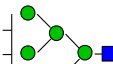



Figure 4-2: Accumulated mass spectrum over the RNase B glycan range; positive ion mode, background subtracted. \*Doubly charged protonated species; <sup>†</sup>doubly charged  $[M+H+HN_4]^{2+}$  species. Protonated ions are more prone to in-source fragmentation.

Table 4-1: Reduced glycans released from the RNase B.

Glycan	Structure	Abbr.	Retention time / min	Ions	M <sub>theoretical</sub> [M+H] <sup>+</sup> /Da	M <sub>measured deconvoluted</sub> [M+H] <sup>+</sup> /Da	Δmass / ppm
(Man) <sub>3</sub> (GlcNAc) <sub>2</sub>		Man3	NA	[M+2H] <sup>2+</sup> [M+H] <sup>+</sup>	913.35071	913.35214	-1.6
(Man) <sub>1</sub> (Man) <sub>3</sub> (GlcNAc) <sub>2</sub>		Man4	NA	[M+H+NH <sub>4</sub> ] <sup>2+</sup> [M+2H] <sup>2+</sup> [M+H] <sup>+</sup>	1075.40353	1075.40498	-1.3
(Man) <sub>2</sub> (Man) <sub>3</sub> (GlcNAc) <sub>2</sub>		Man5	23.8	[M+H+NH <sub>4</sub> ] <sup>2+</sup> [M+2H] <sup>2+</sup> [M+H] <sup>+</sup> [M+Na] <sup>+</sup>	1237.45635	1237.45556	0.6
(Man) <sub>3</sub> (Man) <sub>3</sub> (GlcNAc) <sub>2</sub>		Man6	24.6	[M+H+NH <sub>4</sub> ] <sup>2+</sup> [M+2H] <sup>2+</sup> [M+NH <sub>4</sub> ] <sup>+</sup> [M+H] <sup>+</sup>	1399.50918	1399.50828	0.6
(Man) <sub>4</sub> (Man) <sub>3</sub> (GlcNAc) <sub>2</sub>		Man7	25.2	[M+H+NH <sub>4</sub> ] <sup>2+</sup> [M+2H] <sup>2+</sup>	1561.56200	1561.56185	0.1
(Man) <sub>5</sub> (Man) <sub>3</sub> (GlcNAc) <sub>2</sub>		Man8	25.7	[M+H+NH <sub>4</sub> ] <sup>2+</sup> [M+2H] <sup>2+</sup>	1723.61482	1723.61387	0.6
(Man) <sub>6</sub> (Man) <sub>3</sub> (GlcNAc) <sub>2</sub>		Man9	25.9	[M+H+NH <sub>4</sub> ] <sup>2+</sup> [M+2H] <sup>2+</sup>	1885.66765	1885.66682	0.4

■ GlcNAc; ● Man; NA-not assigned, observed only as in-source fragments of larger glycans.



### 4.3.2. Separation of glycans originating from monoclonal antibody

Reduced MAb3 glycans were analysed using nano ZIC-HILIC coupled with ESI-TOF-MS. The same gradient conditions as for high mannose glycans were used due to expected similar retention properties, as described previously. The lower retention of complex glycans compared to the high mannose glycans with comparable mass, Figure 4-3, was consistent with the results obtained on conventional size ZIC-HILIC. Using nano ZIC-HILIC, higher sensitivity compared to conventional ZIC-HILIC chromatography was achieved. The MAb3 glycan sample was measured in positive and negative ion mode which allowed identification of all previously observed glycans commonly present in this monoclonal antibody (Table 4-2; h-k), which are generally of the biantennary complex type. Furthermore, nine new peaks for low-abundant glycans were observed with the proposed structures summarised in Table 4-2 (a-g, l-m). When 2-AB labelled glycans from the same MAb were analysed by amide HILIC coupled with fluorescence detection, several minor species were observed. However, due to the lower sensitivity of MS in comparison to fluorescence detection and lack of appropriate standards, they have not been previously characterised [81].

For all the known complex glycans, the dominant ions in the positive ion mode were doubly charged protonated ions (Figure 4-4), which is different to the high mannose glycans, where under the same experimental conditions predominantly the  $[M+H+NH_4]^{2+}$  has been observed. The difference in the ionisation pattern suggests that the formation of pseudo molecular ions depends strongly on the structure of the glycan and it is expected that the same structural type of glycans will exhibit the same ionisation pattern. The doubly charged protonated ions could be predicted for peaks that were not previously observed using a conventional-size column.

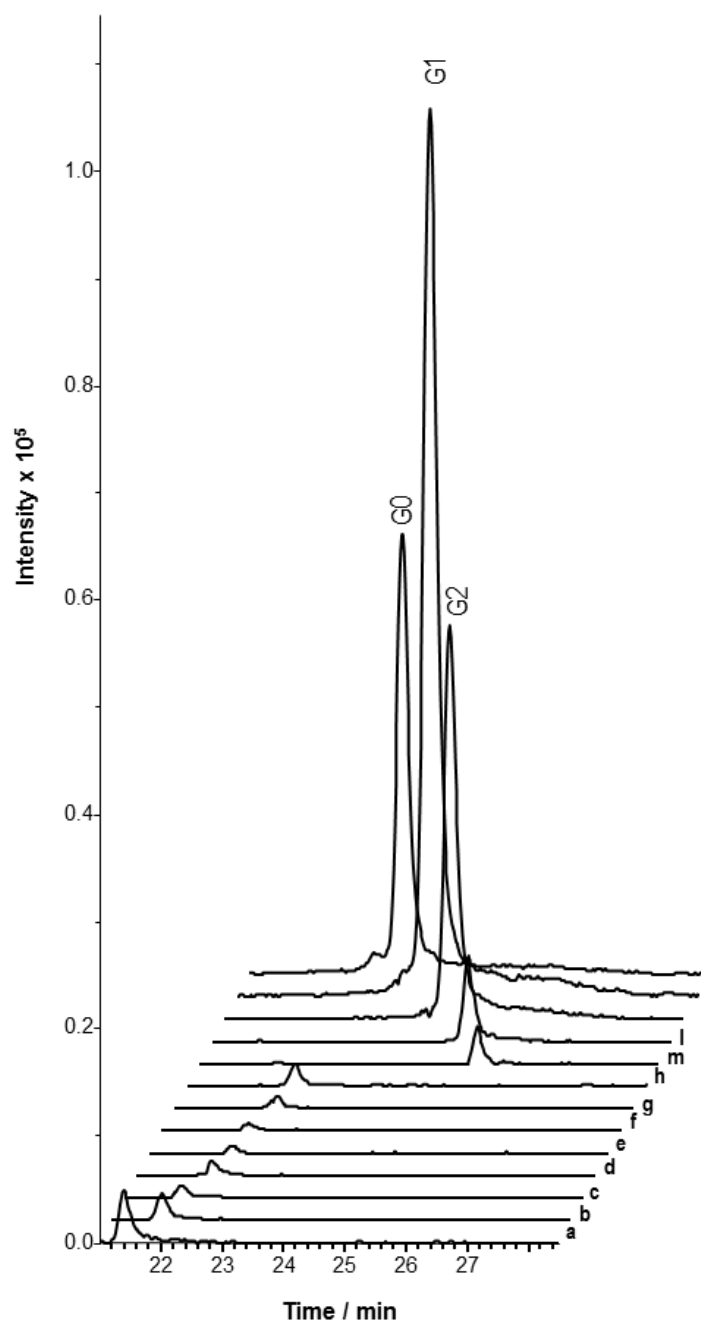
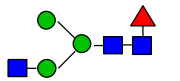
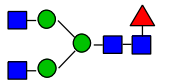
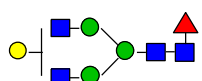
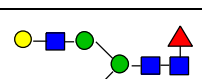
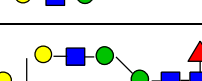
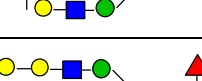


Figure 4-3: Separation of reduced glycans from the MAb3. Gradient elution, 10 to 45% B; mobile phase A (acetonitrile) and mobile phase B (2 mM ammonium acetate pH 6.9 in water); ESI-MS, positive ion mode. HrEICs,  $m/z$ : (a)  $866.3192 \pm 0.002$ ; (b)  $967.8589 \pm 0.002$ ; (c)  $947.3456 \pm 0.002$ ; (d)  $1048.8853 \pm 0.002$ ; (e)  $955.3431 \pm 0.003$ ; (f)  $1028.3720 \pm 0.005$ ; (g)  $1129.9117 \pm 0.005$ ; (h)  $631.7476 \pm 0.002$ ; (i)  $1057.3930 \pm 0.003$ ; (m)  $976.3666 \pm 0.002$ ; (G2)  $895.3401 \pm 0.002$ ; (G1)  $814.3137 \pm 0.002$ ; (G0)  $733.2873 \pm 0.002$ . The proposed structures are listed in Table 4-2.

Table 4-2: Reduced glycans released from the MAb3.

Glycan	Structure	Abbr.	Retention time / min	Ions	M <sub>theoretical</sub> [M+H] <sup>+</sup> / Da	M <sub>measured</sub> deconvoluted [M+H] <sup>+</sup> / Da	Δmass / ppm
(Hex) <sub>1</sub> (HexNAc) <sub>1</sub> (dHex) <sub>1</sub> (NeuGc) <sub>1</sub> (Man) <sub>3</sub> (GlcNAc) <sub>2</sub>		a / G1- GlcNAc+NeuGc	21.4	[M+2H] <sup>2+</sup>	1731.63114	1731.63040	0.4
(Hex) <sub>1</sub> (HexNAc) <sub>2</sub> (dHex) <sub>1</sub> (NeuGc) <sub>1</sub> (Man) <sub>3</sub> (GlcNAc) <sub>2</sub>		b / G1+NeuGc	21.8	[M+2H] <sup>2+</sup>	1934.71052	1934.71046	0.0
(Hex) <sub>2</sub> (HexNAc) <sub>1</sub> (dHex) <sub>1</sub> (NeuGc) <sub>1</sub> (Man) <sub>3</sub> (GlcNAc) <sub>2</sub>		c / Hyb1F+NeuGc	21.9	[M+2H] <sup>2+</sup>	1893.68397	1893.68235	0.9
(Hex) <sub>2</sub> (HexNAc) <sub>2</sub> (dHex) <sub>1</sub> (NeuGc) <sub>1</sub> (Man) <sub>3</sub> (GlcNAc) <sub>2</sub>		d / G2+NeuGc	22.2	[M+2H] <sup>2+</sup> [M+3H] <sup>3+</sup>	2096.76334	2096.76136	0.9
(Hex) <sub>3</sub> (HexNAc) <sub>1</sub> (NeuGc) <sub>1</sub> (Man) <sub>3</sub> (GlcNAc) <sub>2</sub>		e / Hyb3+NeuGc	22.3	[M+2H] <sup>2+</sup>	1909.67888	1909.67934	-0.2
(Hex) <sub>3</sub> (HexNAc) <sub>1</sub> (dHex) <sub>1</sub> (NeuGc) <sub>1</sub> (Man) <sub>3</sub> (GlcNAc) <sub>2</sub>		f / Hyb3F+NeuGc	22.3	[M+2H] <sup>2+</sup>	2055.73679	2055.73537	0.7
(Hex) <sub>3</sub> (HexNAc) <sub>2</sub> (dHex) <sub>1</sub> (NeuGc) <sub>1</sub> (Man) <sub>3</sub> (GlcNAc) <sub>2</sub>		g / G3+NeuGc	22.6	[M+2H] <sup>2+</sup> [M+3H] <sup>3+</sup>	2258.81616	2258.82237	-2.7

Table 4-2 continued...

(HexNAc) <sub>1</sub> (dHex) <sub>1</sub> (Man) <sub>3</sub> (GlcNAc) <sub>2</sub>		h / G0-GlcNAc	22.8	[M+2H] <sup>2+</sup>	1262.48799	1262.48923	-1.0
(HexNAc) <sub>2</sub> (dHex) <sub>1</sub> (Man) <sub>3</sub> (GlcNAc) <sub>2</sub>		i / G0	23.5	[M+2H] <sup>2+</sup>	1465.56736	1465.56786	-0.3
(Hex) <sub>1</sub> (HexNAc) <sub>2</sub> (dHex) <sub>1</sub> (Man) <sub>3</sub> (GlcNAc) <sub>2</sub>		j / G1	24.1	[M+2H] <sup>2+</sup>	1627.62018	1627.61994	0.1
(Hex) <sub>2</sub> (HexNAc) <sub>2</sub> (dHex) <sub>1</sub> (Man) <sub>3</sub> (GlcNAc) <sub>2</sub>		k / G2	24.7	[M+2H] <sup>2+</sup> [M+3H] <sup>3+</sup>	1789.67301	1789.67291	0.1
(Hex) <sub>3</sub> (HexNAc) <sub>2</sub> (dHex) <sub>1</sub> (Man) <sub>3</sub> (GlcNAc) <sub>2</sub>		l / G3	25.1	[M+2H] <sup>2+</sup> [M+3H] <sup>3+</sup>	1951.72583	1951.72641	-0.3
(Hex) <sub>4</sub> (HexNAc) <sub>2</sub> (dHex) <sub>1</sub> (Man) <sub>3</sub> (GlcNAc) <sub>2</sub>		m / G4	25.5	[M+2H] <sup>2+</sup> [M+3H] <sup>3</sup>	2113.77865	2113.77827	0.2

■ GlcNAc; ● Man; ▲ Fuc; ● Gal; ◆ NeuGc

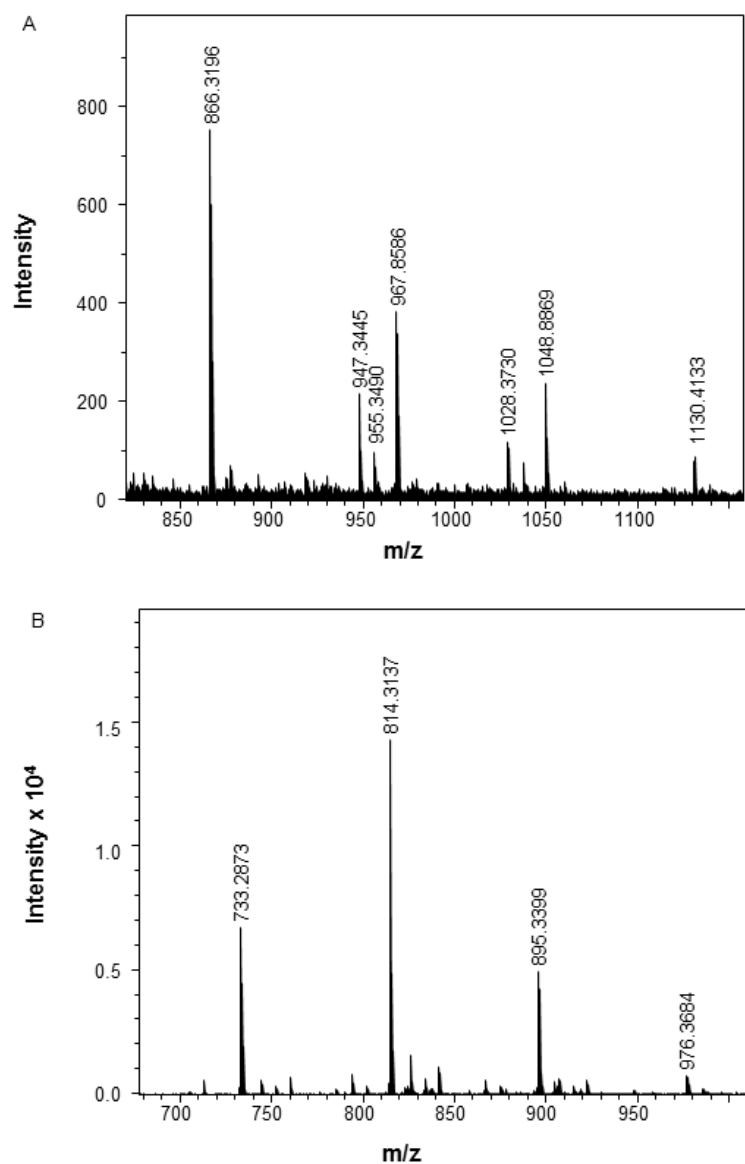


Figure 4-4: Accumulated mass spectrum over the MAb3 sialylated (A) and neutral (B) glycan elution range obtained by nano ZIC-HILIC; positive ion mode, background subtracted. Doubly protonated ions  $[M+2H]^{2+}$  are observed for the complex-type glycans.

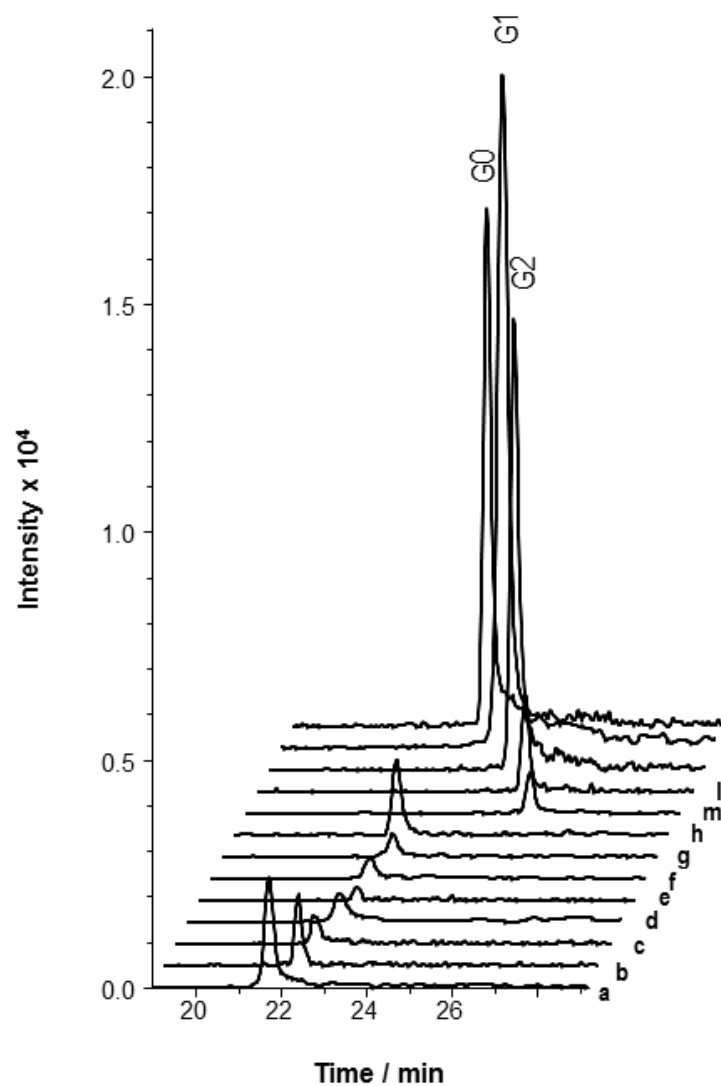


Figure 4-5: Separation of reduced glycans from the MAb3. Gradient elution, 10 to 45% B; mobile phase A (acetonitrile) and mobile phase B (2 mM ammonium acetate pH 6.9 in water); ESI-MS, negative ion mode. HrEICs from top to bottom, m/z: (a)  $864.3036 \pm 0.005$ ; (b)  $965.8432 \pm 0.005$ ; (c)  $945.3300 \pm 0.005$ ; (d)  $1046.8697 \pm 0.01$ ; (e)  $953.3274 \pm 0.005$ ; (f)  $1026.3564 \pm 0.010$ ; (g)  $1127.8961 \pm 0.01$ ; (h)  $629.7320 \pm 0.005$ ; (m)  $1055.3773 \pm 0.010$ ; (l)  $974.3509 \pm 0.005$ ; (G2)  $893.3245 \pm 0.005$ ; (G1)  $812.2981 \pm 0.005$ ; (G0)  $731.2717 \pm 0.005$ .

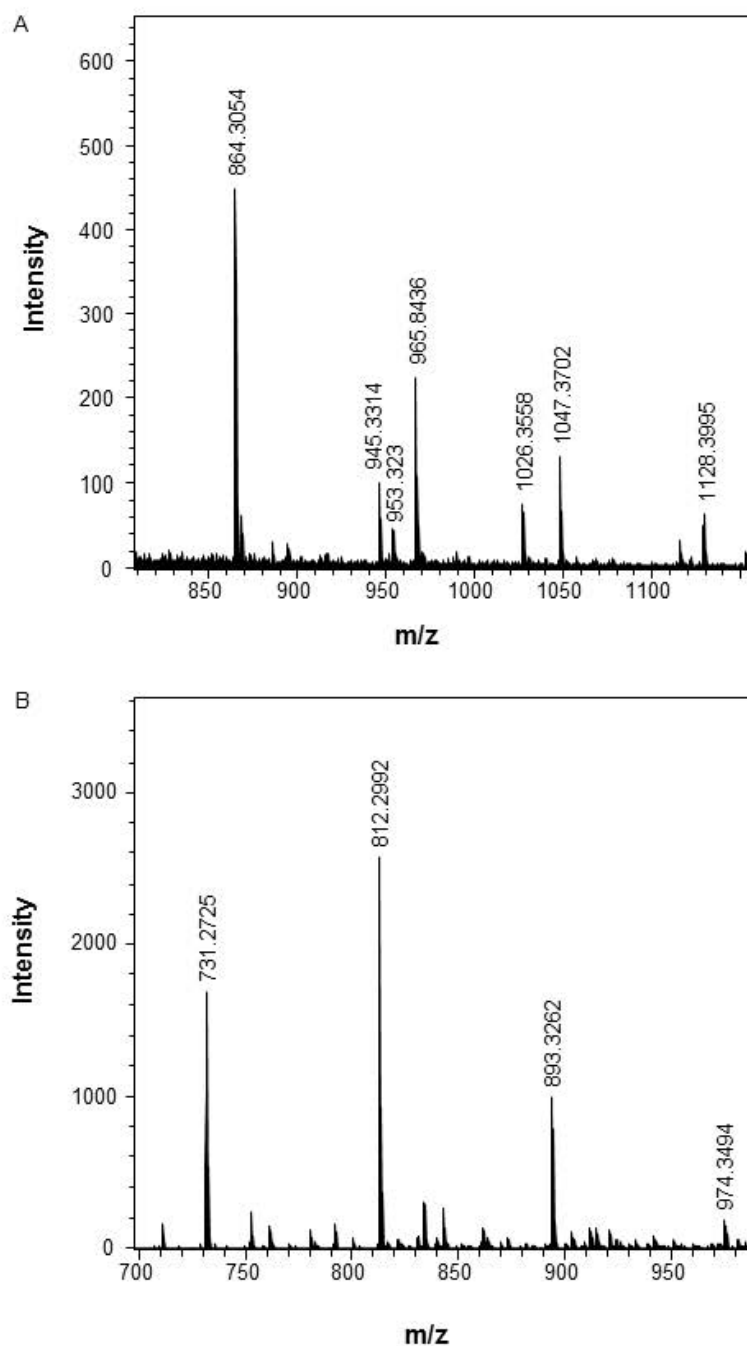


Figure 4-6: Accumulated mass spectrum over the MAb3 sialylated (A) and neutral (B) glycan elution range obtained by nano ZIC-HILIC; negative ion mode, background subtracted.

Considering high mass accuracy, two possible glycan structures with the same elemental composition can be predicted for most of the observed peaks. The average error in mass determination for most of the glycans was below 2 ppm. With the achieved high mass accuracy it is possible to predict a limited number of possible structures for the observed ions. Two probable series of seven related complex and hybrid glycans which were eluted before the neutral G0, G1 and G2 glycans could be identified, either containing a combination of dHex<sub>1</sub>NeuGc<sub>1</sub> or Hex<sub>1</sub>NeuAc<sub>1</sub> residues of which the first is more likely to occur in the sample, as will be further discussed. For the ion (e), only one possible structure can be assigned which confirms the presence of NeuGc in the sample. This result is consistent with the fact that the MAb3 was expressed in a NS0 murine cell line which is known to produce glycans with a high content of NeuGc [15]. In addition, the high degree of fucosylation in the cell line producing the MAb3 leads to the deduction that the glycans observed belong to the group of core-fucosylated complex and hybrid glycans containing NeuGc rather than NeuAc. The structures (a-g) in the Table 4-2 most likely correspond to the peaks observed in the chromatogram (Figure 4-3). The relative intensities for the proposed complex sialylated glycans are higher than those of hybrid sialylated glycans (Figure 4-4), which is in agreement with the high content of neutral complex glycan species in the sample.

Elution of glycans containing sialic acid prior to elution of the neutral glycans indicated that the separation of glycans was not governed by hydrophilic interaction alone, but also by electrostatic repulsion between the ZIC-HILIC stationary phase and the glycans. This contributed to the earlier elution of negatively charged glycans. The observed behaviour of negatively charged glycans under the applied conditions was expected due to the low ionic strength of the mobile phase, where the repulsion interaction was not shielded effectively by the eluent counter-ions. The electrostatic repulsion interaction has been previously observed for 2-aminopyridine labelled sialic acid glycans [80]. Under the conditions applied, the proposed hybrid glycans were eluted later than complex biantennary glycans with similar molecular weight, which is in



agreement with the previous observation that the high mannose glycans were retained more strongly compared to complex glycans of the same size.

Other minor species observed in the sample were the highly galactosylated complex glycans (l, m), which were eluted after the G2 peak. The presence of these glycans in the MAb3 was consistent with the other species observed in the sample and as expected their retention time increased with the higher degree of galactosylation. Due to the  $\alpha$ -galactosyltransferase activity observed in murine systems, hypergalactosylated glycans with additional  $\alpha$ -linked galactose attached to the terminal  $\beta$ -linked galactose can be expected to be found in MAbs expressed in NS0 cell line [18].

The MAb3 glycans were also analysed under the same separation conditions in the negative ion mode. For all the neutral and charged glycans, the doubly deprotonated ions were observed (Figure 4–6) with the main peaks corresponding to the glycans observed in the positive ion mode. However, the overall sensitivity in negative ion mode was lower. In negative ion mode, better ionisation efficiency for glycans containing sialic acids was expected compared to that of the neutral glycans. The relative peak intensity for the early eluted glycans was higher in the negative ion mode, which additionally confirmed the presence of sialic acids (Figure 4–5). The observed ionisation pattern allows the proposed glycan composition to be confirmed with high confidence. The mass spectrum of charged glycans obtained in the negative ion mode gave higher relative intensities for the proposed complex glycans compared to hybrid species (Figure 4–6A) and this was in agreement with the mass spectrum obtained in the positive ion mode (Figure 4–4A). Similar relative intensities in positive and negative ion modes were observed also for neutral glycans (Figure 4–4B and Figure 4–6B).

The complexity of the sample and the presence of a wide range of minor species required downscaling to enable detailed characterisation of the glycan profile, which is not possible with conventional-scale columns due to the lower sensitivity obtainable. Significant information can therefore be lost when

conventional-scale columns are used. Alternatively, separation of fluorescently-labelled glycans coupled with fluorescence detection might be necessary in order to ensure adequate sensitivity. Despite some advantages of fluorescence detection, such as high sensitivity and the possibility of relative quantification, this approach does not provide direct information about the structure of glycans and the profiling can be especially challenging when less common glycans are present in the sample. For the analysis of less abundant species the use of high resolution mass spectrometry may be required to confirm the composition with high confidence.

#### 4.4. Conclusions

In this chapter, a rapid and sensitive technique for the HILIC separation of reduced high mannose and complex glycans using a nano ZIC-HILIC column coupled with high resolution ESI-TOF-MS has been described. It is demonstrated that downscaling can be an efficient way to enhance sensitivity. The new approach allowed glycan profiling without the need for fluorescence labelling. The column exhibited good selectivity for neutral and sialylated glycans and due to the improved sensitivity and high mass accuracy, the composition of several less abundant species could be identified. High resolution mass spectrometry has proven to be a powerful tool in glycosylation analysis as it enables structures with similar composition to be resolved. Using the new method, a range of charged glycans that were not previously observed by standard bore ZIC-HILIC was identified in MAb3 sample. Based on the fact that MAb3 originates from murine cell line and a high level of fucosylation and  $\alpha$ -galactosylation was confirmed in this monoclonal antibody, it is suggested that the sialylated glycans contain NeuGc rather than NeuAc; however, for the complete structural elucidation, exoglycosidase digestions and tandem mass spectrometry will be employed in the following chapter.

## Chapter Five

### *5. Exoglycosidase digestions and tandem mass spectrometry*

#### **5.1. Introduction**

Due to the large number and complexity of glycan structures, various approaches for structural elucidation have been developed. The first common strategy involves LC separation of labelled glycans, in combination with digestions with highly specific exoglycosidases, either simultaneously or sequentially [47, 67]. Chromatography of standard glycans or MS is usually required for confirmation of structures, which makes this method extremely tedious and increases costs of the analysis. To simplify the assignment of chromatographic peaks, methods have been standardised and software for automatic prediction of structures has been developed [46].

The second strategy for structural characterisation of glycans uses MS/MS, either on its own or in combination with LC or other separation techniques [48, 50]. The quality of structural information largely depends on the ions selected for fragmentation. Glycans can be fragmented in the native, labelled or permethylated forms. Fragmentation of protonated species is generally avoided due to poorly informative B- and Y-type glycosidic bond cleavages [100] and rearrangement reactions [107, 108]. More structural information can be obtained by fragmentation of sodiated species, which increases the amount of cross-ring cleavages [100]. Due to the improved MS sensitivity and quality fragmentation data, MS/MS often involves permethylation of glycans [98]. This method is highly suitable for MALDI-MS/MS analysis of glycans without prior separation and can also involve exoglycosidase digestions [48, 50]. Sample preparation has been greatly improved and enzymatic digestion can be performed directly on the MALDI target which simplifies the sample handling [53]. When combined with

LC, permethylation of glycans can represent an additional analytical challenge due to the loss of chromatographic resolution [132].

In this chapter, both analytical approaches were employed for the characterisation of glycans observed by the PGC separation method and the suitability of both approaches was evaluated.

## 5.2. Materials and Methods

### 5.2.1. Reagents and chemicals

$\alpha$ -galactosidase (from green coffee beans),  $\alpha$ (2-3,6,8,9) neuraminidase (from *Arthrobacter ureafaciens*) and  $\alpha$ -mannosidase (from jack bean) were obtained from Sigma (St. Louis, MO, USA).  $\beta$ -N-acetylhexosaminidase (from jack bean) was purchased from Prozyme (CA, USA).

### 5.2.2. Sample preparation

Monoclonal antibody (MAb3, 590  $\mu$ g) was desalted prior to the digestion using centrifugal filter units (Amicon Ultra, 10,000 MWCO, Millipore). Glycans were released from MAb3 with 3  $\mu$ L PNGase F (500 units/mL) digestion at 37 °C per 100  $\mu$ L of ammonium bicarbonate buffer (50 mM, pH 8.0) for 24 h. Proteins were removed by precipitation with 400  $\mu$ L ice-cold ethanol and dried in a vacuum oven. The samples were reduced with 30  $\mu$ L of 0.5 M sodium borohydride in 0.025 mM sodium hydroxide in 50% ethanol (v/v) at room temperature overnight. The reaction was terminated by adding 5  $\mu$ L of glacial acetic acid and the samples were desalted by ion-exchange chromatography (Dowex MR-3 mixed bed, Sigma). The samples were dried in the vacuum oven prior to the exoglycosidase treatment.

The exoglycosidase digestions were carried out using the following enzymes and conditions:  $\alpha$ -galactosidase: 20 mU in 80  $\mu$ L of 50 mM ammonium acetate pH 6.5, for 48 h, at room temperature;  $\beta$ -N-acetylhexosaminidase: 250 mU in 80  $\mu$ L of 50 mM ammonium formate pH 4.8 for 48 h, at 37 °C; neuraminidase: 2.5 mU in 80

μL of 50 mM ammonium formate pH 4.8 for 48 h, at 37 °C; α-mannosidase: 680 mU in 80 μL of 250 mM ammonium formate pH 4.5 for 48 h, at 37 °C. The enzymes were removed prior to analysis by filtration using 10,000 MWCO centrifugal filter units. Analysis was done using the PGC method as previously described in Chapter 3.

### **5.2.3. Tandem mass spectrometry**

The PGC separation method described in Chapter 3 was used for coupling with MS/MS. For the measurement of the effect of collision cell energy, it was raised in 5 eV steps. Collision cell energy was used as noted.

## **5.3. Results and discussion**

The most complex sample used in this study, MAb3, was further analysed to confirm the proposed structures. Several glycan species with multiple possible structures were observed in this MAb and two strategies were used in order to identify the unassigned peaks, observed by the PGC and nano ZIC-HILIC separation methods. The first strategy involved the use of exoglycosidases, which specifically cleave terminal residues, based on the type of the residue and the linkage. Additionally, the tandem MS analysis of glycans was used to obtain additional structural information. The advantages and limitations of both analytical strategies were compared.

### **5.3.1. Exoglycosidase digestions**

Graphitized carbon was chosen as the most suitable stationary phase for analysis of neutral glycans from MAb3 due to the excellent capability to separate isobaric structures, as discussed in Chapter 3. The results of exoglycosidase digestions are summarised in Table 5-1. Compared to the experiments described before, additional glycan species, such as defucosylated complex and oligomannosidic glycans, were observed, since more starting material was used for the PNGase F digestion (Figure 5-1 to Figure 5-3). The presence of these species in the MAb3 is

not surprising; however, a series of less common glycans was identified and exoglycosidase digestions were used for confirmation of the proposed structures.

For several observed  $m/z$  values in the control sample, multiple possible glycan structures can be assigned. Furthermore, for the same  $m/z$  chromatogram traces, several peaks were observed in the PGC chromatogram. Additional analysis is required to confirm whether the observed glycans are structural isomers or glycans with different monosaccharide composition. The high degree of galactosylation and mannosylation observed in MAb3 allows for a large number of possible hybrid structures.

The most likely structures for observed  $m/z$  values are presented in the List of glycans (page XII). The proposed structures were selected based on the glycan mass and previous reports of glycans found with the GlycoMod tool (<http://expasy.org/tools/glycomod/>). The accurate mass was used for the determination of monosaccharide composition and all the measured  $m/z$  were within 20 mDa error range, which allowed confirmation of the composition with high confidence. Due to the acidic mobile phase used in the PGC separation method, the dominant ions were singly and doubly charged protonated ions. A preference to form doubly charged ions was observed for larger glycans. Where isobaric species were observed in the sample, a different ratio between the singly and doubly charged species was observed. This indicated a different glycan composition, most likely due to various degrees of galactosylation and mannosylation.

MAb3 glycans were first analysed to confirm the presence of the  $\alpha$ -galactose epitope, Figure 5-2, which is potentially immunogenic in humans and is expected to be found in the MAb expressed in a murine cell line. As described in Chapter 3, multiple peaks for  $m/z$  895.34 and 976.37 and a peak for 1057.40 were found in MAb3. As previously suggested, the larger peak for  $m/z$  895.34 was not affected by  $\alpha$ -galactosidase digestion (Figure 5-4), which confirmed the proposed structure for this glycan with two  $\beta$ -linked galactose residues.

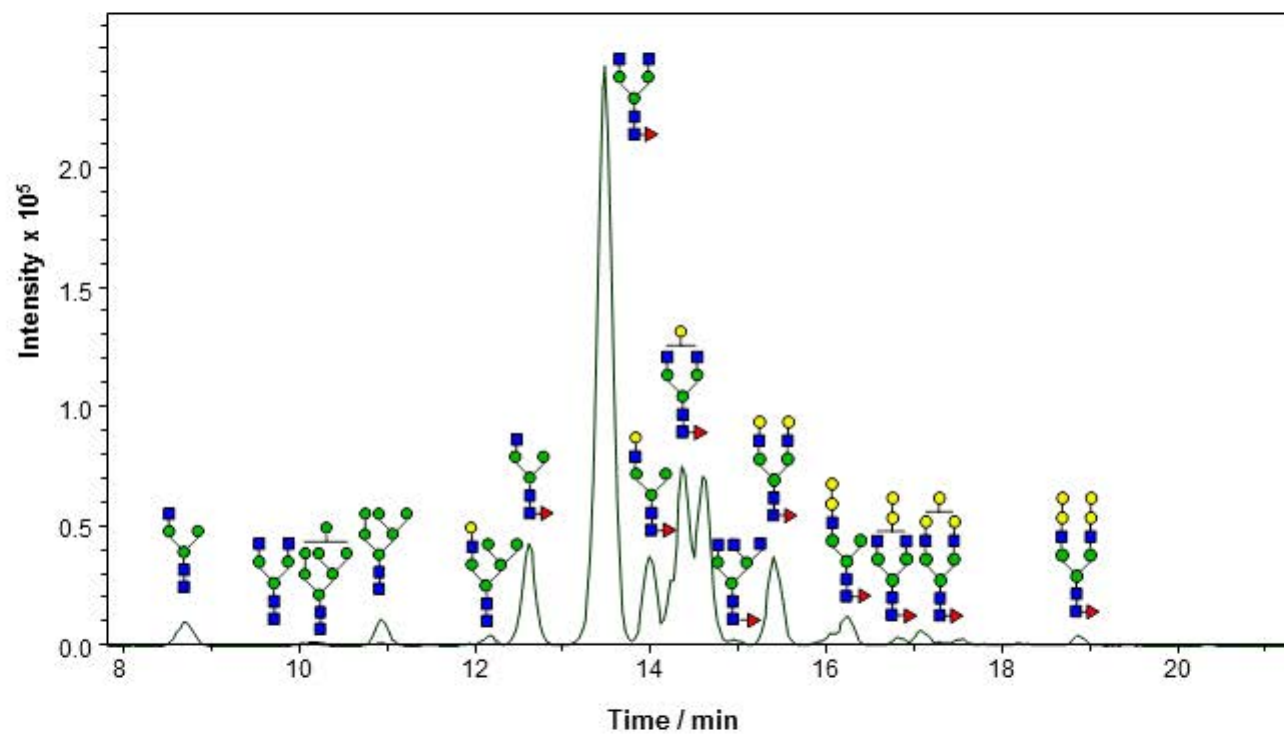


Figure 5–1: PGC separation of neutral reduced glycans found in MAb3, positive ion mode, BPC ( $m/z = 800\text{--}3000$ ). Gradient elution: mobile phase A-acetonitrile, mobile phase B-0.1% (v/v) acetic acid. The sample was highly heterogeneous with multiple low abundant isobaric complex and hybrid species.

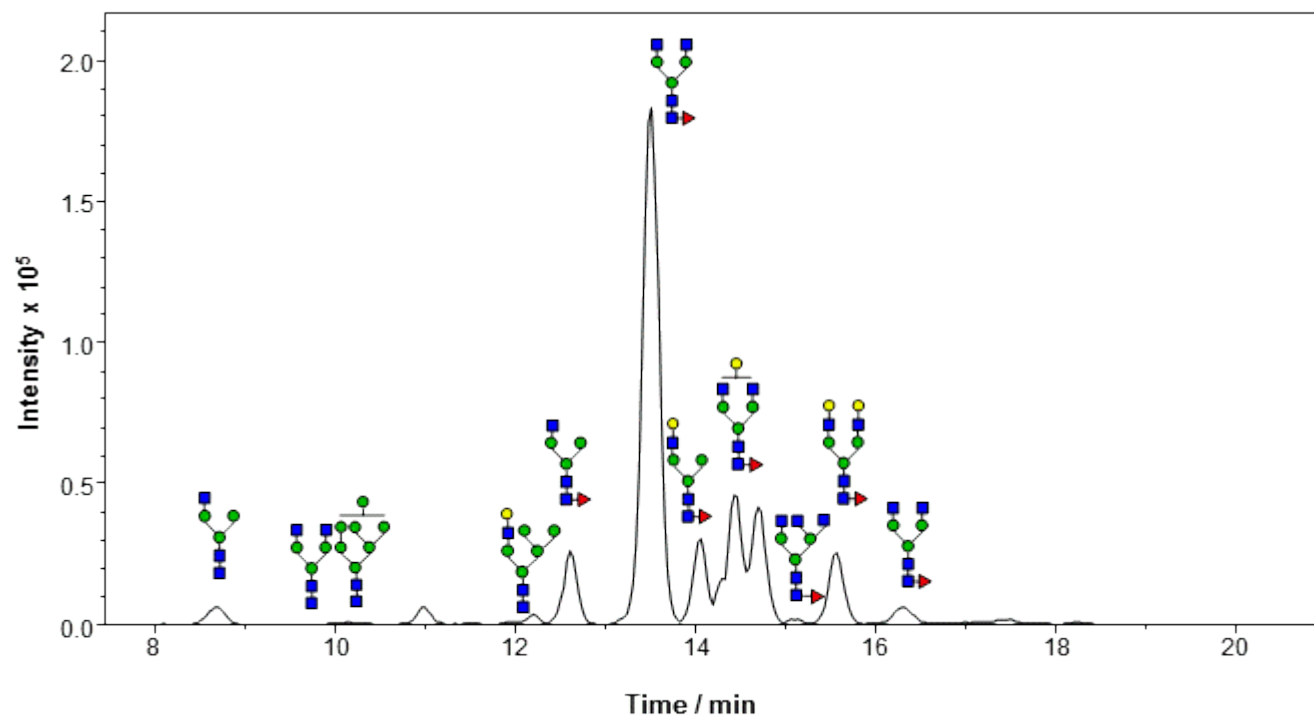


Figure 5–2: PGC separation of neutral reduced glycans found in MAb3 after the digestion with  $\alpha$ -galactosidase, positive ion mode, BPC ( $m/z$  = 800-3000). Gradient elution: mobile phase A-acetonitrile, mobile phase B-0.1% (v/v) acetic acid. Simpler gradient profile compared to the control was obtained. Some unreduced G0 was found in the sample and it was eluted later than reduced G0.



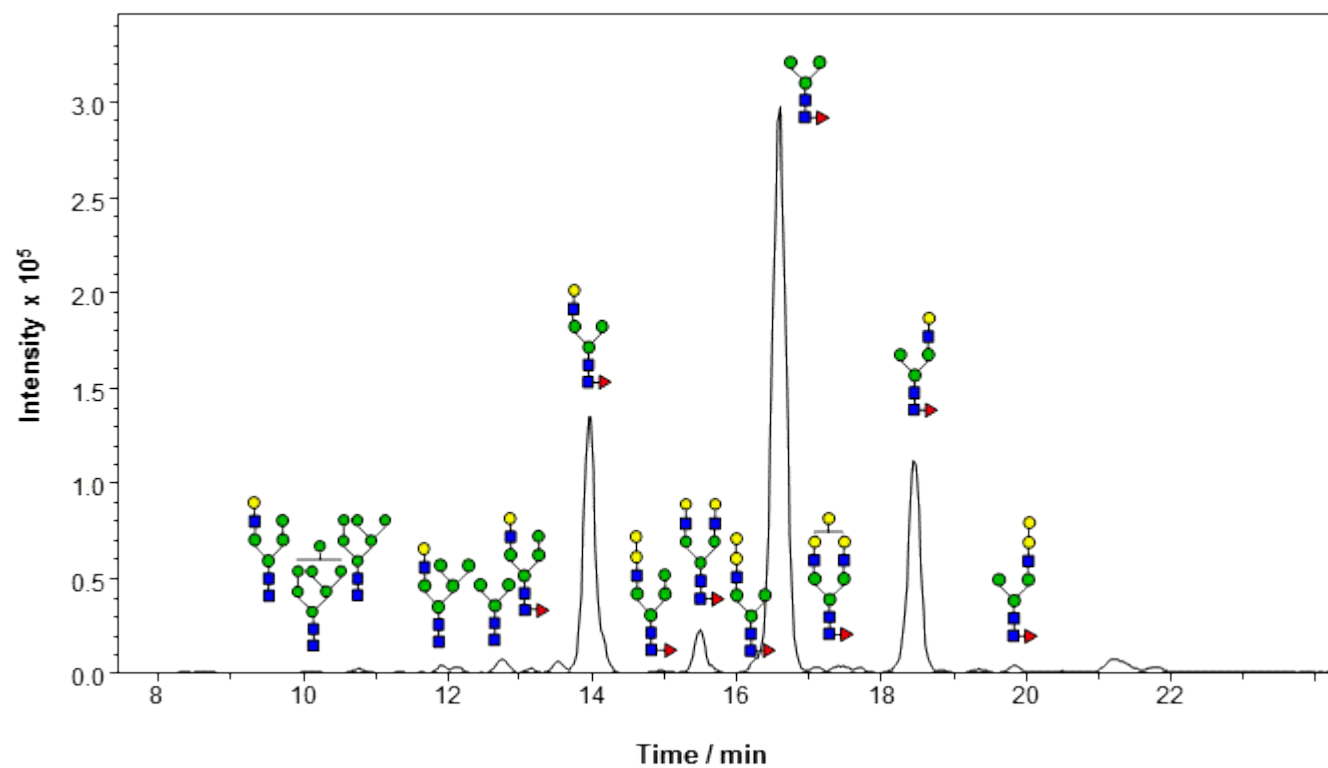


Figure 5–3: PGC separation of neutral reduced glycans found in MAb3 after the digestion with  $\beta$ -N-acetylhexosaminidase, positive ion mode, BPC ( $m/z$  = 800-3000). Gradient elution: mobile phase A-acetonitrile, mobile phase B-0.1% (v/v) acetic acid. Strong peaks for degradation products of G0 and G1 were observed in the chromatogram. A low amount of unreduced glycans was present in the sample.

The other two minor peaks corresponded to two  $\alpha$ -galactosylated G2 glycans. No preference for either of the antennae was expected and the similar peak intensity observed for both isomers was in agreement with the predicted structures. Additionally, two peaks for G3 and a peak for G4 glycans were found in MAb3, with confirmed terminal  $\alpha$ -galactose. The similar peak intensity for G3 glycans suggested that there is no arm-preference for this structural motif as observed for  $\alpha$ -galactosylated G2 glycan. On the other hand, only one peak was observed for G0-GlcNAc(-Fuc), G1-GlcNAc(-Fuc) and G2-GlcNAc glycan species, indicating the arm-preference when only one arm is elongated by GlcNAc, which is in agreement with previously reported structures found in the GlycoSuite database. It is suggested that GlcNAc is linked to the 3-arm of the core and the 6-arm is free or further mannosylated to form hybrid structures.

$\alpha$ -galactosylation was confirmed in complex and hybrid structures; however, several peaks were found that could not be explained by  $\alpha$ -galactosylation alone. The presence of isobaric hybrid species in the sample was also confirmed. By  $\alpha$ -galactosidase digestion it was possible to distinguish between the hybrid glycans with the same molecular weight and containing either mannose or  $\alpha$ -linked galactose. However, without further digestions, it was not possible to conclude if the remaining hybrids were  $\beta$ -galactosylated or with the additional mannose on the 3-arm. N-acetylhexosaminidase and  $\alpha$ -mannosidase digestions were performed to confirm the proposed hybrid structures. After the sample was digested with N-acetylhexosaminidase, the most abundant glycans G0 and G1 could not be found in the PGC chromatogram and intense peaks for enzyme reaction products, fucosylated core and G1-GlcNAc, were observed (Figure 5–3). Furthermore, digestion of the G1 glycans resulted in an additional intense peak for G1-GlcNAc with GlcNAc cleaved from the 3-arm. Similar results were observed for G2-GlcNAc, as a digestion product of  $\alpha$ -galactosylated G2 glycan. These results confirmed that glycans from MAb3 formed only one structural isomer, when there is only one complex-type antenna in the molecule, as previously suggested.

By using N-acetylhexosaminidase digestion it was possible to further confirm the proposed hybrid structures. If the hybrid glycans were not digested by the enzyme, it is suggested that the GlcNAc is further elongated by  $\beta$ -linked galactose. As shown for the chromatographic traces for  $m/z$  1440.54, 793.80, and 874.83, several isobaric hybrid species with various degrees of mannosylation and galactosylation were confirmed in the sample (Figure 5-5 to Figure 5-7). This practical example demonstrates the importance of the separation of glycan species with the same molecular weight to obtain complete information regarding the complexity of glycosylation in a given glycoprotein.

Digestion with  $\alpha$ -mannosidase provided additional information on mannosylation in the hybrid structures. As opposed to other enzyme reactions,  $\alpha$ -mannosidase digestion was not complete. The result is not surprising, considering that some mannosidic linkages are more resistant to  $\alpha$ -mannosidase cleavage. It is suggested that the  $\alpha 1 \rightarrow 6$  linkage is harder to digest compared to the  $\alpha 1 \rightarrow 3$  and  $\alpha 1 \rightarrow 2$  [6]. The digestion of glycans with the proposed free 6-arm was very poor, which was consistent with the fact that core mannose is extremely resistant to  $\alpha$ -mannosidase digestions. Similarly, the proposed glycans with one mannose residue on the 6-arm were only partially digested, indicating the presence of an  $\alpha 1 \rightarrow 6$  mannosidic linkage. On the other hand, proposed hybrid glycans with two mannose residues on the 6-arm were readily digested, which confirmed the likely structures with  $\alpha 1 \rightarrow 3$  and  $\alpha 1 \rightarrow 6$  linkages in the glycan molecule. The presence of additional closely eluted peaks in  $\alpha$ -mannosidase digested samples suggests the possible presence of isomeric digestion products of higher mannosylated glycans. For the chromatogram trace  $m/z$  793.80 (Figure 5-5), two hybrid glycans were proposed. The intense peak at 13.2 min is most likely a hybrid structure with one  $\alpha 1 \rightarrow 6$  linked mannose on the 6-arm, whereas the smaller peak at 14.9 min most likely corresponds to the structural isomer with an  $\alpha 1 \rightarrow 3$  linked mannose, as shown in Figure 5-5. The possible glycan structure with two mannose residues was excluded after the digestion with N-acetylhexosaminidase.

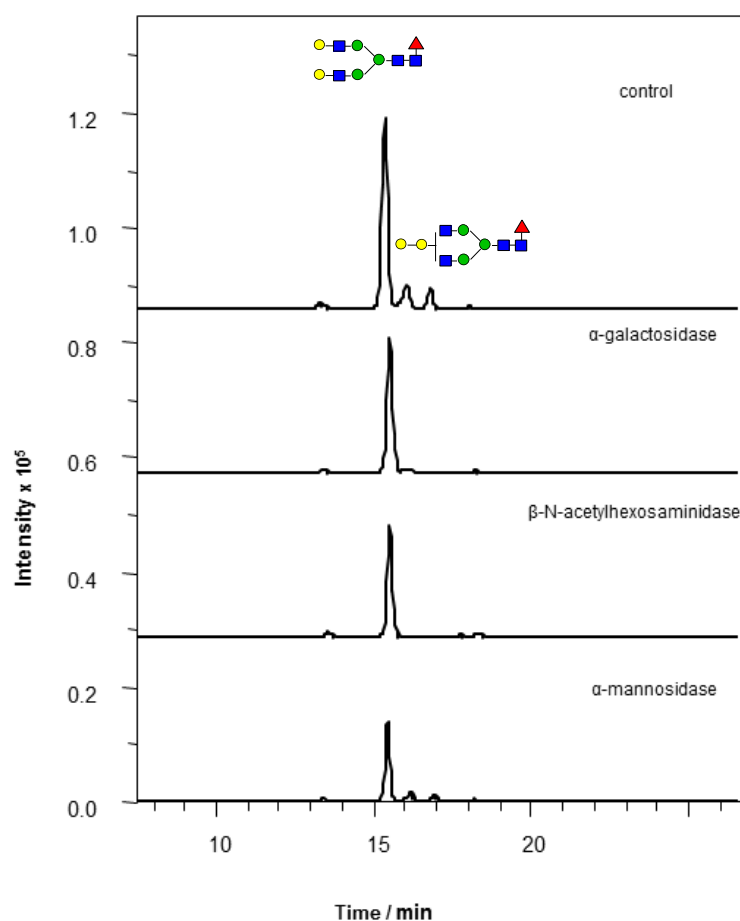


Figure 5-4: PGC EICs of G2 chromatogram trace ( $m/z$  895.34) prior to the digestion and after the digestion with  $\alpha$ -galactosidase,  $\beta$ -N-Acetylhexosaminidase and  $\alpha$ -mannosidase. Digestions with  $\alpha$ -galactosidase and  $\beta$ -N-acetylhexosaminidase confirmed the presence of  $\alpha$ -galactosylated epitope in late eluting low abundance G2 glycans. The same intensity of both peaks indicates that there is no arm-preference for  $\beta$ -linked galactose when two terminal GlcNAcs are present in the molecule.

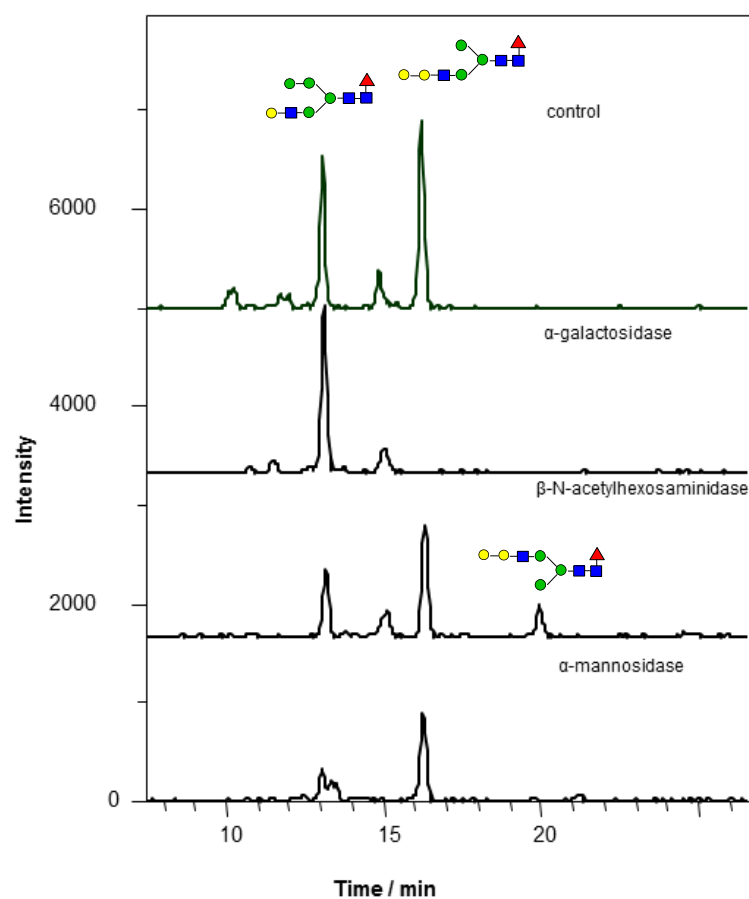


Figure 5-5: PGC EICs of G2-GlcNAc glycan ( $m/z$  793.80) prior to and after the digestions.  $\alpha$ -galactosidase digestion confirmed the presence of  $\alpha$ -linked galactose in the glycan eluting at 16.3 min. After the  $\beta$ -N-acetylhexosaminidase digestion, a new peak was observed, most likely corresponding to digestion product of G2 where GlcNAc was cleaved from the 3-arm of the glycan. After  $\alpha$ -mannosidase digestion new peaks are observed, most likely the digestion products of different mannose cleavages from larger hybrid glycans.

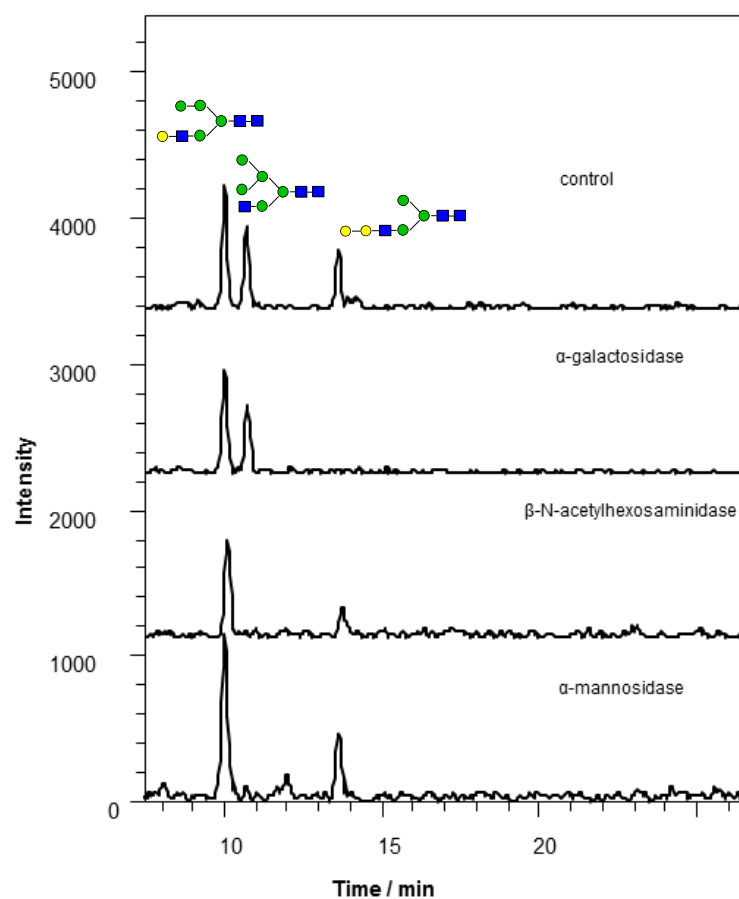


Figure 5–6: PGC EICs of  $m/z$  1440.53 prior to and after the digestions with  $\alpha$ -galactosidase.  $\alpha$ -galactosidase digestion confirmed presence of the  $\alpha$ -linked galactose in the glycan eluting at 13.8 min.  $\beta$ -acetylhexosaminidase and  $\alpha$ -mannosidase digestions confirmed that the peak at 10.9 min contains terminal GlcNAc and most likely contains two mannose residues one of which is  $\alpha 1 \rightarrow 3$  linked.

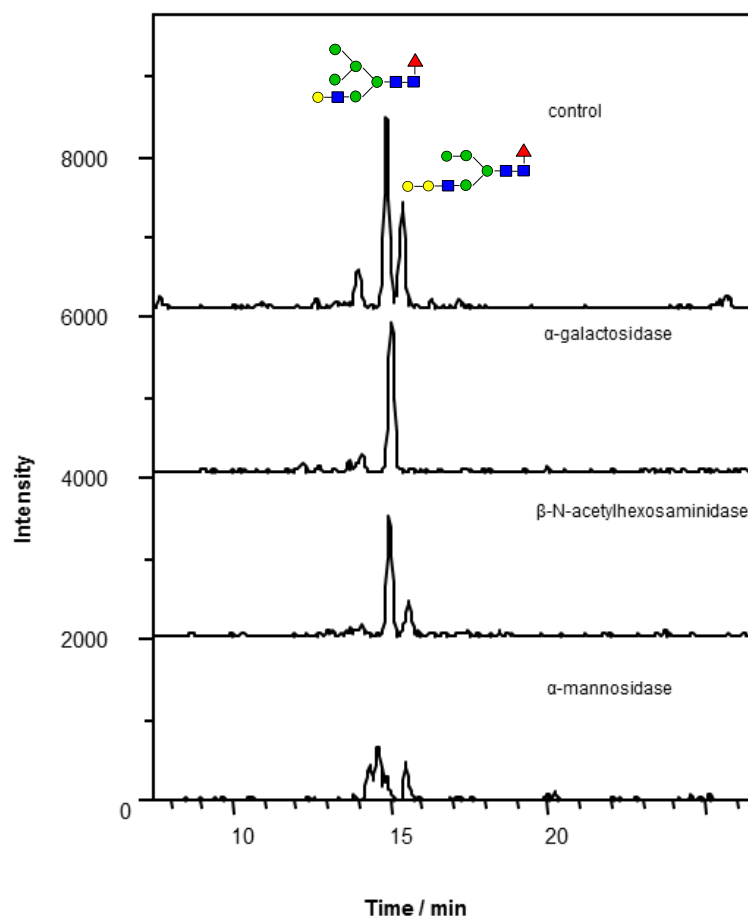


Figure 5-7: PGC EICs of m/z 874.83 prior to the digestion and after the digestion with  $\alpha$ -galactosidase,  $\beta$ -N-acetylhexosaminidase and  $\alpha$ -mannosidase. The digestions confirmed the proposed hybrid structures with none and one galactose residues on the 3-arm. Low abundant peaks could not be fully characterised.

Table 5-1: Exoglycosidase digestions of glycans from MAb3.

Glycan composition	Proposed structures	Abbr.	$M_{\text{theor.}}/\text{Da}$ [M+H] <sup>+</sup> [M+2H] <sup>2+</sup>	Ions found	Control	$\alpha$ -gal	$\alpha$ -sialidase	$\beta$ -AcHex	$\alpha$ -mann
(HexNAc) <sub>1</sub> (Man) <sub>3</sub> (GlcNAc) <sub>2</sub>		G0- GlcNAc- Fuc	1116.4301 558.7187	[M+H] <sup>+</sup>	8.7	8.7	8.8	-	8.8
(HexNAc) <sub>2</sub> (Man) <sub>3</sub> (GlcNAc) <sub>2</sub>		G0-Fuc	1319.5095 660.2584	[M+H] <sup>+</sup>	10.1	10.1	10.3	-	10.2
(Hex) <sub>2</sub> (HexNAc) <sub>1</sub> (Man) <sub>3</sub> (GlcNAc) <sub>2</sub>		Hyb1	1440.5357 720.7715	[M+H] <sup>+</sup> [M+2H] <sup>2+</sup>	10.2	10.2	10.3	10.2	10.2
(Hex) <sub>4</sub> (Man) <sub>3</sub> (GlcNAc) <sub>2</sub>		Man7	1561.56 781.28	[M+H] <sup>+</sup> [M+2H] <sup>2+</sup>	10.2 10.9	10.2 11.8	10.3 11.0	10.1 10.8	- -
(Hex) <sub>2</sub> (HexNAc) <sub>1</sub> (Man) <sub>3</sub> (GlcNAc) <sub>2</sub>		Hyb1	1440.5357 720.7715	[M+H] <sup>+</sup> [M+2H] <sup>2+</sup>	10.9	10.9	10.9	-	-
(Hex) <sub>1</sub> (HexNAc) <sub>1</sub> (Man) <sub>3</sub> (GlcNAc) <sub>2</sub>		G1- GlcNAc- Fuc	1278.4829 639.7451	[M+H] <sup>+</sup>	10.9	10.9	11.0	10.9	10.9



Table 5-1 continued...

(Hex) <sub>3</sub> (Man) <sub>3</sub> (GlcNAc) <sub>2</sub>		Man6	1399.5092 700.2582	[M+H] <sup>+</sup>	10.9	10.9	11.0	10.8	-
(Hex) <sub>3</sub> (HexNAc) <sub>1</sub> (Man) <sub>3</sub> (GlcNAc) <sub>2</sub>		Hyb2	1602.5885 801.7979	[M+H] <sup>+</sup> [M+2H] <sup>2+</sup>	12.2	12.2	12.2	12.1	-
(HexNAc) <sub>1</sub> (dHex) <sub>1</sub> (Man) <sub>3</sub> (GlcNAc) <sub>2</sub>		G0- GlcNAc	1262.4880 631.7476	[M+H] <sup>+</sup>	12.6 13.5 14.4 14.6	12.6 13.5 14.4 14.7	12.6 13.6 14.5 14.8	- - - -	12.5 13.5 14.4 14.7
(HexNAc) <sub>2</sub> (dHex) <sub>1</sub> (Man) <sub>3</sub> (GlcNAc) <sub>2</sub>		G0	1465.5674 733.28.73	[M+H] <sup>+</sup>	10.9 13.5	11.0 13.5	11.2 13.6	- -	11.1 13.5
(Hex) <sub>3</sub> (HexNAc) <sub>1</sub> (Man) <sub>3</sub> (GlcNAc) <sub>2</sub>		Hyb2	1602.5885 801.7979	[M+H] <sup>+</sup>	13.1	-	13.2	13.1	13.2
(Hex) <sub>2</sub> (HexNAc) <sub>1</sub> (dHex) <sub>1</sub> (Man) <sub>3</sub> (GlcNAc) <sub>2</sub>		Hyb1F	1586.5936 793.8005	[M+H] <sup>+</sup> [M+2H] <sup>2+</sup>	13.2 14.9	13.2 15.1	13.3 15.1	13.1 15.1	13.3 -
(Hex) <sub>2</sub> (HexNAc) <sub>1</sub> (Man) <sub>3</sub> (GlcNAc) <sub>2</sub>		Hyb1	1440.5357 720.7715	[M+H] <sup>+</sup>	13.7	-	13.8	13.7	13.7

Table 5-1 continued...

(Hex) <sub>1</sub> (HexNAc) <sub>1</sub> (dHex) <sub>1</sub> (Man) <sub>3</sub> (GlcNAc) <sub>2</sub>		G1- GlcNAc	1424.5408 712.7740	[M+H] <sup>+</sup>	11.9 14.0 14.4 14.6 15.4	11.9 14.1 14.4 14.7 15.6	12.0 14.1 14.5 14.8 15.6	11.9 14.0 14.0	11.9 14.0 14.4 14.7 15.5
(Hex) <sub>2</sub> (Man) <sub>3</sub> (GlcNAc) <sub>2</sub>		Man5	1237.4564 619.2318	[M+H] <sup>+</sup>	14.3	14.3	14.2	14.1	-
(Hex) <sub>1</sub> (HexNAc) <sub>2</sub> (dHex) <sub>1</sub> (Man) <sub>3</sub> (GlcNAc) <sub>2</sub>		G1	1627.6202 814.3137	[M+H] <sup>+</sup> [M+2H] <sup>2+</sup>	12.1 12.4 14.4 14.6	12.2 12.5 14.4 14.7	12.3 12.6 14.5 14.8	- - - -	12.2 12.5 14.4 14.7
(Hex) <sub>4</sub> (HexNAc) <sub>1</sub> (Man) <sub>3</sub> (GlcNAc) <sub>2</sub>		Hyb3	1764.6414 882.8243	[M+H] <sup>+</sup> [M+2H] <sup>2+</sup>	14.7	-	14.9	14.9	-
(HexNAc) <sub>3</sub> (dHex) <sub>1</sub> (Man) <sub>3</sub> (GlcNAc) <sub>2</sub>		T0	1668.6467 834.8270	[M+H] <sup>+</sup> [M+2H] <sup>2+</sup>	15.0	15.1	15.1	-	-

Table 5-1 continued...

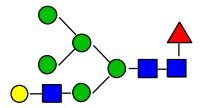
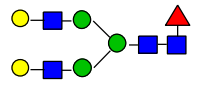
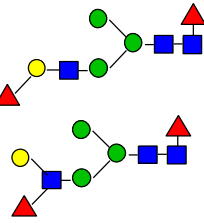
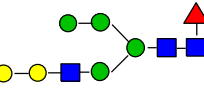
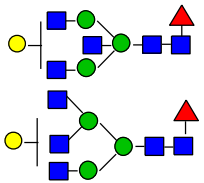
(Hex) <sub>3</sub> (HexNAc) <sub>1</sub> (dHex) <sub>1</sub> (Man) <sub>3</sub> (GlcNAc) <sub>2</sub>		Hyb2F	1748.6465 874.8269	[M+H] <sup>+</sup> [M+2H] <sup>2+</sup>	- 15.0	- 15.1	- 15.1	- 15.0	14.4 14.7 14.9
(Hex) <sub>2</sub> (HexNAc) <sub>2</sub> (dHex) <sub>1</sub> (Man) <sub>3</sub> (GlcNAc) <sub>2</sub>		G2	1789.6730 895.3401	[M+H] <sup>+</sup> [M+2H] <sup>2+</sup>	15.4	15.6	15.6	15.5	15.5
(Hex) <sub>1</sub> (HexNAc) <sub>1</sub> (dHex) <sub>2</sub> (Man) <sub>3</sub> (GlcNAc) <sub>2</sub>		F1- GlcNAc	1570.60 785.80	[M+H] <sup>+</sup>	15.5	15.7	15.6	15.6	15.5
(Hex) <sub>3</sub> (HexNAc) <sub>1</sub> (dHex) <sub>1</sub> (Man) <sub>3</sub> (GlcNAc) <sub>2</sub>		Hyb2F	1748.6465 874.8269	[M+H] <sup>+</sup> [M+2H] <sup>2+</sup>	15.5	-	15.7	15.5	15.5
(Hex) <sub>1</sub> (HexNAc) <sub>3</sub> (dHex) <sub>1</sub> (Man) <sub>3</sub> (GlcNAc) <sub>2</sub>		T1	1830.6996 915.8534	[M+2H] <sup>2+</sup>	15.9 17.2	16.1 17.3	16.1 17.2	- -	16.0 17.2

Table 5-1 continued...

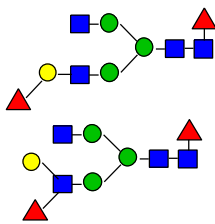
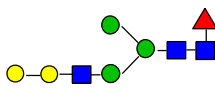
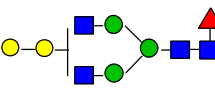
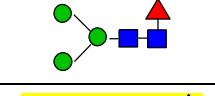
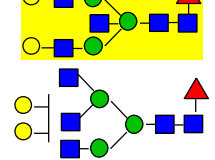
$(\text{Hex})_1(\text{HexNAc})_2$ $(\text{dHex})_2$ $(\text{Man})_3(\text{GlcNAc})_2$		F1	1773.6781 887.3427	$[\text{M}+\text{H}]^+$ $[\text{M}+2\text{H}]^{2+}$	16.1 16.6	16.1 16.6	16.3	-	16.2
$(\text{Hex})_2(\text{HexNAc})_1$ $(\text{dHex})_1$ $(\text{Man})_3(\text{GlcNAc})_2$		G2-GlcNAc	1586.5936 793.8005	$[\text{M}+\text{H}]^+$ $[\text{M}+2\text{H}]^{2+}$	16.2	-	16.4	16.3	16.3
$(\text{Hex})_2(\text{HexNAc})_2$ $(\text{dHex})_1$ $(\text{Man})_3(\text{GlcNAc})_2$		G2	1789.6730 895.3401	$[\text{M}+\text{H}]^+$ $[\text{M}+2\text{H}]^{2+}$	16.1 16.8	- -	16.2 17.0	- -	16.2 17.0
$(\text{dHex})_1$ $(\text{Man})_3(\text{GlcNAc})_2$		G0-2GlcNAc	1059.4086 530.2079	$[\text{M}+\text{H}]^+$	-	-	-	16.6	-
$(\text{Hex})_2(\text{HexNAc})_3$ $(\text{dHex})_1$ $(\text{Man})_3(\text{GlcNAc})_2$		T2	1992.7524 996.8798	$[\text{M}+2\text{H}]^{2+}$	16.7 17.6	16.8 17.7	16.8 17.7	-	-

Table 5-1 continued...

$(\text{Hex})_2(\text{HexNAc})_2$ $(\text{dHex})_2$ $(\text{Man})_3(\text{GlcNAc})_2$		F2	1935.7309 968.3691	$[\text{M}+2\text{H}]^{2+}$	16.8 17.2	17.0 17.4	17.0 17.2	16.9 17.2	16.9 17.2
$(\text{Hex})_3(\text{HexNAc})_2$ $(\text{dHex})_1$ $(\text{Man})_3(\text{GlcNAc})_2$		G3	1951.7258 976.3666	$[\text{M}+2\text{H}]^{2+}$	17.1 17.5	-	17.2 17.7	17.1 17.6	17.1 17.6
$(\text{Hex})_4(\text{HexNAc})_1$ $(\text{dHex})_1$ $(\text{Man})_3(\text{GlcNAc})_2$		Hyb3F	1910.6993 955.8533	$[\text{M}+2\text{H}]^{2+}$	17.1	-	17.4	17.1	-
$(\text{Hex})_3(\text{HexNAc})_3$ $(\text{dHex})_1$ $(\text{Man})_3(\text{GlcNAc})_2$		T3	2154.8052 1077.9062	$[\text{M}+2\text{H}]^{2+}$	18.2	18.3	18.2	18.2	-
$(\text{Hex})_3(\text{HexNAc})_2$ $(\text{dHex})_2$ $(\text{Man})_3(\text{GlcNAc})_2$		F3	2097.7837 1049.3955	$[\text{M}+2\text{H}]^{2+}$	18.2 18.8	-	18.4 18.9	18.3 18.8	18.2 18.8

Table 5-1 continued...

(Hex) <sub>1</sub> (HexNAc) <sub>1</sub> (dHex) <sub>1</sub> (Man) <sub>3</sub> (GlcNAc) <sub>2</sub>		G1- GlcNAc			-	-	-	18.4	-
(Hex) <sub>4</sub> (HexNAc) <sub>2</sub> (dHex) <sub>1</sub> (Man) <sub>3</sub> (GlcNAc) <sub>2</sub>		G4	2113.7787 1057.3930	[M+2H] <sup>2+</sup>	18.8	-	19.0	18.9	18.9
(Hex) <sub>2</sub> (HexNAc) <sub>1</sub> (dHex) <sub>1</sub> (Man) <sub>3</sub> (GlcNAc) <sub>2</sub>		G2- GlcNAc	1586.5936 793.8005	[M+H] <sup>+</sup> [M+2H] <sup>2+</sup>	-	-	-	19.9	-
(Hex) <sub>3</sub> (HexNAc) <sub>1</sub> (NeuGc) <sub>1</sub> (Man) <sub>3</sub> (GlcNAc) <sub>2</sub>		Hyb2+ NeuGc	1909.6789 955.3431	[M+2H] <sup>2+</sup>	27.1	25.0	-	24.3	-
(Hex) <sub>2</sub> (HexNAc) <sub>1</sub> (dHex) <sub>1</sub> (NeuGc) <sub>1</sub> (Man) <sub>3</sub> (GlcNAc) <sub>2</sub>		Hyb1F+ NeuGc	1893.6840 947.3456	[M+2H] <sup>2+</sup>	28.4	26.0	-	25.5	23.0
(Hex) <sub>1</sub> (HexNAc) <sub>2</sub> (dHex) <sub>1</sub> (NeuGc) <sub>1</sub> (Man) <sub>3</sub> (GlcNAc) <sub>2</sub>		G1+NeuGc	1934.7105 967.8589	[M+2H] <sup>2+</sup>	29.8	26.8	-	-	24.1
(Hex) <sub>3</sub> (HexNAc) <sub>1</sub> (dHex) <sub>1</sub> (NeuGc) <sub>1</sub> (Man) <sub>3</sub> (GlcNAc) <sub>2</sub>		Hyb2F+ NeuGc	2055.7368 1028.3720	[M+2H] <sup>2+</sup>	29.9	27.7	-	27.3	-
(Hex) <sub>1</sub> (HexNAc) <sub>1</sub> (dHex) <sub>1</sub> (NeuGc) <sub>1</sub> (Man) <sub>3</sub> (GlcNAc) <sub>2</sub>		G1+NeuGc -GlcNAc	866.3192 1731.6311	[M+H] <sup>+</sup> [M+2H] <sup>2+</sup>	30.2	27.6	-	27.0	24.4



All hybrid structures in the MAb3 sample were found in the fucosylated and defucosylated forms, whereas fucosylated species were dominant for complex glycans and only defucosylated high mannose glycans were found in the sample. Since fucose is generally attached to the glycan core after the glycoprotein has already been processed by mannosidase enzymes (Figure 1–2), this result is not surprising. A glycan profile with a large variety of unprocessed glycans suggests the lower activity of specific enzymes involved in the biosynthetic pathway of N-glycans in this NS0 cell line.

Using the improved procedure, sialylated species previously identified by nano ZIC-HILIC were observed in the PGC chromatogram of MAb3 glycans. As previously suggested, the charged glycans were much more strongly retained by PGC under the applied conditions, with broader peaks being observed compared to those of neutral glycans. Exoglycosidase digestions confirmed the proposed structures, which are mainly core-fucosylated containing NeuGc rather than NeuAc. NeuGc was expected for the MAb expressed in the murine system and is consistent with previously reported data.

Using PGC with optimised sample preparation, another series of complex glycans with additional GlcNAc was identified that was not previously observed by any ZIC-HILIC method due to the low abundance (Figure 5–8). There are two likely series of glycans with the same monosaccharide compositions, either with an additional bisecting GlcNAc or a GlcNAc attached to one of the arms forming triantennary glycans. Since GlcNAc is usually  $\beta$ -linked to the core, it is difficult to distinguish between the two possible glycan series by using exoglycosidase digestions alone. However, some indications were found suggesting that triantennary glycans are more likely to correspond to the observed peaks. For the  $m/z$  996.88, which most likely corresponds to one of the suggested structures with two additional galactose units on the antennae, several peaks were observed, indicating multiple positional isomers. For the glycan with bisecting GlcNAc, the possible isobaric structures would contain one  $\beta$ -linked galactose on each antenna or  $\beta$ - and  $\alpha$ -linked galactose on either arm. The latter structural



motif was not consistent with the  $\alpha$ -galactosidase digestion (Table 5-1, shaded in yellow). On the other hand, the triantennary glycan structures are consistent with the results of  $\alpha$ -galactosidase digestion. These results are in agreement with the chromatograms for  $m/z$  1077.91, where no  $\alpha$ -galactosylation was confirmed which would indicate the presence of the glycan with bisecting GlcNAc. Two structures were therefore confirmed as triantennary and it is possible to deduce that all the observed glycans belong to the same structural group.

Using PGC, a series of glycans with additional fucose (F1-GlcNAc, F1, F2, F3) was observed in the MAb3 sample (Figure 5-9). Using the GlycoSuite database (<http://glycosuitedb.expasy.org/glycosuite/glycodb>) two previously reported likely structures were found for most of the observed  $m/z$  values; one with the additional fucose linked to GlcNAc and the other with fucose linked to terminal galactose. Since this glycosylation pattern is quite unusual, further digestions with linkage-specific fucosidase are required to elucidate these structures. However, due to extremely low amounts of these glycans in the sample, further experiments have not been conducted. It is likely that all the observed glycans from the same glycoprotein would exhibit similar glycosylation pattern, as evident in the case of the hybrid and complex glycans found in this MAb. It is assumed that all the additionally fucosylated glycans belong to the same structural class and differ only in the degree of galactosylation. Another four peaks indicating possible terminal fucosylation, are early eluting G0, G1 and G1-GlcNAc (shaded with green). However, it is possible that these peaks are artefacts.

As demonstrated here, the use of PGC was extremely useful in analysis of highly complex samples, such as the glycans released from MAb3. Previously described HILIC approaches provided only limited information regarding the isobaric species present in the sample, and MS sensitivity was somewhat low due to a higher background originating from the higher acetonitrile content in the mobile phase. On the other hand, the use of PGC was found to be less suitable for the analysis of sialylated glycans due to poor reproducibility of the retention times of

charged glycans under the applied conditions, with retention decreasing over time. This could be due to ageing of the PGC surface [87]. It was shown that PGC is superior for structural elucidation of neutral isobaric glycans compared to HILIC, with more detailed information being provided for hybrid structures. However, the PGC method is less suitable for glycan quantification and routine analysis in quality control of biopharmaceuticals. It is believed that methods based on fluorescence detection will continue developing in the future due to the high sensitivity, quantitative analysis and simplicity of data interpretation.

The improved sample preparation was used also for MAb1 and MAb2 samples; however, no additional glycans were observed by the PGC method. These results confirmed a more uniform glycan profile of the MAbs expressed in CHO cells, as observed also by amide HILIC and ZIC-HILIC approaches.

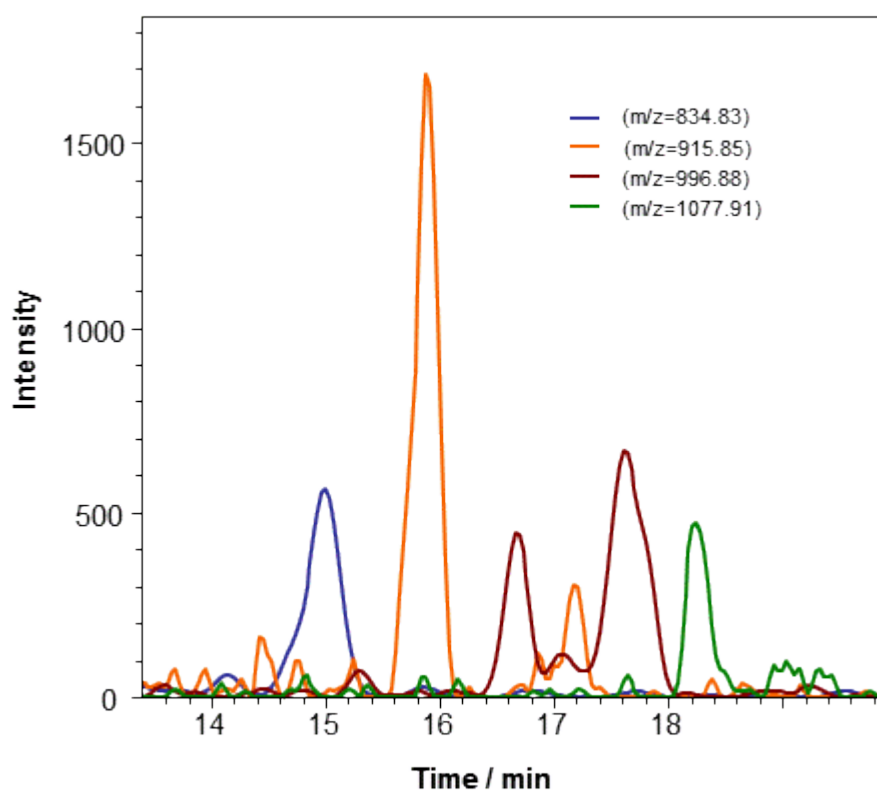


Figure 5-8: EICs of triantennary glycans found in MAb3 obtained by PGC. Multiple isomeric structures were found for T1 and T2 chromatogram traces, whereas only one isomer was observed for T0 and T3 glycans.

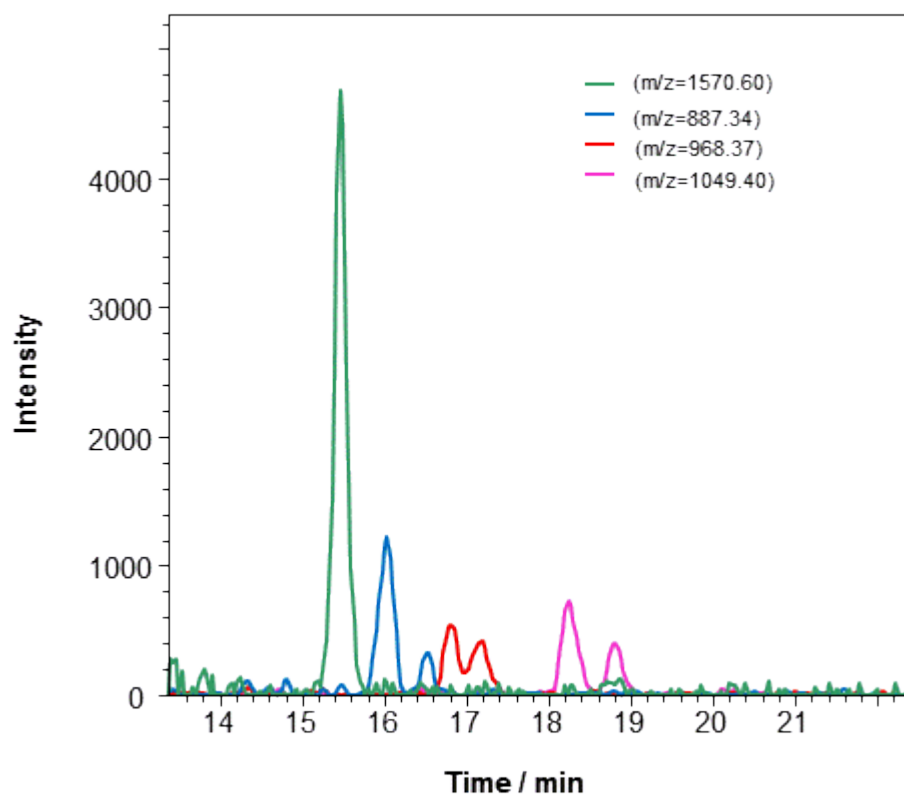


Figure 5-9: EICs of fucosylated glycans found in MAb3 obtained by PGC. Two isobaric species were observed for F1-F3 glycans, indicating the presence of structural isomers. Only one peak was observed for F1-GlcNAc, most likely with the free 6-arm as confirmed for other glycan species in the sample.

### 5.3.2. Tandem mass spectrometry

Glycans separated by graphitized carbon were further fragmented by collision induced dissociation (CID) in the QTOF mass spectrometer in order to evaluate the benefits and limitations of tandem mass spectrometry. Since acetic acid was used as the mobile phase, glycans were mainly detected as singly and doubly protonated species, which was expected to reduce the quality of fragmentation information. Fragmentation of protonated ions usually results in glycosidic bond cleavages producing B- and Y- type ions. This type of fragmentation generally provides information on monosaccharide residues constituting the glycan; however, information on branching and linkages cannot be obtained.

Fragmentation under the applied conditions was studied on the most abundant high mannose and complex glycans, Man5 and G0, respectively (Figure 5–10 to Figure 5–12).

The Man5 fragment spectrum was relatively simple with two glycosidic cleavages observed. As expected, Y-type cleavage of mannose and B-type cleavage of GlcNAc from the core with further fragmentation of B- and Y-fragments by successive losses of mannose residues was observed. The MS/MS spectrum was not very informative and only information on monosaccharide units could be obtained. Since the monosaccharide composition was already determined by accurate mass, tandem MS did not provide any additional information regarding glycan structure.

The fragment spectrum of G0 glycan was more complex compared to the Man5 spectrum. Since G0 formed intense singly and doubly protonated species, both ions were fragmented in order to choose optimum conditions for quality mass spectra (Figure 5–11 and Figure 5–12). Despite a lower collision energy used for fragmentation of the doubly protonated G0 ion, more extensive fragmentation was observed compared to the singly protonated ion, resulting in the loss of information on cleavages of terminal residues. Various collision energies were tested to achieve appropriate fragmentation conditions (not shown) and singly

protonated ions were selected as more suitable for further investigation. For all of the selected ions, glycosidic bond cleavage was observed, producing B- and Y-type fragment ions. As expected, for the Y ion series the loss of terminal GlcNAcs was observed, followed by the loss of fucose and mannose residues, respectively. On the other hand, B ion series exhibited unusual fragmentation pattern. For protonated core-fucosylated glycans, B-type cleavage of GlcNAcFuc residue from the reducing end is generally expected [100]. However, in the mass spectrum of G0 glycan, two B-type ions, 1039.38 and 1242.46, were observed. The first one most likely resulted from the loss of GlcNAcFuc residues at the reducing end of the molecule. The 1242.46 B-type ion indicated the loss of GlcNAc, which would not be possible without additional fucose transfer within the molecule. This result indicates the occurrence of rearrangement reactions which appeared as an internal loss of GlcNAc residue and could lead to incorrect interpretation of fragment spectra.

Tandem MS was used also for confirmation of the structure of Hyb2 glycan, eluted at 12.2 min, which was previously studied by exoglycosidase digestions (Figure 5–13). As expected, the B- and Y- type fragmentations were observed. Both series of fragment ions suggest loss of hexose and subsequent loss of GlcNAc, which excluded the possibility of the hybrid structure with  $\alpha$ -galactosylation on the 3-arm, which was in agreement with the results obtained by exoglycosidase digestions. Since for all the glycans terminating with GlcNAc extensive loss of the GlcNAc residue was observed, it can be deduced that the fragment spectrum in Figure 5–13 belongs to the hybrid glycan with terminal galactose in the 3-arm. The proposed glycan is in agreement with other hybrid glycan species found in MAb3.

It is noted that all glycan structures presented in this study were proposed based on literature reviews, previous reports, and knowledge of possible synthetic pathways found in the cell systems used for expression of the MAbs.

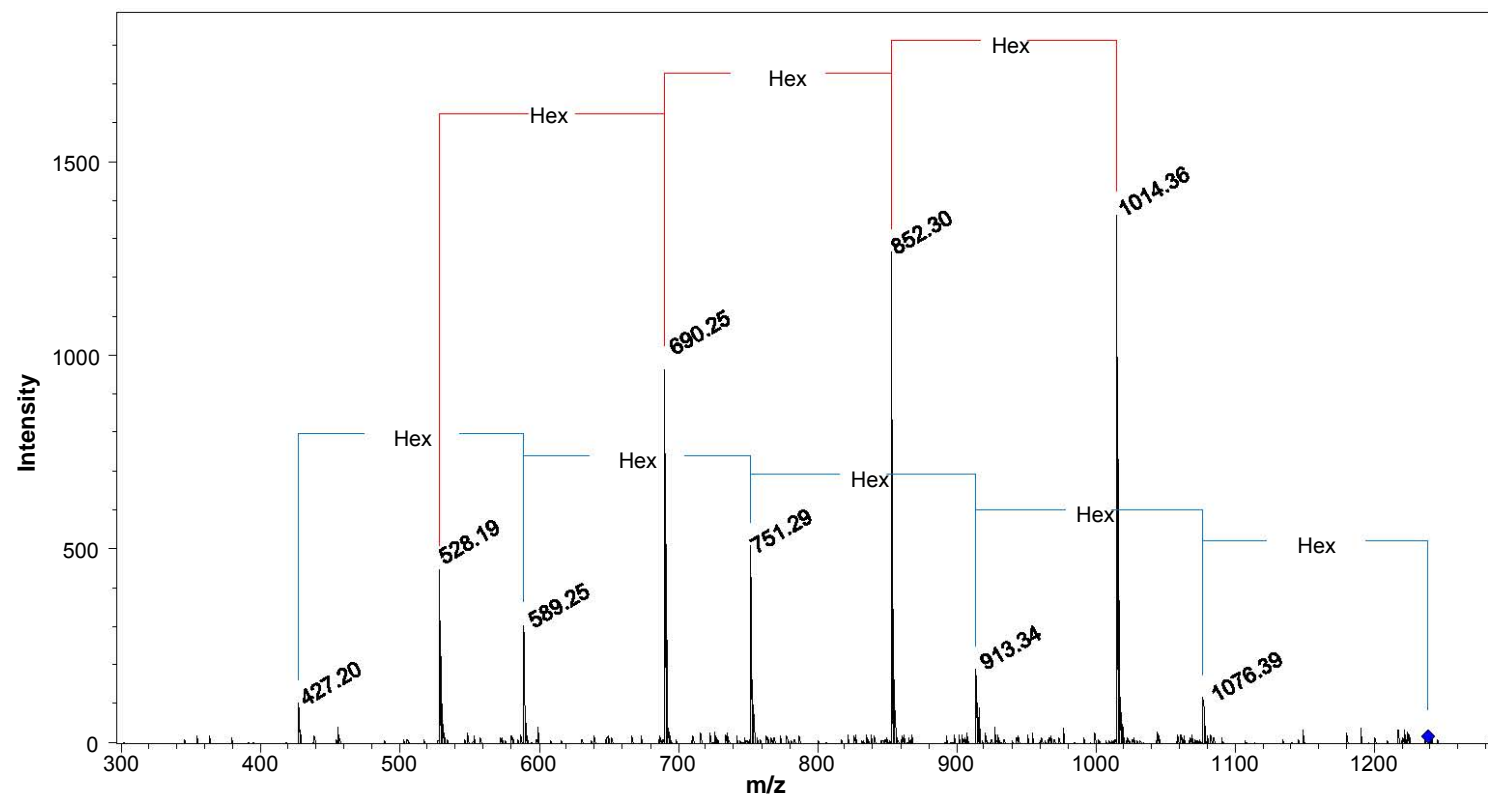


Figure 5–10: CID fragment spectrum of Man5 glycan, positive ion mode, collision cell energy 27 eV.

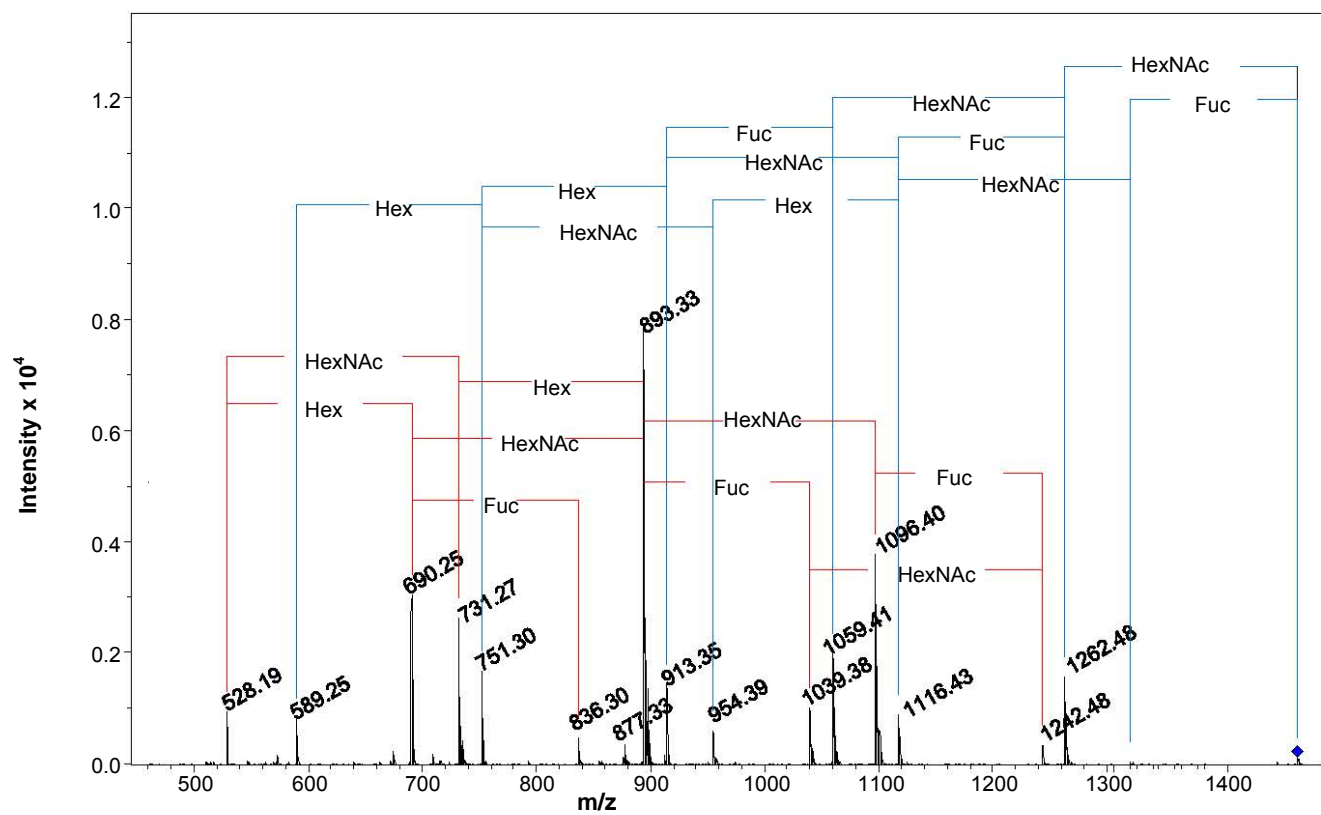


Figure 5-11: CID fragment spectrum of singly protonated G0 glycan, positive ion mode, collision cell energy 30 eV.

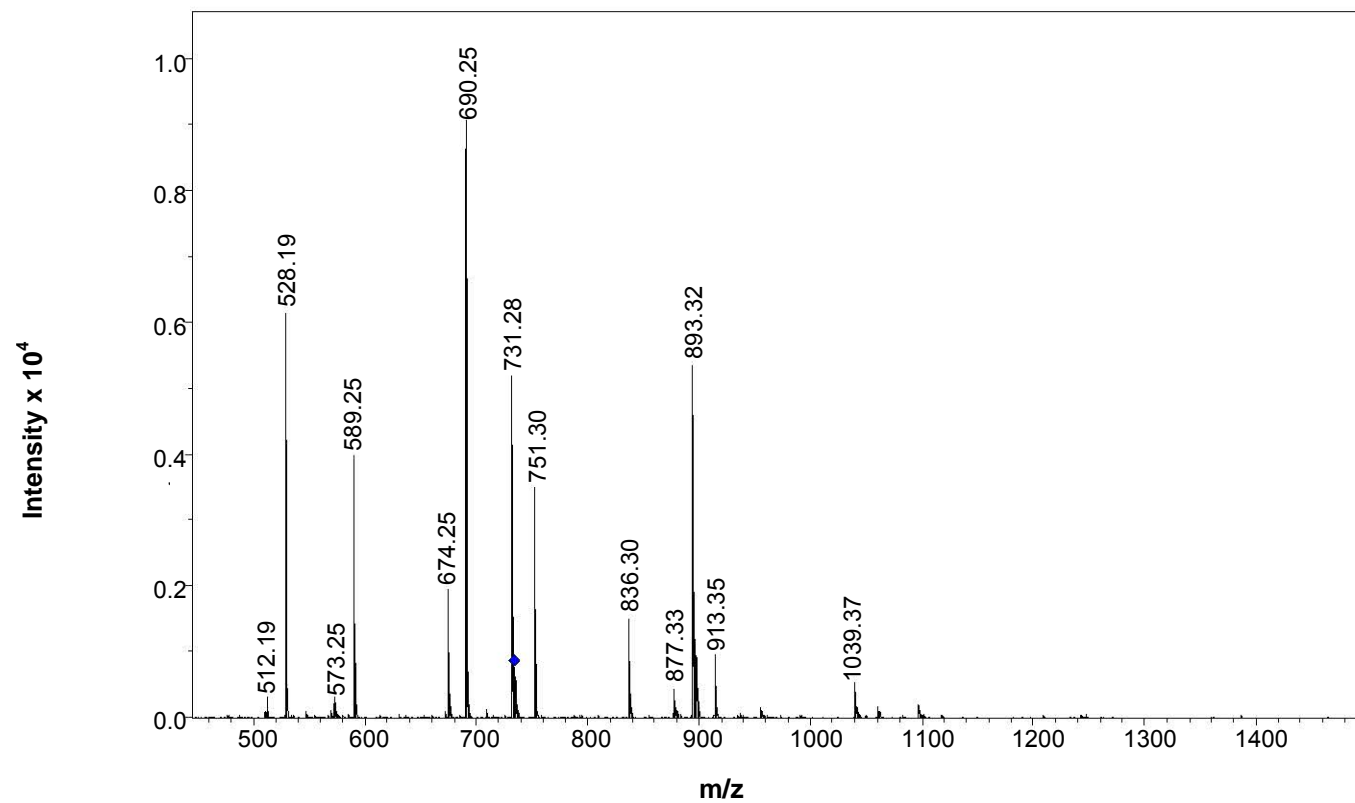


Figure 5-12: CID fragment spectrum of doubly protonated G0 glycan, positive ion mode, collision cell energy 17 eV.



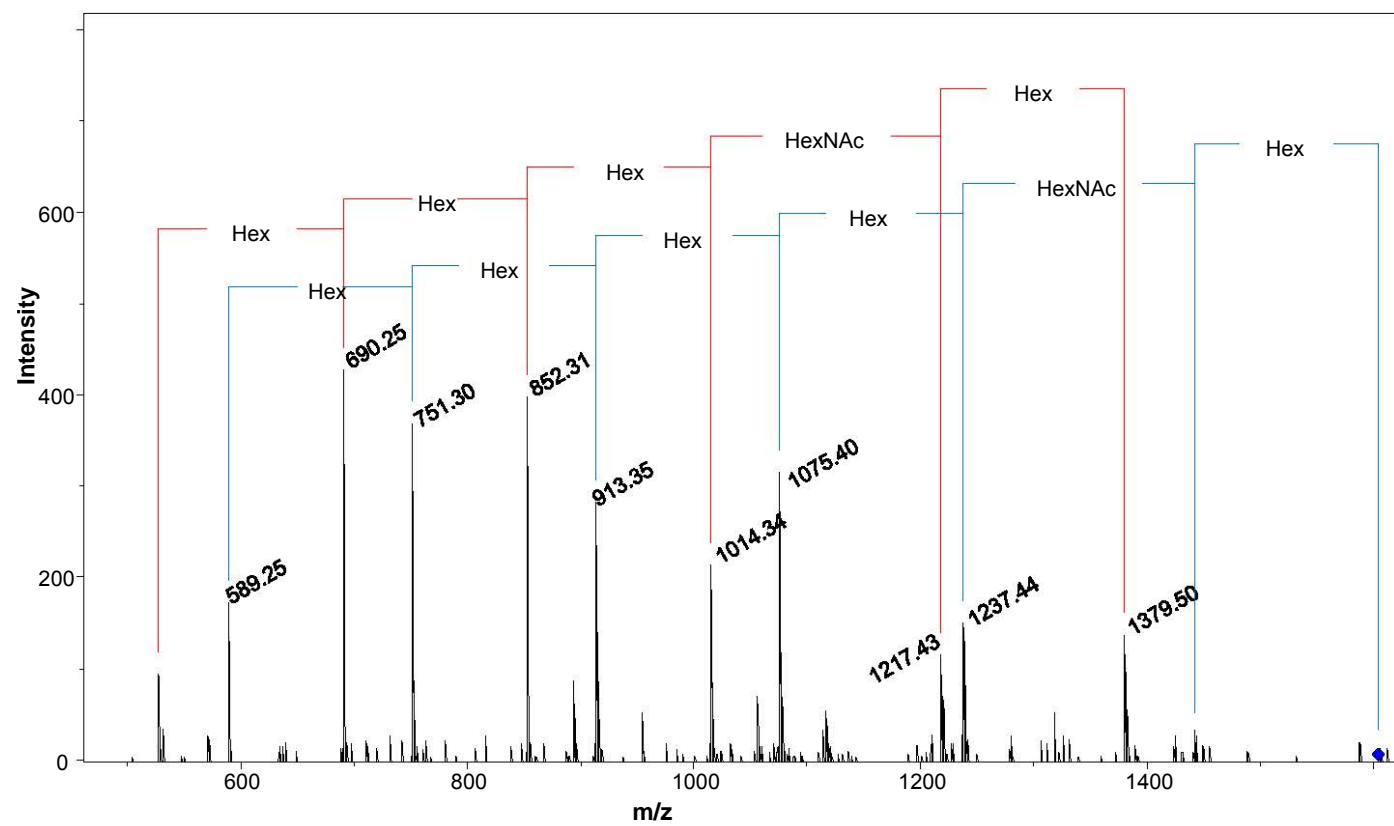


Figure 5–13: CID fragment spectrum of doubly protonated Hyb2 glycan, positive ion mode, collision cell energy 31 eV.

Exoglycosidase digestions and tandem MS were used for confirmation of the proposed structures. However, none of the described methods provided sufficient information for absolute structural elucidation. Due to the large amount of information available on glycosylation of hamster and mouse systems available, the proposed structures can however be confirmed with high confidence.

There are several limitations of the procedures used in this study. Exoglycosidase digestions require additional sample preparation; however, the higher the specificity of the enzyme, the more conclusive is the information on branching and linkages which can be obtained.

MS on the other hand, provides information on the mass of the glycan. If high mass resolution analysers are used, measured accurate mass alone can provide sufficient information to deduce the monosaccharide composition, which would allow only a limited number of possible glycan species. As shown in this study, PGC is a highly suitable stationary phase for the separation of isobaric species, which enables further analysis of glycans either by tandem MS or exoglycosidase digestions. Since PGC separation with an acidic mobile phase, as used in this study, resulted in ESI formation of protonated ions, only limited information could be obtained by MS/MS. Another drawback of the proposed method was insufficient sensitivity. Since most of the hybrid and complex fucosylated and sialylated glycans of interest were present in the sample in extremely low amounts, it was impossible to obtain any quality MS/MS spectra. Possible rearrangements observed under the described conditions could provide misleading information, especially for glycans with additional fucosylation [107]. It is suggested that the proposed MS/MS approach is not suitable for structural elucidation, although some additional information may be obtained and MS/MS spectra of protonated glycans should be interpreted with great care.

It is believed that better quality MS/MS information providing details on structures could be achieved in the negative ion mode [110]. Since sensitivity in the negative mode is much lower compared to the positive mode, this approach

could not be used in combination with the described PGC separation. It is suggested that the use of nano PGC could significantly improve MS sensitivity and therefore more structural information could be obtained either in positive, or even more likely, in negative ion mode [88].

Another MS/MS based approach for structural elucidation would include permethylation of glycans to improve sensitivity and quality of fragment spectra with extensive cross-ring cleavages that could provide information on linkages and branching. In the case of complex samples with several isobaric species present, separation of permethylated glycans prior to MS/MS would be recommended; however, chromatographic resolution might be lower using this approach [132].

As shown in this study, currently there is no universal analytical approach that could provide complete information on glycosylation of complex samples. PGC was shown to be very useful for analysis of neutral glycans due to the high capability for separation of isobaric species; however, due to the ageing of the PGC surface stable retention times for sialylated glycans could not be achieved. Advantages and limitations of various approaches for structural elucidation were demonstrated for an extremely complex monoclonal antibody. Exoglycosidase digestions are commonly used in combination with separation techniques and MS based approaches. The sample preparation and LC analysis of digests are time consuming; however, the results are clear and easy to interpret. On the other hand, analysis of MS/MS spectra is extremely challenging, and the optimum results are usually achieved after permethylation of glycans. It is suggested that combination of separation and MS based strategies is required for detailed glycosylation analysis, either in the field of glycomics or in quality control of pharmaceutical glycoproteins.

## 5.4. Conclusions

Two approaches for structural elucidation, namely exoglycosidase digestions and tandem MS, coupled with chromatographic separation have been studied.

PGC was used as the most suitable stationary phase for separation of neutral glycans. It was shown that several isobaric species were separated using this approach and exoglycosidase digestions confirmed the proposed structures. Several isobaric species with various degrees of galactosylation/mannosylation were confirmed in the MAb3 sample, including the potentially immunogenic  $\alpha$ -galactose and NeuGc epitopes.

The PGC method was further coupled to tandem MS. Due to the use of an acidic mobile phase, the most abundant protonated ions were selected for CID fragmentation. Using this approach, the extensive B- and Y-type glycosidic bond cleavages were observed for all selected ions, providing only limited information on glycan structure. Since most of the unknown glycans in MAb3 were present only in very low amounts, quality MS/MS spectra could not be obtained. Due to the lower sensitivity in negative ion mode, the method was not suitable for fragmentation of deprotonated species, although it is believed that negative MS/MS spectra could provide more structural information.

It was shown that high resolution mass spectrometry can provide sufficient information on monosaccharide composition, which in combination with separation techniques and exoglycosidase digestions allows detailed analysis of very complex samples.

## Chapter Six

### ***6. Conclusions and future work***

#### **6.1. Project summary**

The aim of this project was to develop new methods for analysis of monoclonal antibody glycosylation in order to simplify the sample preparation, improve the separation and improve sensitivity in ESI-MS detection. Several new methods were developed using zwitterionic-type hydrophilic interaction chromatography. A model glycoprotein RNase B and three monoclonal antibodies expressed in different cell lines were used in this study. The new methods were compared to the standard procedure for separation of 2-AB labelled glycans performed on a HILIC stationary phase with amide functionality, as currently used in the pharmaceutical industry. It was demonstrated that ZIC-HILIC was a suitable stationary phase for separation of 2-AB labelled glycans and the method was coupled to fluorescence detection, which allowed relative quantification of glycan species. The method was optimised for on-line coupling with ESI-MS, which provided additional information on glycan composition. A significant difference in glycan profiles between MAbs expressed in CHO and NS0 cell lines has been observed; however, limited sensitivity did not allow the identification of minor glycan species in these samples.

In order to simplify the sample preparation, the ZIC-HILIC column was tested for the separation of native and reduced glycans from RNase B and MAbs. Since chromatography of native glycans resulted in undesirable separation of anomers, the work focused on the separation of reduced glycans, which improved sensitivity and simplified chromatograms. Lower sensitivity compared to the fluorescence detection of 2-AB labelled glycans was achieved; however, all the major glycan species previously identified by the standard procedure were identified by the new proposed method.

To obtain a relevant comparison of methods for the separation of reduced glycans, a conventional graphitized carbon column was compared to ZIC-HILIC. The graphitized carbon column exhibited a superior capability for separation of reduced glycans and several isobaric species were effectively separated using this procedure. The sensitivity was higher than for the ZIC-HILIC method and several new glycan species were observed by this method. The graphitized carbon method confirmed the difference between the profiles of MAbs expressed in CHO cell line to that expressed in murine NS0 cell line. MAb3 from the murine expression system exhibited a relatively high degree of  $\alpha$ -galactosylation, which was absent in the CHO MAbs. At the same time several hybrid structures were found in the glycan profile of MAb3. However, the graphitized carbon method alone was not sufficient for structural elucidation of glycan species found in MAb3 and for several observed  $m/z$  values, multiple structures with various degrees of mannosylation and galactosylation could be assigned.

All the standard-bore methods used exhibited lower sensitivity compared to the standard amide HILIC procedure coupled with fluorescence detection and no charged glycans were confirmed in the MAbs, although low amounts of sialylated glycans were expected to be present in the samples. To improve the ESI-MS sensitivity of the ZIC-HILIC method for separation of reduced glycans, a nanoscale ZIC-HILIC column with internal diameter of 75  $\mu\text{m}$  was employed. Using nano ZIC-HILIC, the sensitivity for neutral glycans increased approximately 70-fold, and seven negatively charged glycans were observed in the MAb3 sample. The nano ZIC-HILIC separation was coupled to a high resolution orthogonal TOF mass spectrometer, which enabled determination of glycan composition with high confidence. For six sialylated glycans two possible glycan structures could be assigned, either containing  $\text{dHex}_1\text{NeuGc}_1$  or  $\text{Hex}_1\text{NeuAc}_1$  combinations of glycan residues. Due to the fact that MAb3 was expressed in a murine cell line, a high level of fucosylation and the confirmed presence of NeuGc in the sample, it was suggested that the first combination is more likely. However, for the complete structural elucidation further

experiments were required. The nano ZIC-HILIC method confirmed once more the presence of hypergalactosylated glycan species in MAb3.

Since many glycans species found using the ZIC-HILIC and PGC methods could not be structurally characterised, exoglycosidase digestions and tandem mass spectrometry were employed in the final part of the project. PGC was chosen to be the most suitable stationary phase for confirmation of the proposed neutral and sialylated glycan structures. By using PGC, several isobaric species with various degrees of galactosylation and mannosylation were confirmed in the sample, which revealed higher complexity of the MAb3 sample than suggested by the standard amide HILIC procedure. Exoglycosidase digestions also confirmed the presence of potentially immunogenic epitopes containing  $\alpha$ -linked galactose and N-glycolylneuraminic acid. Furthermore, two series of previously unobserved triantennary and additionally fucosylated glycans were identified in MAb3.

In contrast to the exoglycosidase digestions, tandem MS coupled with PGC provided only limited information on glycan structure. Due to the low abundance of the unknown glycans present in the MAb3 sample, quality MS/MS spectra for most of the species could not be obtained. Furthermore, due to the use of acidic mobile phase only protonated glycans could be selected for fragmentation, which exhibited only B- and Y-type cleavage of glycosidic bonds with no additional structural information. It was demonstrated that high resolution mass spectrometry can provide sufficient information on glycan composition, which in combination with a suitable separation technique and exoglycosidase digestions, allows detailed analysis of complex real samples.

## 6.2. Suggested future work

This project has investigated in detail two LC-based approaches for glycosylation analysis of monoclonal antibodies. Whereas ZIC-HILIC was shown to be suitable for the separation of fluorescently-labelled and reduced glycans, the PGC method was shown to be superior for the separation of reduced neutral isobaric species.

The proposed methods exhibited enhanced sensitivity, separation of isobaric species, and high resolution MS data and allowed identification of glycan species that could not be confirmed by the standard amide HILIC procedure. However, several questions regarding the structure of less common minor glycan species remain unanswered. For the structural characterisation of these glycan species further analysis employing highly specific exoglycosidases, possibly in combination with tandem MS, would be required. To obtain sufficient chromatographic resolution and ESI-MS sensitivity, the use of nano PGC would be suggested. The miniaturised system could potentially allow detection and fragmentation of the unknown species in negative ion mode, which could provide additional structural information. It is believed that downscaling, not only in nano column format but also in chip format, will become a standard in the glycosylation analysis.

In this project, the use of ZIC-HILIC was demonstrated primarily on oligomannosidic and biantennary complex glycans which are expected to be found in monoclonal antibodies expressed in mammalian systems. It is suggested that the ZIC-HILIC stationary phase could be further tested for the separation of a broader spectrum of neutral and charged glycan species, which could increase its applicability in biotechnology and glycomics research.

Sensitivity and quality of fragmentation data for structural elucidation and quantification could be additionally improved by permethylation. When complex samples with multiple isobaric species are to be analysed, the method would require separation of glycans prior to MS detection. Development of new methods and stationary phases for separation of permethylated glycans could be required to achieve suitable chromatographic resolution of closely related glycan species and structural isomers. Furthermore, additional fluorescent tags could be tested for use in combination with ZIC-HILIC or PGC in order to improve chromatographic separation or sensitivity in ESI-MS and fluorescence detection. Due to the good selectivity of ZIC-HILIC for the separation of neutral and charged glycans either in reduced or 2-AB labelled form, it is believed that



labelling with 2-aminobenzoic acid could be compatible with this stationary phase.

There is a high demand for establishing databases of retention properties of glycans on various stationary phases for simpler assignment of chromatographic peaks. Currently, only databases for amide HILIC are generally available; however, some research groups develop their own databases of glycan structure-retention properties for PGC. Simplified data analysis and peak assignment could make the new methods more attractive also for the use in glycomics research.

### **6.3. Conclusions**

This project has investigated several techniques and approaches in glycosylation analysis of recombinant therapeutic monoclonal antibodies. Two strategies for glycan analysis were employed. The first approach was focused on separation of 2-AB labelled glycans using two HILIC stationary phases coupled with fluorescence detection, whereas the other approach was focused on separation of reduced glycans in order to simplify the sample preparation, and miniaturisation which allowed MS detection of glycans with improved sensitivity. The combination of different approaches enabled detailed analysis of extremely complex real samples containing neutral and charged, complex and hybrid glycans. The newly developed methods were used in combination with exoglycosidase digestions and tandem mass spectrometry for the study of minor glycan species that are potentially immunogenic in humans. The practical value of rapid and sensitive methods for glycosylation analysis in quality control of biopharmaceuticals was demonstrated. Since the same principles apply to the analysis of glycans from organisms, glycomics may be another field for potential application of the presented methods.

## 7. References

- [1] Mann, M., Jensen, O. N., *Nat. Biotech.* 2003, 21, 255-261.
- [2] Walsh, G., Jefferis, R., *Nat. Biotech.* 2006, 24, 1241-1252.
- [3] Spiro, R. G., *Glycobiology* 2002, 12, 43R-56R.
- [4] Varki, A., Cummings, R. D., Esko, J. D., Freeze, H. H., *et al.* (Eds.), *Essentials of Glycobiology*, Cold Spring Harbor Laboratory Press 2009.
- [5] Freeze, H. H., *Nat. Rev. Genet.* 2006, 7, 537-551.
- [6] Winchester, B., *Glycobiology* 2005, 15, 1R-15R.
- [7] Varki, A., Cummings, R. D., Esko, J. D., Freeze, H. H., *et al.*, *Proteomics* 2009, 9, 5398-5399.
- [8] Harvey, D. J., Merry, A. H., Royle, L., P. Campbell, M., *et al.*, *Proteomics* 2009, 9, 3796-3801.
- [9] Dwek, R. A., Butters, T. D., Platt, F. M., Zitzmann, N., *Nat. Rev. Drug Discov.* 2002, 1, 65-75.
- [10] Jefferis, R., Amer. Chemical. Soc. 2005, pp. 11-16.
- [11] Griggs, J., Zinkewich-Peotti, K., *Br J. Cancer* 2009, 101, 1807-1812.
- [12] Jiang, X.-R., Song, A., Bergelson, S., Arroll, T., *et al.*, *Nat. Rev. Drug Discov.* 2011, 10, 101-111.
- [13] Solá, R. J., Griebenow, K., *J. Pharm. Sci.* 2009, 98, 1223-1245.
- [14] Isaacs, J. D., *Arthritis Res. Ther.* 2009, 11, 11.
- [15] Baker, K. N., Rendall, M. H., Hills, A. E., Hoare, M., *et al.*, *Biotech. Bioeng.* 2001, 73, 188-202.
- [16] Beck, A., Wagner-Rousset, E., Bussat, M.-C., Lokteff, M., *et al.*, *Curr. Pharm. Biotech.* 2008, 9, 482-501.
- [17] Jefferis, R., *Nat. Rev. Drug Discov.* 2009, 8, 226-234.
- [18] Sheeley, D. M., Merrill, B. M., Taylor, L. C. E., *Anal. Biochem.* 1997, 247, 102-110.
- [19] Bosques, C. J., Collins, B. E., Meador, J. W., Sarvaiya, H., *et al.*, *Nat. Biotech.* 2010, 28, 1153-1156.

- [20] Noguchi, A., Mukuria, C. J., Suzuki, E., Naiki, M., *J. Biochemistry* 1995, 117, 59-62.
- [21] Ghaderi, D., Taylor, R. E., Padler-Karavani, V., Diaz, S., Varki, A., *Nat. Biotech.* 2010, 28, 863-867.
- [22] Saint-Jore-Dupas, C., Faye, L., Gomord, V., *Trends Biotech.* 2007, 25, 317-323.
- [23] Chen, X., Liu, Y. D., Flynn, G. C., *Glycobiology* 2009, 19, 240-249.
- [24] Castilho, A., Gattinger, P., Grass, J., Jez, J., *et al.*, *Glycobiology* 2011.
- [25] Mori, K., Iida, S., Yamane-Ohnuki, N., Kanda, Y., *et al.*, *Cytotechnology* 2007, 55, 109-114.
- [26] Kanda, Y., Yamada, T., Mori, K., Okazaki, A., *et al.*, *Glycobiology* 2007, 17, 104-118.
- [27] Kaneko, Y., Nimmerjahn, F., Ravetch, E. V., *Science* 2006, 313, 670-673.
- [28] Raman, R., Raguram, S., Venkataraman, G., Paulson, J. C., Sasisekharan, R., *Nat. Meth.* 2005, 2, 817-824.
- [29] Kamoda, S., Ishikawa, R., Kakehi, K., *J. Chromatogr. A* 2006, 1133, 332-339.
- [30] Wagner-Rousset, E., Bednarczyk, A., Bussat, M. C., Colas, O., *et al.*, *J. Chromatogr. B* 2008, 872, 23-37.
- [31] Dillon, T. M., Bondarenko, P. V., Rehder, D. S., Pipes, G. D., *et al.*, *J. Chromatogr. A* 2006, 1120, 112-120.
- [32] Huhn, C., Selman, M. H. J., Ruhaak, L. R., Deelder, A. M., Wuhrer, M., *Proteomics* 2009, 9, 882-913.
- [33] Bailey, M. J., Hooker, A. D., Adams, C. S., Zhang, S. H., James, D. C., *J. Chromatogr. B* 2005, 826, 177-187.
- [34] Wuhrer, M., Stam, J. C., van de Geijn, F. E., Koeleman, C. A. M., *et al.*, *Proteomics* 2007, 7, 4070-4081.
- [35] Dalpathado, D. S., Desaire, H., *Analyst* 2008, 133, 731-738.
- [36] Wuhrer, M., Deelder, A. M., Hokke, C. H., *J. Chromatogr. B* 2005, 825, 124-133.
- [37] Stadlmann, J., Pabst, M., Kolarich, D., Kunert, R., Altmann, F., *Proteomics* 2008, 8, 2858-2871.
- [38] Takegawa, Y., Deguchi, K., Keira, T., Ito, H., *et al.*, *J. Chromatogr. A* 2006, 1113, 177-181.

- [39] Palms, A. K., Novotny, M. V., *Rapid Commun. Mass Spectrom.* 2005, 19, 1730-1738.
- [40] Krenkova, J., Lacher, N. A., Svec, F., *J. Chromatogr. A* 2009, 1216, 3252-3259.
- [41] Bynum, M. A., Yin, H., Felts, K., Lee, Y. M., *et al.*, *Anal. Chem.* 2009, 81, 8818-8825.
- [42] Patel, T. P., Parekh, R. B., in: William J. Lennarz, G. W. H. (Ed.), *Methods Enzymol.*, Academic Press 1994, pp. 57-66.
- [43] Bigge, J. C., Patel, T. P., Bruce, J. A., Goulding, P. N., *et al.*, *Anal. Biochem.* 1995, 230, 229-238.
- [44] Amon, S., Zamfir, A. D., Rizzi, A., *Electrophoresis* 2008, 29, 2485-2507.
- [45] Anumula, K. R., *Anal. Biochem.* 2006, 350, 1-23.
- [46] Campbell, M. P., Royle, L., Radcliffe, C. M., Dwek, R. A., Rudd, P. M., *Bioinformatics* 2008, 24, 1214-1216.
- [47] Prime, S., Dearnley, J., Ventom, A. M., Parekh, R. B., Edge, C. J., *J. Chromatogr. A* 1996, 720, 263-274.
- [48] Qian, J., Liu, T., Yang, L., Daus, A., *et al.*, *Anal. Biochem.* 2007, 364, 8-18.
- [49] Morelle, W., Donadio, S., Ronin, C., Michalski, J.-C., *Rapid Commun. Mass Spectrom.* 2006, 20, 331-345.
- [50] Morelle, W., Michalski, J.-C., *Nat. Protocols* 2007, 2, 1585-1602.
- [51] Yang, Y., Orlando, R., *Anal. Chem.* 1996, 68, 570-572.
- [52] Colangelo, J., Orlando, R., *Anal. Chem.* 1999, 71, 1479-1482.
- [53] Küster, B., Naven, T. J. P., Harvey, D. J., *J. Mass Spectrom.* 1996, 31, 1131-1140.
- [54] Harvey, D., Crispin, M., Moffatt, B., Smith, S., *et al.*, *Glycoconjugate J.* 2009, 26, 1055-1064.
- [55] Aoki, K., Perlman, M., Lim, J.-M., Cantu, R., *et al.*, *J. Biol. Chem.* 2007, 282, 9127-9142.
- [56] Balaguer, E., Demelbauer, U., Pelzing, M., Sanz-Nebot, V., *et al.*, *Electrophoresis* 2006, 27, 2638-2650.
- [57] Raju, T. S., Briggs, J. B., Borge, S. M., Jones, A. J. S., *Glycobiology* 2000, 10, 477-486.
- [58] Gennaro, L. A., Salas-Solano, O., *Anal. Chem.* 2008, 80, 3838-3845.

- [59] Kamoda, S., Nomura, C., Kinoshita, M., Nishiura, S., *et al.*, *J. Chromatogr. A* 2004, 1050, 211-216.
- [60] Ma, S., Nashabeh, W., *Anal. Chem.* 1999, 71, 5185-5192.
- [61] Kamoda, S., Kakehi, K., *Electrophoresis* 2008, 29, 3595-3604.
- [62] Behan, J. L., Smith, K. D., *Biomed. Chromatogr.* 2011, 25, 39-46.
- [63] Bruggink, C., Wuhrer, M., Koeleman, C. A. M., Barreto, V., *et al.*, *J. Chromatogr. B* 2005, 829, 136-143.
- [64] Grey, C., Edebrink, P., Krook, M., Jacobsson, S. P., *J. Chromatogr. B* 2009, 877, 1827-1832.
- [65] Deguchi, K., Keira, T., Yamada, K., Ito, H., *et al.*, *J. Chromatogr. A* 2008, 1189, 169-174.
- [66] Wuhrer, M., de Boer, A. R., Deelder, A. M., *Mass Spectrom. Rev.* 2009, 28, 192-206.
- [67] Guile, G. R., Rudd, P. M., Wing, D. R., Prime, S. B., Dwek, R. A., *Anal. Biochem.* 1996, 240, 210-226.
- [68] Royle, L., Campbell, M. P., Radcliffe, C. M., White, D. M., *et al.*, *Anal. Biochem.* 2008, 376, 1-12.
- [69] Bones, J., Mittermayr, S., O'Donoghue, N., Guttman, A. s., Rudd, P. M., *Anal. Chem.* 2010, 82, 10208-10215.
- [70] Melmer, M., Stangler, T., Schiefermeier, M., Brunner, W., *et al.*, *Anal. Bioanal. Chem.* 2010, 398, 905-914.
- [71] Anumula, K. R., Dhume, S. T., *Glycobiology* 1998, 8, 685-694.
- [72] Ruhaak, L. R., Huhn, C., Waterreus, W. J., de Boer, A. R., *et al.*, *Anal. Chem.* 2008, 80, 6119-6126.
- [73] Maslen, S., Sadowski, P., Adam, A., Lilley, K., Stephens, E., *Anal. Chem.* 2006, 78, 8491-8498.
- [74] Neville, D. C. A., Dwek, R. A., Butters, T. D., *J. Proteome Res.* 2008, 8, 681-687.
- [75] Wuhrer, M., Koeleman, C. A. M., Deelder, A. M., Hokke, C. N., *Anal. Chem.* 2004, 76, 833-838.
- [76] Bereman, M. S., Williams, T. I., Muddiman, D. C., *Anal. Chem.* 2008, 81, 1130-1136.

- [77] Zhao, J., Qiu, W. L., Simeone, D. M., Lubman, D. M., *J. Proteome Res.* 2007, 6, 1126-1138.
- [78] Wohlgemuth, J., Karas, M., Jiang, W., Hendriks, R., Andrecht, S., *J. Sep. Sci.* 2010, 33, 880-890.
- [79] Mysling, S., Palmisano, G., Højrup, P., Thaysen-Andersen, M., *Anal. Chem.* 2010, 82, 5598-5609.
- [80] Takegawa, Y., Deguchi, K., Ito, H., Keira, T., *et al.*, *J. Sep. Sci.* 2006, 29, 2533-2540.
- [81] Mauko, L., Nordborg, A., Hutchinson, J. P., Lacher, N. A., *et al.*, *Anal. Biochem.* 2011, 408, 235-241.
- [82] Kawasaki, N., Ohta, M., Hyuga, S., Hashimoto, O., Hayakawa, T., *Anal. Biochem.* 1999, 269, 297-303.
- [83] Pabst, M., Bondili, J. S., Stadlmann, J., Mach, L., Altmann, F., *Anal. Chem.* 2007, 79, 5051-5057.
- [84] Kolarich, D., Weber, A., Pabst, M., Stadlmann, J., *et al.*, *Proteomics* 2008, 8, 254-263.
- [85] Kawasaki, N., Haishima, Y., Ohta, M., Itoh, S., *et al.*, *Glycobiology* 2001, 11, 1043-1049.
- [86] Ruhaak, L. R., Deelder, A. M., Wührer, M., *Anal. Bioanal. Chem.* 2009, 394, 163-174.
- [87] Pabst, M., Altmann, F., *Anal. Chem.* 2008, 80, 7534-7542.
- [88] Karlsson, N. G., Wilson, N. L., Wirth, H.-J., Dawes, P., *et al.*, *Rapid Commun. Mass Spectrom.* 2004, 18, 2282-2292.
- [89] Chu, C. S., Ninonuevo, M. R., Clowers, B. H., Perkins, P. D., *et al.*, *Proteomics* 2009, 9, 1939-1951.
- [90] Chen, X., Flynn, G. C., *Anal. Biochem.* 2007, 370, 147-161.
- [91] Prater, B. D., Connelly, H. M., Qin, Q., Cockrill, S. L., *Anal. Biochem.* 2009, 385, 69-79.
- [92] Takegawa, Y., Deguchi, K., Ito, S., Yoshioka, S., *et al.*, *Anal. Chem.* 2004, 76, 7294-7303.

- [93] Charlwood, J., Birrell, H., Tolson, D., Camilleri, P., *Anal. Chem.* 1998, 70, 2530-2535.
- [94] Wojczyk, B. S., Takahashi, N., Levy, M. T., Andrews, D. W., *et al.*, *Glycobiology* 2005, 15, 655-666.
- [95] Ciucanu, I., Kerek, F., *Carbohydr. Res.* 1984, 131, 209-217.
- [96] Delaney, J., Vouros, P., *Rapid Commun. Mass Spectrom.* 2001, 15, 325-334.
- [97] Wada, Y., Azadi, P., Costello, C. E., Dell, A., *et al.*, *Glycobiology* 2007, 17, 411-422.
- [98] Morelle, W., Michalski, J. C., *Curr. Pharm. Design* 2005, 11, 2615-2645.
- [99] Domon, B., Costello, C. E., *Glycoconjugate J.* 1988, 5, 397-409.
- [100] Harvey, D. J., *J. Mass Spectrom.* 2000, 35, 1178-1190.
- [101] Ngoka, L. C., Gal, J. F., Lebrilla, C. B., *Anal. Chem.* 1994, 66, 692-698.
- [102] Cancilla, M. T., Penn, S. G., Carroll, J. A., Lebrilla, C. B., *J. Am. Chem. Soc.* 1996, 118, 6736-6745.
- [103] Stephens, E., Maslen, S. L., Green, L. G., Williams, D. H., *Anal. Chem.* 2004, 76, 2343-2354.
- [104] Morelle, W., Page, A., Michalski, J.-C., *Rapid Commun. Mass Spectrom.* 2005, 19, 1145-1158.
- [105] Pabst, M., Kolarich, D., Pörtl, G., Dalik, T., *et al.*, *Anal. Biochem.* 2009, 384, 263-273.
- [106] Prien, J. M., Prater, B. D., Qin, Q., Cockrill, S. L., *Anal. Chem.* 2010, 82, 1498-1508.
- [107] Wührer, M., Koeleman, C. A. M., Hokke, C. H., Deelder, A. M., *Rapid Commun. Mass Spectrom.* 2006, 20, 1747-1754.
- [108] Wührer, M., Koeleman, C. A. M., Deelder, A. M., *Anal. Chem.* 2009, 81, 4422-4432.
- [109] Harvey, D. J., *J. Am. Soc. Mass Spectrom.* 2005, 16, 631-646.
- [110] Harvey, D. J., *J. Am. Soc. Mass Spectrom.* 2005, 16, 647-659.
- [111] Wong, A. W., Wang, H., Lebrilla, C. B., *Anal. Chem.* 2000, 72, 1419-1425.
- [112] Zhu, J., Cole, R. B., *J. Am. Soc. Mass Spectrom.* 2001, 12, 1193-1204.
- [113] Wührer, M., Deelder, A. M., *Anal. Chem.* 2005, 77, 6954-6959.

- [114] Mechref, Y., Kang, P., Novotny, M. V., *Rapid Commun. Mass Spectrom.* 2006, 20, 1381-1389.
- [115] Wheeler, S. F., Harvey, D. J., *Anal. Chem.* 2000, 72, 5027-5039.
- [116] Jang, K.-S., Kim, Y.-G., Gil, G.-C., Park, S.-H., Kim, B.-G., *Anal. Biochem.* 2009, 386, 228-236.
- [117] Gil, G.-C., Iliff, B., Cerny, R., Velander, W. H., Cott, K. E. V., *Anal. Chem.* 2010, 82, 6613-6620.
- [118] Alley, W. R., Novotny, M. V., *J. Proteome Res.* 2010, 9, 3062-3072.
- [119] Ashline, D. J., Lapadula, A. J., Liu, Y.-H., Lin, M., *et al.*, *Anal. Chem.* 2007, 79, 3830-3842.
- [120] Prien, J. M., Huysentruyt, L. C., Ashline, D. J., Lapadula, A. J., *et al.*, *Glycobiology* 2008, 18, 353-366.
- [121] Morelle, W., Canis, K., Chirat, F., Faïd, V., Michalski, J. C., *Proteomics* 2006, 6, 3993-4015.
- [122] Fan, J. Q., Kondo, A., Kato, I., Lee, Y. C., *Anal. Biochem.* 1994, 219, 224-229.
- [123] Koizumi, K., *J. Chromatogr. A* 1996, 720, 119-126.
- [124] ThermoFisherScientific, 2007.
- [125] Wilson, N. L., Robinson, L. J., Donnet, A., Bovetto, L., *et al.*, *J. Proteome Res.* 2008, 7, 3687-3696.
- [126] Itoh, S., Kawasaki, N., Ohta, M., Hyuga, M., *et al.*, *J. Chromatogr. A* 2002, 968, 89-100.
- [127] Hashii, N., Kawasaki, N., Itoh, S., Hyuga, M., *et al.*, *Proteomics* 2005, 5, 4665-4672.
- [128] Lipniunas, P. H., Neville, D. C. A., Trimble, R. B., Townsend, R. R., *Anal. Biochem.* 1996, 243, 203-209.
- [129] Yuan, J., Hashii, N., Kawasaki, N., Itoh, S., *et al.*, *J. Chromatogr. A* 2005, 1067, 145-152.
- [130] Hashii, N., Kawasaki, N., Itoh, S., Harazono, A., *et al.*, *Rapid Commun. Mass Spectrom.* 2005, 19, 3315-3321.
- [131] Thomsson, K. A., Backstrom, M., Holmén Larsson, J. M., Hansson, G. C., Karlsson, H., *Anal. Chem.* 2010, 82, 1470-1477.



- [132] Costell, C., Contado-Miller, J., Cipollo, J., *J. Am. Soc. Mass Spectrom.* 2007, 18, 1799-1812.
- [133] Ninonuevo, M., An, H. J., Yin, H. F., Killeen, K., *et al.*, *Electrophoresis* 2005, 26, 3641-3649.
- [134] Bynum, M. A., Yin, H. F., Felts, K., Lee, Y. M., *et al.*, *Anal. Chem.* 2009, 81, 8818-8825.
- [135] Nischang, I., Svec, F., Fréchet, J. M. J., *Anal. Chem.* 2009, 81, 7390-7396.
- [136] Barroso, B., Dijkstra, R., Geerts, M., Lagerwerf, F., *et al.*, *Rapid Commun. Mass Spectrom.* 2002, 16, 1320-1329.
- [137] Luo, Q., Rejtar, T., Wu, S.-L., Karger, B. L., *J. Chromatogr. A* 2009, 1216, 1223-1231.
- [138] Alley, W. R., Madera, M., Mechref, Y., Novotny, M. V., *Anal. Chem.* 2010, 82, 5095-5106.
- [139] Prien, J. M., Ashline, D. J., Lapadula, A. J., Zhang, H., Reinhold, V. N., *J. Am. Soc. Mass Spectrom.* 2009, 20, 539-556.